Specific bromination of fluorinated oligophenylenes, towards cyclo-para- and cyclo-meta-phenylenes.

Dissertation

zur Erlangung des Doktorgrades der Naturwissenschaften

(Dr. rer. nat.)

der

Naturwissenschaftlichen Fakultät II

Chemie, Physik und Mathematik

der Martin-Luther-Universität

Halle-Wittenberg

vorgelegt von

NOUR-EDDINE EL ALAOUI

Gutachter	**Prof. Dr. Konstantin Amsharov** **Prof. Dr. Norbert Jux**
Tag der Verteidigung	**28.01.2026**

Danksagung

Ich möchte mich herzlich bedanken bei Prof. Dr. Konstantin Amsharov für das Bereit-stellen dieses interessanten Forschungsthemas. Außerdem hat er auch große Unter-stützung bei Fragen oder Problemen geleistet.

Zudem gilt mein Dank allen Mitarbeitern seines Arbeitskreises, die mich sehr herzlich aufgenommen haben und mir immer mit Rat und Tat zur Seite gestanden haben.

Zusätzlich möchte ich mich noch bei allen Angestellten des Institutes für Organische Chemie für die Unterstützung bedanken, vor allem Anne Hauptmann für alle organi-satorischen Aufgaben.

Zum Schluss möchte ich mich noch bei meiner Familie bedanken, die mich nicht nur während der Doktorarbeit, sondern auch während des gesamten Studiums immer unterstützt und motiviert hat.

List of Symbols

Symbol	Meaning
δ	Chemical shift (NMR)
J	Coupling constant (NMR)

List of Abbreviations

Abbreviation	Meaning
AcOH	Acetic acid
aq.	Aqueous
B_2pin_2	Bis(pinacolato)diboron
^{13}C NMR	Carbon-13 nuclear magnetic resonance
conc.	Concentrated
d	Doublet (NMR) / Day(s) (context-dependent)
DCM	Dichloromethane
DDQ	4,5-Dichloro-3,6-dioxocyclohexa-1,4-diene-1,2-dicarbonitrile
EtOAc	Ethyl acetate
^{19}F NMR	Fluorine-19 nuclear magnetic resonance
FLC	Flash liquid chromatography
g	Gram(s)
^{1}H NMR	Proton nuclear magnetic resonance
h	Hour(s)
HPLC	High performance liquid chromatography
Hz	Hertz
eq.	Equivalent(s)
ESI	Electrospray ionization
HMPA	Hexamethylphosphoramide
HR-MS	High-resolution mass spectrometry
IUPAC	International Union of Pure and Applied Chemistry
Me	Methyl
M	Molar
MeOH	Methanol
MHz	Megahertz
m-	Meta
m	Multiplet (NMR)
M.W	Microwave (assisted experiments)
m/z	Mass-to-charge ratio
min	Minute(s)

Abbreviation	Meaning
mL	Milliliter(s)
MS	Mass spectrometry
n-BuLi	n-Butyllithium
NGs	Nanographenes
NMR	Nuclear magnetic resonance
o-	Ortho
p-	Para
PBr	Pentabromobenzyl bonded silica
PAH	Polycyclic aromatic hydrocarbon
$Pd(dppf)Cl_2$	[1,1′-Bis(diphenylphosphino)ferrocene]dichloropalladium(II)
$Pd(P(Ph)_3)_4$	Tetrakis(triphenylphosphine)palladium(0)
ppm	Parts per million
t-BuOK	Potassium tert-butoxide
LooP	Ladderization of fluorinated oligophenylenes
rt	Room temperature
s	Singlet (NMR)
SM	Starting material
TLC	Thin-layer chromatography
Tol	Toluene
t	Triplet (NMR)
THF	Tetrahydrofurane
TMP	2,2,6,6-Tetramethylpipiridine
TBAB	Tetrabutylammonium bromide
TfOH	Trifluoromethanesulfonic acid

Table of Content

I. Introduction

Carbon is one of the most versatile elements on Earth, playing a fundamental role in life due to its ability to form long and stable carbon-carbon (C–C) bonds. Beyond its biological importance, carbon-based materials like fullerenes, carbon nanotubes, and graphene have attracted significant scientific attention because of their unique structural and electronic properties. The groundbreaking discoveries of fullerenes and graphene were even recognized with Nobel Prizes in Chemistry and Physics in 1996 and 2010, respectively.

The isolation of a single graphene layer by *Novoselov*[1] *et al.* (2004) marked a major breakthrough in materials science. Until then, it was widely believed that two-dimensional (2D) materials would be thermodynamically unstable and could not exist in a free-standing form[2,3]. However, this discovery proved otherwise and opened up new possibilities for research in chemistry, physics, and materials science. Graphene stands out due to its exceptional chemical stability, optical transparency[4], flexibility, porosity, biocompatibility, and tunable electronic properties, making it one of the most studied nanomaterials today.

Structurally, graphene consists of a single layer of carbon atoms arranged in a honeycomb lattice. Each carbon atom is sp^2 hybridized, forming strong sigma bonds with three neighboring atoms at 120° angles. The remaining p-orbitals interact to create a delocalized π-electron system, which is responsible for graphene's high electrical conductivity. Unlike conventional semiconductors, which have a finite bandgap, graphene is classified as a zero-bandgap semiconductor[1] due to the overlap of its conduction and valence bands at the Dirac point. This unique band structure gives graphene exceptional carrier mobility and electronic performance. Apart from its electrical properties, graphene is extremely lightweight yet incredibly strong-about 100 times stronger than steel[5], and has outstanding thermal and electrical conductivity[6,7]. These remarkable features make it a promising material for next-generation electronic and optoelectronic devices, including transistors[8], light-emitting diodes LEDs[9], solar cells[10–12], and flexible displays. In addition, graphene is also being explored for applications in filtration membranes[13], energy storage systems[14], and chemical sensors[15–17], broadening its impact beyond electronics.

Graphene can be regarded as an infinitely extended polycyclic aromatic hydrocarbon (PAH). Large PAHs, also known as nanographenes, are often used as model systems to study its properties. Since the size, shape, and edge topology of these PAHs influence their electronic structure[18,19], they play a key role in molecular electronics and optoelectronics, such as in donor-acceptor photovoltaics, organic field-effect transistors (OFETs)[18,20], and liquid crystal-based displays. The ability to fine-tune these characteristics makes nanographenes an exciting area of research with promising technological applications[21].

Generally, the discovery of graphene marked a groundbreaking milestone in the world of science, attracting a wide array of research due to its exceptional electrical[22], thermal[5], mechanical[9], and structural properties.

I.1. Introduction to nanographenes

The term in question combines "nano" (10^{-9}) and "graphene," a recently discovered carbon-based nanosheet material. The International Union of Pure and Applied Chemistry (IUPAC) defined "graphene" in 1986. This semi-metal, with a slight overlap between valence and conduction bands[23], is a carbon allotrope consisting of a single layer of carbon atoms in a hexagonal lattice.

Professor Han-Peter Boehm and Eberhard Stumpp identified single graphene sheets using TEM and X-ray diffraction in the early 1960s. Despite this, the 2010 Nobel Prize recognized later research on graphene's exceptional properties, ushering in a new era of optical and electronic materials[24]. Nanographenes, still in development, exhibit remarkable properties e.g. high electrical conductivity and near-transparency. They can be viewed as large aromatic molecules or polycyclic aromatic hydrocarbons (PAHs). Recent interest has grown in 3D-nanographenes, including curved and chiral variants, due to their potential in nanoelectronics and novel optical devices.

Over the past decade, PAHs and graphene nanoribbons (GNRs) have gained prominence in materials chemistry, finding applications in polymer films[25], sensors[26], electronic devices[27], and photovoltaic studies[28,29]. Aryl-aryl bond formation has been crucial in expanding these structures, significantly impacting synthetic approaches for large organic molecules[30,31]. Graphene's structure consists of sp^2-hybridized carbon atoms in a honeycomb pattern, forming the basis of graphite. While nanographenes and PAHs share similar frameworks, they differ in properties. Recent interest in nanographenes stems from their high electron mobility and flexibility, making them attractive in organic chemistry research[24,26].

I.2. Bromination

Brominated aromatic compounds represent a significant category of organic intermediates, valued for their diverse applications in agrochemicals[32], as biologically active agents[33,34], and important reagents in synthetic organic chemistry. Specifically, aromatic bromides are extensively utilized as precursors in various carbon-carbon and carbon-heteroatom bond-forming reactions, including Suzuki-Miyaura[35], Sonogashira[36], Heck[37], Stille[38], Buchwald-Hartwig[39], and cross-coupling reactions. Additionally, they serve as effective precursors for Yamamoto coupling[40,41] and are employed as key precursors in on surface synthesis in Scanning Tunneling Microscopy (STM) studies[42]. Significant research has been dedicated to developing selective[43], efficient, and straightforward synthetic routes for fluorinated aromatic bromide compounds. For instance, Gottfried[44] et al. explored intermolecular aryl-aryl coupling through C-F activation, highlighting the HF-zipping method as a robust alternative for producing nonbenzenoid carbon allotropes. *Kolmer*[45,46] *et al.* achieved a complex synthesis of nanographenes and nanoribbons by facilitating intramolecular aryl-aryl coupling on rutile titania surfaces. *Feofanov*[47,48] *et al.* synthesized a variety of fluorinated oligophenylenes, leading to the formation of O-heteroacenes via ladderization of fluorinated oligophenylenes (LooP). In another study, *Steiner* [49]*et al.* investigated the lithiation of 1-bromo-2-fluorobenzene using n-BuLi and 2,2,6,6-tetramethylpiperidine (TMP) in the presence of $CuBr_2$, yielding 3,3'-dibromo-2,2'-difluoro-1,1'-biphenyl with a 73% yield.

These advancements underscore the importance of brominated aromatic compounds in various chemical syntheses and their potential for further innovation in organic chemistry.

I.2.1. Metal-Mediated Aryl Aryl coupling.

- Palladium-Catalyzed Aryl-Aryl Coupling.

The Suzuki-Miyaura[35] cross-coupling reaction is widely recognized as a superior methodology for carbon–carbon bond formation compared to Negishi and Stille couplings, primarily due to the advantageous use of organoboranes. Organoboronic acids and their derivatives are commercially available, air-stable, and exhibit significantly lower toxicity than the organozinc reagents required for Negishi couplings or the toxic tin derivatives utilized in Stille reactions. A critical feature of this reaction is the mandatory inclusion of a base, which plays dual mechanistic roles. First, the base facilitates transmetallation by deprotonating the organoborane to form a tetracoordinated borate complex, thereby enhancing its nucleophilicity toward the palladium center. Second, weaker bases promote ligand exchange at the palladium intermediate, generating a hydroxypalladium species that exhibits greater reactivity in the transmetallation step compared to halogenated analogues. The original catalytic system developed by Suzuki employed $Pd(PPh_3)_4$ as the precatalyst with Na_2CO_3 in Benzene, THF or DMF at 60–80°C over 12–20 hours. Subsequent advancements have optimized ligand architectures, solvent systems, and base selection, expanding substrate scope and improving reaction efficiency while maintaining the inherent practicality and environmental compatibility of the process.

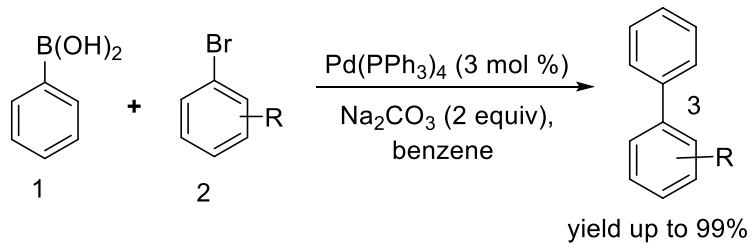

Scheme 1.1: Suzuki-Miyaura Cross-coupling.

- Ullmann Couplings of Brominated Aryl.

The origins of copper-mediated aryl–aryl bond formation date back to 1901, when Fritz Ullmann[50] and Jean Bielecki first demonstrated that heating o-bromonitrobenzene with 1.9 equiv of copper powder at high temperatures (210- 220 °C) produced 2,2′-dinitrobiphenyl in significant yield 76%, marking the inception of what is now known as the Ullmann reaction. This pioneering work not only showcased the ability of copper to facilitate the coupling of aryl halides but also established a foundation for transition-metal-catalyzed carbon–carbon bond formation in organic synthesis. Since its discovery, the Ullmann reaction has been extensively studied and refined, although the classical version required harsh conditions and often gave variable results; nevertheless, ongoing research and methodological improvements have broadened its scope and applications, making it a valuable tool in the synthesis of biaryl compounds and beyond.

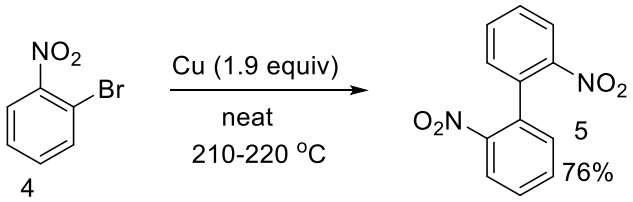

Scheme 1.2: Dimirization using Ullmann Couplings.

I.2.2. On-Surface Synthesis of Graphene Nanoribbons and Related Structures.

R. Fasel et al[42]. described a straightforward approach for creating precise graphene nanoribbons with varied structures and dimensions by employing 10,10'-dibromo-9,9'-bianthryl as a starting material in a surface-assisted coupling process. The technique involves thermally sublimating the monomers onto a solid substrate, which triggers the removal of halogen groups, resulting in surface-stabilized biradical entities. These entities serve as the fundamental components for the desired graphene ribbons. The initial thermal activation allows the biradicals to move across the surface, engaging in addition reactions to form linear polymers, guided by the monomers' specific chemical patterns. A subsequent thermal step induces surface-assisted cyclodehydrogenation, leading to the formation of an extensive aromatic system.

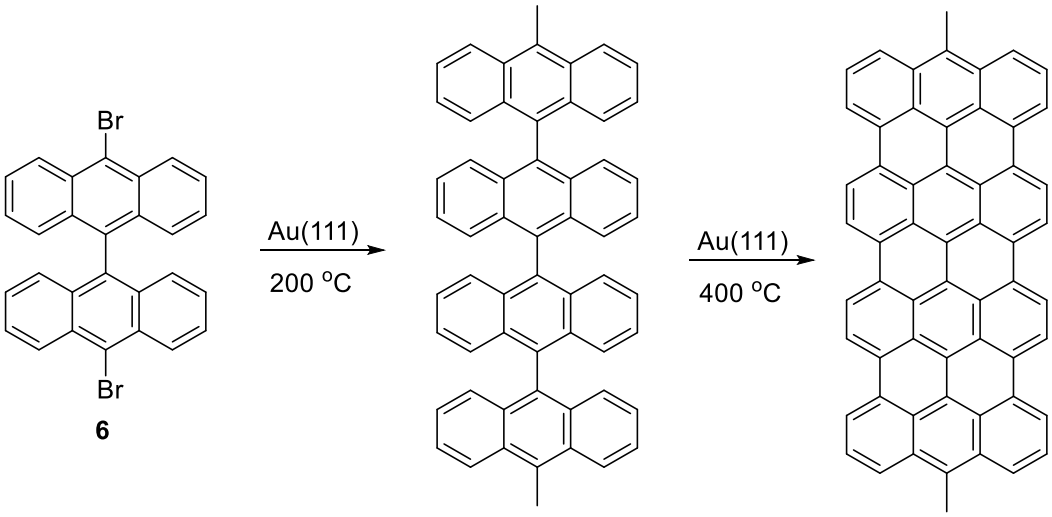

Scheme 1.3: On-surface synthesis of the linear GNR on an Au(111) surface.

Gottfried et al[44]. presented a novel approach for creating nonbenzenoid structures without incorporating them in the initial precursor. Instead, these elements form during the lateral dehydrofluorination fusion of benzenoid polyphenylene chains, a process termed "HF-zipping." This method utilizes 4,4″-dibromo-2,2′,2″,5,5′,5″-hexafluoro-1,1′:4′,1″-terphenyl (DHTP) as a starting material. When deposited on a Au(111) surface, DHTP undergoes polymerization via debrominative coupling, creating well-organized assemblies of poly(2,5-difluoro-para-phenylene) (PFPP) chains. Subsequently, these chains participate in C-C coupling via HF-zipping, leading to the formation of a biphenylene network. This interchain process selectively facilitates C-C bond formation between C-F and C-H moieties, resulting in

the creation of four- and eight-membered rings between the chains. The strategic positioning of C-F groups is crucial for generating this nonbenzenoid structure, as their absence would result in dehydrogenative C-C coupling, forming six-membered rings and regular graphene instead.

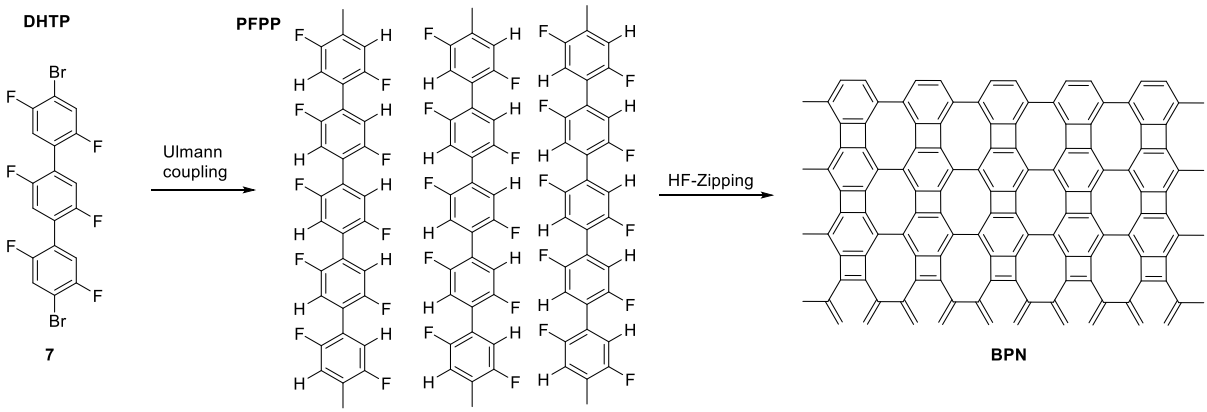

Scheme 1.4: BPN was synthesized from DHTP (7) monomers through a two-step process, first forming linear polymers and then connecting these chains via interchain HF-zipping.

I.3. Synthesis of Cycloparaphenylenes.

Since the initial discovery by Iijima in 1991[51], carbon nanotubes (CNTs) have garnered significant attention from researchers due to their exceptional physical characteristics and potential technological applications[9,52–55]. Single-walled CNTs are essentially graphene sheets rolled into cylindrical forms, with their specific structure determined by the chiral index, denoted as (n, m). Depending on the values of n and m, CNTs are categorized into three types: "zigzag" (m = 0), "armchair" (n = m), and "chiral" (n > m > 0).

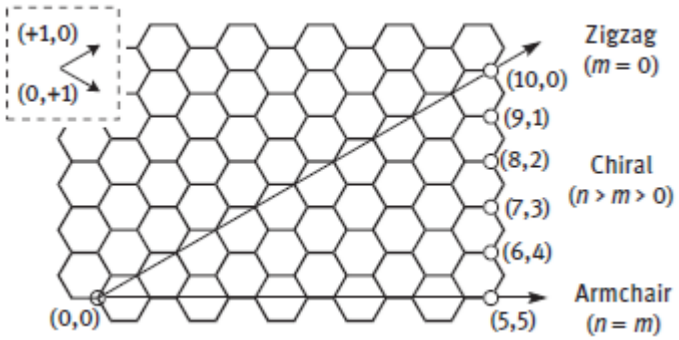

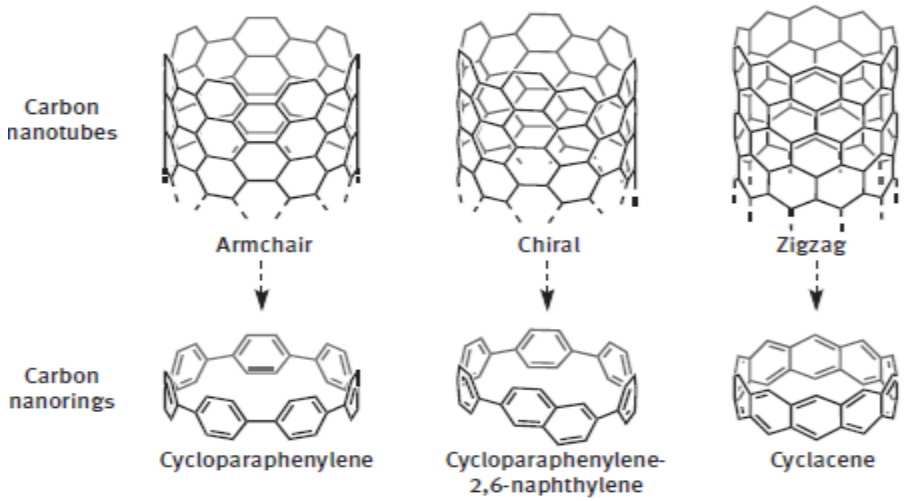

Scheme 1.5: Structures, the chiral index of carbon nanotubes (CNTS) and carbon nanorings.

In 2008, Bertozzi and Jasti[56] achieved the initial synthesis of CPP, followed shortly by the Itami group[57], which introduced the first size-selective synthesis of CPP in 2009. Yamago[58] later contributed an alternative method in 2010. Through the efforts of Jasti, Itami, and Yamago's teams, synthetic strategies were established for both selective and random formation of CPPs, leading to the successful creation of [n]CPPs with ring sizes ranging from n = 5–18. This outstanding work in cycloparaphenylene synthesis has opened up new avenues for research in carbon nanostructures.

I.3.1. Synthesis of [9], [12] and [18]CPP by Bertozzi and Jasti[56].

The first synthesis of CPP was accomplished by Bertozzi and Jasti in 2008. To construct the macrocyclic CPP precursor, their approach began with the creation of an L-shaped building block, derived from the reaction of monolithiated 1,4-diiodobenzene with p-benzoquinone. This key component was then modified through borylation. The researchers employed a suzuki-miyaura cross-coupling reaction to combine these units, resulting in the formation of three distinct macrocyclic structures. The final step involved a reductive aromatization process using lithium naphthalenide, which successfully transformed these precursors into the desired CPPs, yielding [9]CPP, [12]CPP, and [18]CPP.

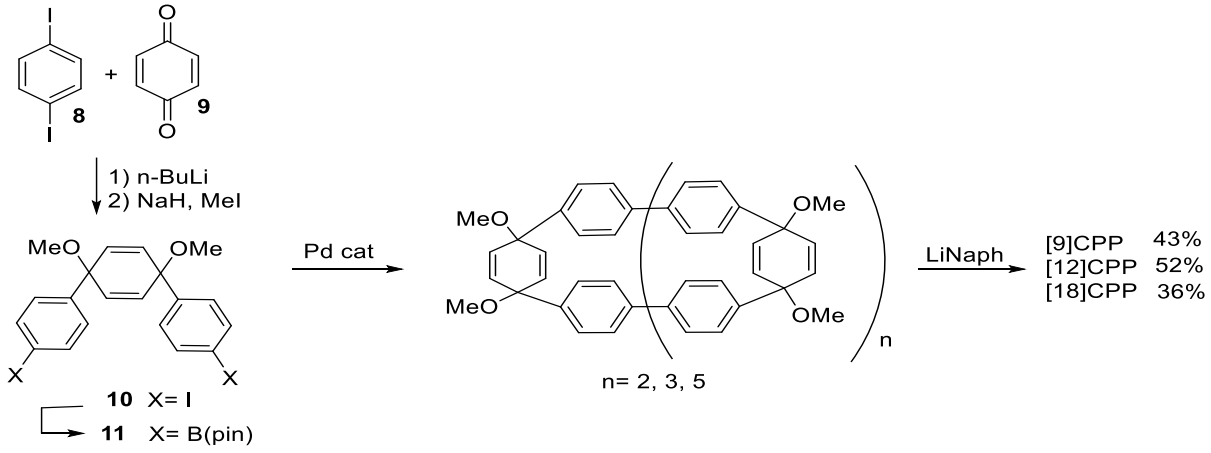

Scheme 1.6: Bertozzi and Jasti approach for the synthesis of [9]CPP, [12]CPP and [18]CPP.

I.3.2. Synthesis of [12]CPP by Itami[57].

In 2009, Itami achieved the first size-selective synthesis of [12]CPP. The process began with the preparation of an L-shaped unit from 1,4-diiodobenzene and cyclohexane-1,4-dione. This unit was then modified to get borylated 13 and MOM-protected 12 (MOM = methoxymethyl) for use in Suzuki–Miyaura coupling. A palladium-catalyzed cross-coupling reaction between 13 and an excess of 12 produced the acyclic C-shaped unit 14, which further reacted with 13 to form 15, which underwent a one-pot reaction involving deprotection, dehydration, and dehydrogenation, facilitated by p-toluenesulfonic acid (TsOH) and microwave irradiation under air, resulting in the successful production of [12] CPP.

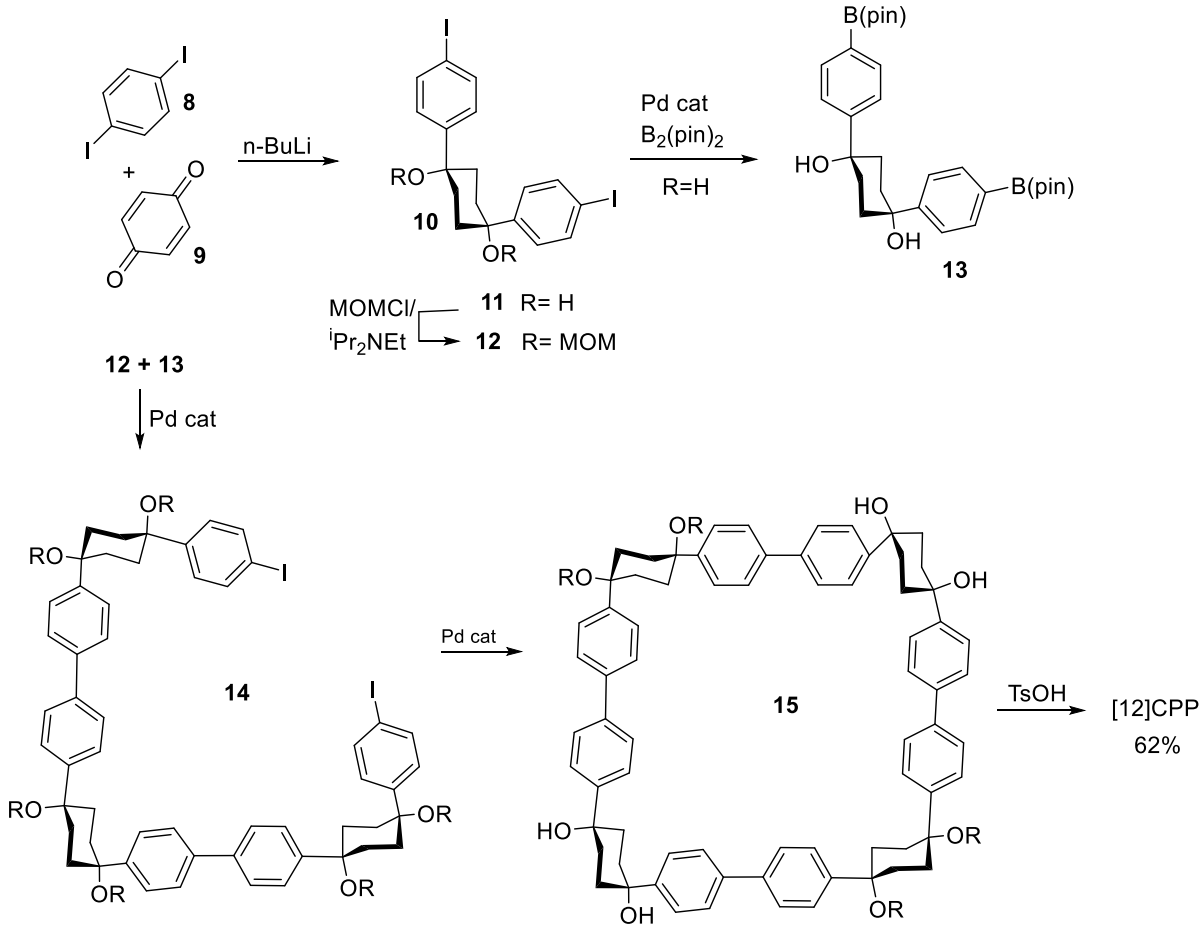

Scheme 1.7: Itami approach for the synthesis of [12]CPP.

I.3.3. Synthesis of [12]CPP by Yamago[59].

In 2011, Yamago introduced a selective synthesis method for [12]CPP by adapting Bäuerle's cycloarene synthesis approach, utilizing platinum-based macrocycles. The process involved the complexation of bis(trimethylstannyl)terphenyl 16 with Pt(cod)Cl2, yielding macrocycle. Subsequent reductive elimination of the aryl groups from the platinum center was facilitated by ligand exchange from cod to dppf (1,1′-bis(diphenylphosphino)ferrocene), followed by oxidation with bromine, ultimately leading to the formation of [12]CPP.

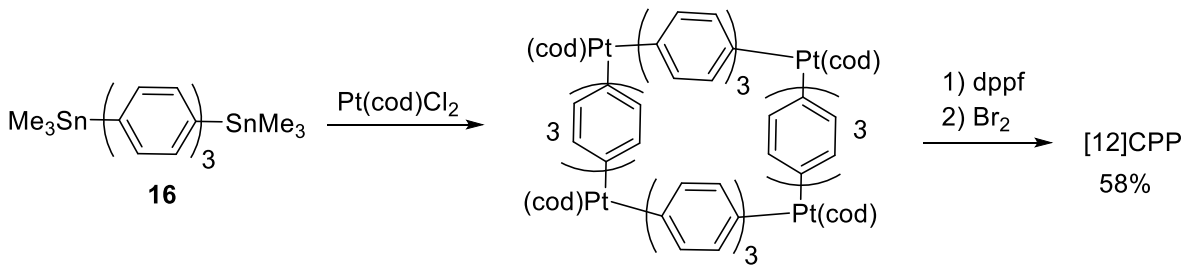

Scheme 1.8: Yamago approach for the synthesis of [12]CPP.

I.4. Synthesis of Cyclo-meta-phenylenes.

Cyclo-meta-phenylenes, cyclic oligomers sharing a benzene ring backbone with poly(p-phenylene)s (PPPs), were first synthesized by Staab in the 1960s[60] and later explored by Cram[61,62] for cation host applications. These macrocycles have received limited attention despite their potential. While recent work by Klaus Müllen's group introduced functionalized derivatives, prior studies primarily featured simple alkyl or alkoxy substituents due to synthetic constraints. Existing synthetic approaches rely on laborious terphenyl precursor preparation before macrocyclization via reductive coupling, which limits structural diversity and functional group compatibility due to harsh reaction conditions. As interest grows in novel functional materials, more efficient synthetic methods are needed to expand the potential applications of cyclohexa-m-phenylenes.

Klaus Müllen et al[63]. reported the synthesis of hexaalkyl CHP through Yamamoto-type dimerization of compound **17**, achieving a 58% yield of hexa-m-phenylene **18** after optimizing reaction conditions. Subsequent ipso substitution replaced trimethylsilyl groups with iodine, yielding a macrocycle with six iodine atoms at 84%. Although the intermediate exhibited limited solubility, a final six-fold Hagihara–Sonogashira coupling with tetradec-1-yne efficiently produced the target alkylated CHP macrocycle (51%).

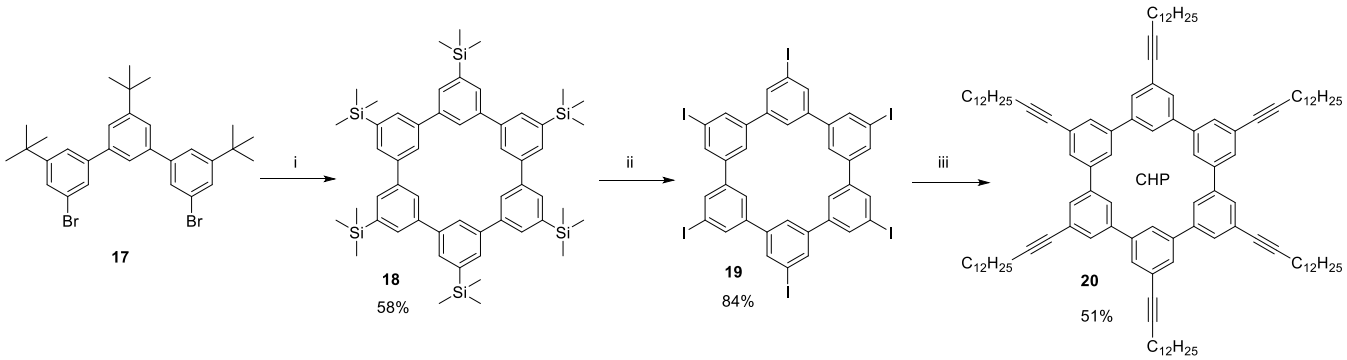

Scheme 1.9: Synthetic routes to CHP, i) cod, bipy, [Ni(cod)$_2$], 58%; ii) ICl, 84%; iii) tetradec-1-yne, PPh3, CuI, [Pd (PPh$_3$)$_4$], 51%.

Swager et al[64]. developed a Straightforward strategy for assembling the cyclohexa-m-phenylene structure in one step by performing a sixfold Suzuki coupling. Their methodology employed two essential monobenzenoid precursors: a pinacol-protected diboronic acid (21) and a dibromide derivative (22), enabling direct macrocyclization without requiring

intermediate isolation steps. This efficient strategy significantly simplifies the construction of the target framework compared to traditional multi-step synthetic routes.

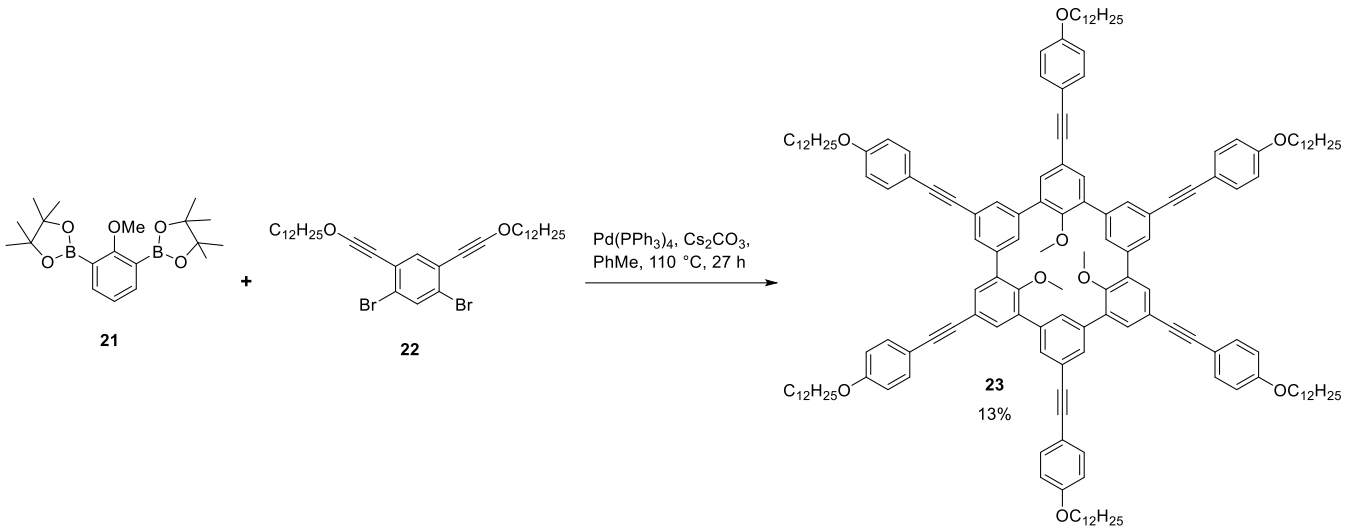

Scheme 1.10: Synthesis of hexa-m-phenylene via sixfold Suzuki coupling.

I.5. The Scholl reaction.

In 1910, Roland Scholl[65] reported an oxidative dimerization of aromatic compounds in the presence of strong Lewis acids, using an excess of neat anhydrous aluminum chloride ($AlCl_3$) at temperatures ranging from 140°C to 145 °C for 45 minutes. Although no yield was reported (Scheme 1.11), this oxidative cyclization process was subsequently named the "Scholl reaction."

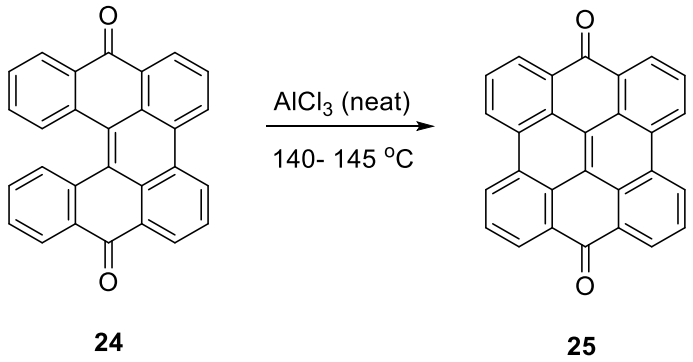

Scheme 1.11: Synthesis of quinones employing the Scholl reaction.

This method enabled the synthesis of extended polycyclic arenes under such harsh conditions. Over time, the Scholl reaction has been widely applied in both intramolecular and intermolecular transformations, employing a variety of oxidants, including $FeCl_3$, $CuCl_2$, $Cu(OTf)_2$, $Tl(O_2CCF_3)_3$ in CF_3CO_2H or BF_3-OEt_2, $Pb(OAc)_4/BF_3$-Et_2O in MeCN, triethyloxonium hexachloroantimonate (Et_3O^+ $SbCl_6^-$), $SbCl_5$, $MoCl_5$, etc.

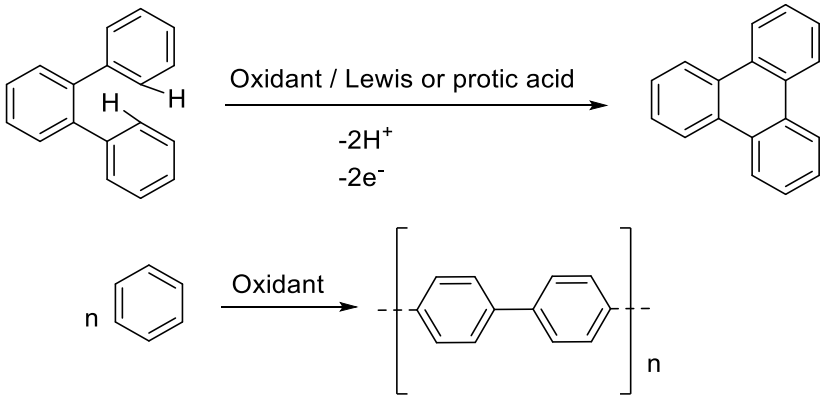

Scheme 1.12: Intramolecular and intermolecular C–C bond formation through the Scholl reaction.

I.5.1. Mechanistic pathways of the Scholl reaction

The Scholl reaction's mechanism has been thoroughly studied and examined, with significant focus to understand its underlying processes. Initially, the precise mechanism was not fully elucidated, resulting in the emergence of two main hypotheses:

- ***The first hypothesis***, known as the ***Arenium Cation Mechanism***, was originally introduced by Baddeley[66]. This mechanism suggests that the reaction proceeds through the formation of a sigma complex between a Lewis acid and an aromatic compound. This intermediate subsequently generates an arenium cation, which undergoes electrophilic attack followed by dehydrogenation. The Arenium Cation Mechanism was later refined by King[67,68] and Rathore[69], offering further clarification and deep insights into this underyling process.
- ***The second hypothesis***, referred to as the ***Radical Cation Mechanism***, was advanced by Kenner[70]. This proposal posits that the reaction proceeds through the formation of radical cations. The Radical Cation Mechanism received further support from researchers, namely Rathore[71], Rooney and Pink[72], and Clover[73], who validated it through experimental and theoretical studies.

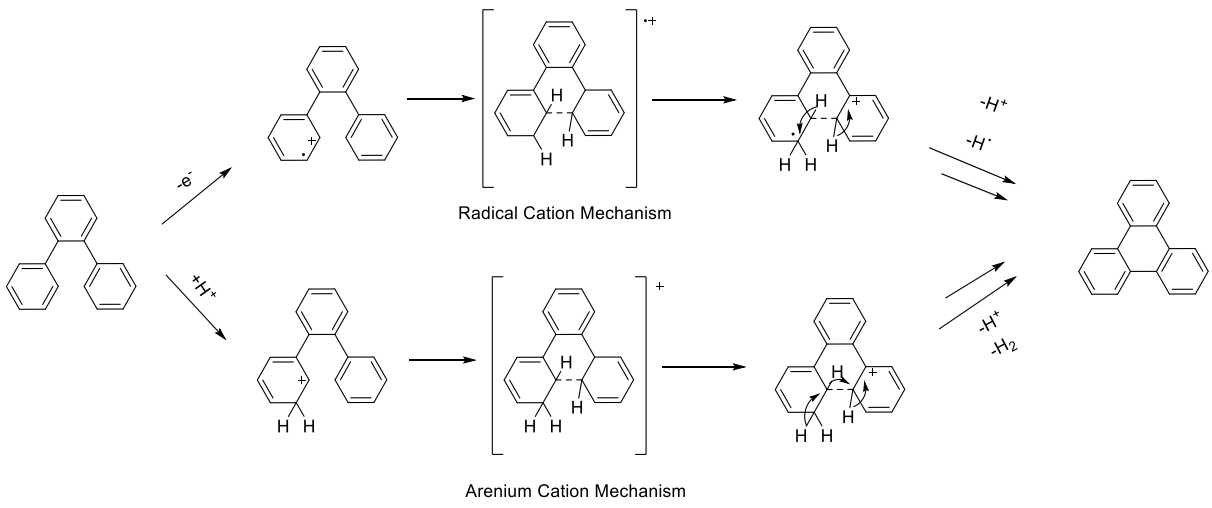

Scheme 1.13: Oxidative coupling of arenes through a radical cation or an arenium ion mechanism according to Scholl reaction conditions.

The Scholl reaction is predominantly characterized by electrophilic aromatic substitution. The presence of electronically activating substituents on the aromatic rings plays a crucial role in enhancing the system's reactivity. Both the Arenium Cation Mechanism and the Radical Cation Mechanism converge in the elimination of H_2 through cyclodehydrogenation. This transformation is driven by the action of an oxidant and a catalyst, yielding the formation of a new carbon-carbon (C–C) bond and the generation of additional aryl rings.

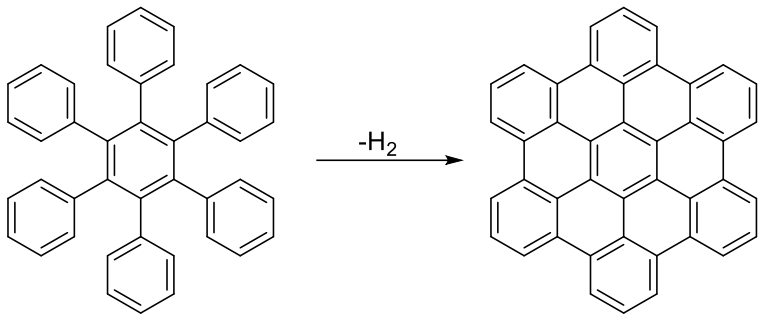

26 **27**

Scheme 1.14: Synthesis of hexa-peri-hexabenzocoronene via cyclodehydrogenation.

I.5.2. Intermolecular Oxidative Aromatic Coupling

Oxidative coupling reactions can be categorized into two main types: Homocoupling and Cross-coupling. In homocoupling, two identical aromatic molecules combine to form a biaryl structure. While Cross-coupling is more challenging, because of involving two different arenes and due to the reaction's low selectivity. which is influenced by steric considerations and the electron density of both aromatic molecules involved. The reaction conditions control is crucial to prevent unwanted homocoupling in cross-coupling reactions. Despite these challenges, substantial advancements have been made in the area of intermolecular oxidative cross-coupling in recent years.

I.5.2.1. Homocoupling of Naphthalene Derivatives

The oxidative coupling of aromatic compounds frequently results in the formation of axially chiral products. which are crucial in the development of optically active catalysts based on biaryl units. Among them, Binaphthyl and its derivatives, particularly 1,1'-Bi-2-naphthol (BINOL)[74], plays a significant role as a precursor of many important ligands used in asymmetric catalysis, with BINAP being a notable example. The synthesis of BINOL and other binaphthyl derivatives through oxidative coupling of corresponding naphthalenes has been achieved using various methods, producing both racemic mixtures and pure enantiomers. Many catalytic systems, oxidants, and metal complexes have been explored for this purpose. In addition to traditional methods using FeCl3, reasonable yields of binaphthyls have been achieved with reagents as thallium(III) and mercury(II) trifluoroacetates, $Pb(OAc)_2$, and CoF_3[75], as well as titanium(IV) chloride[76] and $CuCl_2$ in the presence of amines[77].

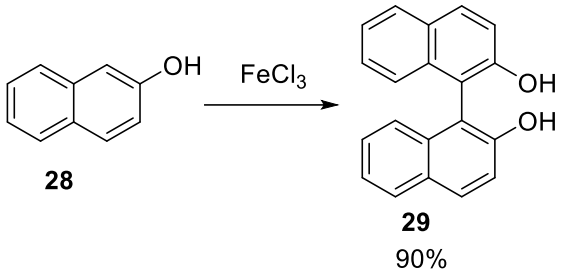

Scheme 1.15: Synthesis of 1,1'-bi-2-naphthol (29) by the oxidation of 2-naphthol (28) in the presence of $FeCl_3$.

Wang and co-workers[78,79] reported two novel systems that effectively oxidize various 2-naphthols into their corresponding racemic binaphthols. In the first system, using m-chloroperoxybenzoic acid (m-CPBA) as an oxidant, whereas iron(III) chloride acting as the catalyst for the reaction. The second approach involved oxidation using a stoichiometric quantity of manganese(IV) oxide in the presence of a tenfold excess of trifluoroacetic acid (TFA). Both methods yield biaryl products in satisfactory quantities.

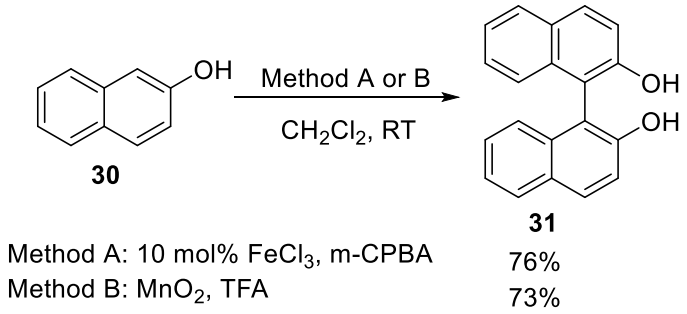

Scheme 1.16: Synthesis of 1,1'-bi-2-naphthol (31) using two method (a) using m-CPBA as an oxidant and $FeCl_3$ as a catalyst, (b) using MnO_2 in excess of TFA.

I.5.2.2. Triphenylene Syntheses

Intermolecular oxidative aromatic coupling is not limited to naphthalene derivatives, it can also be successfully applied to various electron-rich benzene derivatives and heteroarenes. A well-known example is the synthesis of 2,3,6,7,10,11-hexamethoxytriphenylene (33), first reported in 1965[80]. Triphenylene was produced in a 73% yield through the oxidative cyclization of 1,2-dimethoxybenzene (veratrole) using chloranil in 70% aqueous sulfuric acid. The authors proposed that the first step of the reaction involves an oxidative dimerization of veratrole to form 3,3',4,4'-tetramethoxybiphenyl as an intermediate. This intermediate then couples with another veratrole molecule, followed by an intramolecular coupling to yield the triphenylene structure. Supporting this hypothesis, the same triphenylene product was obtained when a mixture of veratrole and 3,3',4,4'-tetramethoxybiphenyl was subjected to the same reaction conditions.

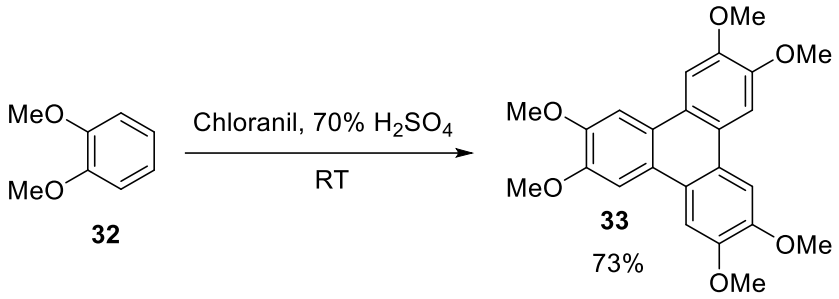

Scheme 1.17: Synthesis of 2,3,6,7,10,11-hexamethoxytriphenylene via oxidative cyclization of 1,2-dimethoxybenzene (32) upon treatment with chloranil in 70% H_2SO_4.

I.5.2.3. Intermolecular Oxidative Cross-Coupling of Aromatic Compounds

Intermolecular oxidative cross-coupling of arenes presents greater challenges and is less predictable compared to homocoupling. To achieve reasonable yields and good selectivity, a careful selection of reaction conditions and starting materials is required[81,82]. The proposed reaction mechanism involves several key steps:

As shown in scheme 1.14, a preferential oxidation of the more electron-rich arene ***34*** (lowest oxidation potential $\boldsymbol{E_p^{ox}}$), forms an electrophilic cation radical ***35***. An electrophilic attack by ***36*** on ***35***, results in an intermediate radical ***37***. Subsequent loss of two protons and an electron yields to the desired cross-coupled biaryl product ***38***.

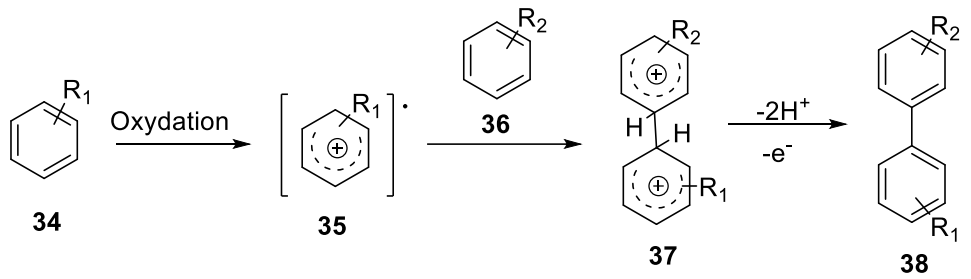

$$\boldsymbol{E_p^{ox}\ 34 < E_p^{ox}\ 36}$$

Scheme 1.18: Mechanism of Intermolecular Oxidative Cross-Coupling of Aromatic Compounds.

Waldvogel et al[83]. introduced an innovative electrochemical method for selective phenol-arene cross-coupling using boron-doped diamond (BDD) electrodes. This approach relies on the presence of a hydroxyl group, as the phenoxyl radical intermediate plays a crucial role in the reaction mechanism[1].The method successfully coupled 4-methylguaiacol with various electron-rich benzene derivatives, yielding to cross-coupled products with moderate efficiency[5]. Notably, this method has also been applied to oxidative homocoupling of phenols, producing yields ranging from 44% to 84%. These reactions are exclusively carried out in hexafluoroisopropanol as the solvent.

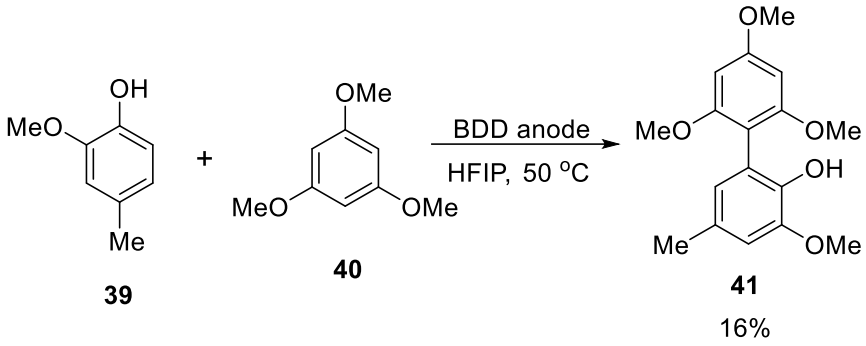

Scheme 1.19: Selective electrochemical cross-coupling reaction between phenols and arenes is achieved utilizing boron-doped diamond (BDD) electrodes.

I.5.3. Intramolecular Oxidative Aromatic Coupling

The intramolecular oxidative coupling of arenes, often referred to as the *"Scholl reaction"*, has recently emerged as a powerful synthetic tool, despite being known for many years. This reaction gained prominence due to the growing importance of research in organic electronics, nanotechnology, and bioimaging, which require efficient methods for creating intramolecular C_{aryl}-C_{aryl} bonds. It became a versatile and widely used method for synthesizing various Polycyclic Aromatic Hydrocarbons (PAHs) including nanographenes, as well as for expanding and planarizing π-conjugated systems and preparing strained, curved, or twisted molecular structures. The increasing demand for this reaction in diverse applications has led to its establishment as a well-recognized synthetic method.

I.5.3.1. Large Planar Polycyclic Aromatic Hydrocarbons (PAHs).

Intramolecular oxidative coupling methods have been proven to be a powerful tool in the synthesis of complex PAHs and nanographenes. These methods excel in their ability to form multiple C_{aryl}-C_{aryl} bonds simultaneously, often creating hundreds or even thousands of such connections in a single reaction step. The efficiency of this approach becomes particularly evident when compared to alternative C_{aryl}-C_{aryl} coupling techniques. Traditional methods would require a strategic placement of numerous activating groups, such as halides or boronic acids/esters, throughout the precursor molecules. This requirement would not only complicate the synthetic process but also potentially render the goal unattainable for larger, more complex structures.

Hexa-peri-hexabenzocoronene (HBC) and its derivatives represents a significant milestone in the synthesis of large PAHs. While these compounds were known previously, their synthesis yielded to extreme low amounts, limiting their practical applications. It was not possible that hexaphenylbenzenes could be transformed to HBC derivatives with significantly improved yields until *Müllen et al*[84]. developed innovative oxidation methods using $Cu^{II}/AlCl_3$ or $FeCl_3$ that. Among these methods, the use of $FeCl_3$ dissolved in nitromethane, followed by its addition to a dichloromethane solution of the precursor, proved to be the most effective. This approach not only delivered superior yields but also demonstrated broad applicability across a wide range of HBC derivatives.

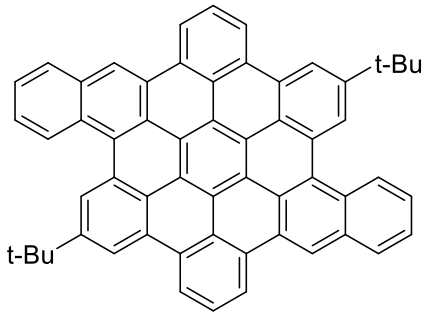

42

68%

Scheme 1.20: Synthesis of an extended hexabenzocoronene 42.

Dichtel et al[85]. synthesized an extended hexabenzocoronene, compound ***42***, through a two-step process. Their research revealed that the initial fusion of four bonds occurs rapidly, resulting in a partially fused intermediate with a twisted structure. This intermediate is stable enough to be isolated and studied. Subsequently, prolonged exposure to the $FeCl_3$ oxidizing agent completes the fusion process, yielding to the fully formed HBC derivative.

Müllen et al[86]. reported an unexpected 1,2-aryl shifts during an oxidative aromatic coupling reaction. While attempting to synthesize tetrabenzo[a,cd,j,lm]perylene using the *Scholl reaction*, they observed that the starting material, 6,7,13,14-tetraphenylbenzo[k]tetraphene, underwent two 1,2-aryl shifts instead of the anticipated cyclization. Their investigation suggested that the initial shift likely proceeds through a *radical cation mechanism*. Building on this serendipitous discovery, the research team later applied this rearrangement strategy to successfully synthesize fused dibenzo[a,m]rubicene, a curved molecule structurally related to a subunit of C70 fullerene. This work highlights how unexpected molecular rearrangements can lead to novel synthetic pathways and structures in polycyclic aromatic hydrocarbon chemistry.

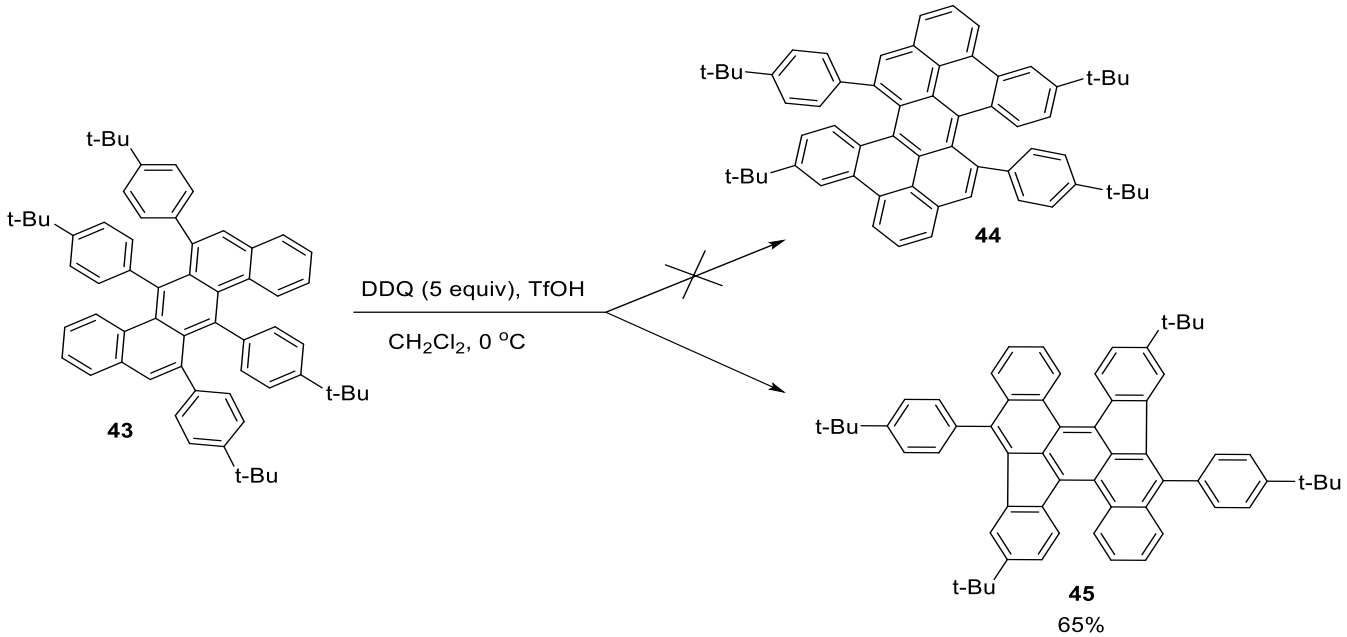

Scheme 1.21: A representative dehydrogenative coupling reaction occurs alongside a double 1,2-aryl shift.

I.6. Ladderization

Organic semiconductors have undergone significant advancements in recent decades, driven by their potential for creating next-generation ultrathin, large-area, and flexible devices. These materials have found applications in organic field-effect transistors (OFETs), organic light-emitting diodes (OLEDs), and organic photovoltaics (OPVs), offering novel features distinct from traditional silicon technologies. The journey of organic semiconductors began in the 1980s with the use of poly(thiophene) in OFETs[87], though initial performance was subpar. Significant breakthroughs in the 1990s, including advancements in materials development, purification methods, and device fabrication techniques[88,89], led to substantial improvements in device performance. The evolution of organic semiconductors has seen the combination of heterocyclic compounds like thiophenes with acene structures, resulting in ladder-type sulfur-containing π-conjugated molecules. These hybrid materials exhibit remarkable stability and effective π-π stacking in the solid state, capitalizing on the advantages of both classes.

I.6.1. Classification of Thienoacene

Thienoacene-based organic semiconductors have evolved into a diverse array of molecular structures, each with unique properties suited for various applications. These compounds can be categorized into four main classes based on their structural features: [n]thienoacenes ([n]TAcs)[90,91], benzene-thiophene alternating molecules (BTAs)[92], acenedithiophenes (AcDTs)[93], and diacene-fused thienothiophenes (DAcTTs)[94]. Each class is represented by notable compounds such as 5thienoacene, benzo[1,2-b:4,5-b']bis[b]benzothiophene (BBBT), anthra[2,3-b:6,7-b']dithiophene (ADT), and dinaphtho[2,3-b:2',3'-f]thieno[3,2-b]thiophene (DNTT), respectively. These molecules exhibit distinct characteristics in terms of their highest occupied molecular orbital (HOMO) energy levels, HOMO geometries, and reorganization energies for hole transport. The structural variations among these classes result in different electronic properties, making them suitable for specific roles in organic semiconductor applications. Understanding these molecular features is crucial for designing and optimizing thienoacene-based materials for use in organic electronics. In the following section, we will examine the synthetic methodologies employed in the formation of Benzene-Thiophene Alternating Molecules (BTAs).

I.6.1.1. Benzene-Thiophene Alternating Molecules (BTAs).

Benzene-thiophene alternating molecules (BTAs) have emerged as promising materials for organic field-effect transistors (OFETs)[95–97], building on the success of their non-fused counterparts, thiophene-phenylene alternating co-oligomers. The first BTA compound investigated for OFET applications was dibenzo[b,b']thieno[2,3-f:5,4-f']bisbenzothiophene (DBTBT), reported by *Sirringhaus et al*[98]. which exhibited impressive performance with a field-effect mobility (μFET) of 0.15 $cm^2\ V^{-1}\ s^{-1}$ and an on/off current ratio (I_{on}/I_{off}) exceeding 10^6. Following this breakthrough, numerous BTA-based materials have been developed and tested as active layers in OFETs, utilizing both vacuum deposition and solution-processing techniques, further highlighting their potential in organic electronics.

I.6.1.2. Synthesis of BTAs

The benzene-thiophene alternating (BTA) system is built upon the fundamental unit of dibenzo[b,d]thiophene (DBT), a well-known compound that can be synthesized from various precursors such as biphenyl, diphenylsulfide, and o-mercaptobiphenyl. However, these traditional synthetic routes are not easily adaptable for creating larger BTA compounds with multiple DBT substructures. A significant advancement in this field came from *Müllen et al*[98].who developed a more efficient and versatile method for thiophene annulation. This approach involves an intramolecular coupling reaction between aromatic methyl sulfoxides and an activated aromatic building block in the presence of strong acids. This innovative synthetic strategy has greatly expanded the possibilities for creating complex BTA-based materials, opening new avenues for the development of advanced organic semiconductors with tailored properties for various electronic applications.

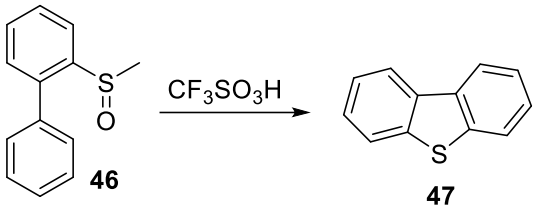

46 **47**

Scheme 1.22: Synthesis of Benzene-Thiophene Alternating Molecules (BTAs).

During the synthesis of compound ***49***, the precursor 3,7-bis[2-(methylsulfinyl)phenyl]DBT was treated with trifluoromethanesulfonic acid, resulting in the formation of two regioisomers. These isomers were difficult to separate due to their minimal differences in sublimation temperatures. In contrast, the synthesis of compounds 52[99] and 54[100] (DTBDT) avoided regioisomer formation by using 1,4-dibromo-2,5-bis(methylsulfinyl)benzene as a key intermediate. This intermediate underwent efficient cross-coupling reactions with phenyl boronic acids or thienyl-trimethylstannanes to produce the necessary precursors. The final step, involving intramolecular coupling induced by trifluoromethanesulfonic acid, yielded to the target compounds in high purity and excellent yields. This synthetic strategy was further validated through its successful application in creating heteroheptacenes containing fused thiophene and pyrrole rings[101,102] .

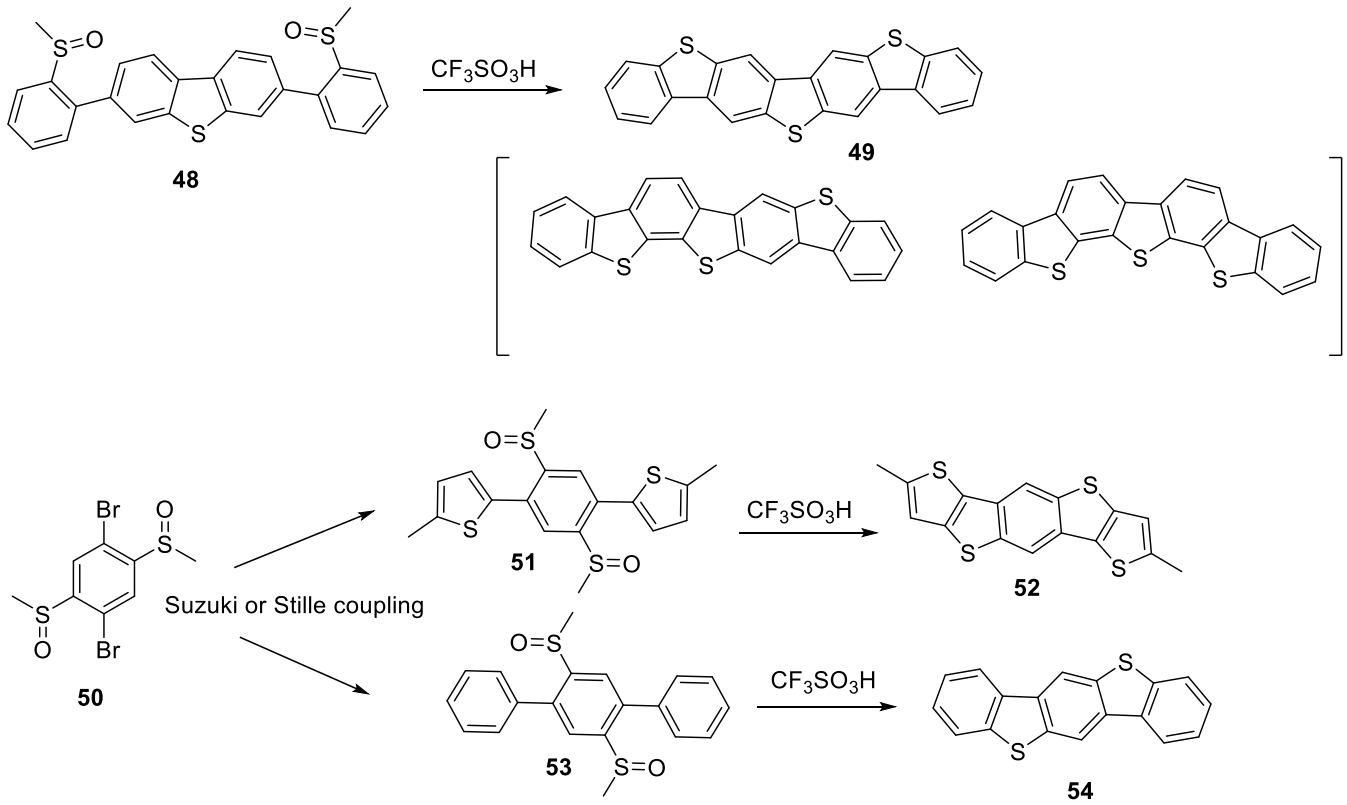

Scheme 1.23: Synthesis of BTAs through an intramolecular coupling reaction of aromatic methyl sulfoxides in acidic conditions.

M. Feofanov et al[103]. have developed an innovative approach to synthesizing sulfur-containing heteroacenes that represents a significant advancement in the field. This transition-metal-free method utilizes fluorinated oligophenylenes as starting materials, offering a versatile and efficient route to complex heteroacenes. Unlike conventional strategies, which typically rely on sulfur-containing precursors to construct the dibenzo[b,d]thiophene (DBT) core*, Feofanov's* innovative technique utilizes sodium sulfide (Na_2S) as an external sulfur source in the presence of tetrabutylammonium bromide (TBAB) in HMPA (hexamethylphosphoramide) for 3h at 180 °C. This shift not only enhances the flexibility of the synthetic process but also expands the potential for designing and producing diverse DBT-based structures, paving the way for new developments in heteroacene chemistry.

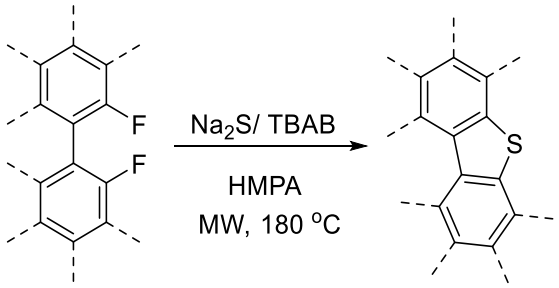

Scheme 1.24: Reaction conditions of S-heteroacenes.

Subsequently, *Itami et al*[104]. achieved the synthesis of highly sought-after thiophene-fused aromatic belts, commonly referred to as thiophene belts, by adapting the conditions developed

by *M. Feofanov* Utilizing partially fluorinated cycloparaphenylenes (CPPs) as precursors, O-heteroacenes.

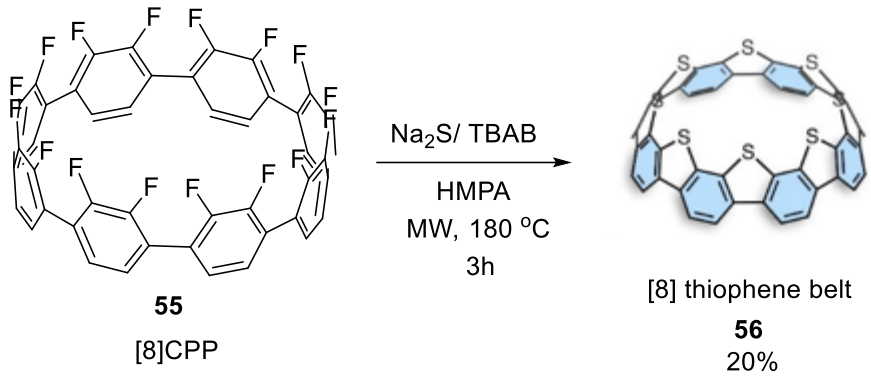

Scheme 1.25: Synthesis of [8]thiophene belt.

Heteroacenes systems incorporating thiophene have been extensively researched for their potential as organic semiconductors, demonstrating impressive performance characteristics. In contrast, furan-based π-conjugated structures have only recently gained significant attention in this field. The oxygen atom's smaller van der Waals radius compared to sulfur suggests that furan-containing compounds could potentially form more compact packing arrangements in solid form. This tighter molecular organization is a crucial factor for enhancing semiconducting properties in organic materials.

Dibenzo[b,d]furan represents the most basic and stable example of O-heteroacenes and is commonly used as a reference compound for developing synthetic methods targeting these systems. Although significant efforts have been made to simplify the formation of the furan ring, the main synthetic strategies remain limited and can be grouped into two categories. The final step typically involves either a transition metal-catalyzed C-C coupling [105–107] reaction using substituted diphenyl ethers or the formation of a [107–110]C-O bond from 2,2-disubstituted biphenyls, generally accomplished through a two-step process of deprotection followed by dehydration.

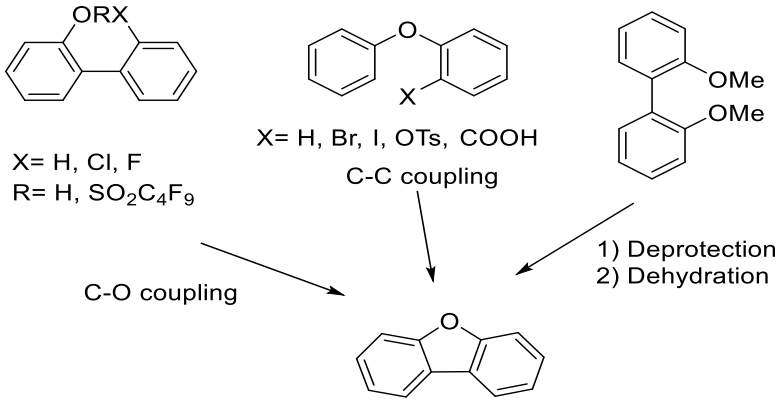

Scheme 1.26: Synthesis of O-heteroacenes.

A novel approach for synthesizing O-heteroacenes has been developed by *Kalyani et al*[107], utilizing palladium-catalyzed intramolecular C-H arylation with tosylates serving as electrophiles. This efficient transformation employs a carefully optimized reaction system, featuring a palladium acetate catalyst (5 mol%), dcype ligand (10 mol%), cesium carbonate

(1.5 equiv), and cesium pivalate (1.1 equiv) in toluene at 120°C. Under these conditions, the intramolecular cyclization proceeds smoothly, affording the desired product in a yield of 86%.

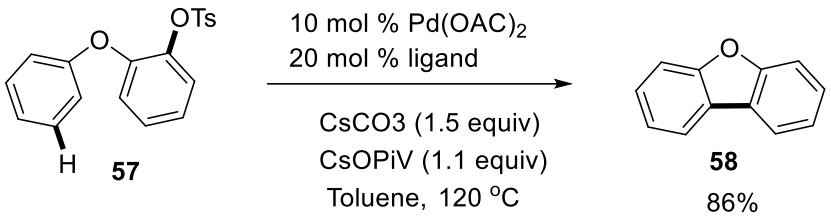

Scheme 1.27: Synthesis of 48 via palladium-catalyzed.

Bedekar et al[111]. conducted a series of experiments involving naphthofuran derivatives. They successfully synthesized 2-hydroxy-7-oxahelicene through the acid-catalyzed dehydration of 1,10-binaphthalenyl-2,20,7-triol.

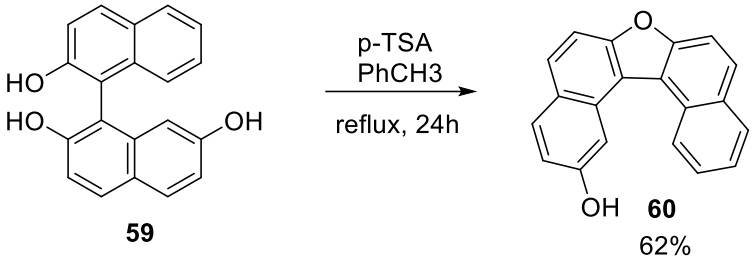

Scheme 1.28: Synthesis of 2-hydroxy-7-oxa[5]helicene (60).

Another example of an O-heteroacene is syn-DBBDF[112], which was effectively synthesized through a double cyclization process. This reaction was carried out under basic conditions at elevated temperatures, achieving a high yield of 92%.

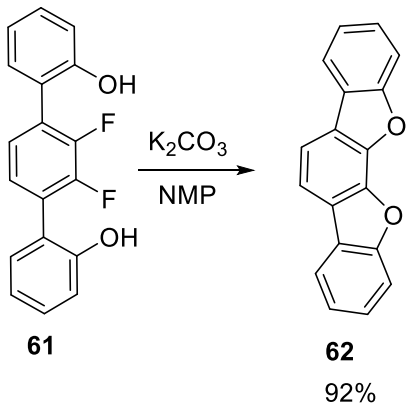

Scheme 1.29: Synthesis of syn-DBBDF (62).

The Amsharov research group has developed two novel approaches for synthesizing Dibenzo[b,d]furan using external oxygen sources. In one method, *Akhmetov et al*[113]. employed γ-Al_2O_3 at 190°C as an oxygen donor to facilitate the formation of benzoannulated-

furan derivatives. Alternatively, *Feofanov et al*[47]. utilized t-BuOK as an oxygen source in hexamethylphosphoramide (HMPA) solvent, applying microwave irradiation at 120°C for 3 hours to achieve the desired transformation. This methodology represents a significant advancement in heteroacene synthesis, offering a more accessible route to these important organic semiconductor materials.

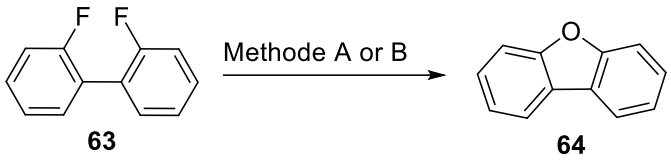

63 **64**

Method A: Al_2O_3, 190 ^oC, 12 h. **65%**
Method B: t-BuOk, HMPA, 120 ^oC, 3h, MW. **93%**

Scheme 1.30: Synthesis of dibenzofuran via two methods, using Al_2O_3 or t-BuOK as an external source of oxygen.

II. Aims

In recent years, cyclophenylene hydrocarbons have once again become a focal point of chemical research. The field originated in the 1940s[114] with the creation of ortho-linked macrocyclic hydrocarbons, known as cyclo-ortho-phenylenes (COP). This was followed by a renewed focus in the 1960s[60] when cyclo-meta-phenylenes (CMP) were introduced. The synthesis of cyclopara-phenylenes (CPP) in the 2000s[56–58] addressed a longstanding challenge and opened up exciting new possibilities, particularly in connection with nanocarbon materials. The aim of this study is dedicated to preparing two varieties of fluorinated cyclophenylene hydrocarbons. This was achieved using two distinct approaches: On-surface chemistry techniques were employed to synthesize CPP derivatives, while a nickel-mediated method was used to obtain CMP compounds. Thus, the study should include the following steps:

- The precursor undergoes bromination and is subsequently deposited onto an Au(111) surface, where its structure is analyzed using scanning tunneling microscopy and spectroscopy (STM/STS). This process facilitates the formation of cyclo-para-phenylenes (CPP).
- Fluorinated oligo-phenylenes are synthesized through the application of BuLi-mediated reactions and Suzuki–Miyaura cross-coupling.
- A novel strategy is employed for direct bromination.
- Cyclo-meta-phenylenes (CMP) are produced utilizing a nickel-catalyzed synthetic route.

III. Results and discussion

In the following sections, all results will be discussed, beginning with the synthesizing of 5,9-dibromodinaphtho[2,1-b:1',2'-d]furan, a precursor employed in on-surface synthesis (OSS) to construct planar cycloparaphenylenes (CPPs). Subsequent work focuses on fluorinated oligophenylene derivatives, prepared via n-BuLi-mediated reactions and Suzuki-Miyaura-coupling, followed by bromination under varied conditions to assess efficiency and regioselectivity. The third phase applies Yamamoto coupling to compound 7a, yielding macrocyclic [8]CMP and [12]CMP, which undergo ladderization of fluorinated oligophenylenes (LOOP reaction) using an external source of sulfur. LOOP conditions are then extended to fluorinated oligophenylenes (5, 6, 7), with using oxygen or sulfur source outcomes. Finally, brominated-fluorinated derivatives (4a, 5a, 6a, and 7a) are functionalized with fluorinated phenyl or naphthalene groups, serving as precursors for LOOP-derived structures.

III.1. Bromination of dinaphtho[2,1-b:1',2'-d]furan 1.

The bromination of **1** was performed with 2.2 equivalents of Br_2 in dry dichloromethane for 22h, yielding dibromodinaphthofuran (5,9-dibromodinaphtho[2,1-b:1',2'-d]furan in 82%. Notably, the process proceeded efficiently without the use of a catalyst; due to the presence of the oxygen atom in the furan ring, which significantly activates the aromatic system for electrophilic substitution without requiring additional catalysts.

Scheme 1. Bromination of dinaphtho[2,1-b:1',2'-d]furan **1**.

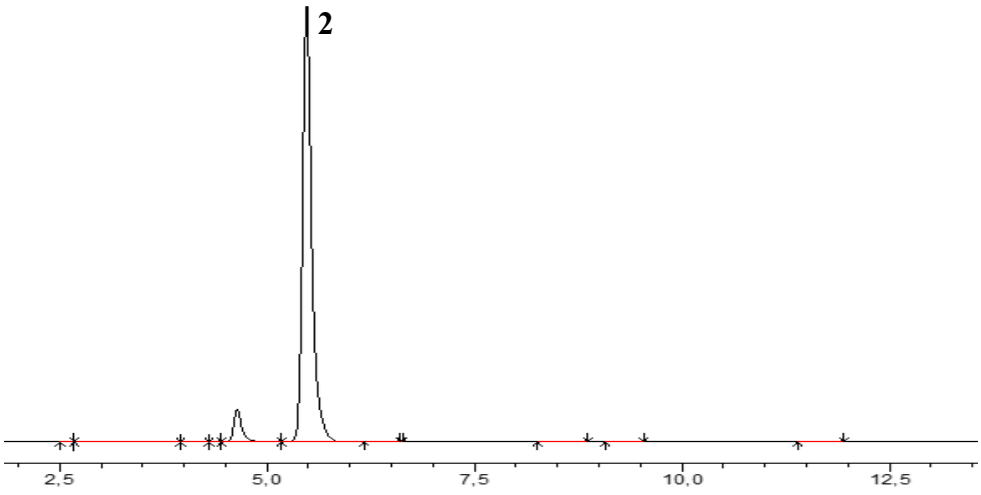

Figure 1. HPLC-profile after reaction of dinaphtho[2,1-b:1',2'-d]furan with bromine in dry dichloromethane. HPLC conditions: PBr column, eluent DCM:MeOH:70:30, 40 °C, 1 mL min-1, detection at 300 nm.

The proton NMR characterization of the dibromodinaphthofuran (5,9-dibromodinaphtho[2,1-b:1',2'-d]furan was done in $CDCl_3$-solvent, and the results are presented in Figure 2 below.

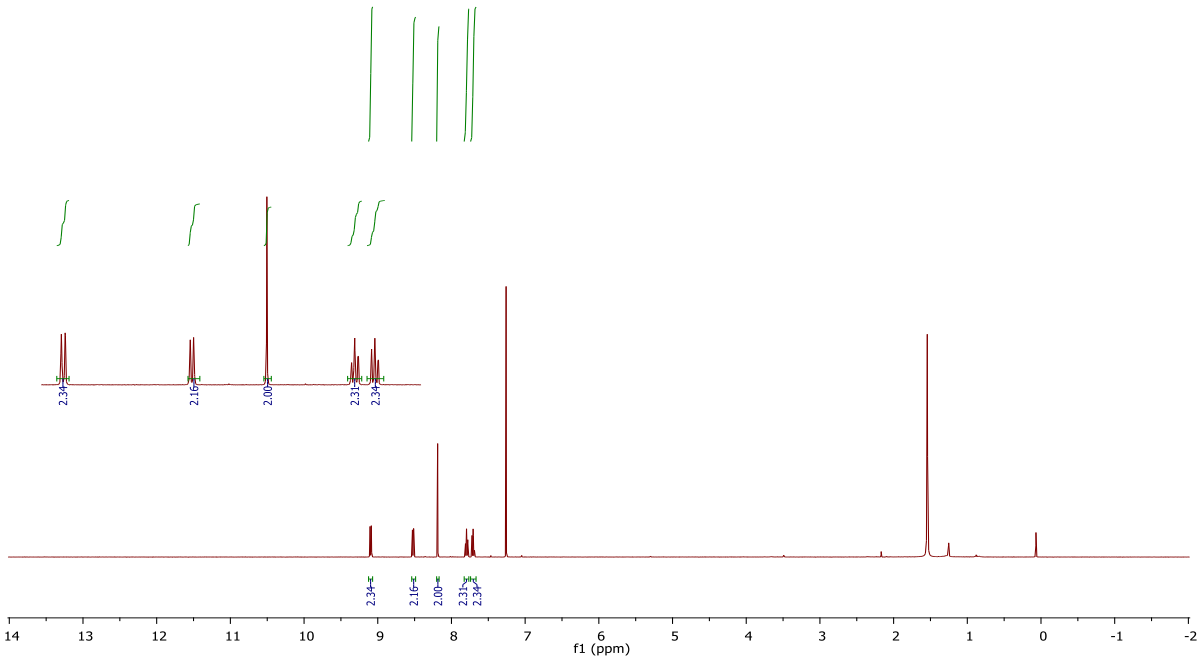

Figure 2. ^{1}H-NMR (400 MHz, $CDCl_3$, RT) of dibromodinaphthofuran (5,9 dibromodinaphtho[2,1-b:1',2'-d]furan **2**.

III.2. Dimerization of 5,9-dibromodinaphtho[2,1-b:1',2'-d]furan.

To achieve the dimerization of dibromodinaphthofuran (5,9-dibromodinaphtho[2,1-b:1',2'-d]furan), the procedure involved reacting compound **2** with 1.1 equivalent of n-butyllithium (n-BuLi) at –78 °C and stirring for 30 minutes, followed by the addition of one equivalent of copper(II) bromide ($CuBr_2$) and continued stirring at –78 °C for another 45 minutes before allowing the reaction to proceed at room temperature for 3 hours. Despite these conditions, the transformation did not go to completion; analysis revealed the presence of only the mono-brominated **3** in a yield of 65% and unreacted starting material **2**, with no evidence of the desired dibrominated compound.

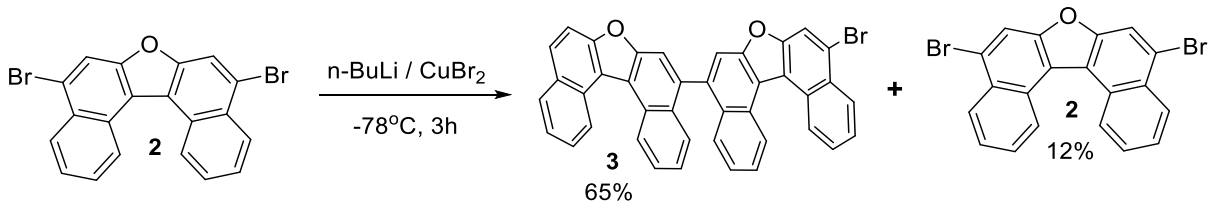

Scheme 2. Homocoupling of 5,9-dibromide naphtho[2,1-b:1',2'-d]furan **2**.

The on-surface synthesis (OSS) of planar cycloparaphenylenes (CPPs) employs a dinaphthofuran derivative substituted with bromine atoms at the 5,9-positions as a precursor. This precursor's fused furan ring induces curvature in the para-linked biphenyl segment, facilitating the formation of a cycloparaphenylene CPP framework through intermolecular coupling. The bromine substituents enable the debrominative coupling via cis or trans configurations, while attached benzo groups (cyan) allow subsequent cyclodehydrogenation to

enhance structural rigidity. DFT calculations (PBE-D3(BJ)) reveals that the angle between C–Br bonds in the nonplanar precursor is 141.4°, favoring 9- or 10-unit macrocycles. Forcing the molecule into a planar conformation reduces this angle to 135.2°, shifting preference toward 8-unit macrocycle.

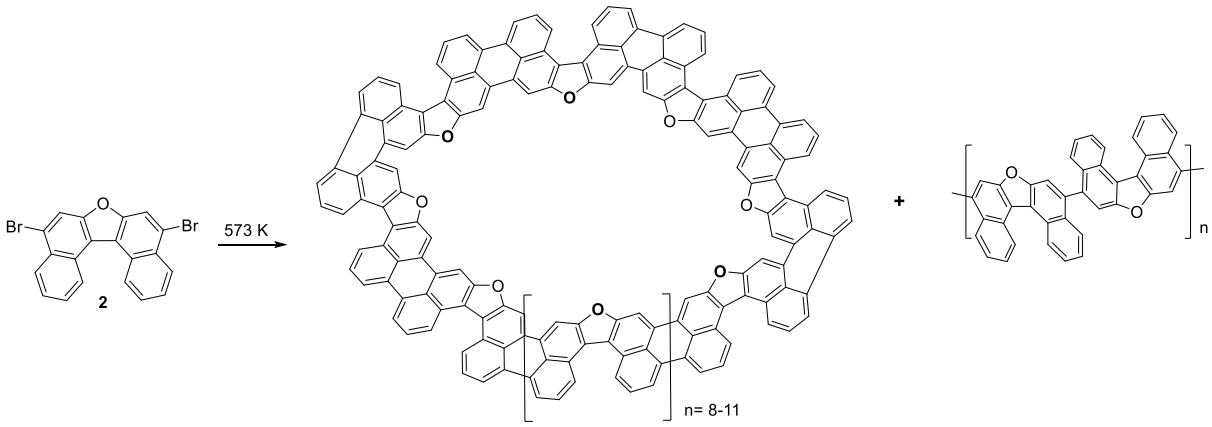

Scheme 3. The formation of the macrocyclics.

Experimentally, depositing the precursor onto Au(111) at 300 K leads to noncovalent self-assembled ribbons in face-centered cubic (fcc) regions, stabilized by Br···Br and O···H interactions. Annealing at 573 K triggers debromination, evidenced by a Br 3p3/2 binding energy shift from 183.6 eV to 181.4 eV, and induces covalent coupling. This results in circular macrocycles (40% yield) and incomplete macrocycles (arc structures) from all-cis linkages, along with chains and macrocycles of other topologies structures from cis-trans combinations. The enhanced ring yield compared to prior studies stems from staggered naphthalene groups in the precursor[44], which mitigate steric hindrance during cis-coupling of monomers, STM imaging confirms macrocycles comprising 8–11 monomers (π-extended [2n]CPPs (n = 8–11)), with cyclodehydrogenated perylene motifs visible as white arrows in Figure 2c–f. These findings underscore the interplay between precursor geometry, surface interactions, and reaction pathways in achieving size-controlled planar CPPs.

III.3. Synthesis of Fluorinated oligophenylenes.

Initially, we synthesized our precursors by two methods, namely, the ortho lithiation and the Suzuki–Miyaura coupling. We began with an ortho lithiation of 2,6-Difluorotoluene **4** followed by an addition of 2eq of Copper (II) bromide at -78 °C, leading to the homocouplings of 2,6-Difluorotoluene (Dimer 2,2',4,4'-tetrafluoro-3,3'-dimethyl-1,1'-biphenyl, Trimer 2,2",4,4',4",6'-hexafluoro-3,3",5'-trimethyl-1,1':3',1"-terphenyl, and Tetramer 2,2"',4,4',4",4"',6',6"-octafluoro-3,3"',5',5"-tetramethyl-1,1':3',1":3",1"'-quaterphenyl) in a yield of 32%, 18%, and 7% respectively (Scheme 4). The structural NMR (^{1}H ^{19}F and ^{13}C) and MS characterization methods confirmed the structural assignments. The Suzuki-Miyaura coupling of 3,4-difluorophenylboronic acid was readily cross-coupled under palladium catalysis with various Brominated-aryl to give isolated 3,3',4,4'-tetrafluoro-1,1'-biphenyl (8) and 3,3",4,4',4",5'-hexafluoro-1,1':2',1"-terphenyl (9) in yields of 78% and 72% (Scheme 5).

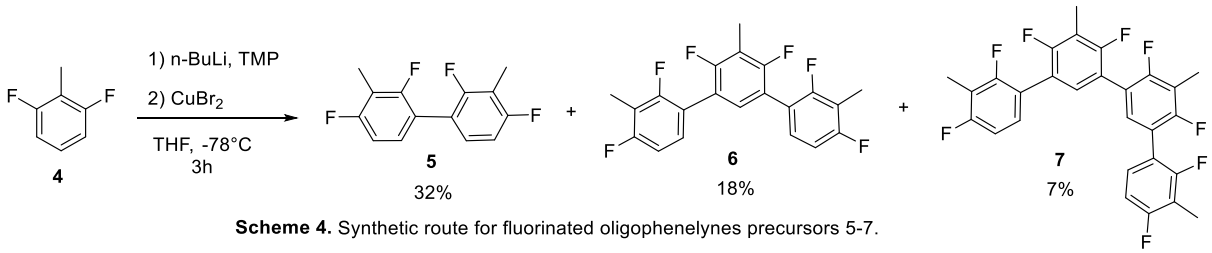

Scheme 4. Synthetic route for fluorinated oligophenelynes precursors 5-7.

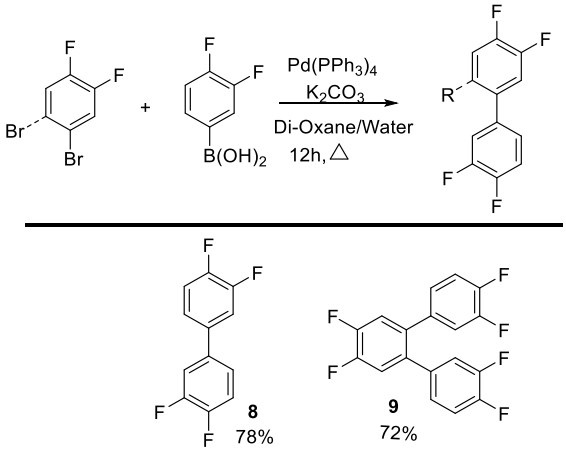

Scheme 5. Synthesis of precursor structures 8-9 via a Suzuki-Miyaura cross-coupling reaction.

With the necessary precursors in hand, we turned our attention to the formation of specific Di-para-iodation or Di, para-borylation.

III.3.1. Iodonation or borylation of 2,2',4,4'-tetrafluoro-3,3'-dimethyl-1,1'-biphenyl.

To attempt the insertion of iodane or boronic acid at the ortho position relative to fluorine, butyl lithium chemistry was employed using various iodine sources, including diiodine and 1,2-diiodoethane, as well as different boronic acid sources such as trimethyl borate and isopropoxy pinacolborane. However, in all cases, the reaction did not take place.

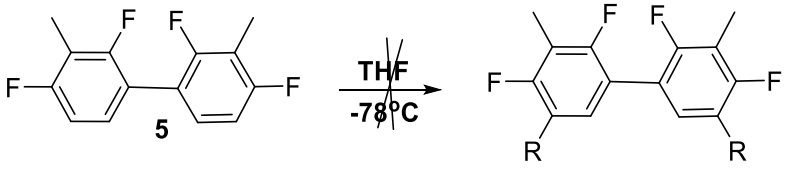

TMP	n-BuLi 2,5M	R	time	Results
2.2 eq	2 eq	Di-iodine	2h	No reaction
2.2 eq	2 eq	1,2-diiodoethane	2 h	No reaction
2.2 eq	2 eq	Trimethyl-Borate	2h	No reaction
2.2 eq	2 eq	isopropoxy pinacolborane	2h	No reaction
7,4 eq	7 eq	isopropoxy pinacolborane	weekend	No reaction

Table 1. Iodonation or borylation of 5.

III.4. Bromination of Fluorinated oligophenylenes.

III.4.1. Bromination of 2,6-difluorotoluene

The reaction of 2,6-difluorotoluene was conducted using two approaches (Scheme 6). The first method employed 3 equivalents of bromine and 10 equivalents of iron at room temperature, yielding 3,5-dibromo-2,6-difluorotoluene (4a) with a high efficiency of 90%. In contrast, the second method utilized conventional conditions with 2 equivalents of iron and 10 equivalents of bromine, producing 3,4,5-tribromo-2,6-difluorotoluene (4b) in an 87% yield. The employed method for synthesizing (4a) showed a remarkable selectivity for bromination at the para position relative to fluorine, even when increasing bromine to 5 or 7 equivalents, leaving the para position to the methyl group unreacted.

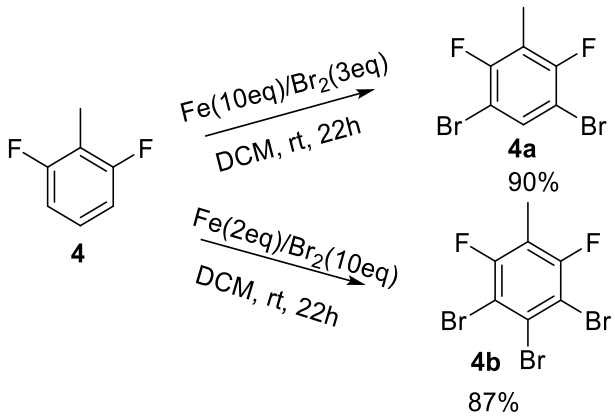

Scheme 6. Bromination of 2,6-difluorotoluene **4**.

III.4.2. Bromination of 2,2',4,4'-tetrafluoro-3,3'-dimethyl-1,1'-biphenyl.

The bromination of dimer (5) was carried out using 3 equivalents of bromine and 10 equivalents of iron at room temperature, resulting in a mixture of the di-brominated compound (5a) and the unreacted starting material (5), as reported in Table 2. To enhance the yield, the amount of iron was increased to 20 equivalents, which improved the reaction outcome but the starting material (5) was observed. The reaction would require more excess of Iron in order to be completed. While using 30eq of Iron, the results showed a total para-specific reaction with a good yield of 90%. However, the usage of 2 equivalents of Iron in the presence of 10 equivalents of Bromine has led to a complex mixture which was difficult to be identified and separated by column chromatography and high-performance liquid chromatography (HPLC).

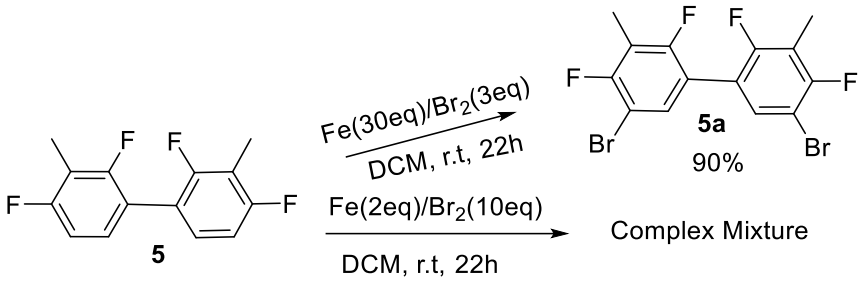

Scheme 7. bromination of 2,2',4,4'-tetrafluoro-3,3'-dimethyl-1,1'-biphenyl **5**.

Fe(eq)	Br_2(eq)	Results
10	3	Mixture (5: 35%, 5a: 65%)
20	3	Mixture (5: 20%, 5a 80%)
30	3	5a: 90%

Table 2. Mixtures of Di-bromination and starting compound were observed.

III.4.2.1. Optimization of the reaction conditions using a series of Copper/Iron Bromides (MXn).

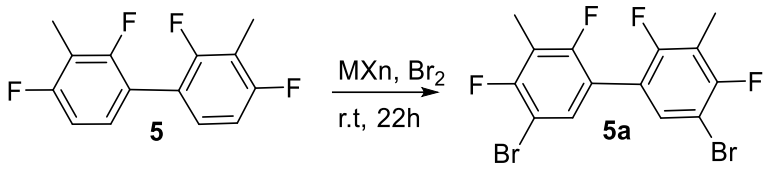

entry	MX_n (eq)	Br_2(eq)	Yield
1	CuBr(4eq)	-	No reaction
2	CuBr(30eq)	-	No reaction
3	CuBr(30eq)	3(eq)	No reaction
4	CuBr(2eq)	10(eq)	No reaction
5	$CuBr_2$(4eq)	-	No reaction

6	$CuBr_2$(30eq)	-	No reaction
7	$CuBr_2$(30eq)	3(eq)	No reaction
8	$CuBr_2$(2eq)	10(eq)	No reaction
9	$FeBr_2$(2eq)	-	No reaction
10	$FeBr_2$(30eq)	-	No reaction
11	$FeBr_2$(30eq)	3(eq)	Mixture[1]
12	$FeBr_2$(2eq)	10(eq)	Mixture[1]
13	$FeBr_3$(2eq)	-	No reaction
14	$FeBr_3$(4eq)	-	Mixture[2](5: 90%, 5a: 10%)
15	$FeBr_3$(10eq)	-	Mixture[2](5: 73%, 5a: 27%)
16	$FeBr_3$(30eq)	3(eq)	Mixture[1]
17	$FeBr_3$(2eq)	20(eq)	Mixture[1]

Table 3. Screening of conditions for selective synthesis of (5a).[1]Complex Mixtures were observed. [2]Mixtures of Di-bromination and starting compound were observed via NMR.

This behavior suggests that the reaction likely occurs on the surface of metallic iron. To support this hypothesis, we investigated direct bromination using alternative brominating agents. Biphenylene 5 was selected as a model compound, with the aim of preferentially obtaining the dibrominated product 5a. However, no bromination was observed when using cupric bromide or cuprous bromide as the brominating agents (entries 1–8). Similarly, attempts using $FeBr_2$ or $FeBr_3$ (2eq) in various stoichiometries (entries 9, 10, 13) did not yield any detectable brominated products. Under more forcing conditions—combinations of Br_2 with $FeBr_2$ a complex mixtures of were observed (entries 11, and 12), Upon increasing the amount of $FeBr_3$, only mixtures of the desired dibrominated product (5a) and unreacted starting material (5) were obtained (entries 14, and 15). use of Bromine with $FeBr_3$ had a disappointing outcome where a complex mixture was detected (entries 16 and 17). Thus, none of the examined conditions matched the selectivity and efficiency achieved with bromination in the presence of excess metallic iron.

III.4.3. Bromination of Trimer and Tetramer.

The same strategy was employed to 6. Where 20 equivalents of Iron was adequate to obtain 6a with a 90% yield. And 10 equivalents of Iron with 3 equivalents of bromine (Br_2) was sufficient for obtaining 7a with a 98% yield. The characterization studies were carried out via NMR (^1H, ^{19}F and ^{13}C), MS. In contrast, employing conventional conditions with 2 equivalents of iron and 10 equivalents of bromine for compounds (6) and (7) resulted in complex mixtures that were difficult to analyze.

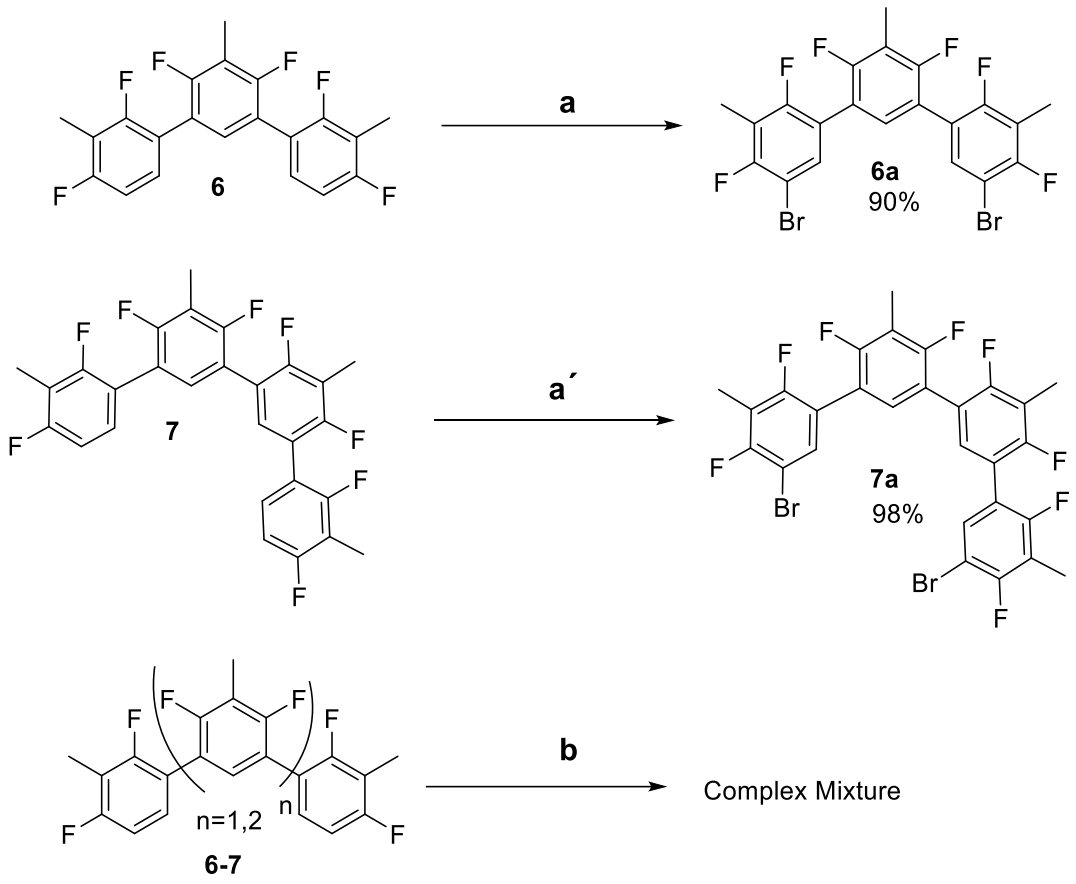

Scheme 8. Bromination of fluorinated oligophenelynes precursors 6-7. Conditions (**a**) Fe(20 eq)/Br_2(3 eq), rt, 22h. (**a´**) Fe(10 eq)/Br_2(3 eq), rt, 22h. (**b**) Fe(2 eq)/Br_2(10 eq), rt, 22h.

III.4.4. Bromination of 3,3',4,4'-tetrafluoro-1,1'-biphenyl.

Additionally, we examined the effect of Bromine/Iron on 3, 3,3',4,4'-tetrafluoro-1,1'-biphenyl (8). The results showed a di-brominated compound which is the 2,2'-dibromo-4,4',5,5'-tetrafluoro-1,1'-biphenyl (8a), with a yield of 76%. On the other hand, using conventional conditions with 2 equivalents of iron and 10 equivalents of bromine resulted in complex mixtures that were difficult to analyze.

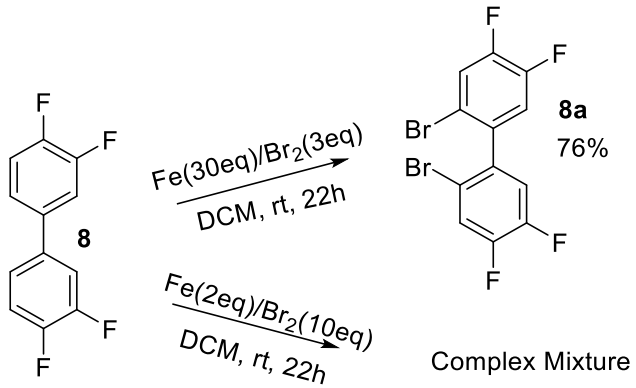

Scheme 9. Bromination of precursors **8**.

III.4.5. Bromination of 3,3'',4,4',4'',5'-hexafluoro-1,1':2',1''-terphenyl.

The bromination of 3,3'',4,4',4'',5'-hexafluoro-1,1':2',1''-terphenyl (9) under both methods produced 2,2''-dibromo-4,4',4'',5,5',5''-hexafluoro-1,1':2',1''-terphenyl (9b) as a major product, with our approach delivering a superior yield of 83%, compared to the 70% yield achieved using the conventional method.

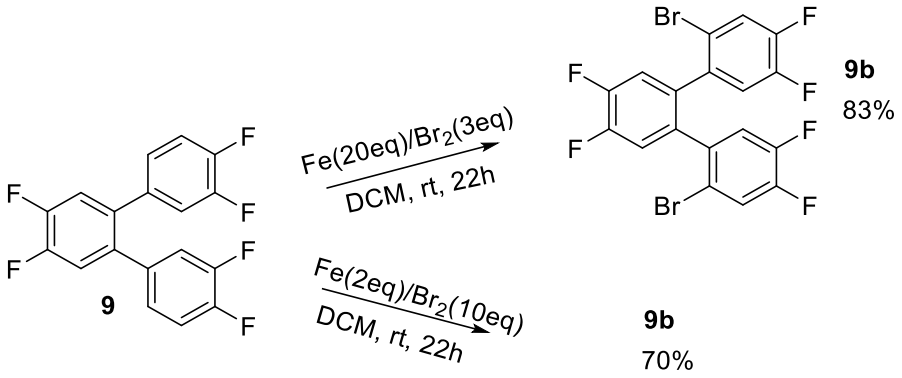

Scheme 10. Bromination of precursors **9**.

III.4.6. Screening the bromination of fluorinated-biphenyl.

For comparison purposes, further reactions were conducted with different types of Fuoro-oligophenelynes, where Fluorine atoms are located in the bay-region. Using the optimised conditions obtained above for the synthesis of 5a from 5 (Table.2) and the conventional conditions.

- **Bromination of 2,2'-difluoro-1,1'-biphenyl.**

Fluorinated biphenyl 10[115] was brominated by employing 30 equivalents of Iron and 3 equivalents of Bromine, affording 5,5'-dibromo-2,2'-difluoro-1,1'-biphenyl (10a) in a yield of 97%. However, conventional bromination gave 4,4',5,5'-tetrabromo-2,2'-difluoro-1,1'-biphenyl (Tetra-bromination, 10b) with a yield of 68%.

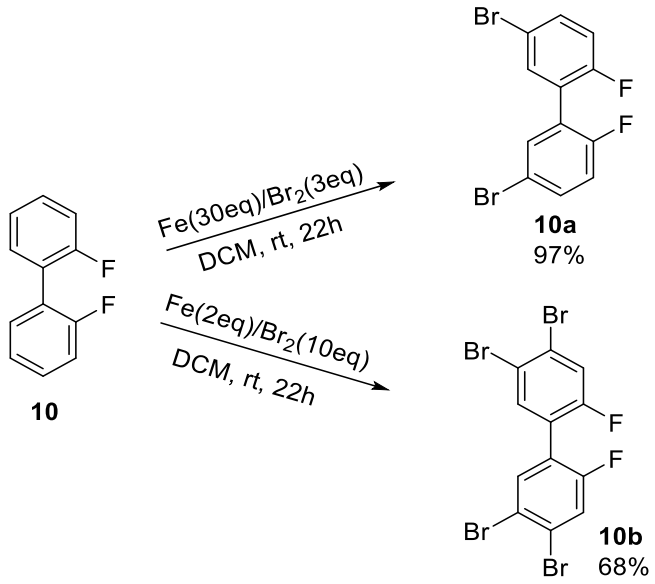

Scheme 11. Bromination of precursors **10**.

- **Bromination of 2,2',6,6'-tetrafluoro-1,1'-biphenyl.**

The bromination of 2,2',6,6'-tetrafluoro-1,1'-biphenyl (11)[116] using our method gives 3,3'-dibromo-2,2',6,6'-tetrafluoro-1,1'-biphenyl (11a) with a yield of 81%. In contrast, utilizing 2 equivalents of Iron and 10 equivalents of Bromine produces a mixture of 3,3'-dibromo-2,2',6,6'-tetrafluoro-1,1'-biphenyl (11a) and 3,3',5-tribromo-2,2',6,6'-tetrafluoro-1,1'-biphenyl (11b) in yields of 7% and 15%, respectively.

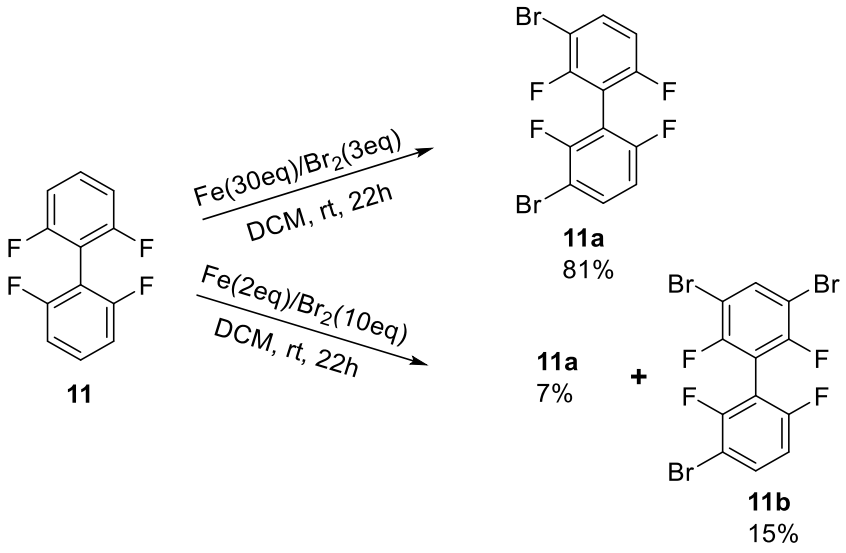

Scheme 12. Bromination of precursors **11**.

- **Bromination of 2,2',4,4'-tetrafluoro-1,1'-biphenyl.**

The bromination of 2,2',4,4'-tetrafluoro-1,1'-biphenyl 12[47] proceeded in both conditions to give 5,5'-dibromo-2,2',4,4'-tetrafluoro-1,1'-biphenyl 12a in a comparable yield (70% and 67%).

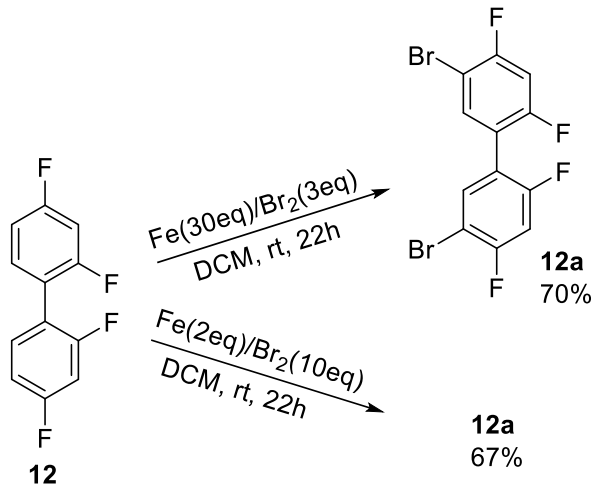

Scheme 13. Bromination of precursors **12.**

➢ **Bromination of 2,2'-difluoro-5,5'-dimethyl-1,1'-biphenyl.**

To investigate the impact of blocking the para position relative to fluorine, 2,2'-difluoro-5,5'-dimethyl-1,1'-biphenyl (13)[47] was selected for bromination. When treated with 30 equivalents of iron and 3 equivalents of bromine, we obtained 3,3'-dibromo-2,2'-difluoro-5,5'-dimethyl-1,1'-biphenyl (13a) with a 73% yield, where the bromination took place at the ortho position relative to fluorine. However, using 2 equivalents of iron and 10 equivalents of bromide, 2,2',4,4',5,5'-hexabromo-6,6'-difluoro-3,3'-dimethyl-1,1'-biphenyl (13b) was obtained with a yield of 85%, where bromination occurred at all positions.

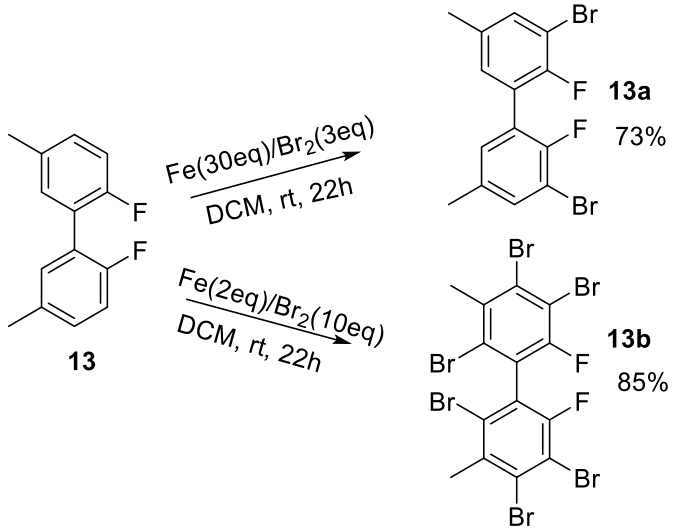

Scheme 14. Bromination of precursors **13**.

➢ **Bromination of 14 and 15.**

Both 4,4'-difluoro-1,1'-biphenyl (14)[117] and 2,2',3,3'-tetrafluoro-1,1'-biphenyl (15)[118] gave a complex mixture under both bromination conditions. The resulting mixtures were challenging to identify and separate using column chromatography and high-performance liquid chromatography (HPLC).

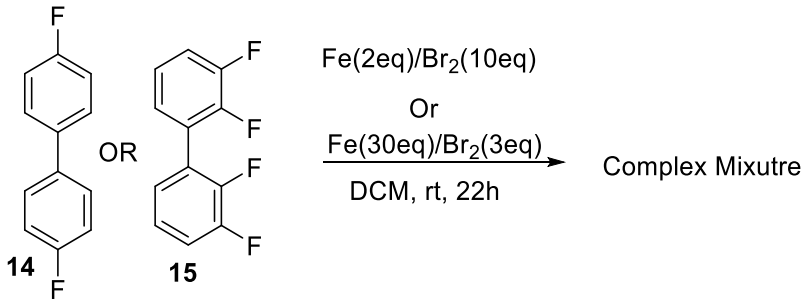

Scheme 15. Bromination of precursors **14** and **15**.

➢ **Bromination of 2,2',5,5'-tetrafluoro-1,1'-biphenyl.**

Under both conditions, the bromination of 2,2',5,5'-tetrafluoro-1,1'-biphenyl (16)[47] resulted in the formation of 4,4'-dibromo-2,2',5,5'-tetrafluoro-1,1'-biphenyl (16a), our method gives a higher yield (93%) compared to the conventional approach (82%).

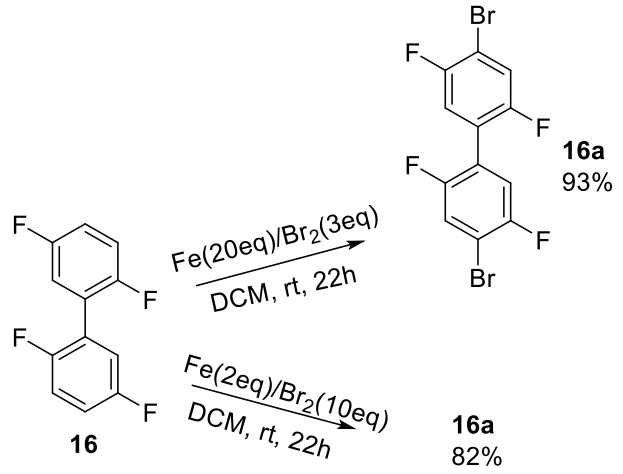

Scheme 16. Bromination of precursors **16**.

➢ **Bromination of 3,3'-difluoro-1,1'-biphenyl.**

For 3,3'-difluoro-1,1'-biphenyl (17)[119], our method yielded compound 17a with a yield of 89%. Interestingly, the first bromination occurred at the para position relative to the fluorine atom, while the second bromination took place at the ortho position. We hypothesize that the initial bromination occurred in the bay region, which subsequently prevented the second bromination from occurring at the same site. In contrast, conventional conditions resulted in complex mixtures that were difficult to analyze.

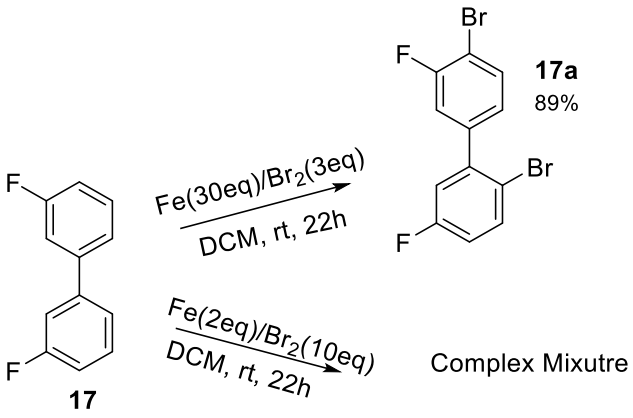

Scheme 17. Bromination of precursors **17**.

III.5. Synthesis of Cyclometaphenylenes [8]CMP.

- **Retrosynthetic analysis.**

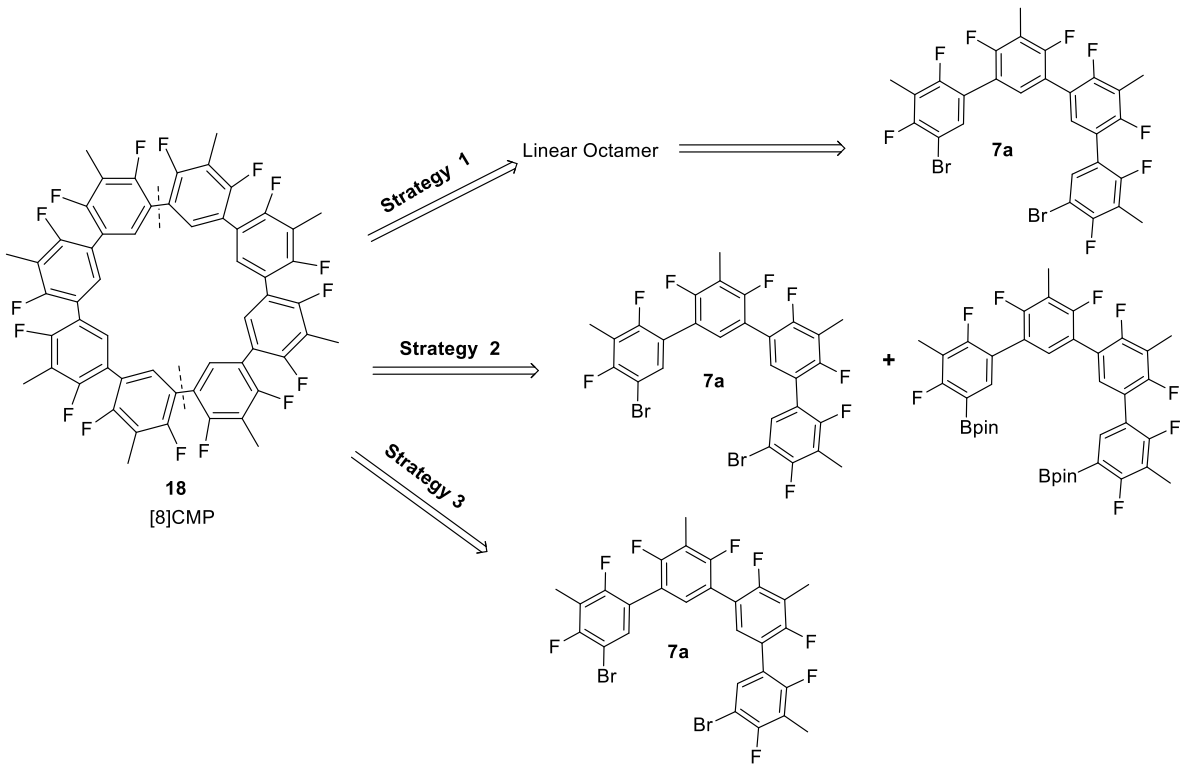

Scheme 18. The synthesis strategy to obtain **[8]CMP.**

To synthesize Cyclometaphenylenes [8]CMP, three strategies were explored:

Strategy 1: began with dimerization of precursor 7a to form a linear di-brominated octamer, followed by conversion of bromine to boronic esters and performing an intramolecular homocoupling to obtain [8]CMP.

Strategy 2: employed bromine-lithium exchange or Miyaura borylation to transform the di-brominated intermediate into boronic esters, then utilized Suzuki-Miyaura cross-coupling to achieve macrocyclization.

Strategy 3: utilised Yamamoto coupling directly on 7a to generate [8]CMP.

i. Examination of the Strategy 1.

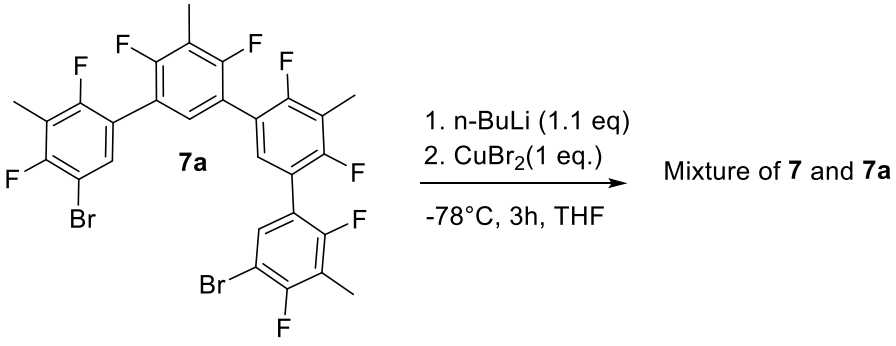

Scheme 19. Homocoupling of **7a** using BuLi chemistry.

To synthesize the di-bromination-octamer, a bromine-lithium exchange was attempted on **7a** using n-BuLi(1,2 eq) in THF at -78C, followed by the addition of $CuBr_2$(1 eq). However, the reaction did not proceed as expected, yielding **7** and **7a** instead, Consequently, the first strategy was unsuccessful due to the failure to synthesize the desired octamer.

ii. Examination of the Strategy 2.

In an attempt to convert the bromine of compound **7a** into boronic acid, the reaction was carried out using various types of BuLi in THF at –78 °C, followed by treatment with an excess amount of $B(OMe)_3$ or B_2pin_2 for 3 hours (Entry 1-4). However, the desired transformation did not occur, and only starting materials **7** and **7a** were recovered.

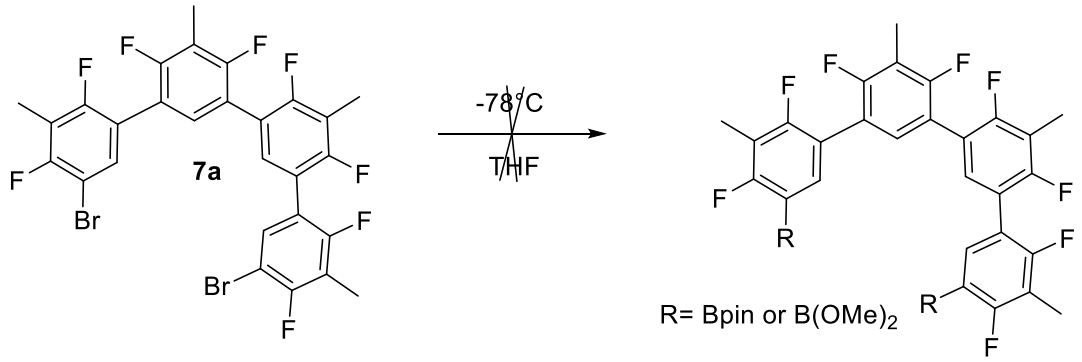

Scheme 20. Borylation of **7a**.

	n-BuLi 2,5M	Boron source	Time	Result
Entry 1	n-BuLi (2 eq)	$B(OMe)_3$	3h	No reaction
Entry 2	Sec-BuLi (2eq)	$B(OMe)_3$	3h	No reaction
Entry 3	t-BuLi (2 eq)	$B(OMe)_3$	3h	No reaction
Entry 4	Sec-BuLi (2eq)	B_2pin_2	3h	No reaction

Table 4. Borylation of **7a** using BuLi chemistry.

In parallel, Miyaura borylation conditions were tested to convert bromine in compound **7a** into its corresponding boronic ester. Standard reaction conditions were employed with variations in reaction time, temperature, and the use of either microwave or solution-based setups (entries 5–16). Further attempts involved modifying the catalyst, replacing $PdCl_2$(dppf) with $Pd(OAc)_2$ for solution-phase reactions lasting 8–12 hours (entry 17). In entry 18, $Pd(dba)_2$ was used as the catalyst under solvent-free conditions in a microwave. Despite these extensive optimizations, none of the reactions succeeded, and the desired transformation was not achieved.

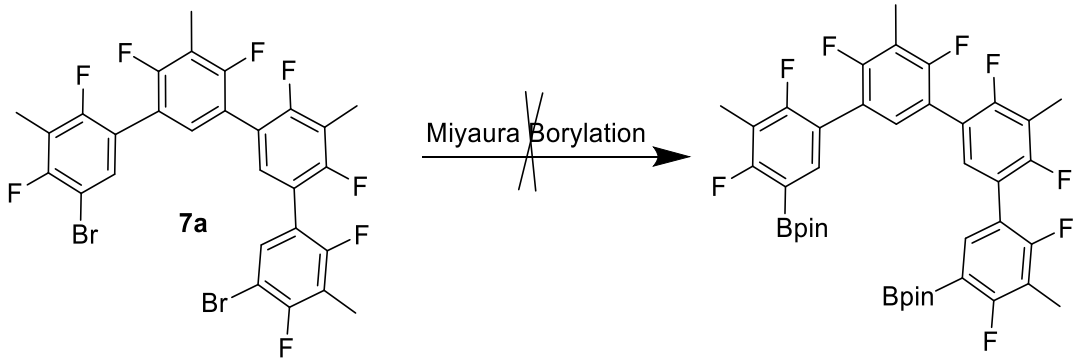

Entry	reactants	Cat	Base	Solvant	Temp °C	Time(h)	Method
5	B_2pin_2	$PdCl_2(dppf)$	KOAc	Dioxane	80	1	M.W
6	B_2pin_2	$PdCl_2(dppf)$	KOAc	Dioxane	80	3	M.W
7	B_2pin_2	$PdCl_2(dppf)$	KOAc	Dioxane	80	6	M.W
8	B_2pin_2	$PdCl_2(dppf)$	KOAc	Dioxane	80	12	M.W
9	B_2pin_2	$PdCl_2(dppf)$	KOAc	Dioxane	110	0.5	M.W
10	B_2pin_2	$PdCl_2(dppf)$	KOAc	Dioxane	110	10	M.W
11	B_2pin_2	$PdCl_2(dppf)$	KOAc	Dioxane	80	8	Solution
12	B_2pin_2	$PdCl_2(dppf)$	KOAc	Dioxane	80	overnight	Solution
13	B_2pin_2	$PdCl_2(dppf)$	KOAc	Dioxane	80	24	Solution
14	B_2pin_2	$PdCl_2(dppf)$	KOAc	Dioxane	110	8	Solution
15	B_2pin_2	$PdCl_2(dppf)$	KOAc	Dioxane	110	overnight	Solution
16	B_2pin_2	$PdCl_2(dppf)$	KOAc	Dioxane	110	24	Solution
17	B_2pin_2	$Pd(OAc)_2$	KOAc	Dioxane	80	8/12	Solution
18	B_2pin_2	$Pd(dba)_2$	KOAc	Free	110	12/24	M.W

Table 5. Borylation of **7a** using Miyaura borylation

Therefore, the second strategy was deemed unsuccessful due to the inability to convert the bromine groups into boronic esters.

iii. Examination oft he Strategy 3.

Under Yamamoto coupling conditions, compound **7a** was reacted with 4 equivalents of $Ni(COD)_2$, 4 equivalents of 2,2′-bipyridine, and 8 equivalents of 1,5-cyclooctadiene (COD) in THF for 1 hour. The reaction, which demands strict exclusion of air and moisture, was performed in a glovebox to maintain anhydrous conditions. Despite these precautions, F_{16}[8]CMP was obtained with a yield of 1%, along with trace amounts of F_{24}[12]CMP.

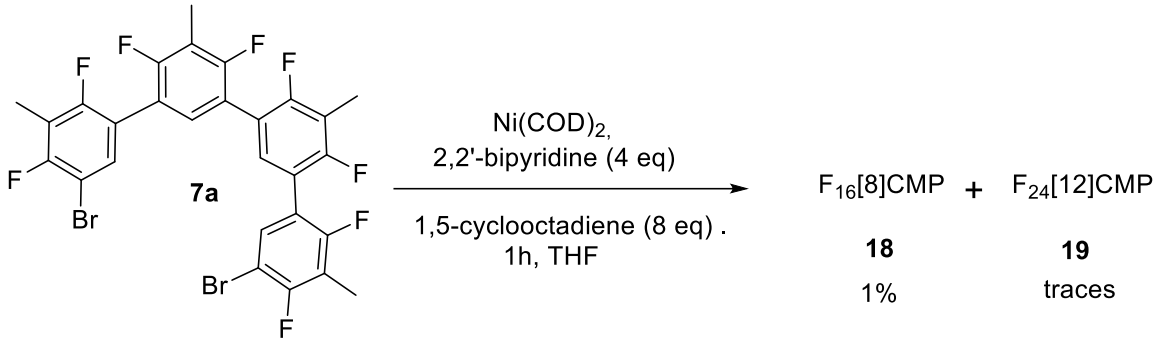

Scheme 21. Yamamoto coupling of **7a**.

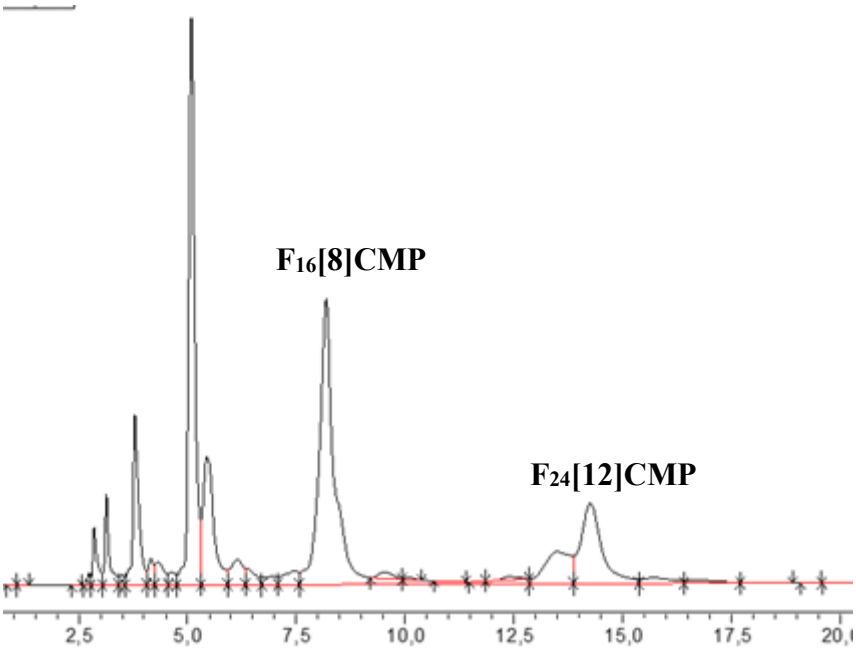

Figure 3. HPLC-profile after reaction Yamamoto coupling of compound **7a**. HPLC conditions: PBr column, eluent DCM:MeOH:30:70, 40 °C, 1 mL min-1, detection at 350 nm.

The NMR characterization of Cyclomethaphenylenes F_{16}[8]CMP was conducted using $CDCl_3$ as the solvent, with the resulting spectrum depicted in Figure 4. The ^1H NMR spectrum of F_{16}[8]CMP is straightforward to interpret, displaying two distinct signals: a peak at 7.09 ppm, which is attributed to the aromatic C–H protons of the benzene rings, and a peak at 2.33 ppm, corresponding to the methyl group protons. This clear separation of signals facilitates the structural elucidation of the macrocyclic F_{16}[8]CMP.

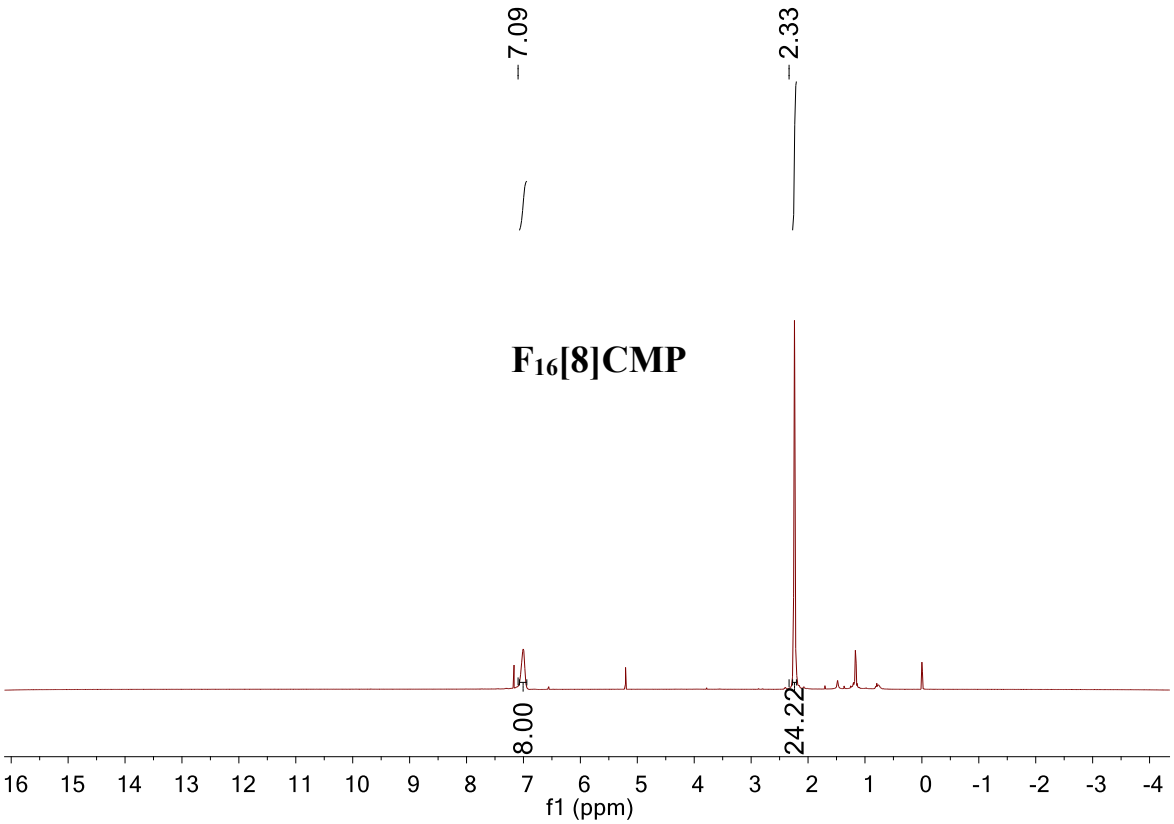

Figure 4. ^{1}H-NMR (400 MHz, $CDCl_3$, RT) of F_{16}[8]CMP **18**.

III.5.1. Ladderization of fluorinated oligophenylenes (LOOP reaction) of F_{16}[8]CMP.

F_{16}[8-S]CMP was synthesized from the precursor F_{16}[8]CMP. utilizing sulfur-embedding nucleophilic aromatic substitution (SNAr) reactions under conditions optimized by Feofanov. Specifically, a reaction mixture of F_{16}[8]CMP (1.0 equivalent), sodium sulfide (Na_2S, 80 equivalents), and tetrabutylammonium bromide (TBAB, 16 equivalents) was dissolved in 1 ml of hexamethylphosphoric triamide (HMPA) and subjected to microwave irradiation at 180 °C for 3 hours, resulting F_{16}[8-S]CMP.

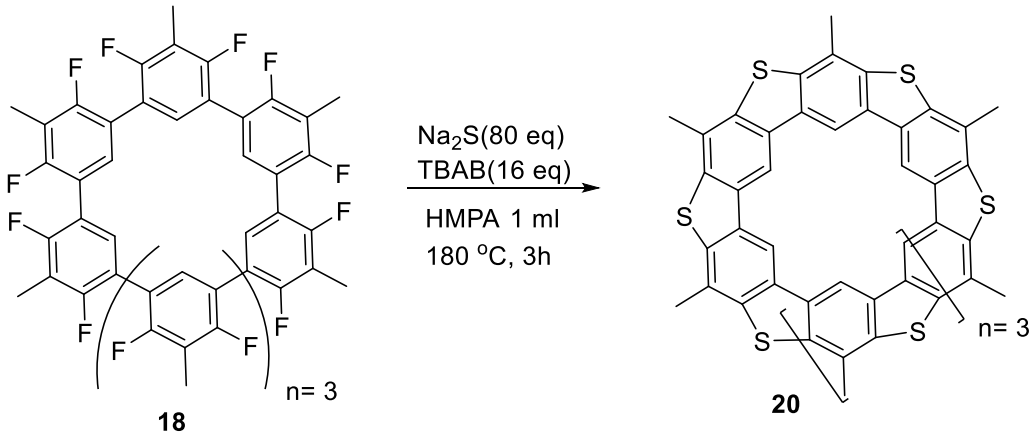

Scheme 22. LOOP reaction of **F_{16}[8]CMP**.

The desired product was successfully detected using mass spectrometry with liquid injection field desorption ionization (MS, LIFDI), showing a measured $[M]^+$ ion at m/z 960.0260, which closely matches the calculated value of m/z 960.0297 for the molecular formula $C_{56}H_{32}S_8$, thereby confirming the identity of the product.

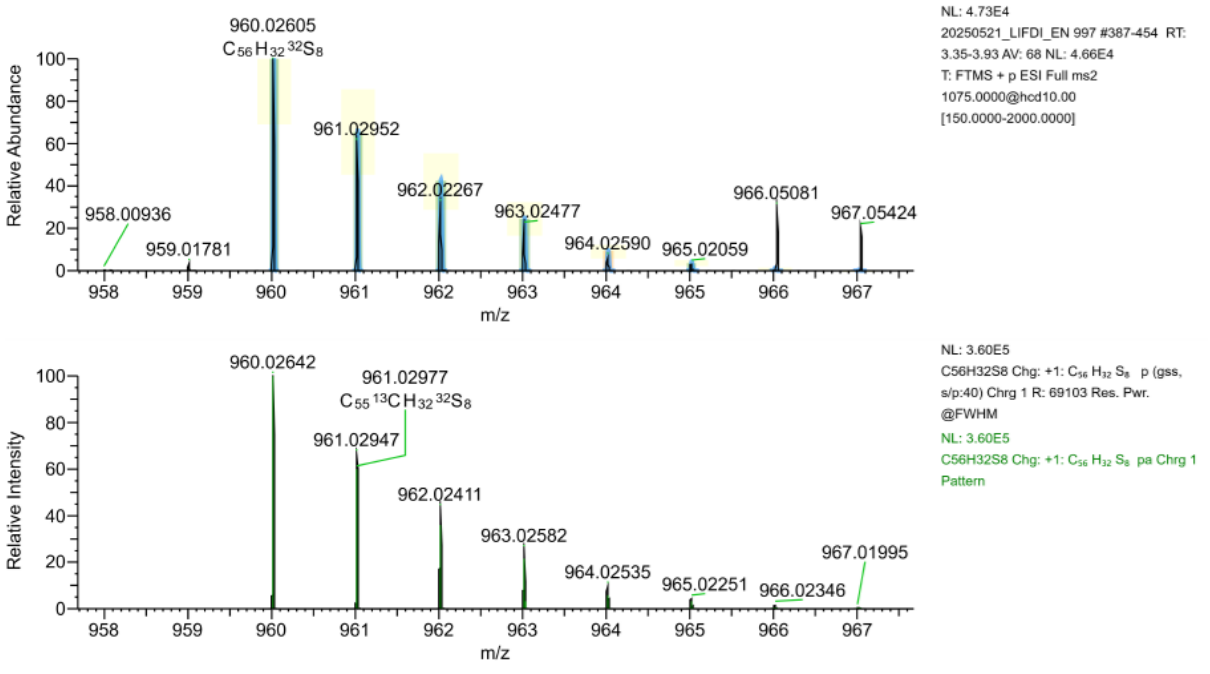

Peak Mass	Display F...	S Fit	RDB	Delta [pp...	Theo. ma...	Rank	Combine...	# Match...	# Missed...	MS Cov....	Pattern C...	MSMS M.
960.02605	$C_{56}H_{32}{}^{32}S_8$	25.90686 7517877 2	41.00	-0.38	960.02642	1	73.71	9	0	76.36	95.36	(Collection)

Figure 5. HRMS (LIFDI) of **20**.

III.6. LOOP of Dimer 5.

The LOOP reaction of the dimer (5), conducted with 12 equivalents of potassium tert-butoxide (t-BuOK) as an external oxygen source in 2 mL of hexamethylphosphoramide (HMPA) under microwave irradiation at 120 °C for 3 hours, produced a complex mixture of products that proved challenging to separate. Increasing the amount of t-BuOK did not improve the outcome. However, elevating the reaction temperature to 150 °C and extending the reaction time to 6 hours while maintaining 12 equivalents of t-BuOK led to the exclusive formation of a single product in 70% yield, as evidenced by NMR spectra indicating that only one terminal fluorine atom had reacted. Further attempts to drive the reaction of the second terminal fluorine by increasing t-BuOK to 20 equivalents at 150 °C for 6 hours, or by raising the temperature to 180 °C for the same duration or 22h, resulted in no additional reactivity, with the second terminal fluorine remaining Unconverted.

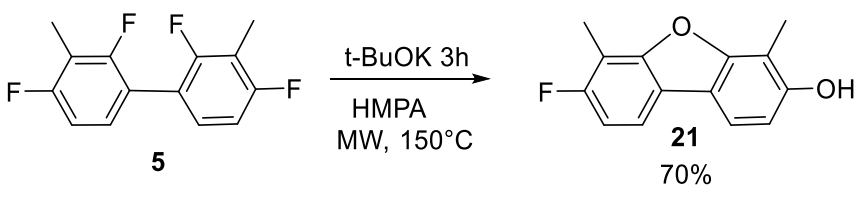

Scheme 23. LOOP reaction of precursor **5**.

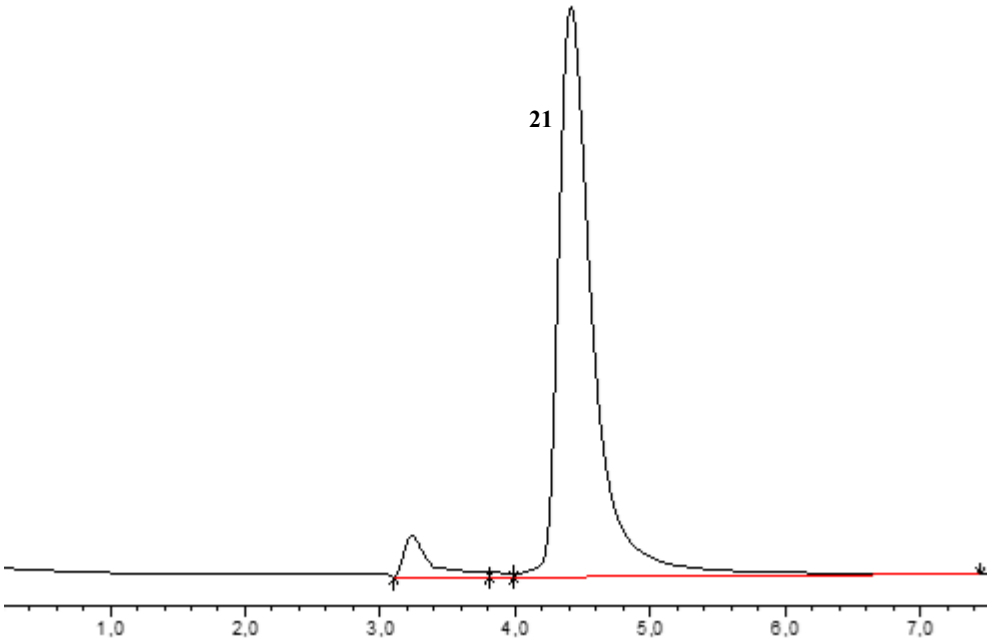

Figure 6. HPLC-profile after reaction of **5** with t-BuOK in HMPA. HPLC conditions: PBr column, eluent DCM:MeOH:70:30, 40 °C, 1 mL min-1, detection at 300 nm.

In contrast, when the same reaction conditions were applied to the trimer (6) and tetramer (7)—utilizing 3 equivalents of t-BuOK for each florine in 2 ml of hexamethylphosphoramide (HMPA) under microwave irradiation at 150 °C for 6 hours—a complex mixture of products was obtained, which could not be identified or separated using either column chromatography or high-performance liquid chromatography (HPLC).

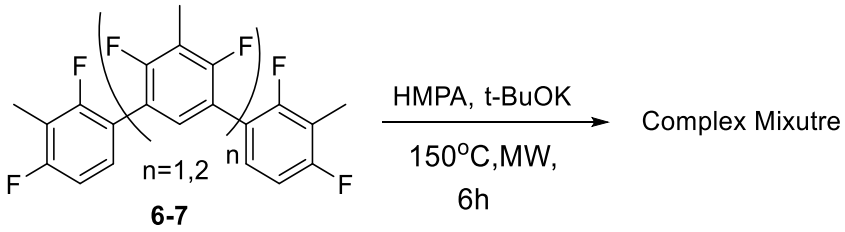

Scheme 24. LOOP reaction of precursors **6,7.**

Under comparable nucleophilic aromatic substitution (SNAr) conditions, a mixture containing Dimer 5 and sodium sulfide (Na2S, 5 equivalents per fluorine atom) and tetrabutylammonium bromide (TBAB, 1 equivalent per fluorine atom) in 1 mL of (HMPA) and exposed to microwave irradiation at 180 °C for a duration of 3 hours. A complex reaction mixture was generated, which proved to be unidentifiable and inseparable through both column chromatography and high-performance liquid chromatography (HPLC) techniques.

III.7. Functionalization of di-brominated derivatives with fluorinated phenyl or naphthalene groups.

III.7.1. Synthesis of 2,2'',4',6'-tetrafluoro-5'-methyl-1,1':3',1''-terphenyl.

In order to investigate bromo-fluorinated-oligophenelynes in more detail and prevent the liberation of terminal fluorine, a series of ortho-fluorinated aryl-boronic derivatives was prepared from the resultant bromo-fluorinated-oligophenelynes using 2-fluorophenyl)boronic acid or 2-(1-fluoronaphthalen-2-yl)-5,5-dimethyl-1,3,2-dioxaborinane via a palladium-catalyzed Suzuki-Miyaura cross-coupling reactions.

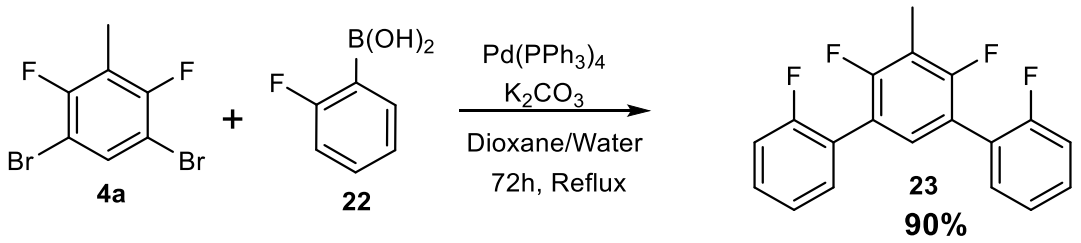

Scheme 25. Synthesis of precursor **23** via a Suzuki–Miyaura cross-coupling reaction.

We began to probe various parameters to optimise the Suzuki-Miyaura cross-coupling reaction between 1,5-dibromo-2,4-difluoro-3-methylbenzene and 2-fluorophenylboronic acid. Preliminary attempts using a toluene-methanol-water (6:3:1) solvent mixture, potassium carbonate (K_2CO_3) as base, and 10 mol% $Pd(PPh_3)_4$ under 12-hour reflux conditions showed no conversion. Subsequently, neither prolonged reaction times (72 hours) nor increased catalyst amount (60 mol%) facilitated the coupling. Changing the solvent to a dioxane-water system of 9:1 similarly yielded no conversion under standard conditions, though a minor amount of monomeric product appeared after extended reaction to 72 h. Ultimately, only when both the reaction duration was extended to 72 hours and the catalyst amount was increased to 60 mol%, the 2,2'',4',6'-tetrafluoro-5'-methyl-1,1':3',1''-terphenyl was formed in high yield (90%). This outcome underscores the significant kinetic and electronic challenges posed by the high number of fluorinated in the presence of substrates, necessitating both elevated catalyst concentrations and prolonged reaction times to achieve efficient coupling.

III.7.2. Synthesis of 2,2'-(4,6-difluoro-5-methyl-1,3-phenylene)bis(1-fluoronaphthalene).

Applying the optimized reaction conditions—specifically, a dioxane-water (9:1) solvent system, K_2CO_3 as the base, and 60 mol% $Pd(PPh_3)_4$ under reflux for 72 hours—to the cross-coupling of 1,5-dibromo-2,4-difluoro-3-methylbenzene with 2-(1-fluoronaphthalen-2-yl)-5,5-dimethyl-1,3,2-dioxaborinane afforded the 2,2'-(4,6-difluoro-5-methyl-1,3-phenylene)bis(1-fluoronaphthalene) in an isolated yield of 87%.

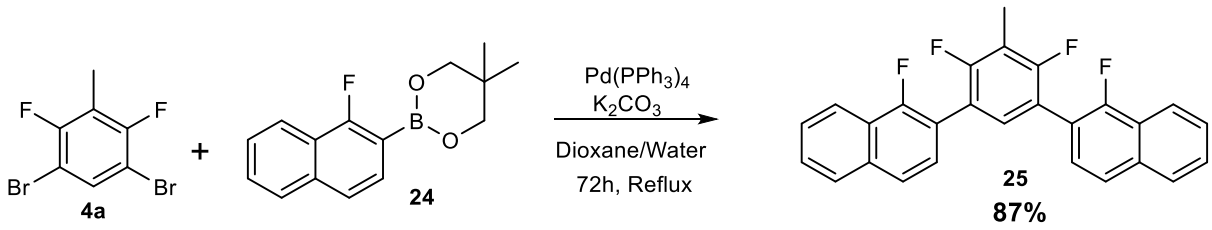

Scheme 26. Synthesis of precursor **25** via a Suzuki–Miyaura cross-coupling reaction.

III.7.3. Synthesis of 2,2''',4',4'',6',6''-hexafluoro-5',5''-dimethyl-1,1':3',1'':3'',1'''-quaterphenyl.

The optimized Suzuki-Miyaura cross-coupling protocol was applied to the 5,5'-dibromo-2,2',4,4'-tetrafluoro-3,3'-dimethyl-1,1'-biphenyl (dimer), utilizing 2-fluorophenylboronic acid as the coupling partner, resulting 2,2''',4',4'',6',6''-hexafluoro-5',5''-dimethyl-1,1':3',1'':3'',1'''-quaterphenyl in an 83% yield.

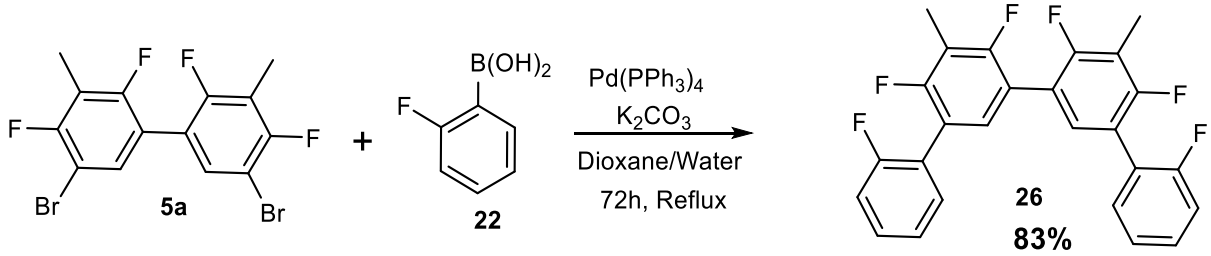

Scheme 27. Synthesis of precursor **26** via a Suzuki–Miyaura cross-coupling reaction.

III.7.4. Synthesis of 2,2'-(4,4',6,6'-tetrafluoro-5,5'-dimethyl-[1,1'-biphenyl]-3,3'-diyl)bis(1-fluoronaphthalene).

The same reaction conditions were applied to the di-brominated dimer, using 2-(1-fluoronaphthalen-2-yl)-5,5-dimethyl-1,3,2-dioxaborinane as coupling partners. yielding 2,2'-(4,4',6,6'-tetrafluoro-5,5'-dimethyl-[1,1'-biphenyl]-3,3'-diyl)bis(1-fluoronaphthalene) in 73%.

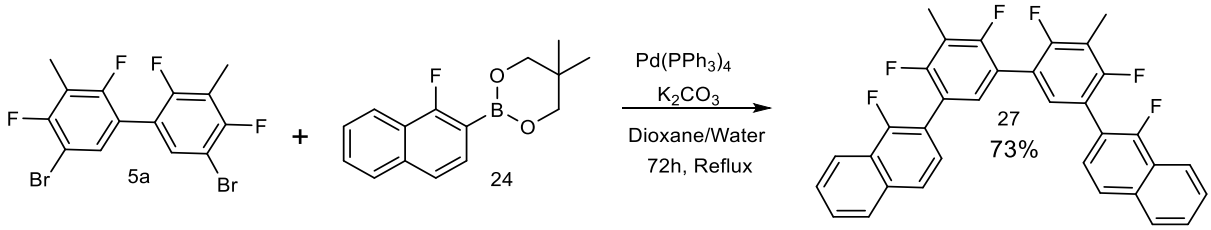

Scheme 28. Synthesis of precursor **27** via a Suzuki–Miyaura cross-coupling reaction.

The optimized reaction conditions were subsequently extended to the di-brominated, trimer and tetramer substrates, employing 2-Fluorophenylboronic acid or Fluoronaphthalen-2-yl)-5,5-dimethyl-1,3,2-dioxaborinane as the coupling partner in each case, to afford 28, 29, 30 and 31 in yields of 81, 65, 63, and 57%, respectively.

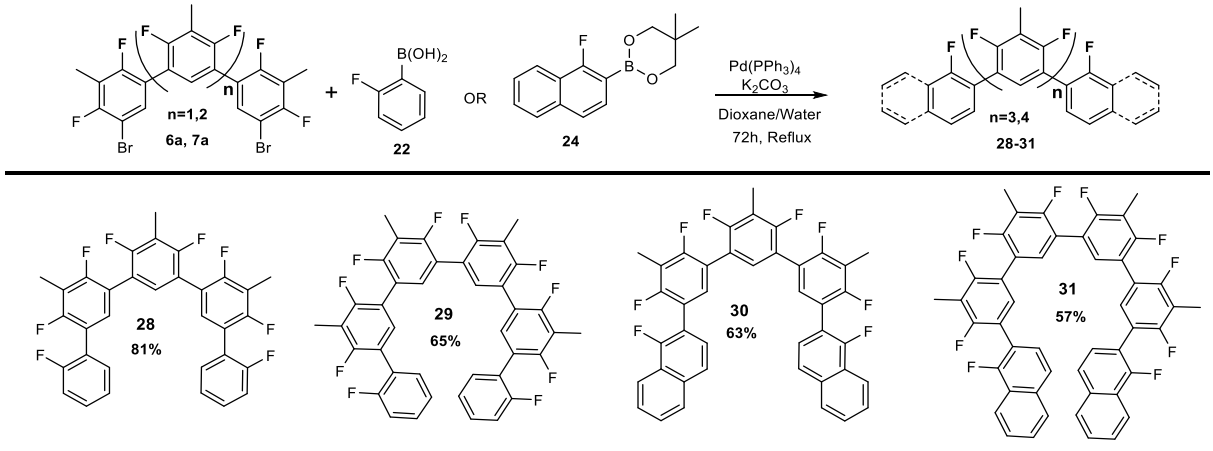

Scheme 29. Synthesis of precursor **28-31** via a Suzuki–Miyaura cross-coupling reaction.

III.8. Scholl reaction of 2,2'-(4,4',4'',4''',6,6',6'',6'''-octafluoro-5,5',5'',5'''-tetramethyl-[1,1':3',1'':3'',1'''-quaterphenyl]-3,3'''-diyl)bis(1-fluoronaphthalene) 31.

The compound 31 was subjected to oxidative conditions using DDQ in the presence of a catalytic amount of trifluoromethanesulfonic acid (TfOH) at 0 °C for 20 minutes under high dilution, with the aim of synthesizing a macrocyclic product. However, instead of the desired macrocyclization, the reaction predominantly resulted in the dimerization of 31, yielding compound 32 with an isolated yield of 30%.

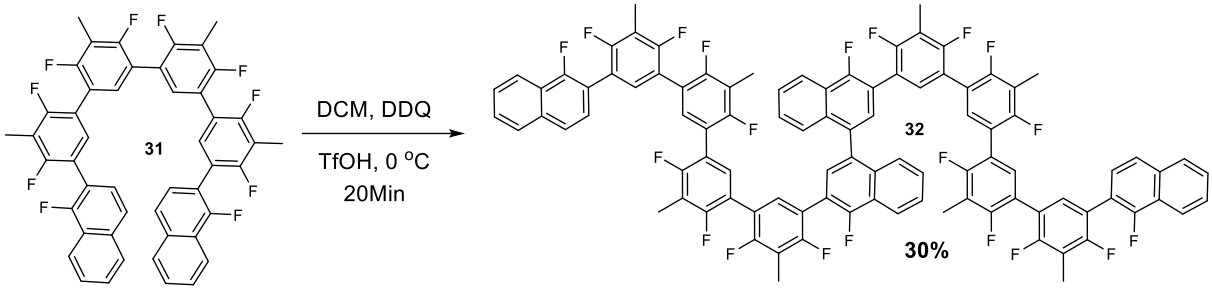

Scheme 30. Synthesis of precursor **32** via a Scholl reaction.

The target compound was unequivocally identified by mass spectrometry employing LIFDI, as evidenced by the observation of the $[M]^+$ ion at m/z 1585.37672 for the molecular formula $C_{96}H_{52}F_{20}$, thereby providing definitive confirmation of the product's molecular structure.

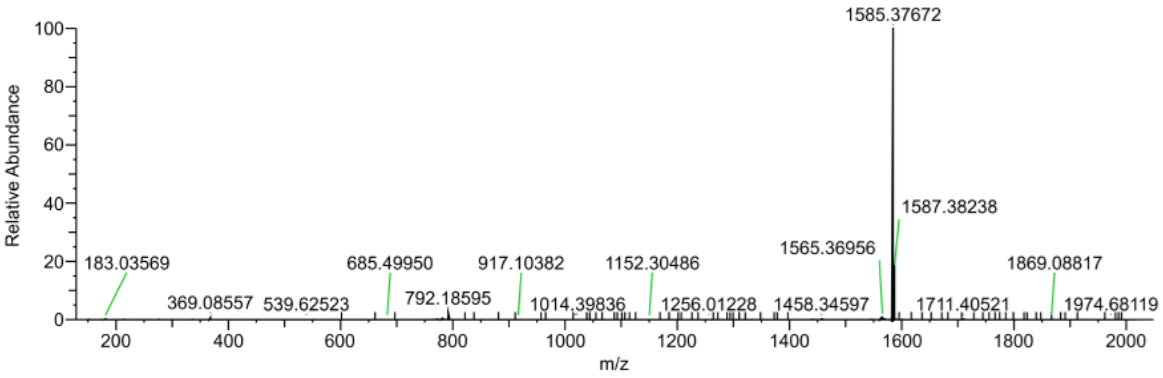

Figure 7. HRMS (LIFDI) of **32**.

III.9. Ladderization of fluorinated oligophenylenes

After obtaining the required precursors, we focused on the ladderization of fluorinated oligophenylenes by employing two distinct external reagents as sources of oxygen and sulfur, specifically tert-butoxide potassium (t-BuOK) and a combination of sodium sulfide with tetrabutylammonium bromide (Na_2S/TBAB), respectively.

III.9.1. LOOP reaction of 2,2'',4',6'-tetrafluoro-5'-methyl-1,1':3',1''-terphenyl.

The LOOP reaction of 2,2'',4',6'-tetrafluoro-5'-methyl-1,1':3',1''-terphenyl (23) employing 12 equivalents of potassium tert-butoxide (t-BuOK) as an external source of oxygen, in 2 ml of hexamethylphosphoramide (HMPA) solvent under microwave irradiation at 120 °C for 3 hours, yielded two distinct products. The major product **33** was isolated in 64% yield, with NMR analysis exhibited complete disappearance of the methyl, consistent with its replacement by a

hydrogen atom. In contrast, the minor product **34** (31% yield) confirming retention of the methyl group at the 5'-position.

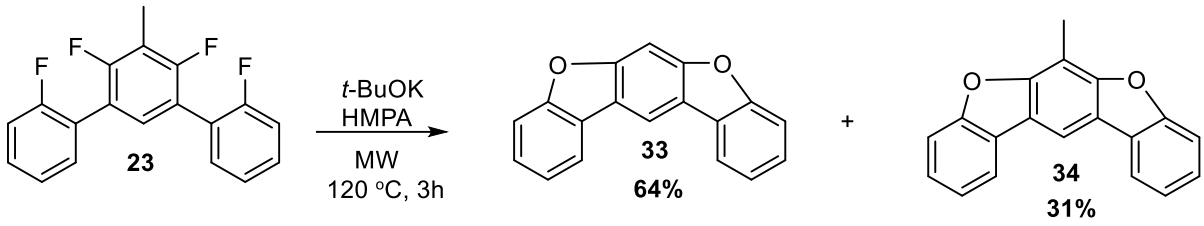

Scheme 31. LOOP reaction of precursor **23** using t-BuOK in HMPA.

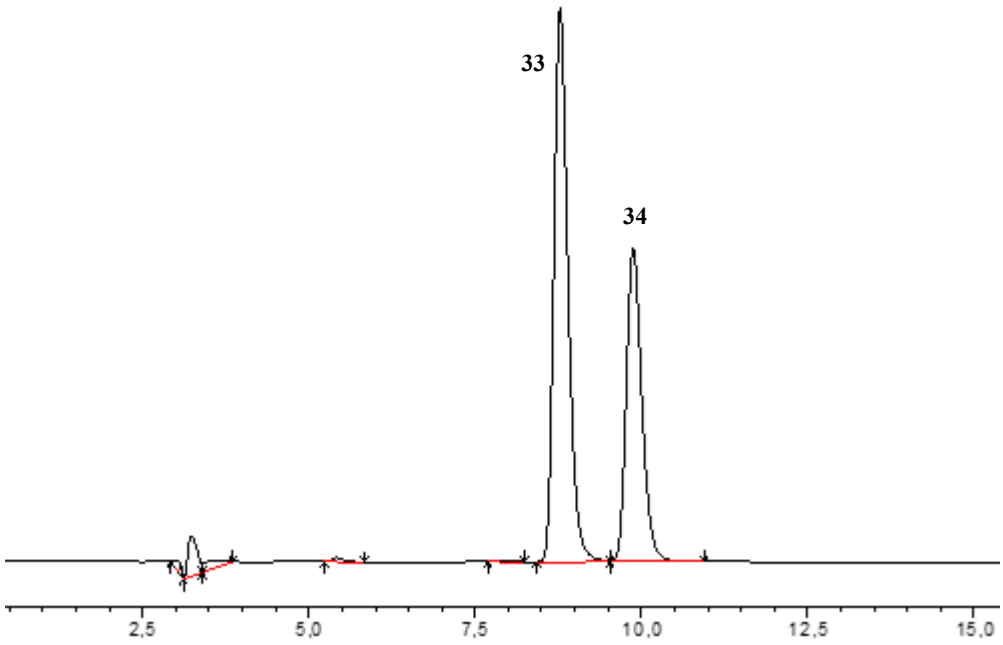

Figure 8. HPLC-profile after reaction of **25** with t-BuOK in HMPA. HPLC conditions: PBr column, eluent DCM:MeOH:70:30, 40 °C, 1 mL min-1, detection at 300 nm.

On the other hand, when 2,2",4',6'-tetrafluoro-5'-methyl-1,1':3',1"-terphenyl is subjected to microwave irradiation at 180 °C for 3 hours in 1 ml of hexamethylphosphoramide (HMPA) using a mixture of 20 equivalents of sodium sulfide and 4 equivalents of tetrabutylammonium bromide as reagents, a single product is obtained in 78% yield. Notably, NMR analysis confirms that the methyl group at the 5' position remains untouchable under these reaction conditions, indicating its stability throughout the process.

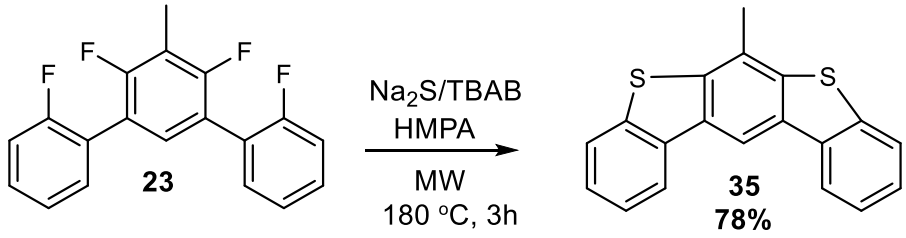

Scheme 32. LOOP reaction of precursor **23** using Na_2S/TBAB in HMPA.

III.9.2. LOOP reaction of 2,2'-(4,6-difluoro-5-methyl-1,3-phenylene)bis(1-fluoronaphthalene).

Applying the same reaction conditions to 2,2'-(4,6-difluoro-5-methyl-1,3-phenylene)bis(1-fluoronaphthalene), utilizing t-BuOK as a source of oxygen, resulted in the formation of two products with isolated yields of 86% and 6%, respectively.

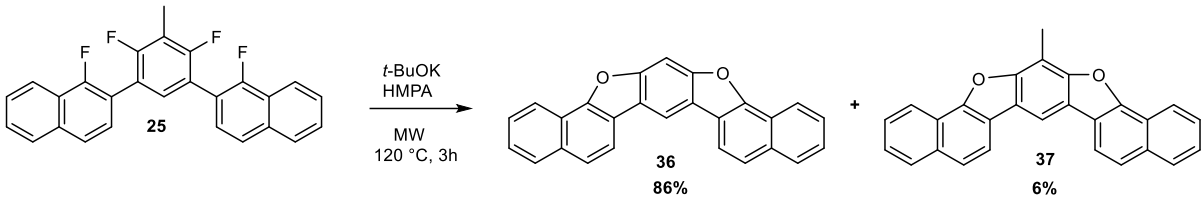

Scheme 7. LOOP reaction of precursor **25** using t-BuOK/HMPA.

Conversely, when 2,2'-(4,6-difluoro-5-methyl-1,3-phenylene)bis(1-fluoronaphthalene) was subjected to similar reaction conditions, employing 20 equivalents of sodium sulfide and 4 equivalents of tetrabutylammonium bromide, a unique product was formed in 56% yield.

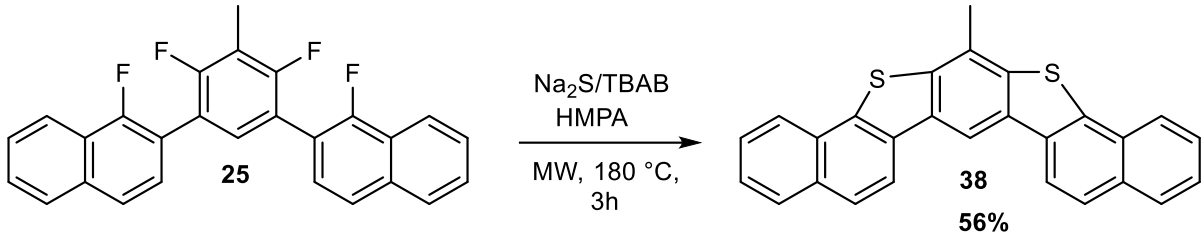

Scheme 24. LOOP reaction of precursor **25** using Na_2S/TBAB in HMPA.

Scheme 33. LOOP reaction of precursor **25** using Na_2S/TBAB in HMPA.

Given the observed instability of the methyl group at the 5-position under t-BuOK/HMPA conditions, subsequent investigations were directed exclusively toward the synthesis of the corresponding sulfur-containing compound.

The ongoing execution of the LOOP reaction using NaS_2 and TBAB in HMPA, can be a future opportunity to continue this work.

IV. Summary

The main goal of this thesis was the synthesis of cyclopara-phenylenes CPP and cyclo-meta-phenylenes CMP via selective dibromide derivatives.

First of all, we successfully prepared a series of quasi-planar π-extended cycloparaphenylenes (CPPs) with varying ring sizes on Au(111) surface through sequential debromination and cyclodehydrogenation reactions. These π-extended CPPs form macrocyclic structures with para-linked phenylene units composing the inner framework. Notably, the 8-unit [16]CPP adopts a nearly flat conformation on the surface, while larger 9- to 11-unit CPPs exhibit slight deviations from planarity due to twisted perylene moieties.

Furthermore, a selective terminal di-bromination approach for fluorinated oligophenylenes, employing a straightforward setup with commonly available reagents and catalysts under mild reaction conditions. The method proves effective for a wide range of fluorinated oligophenylenes that are otherwise difficult to access through conventional synthetic routes. Key findings reveal that the fluorine substituent's position critically influences bromination selectivity, allowing for high-yielding and regioselective formation of dibrominated products. This technique offers a flexible platform for assembling more intricate molecular frameworks, with significant potential for applications in synthetic and materials chemistry.

Finally, we achieved the synthesis of highly symmetrical, fluorinated cyclometaphenylenes F_{16}[8]CMP F_{24}[12]CMP through Yamamoto-coupling. This research advances the chemistry of CMPs and fluoroarenes while introducing a novel approach for designing complex nanorings and nanobelts.

V. Zusammenfassung

Das Hauptziel dieser Arbeit war die Synthese von Cyclopara-Phenylenen CPP und Cyclo-Meta-Phenylenen CMP über selektive Dibromid-Derivate.

Zunächst haben wir erfolgreich eine Reihe von quasi-planaren π-verlängerten Cycloparaphenylenen (CPP) mit unterschiedlichen Ringgrößen auf der Au(111)-Oberfläche durch aufeinanderfolgende Debromierungs- und Cyclodehydrierungsreaktionen hergestellt. Diese π-verlängerten CPPs bilden makrozyklische Strukturen mit para-verknüpften Phenyleneinheiten, die das innere Gerüst bilden. Insbesondere das 8-gliedrige [16]CPP nimmt auf der Oberfläche eine nahezu flache Konformation an, während die größeren 9- bis 11-gliedrigen CPPs aufgrund von verdrehten Peryleneinheiten leichte Abweichungen von der Planarität aufweisen.

Darüber hinaus wurde ein selektiver Ansatz für die terminale Di-Bromierung von fluorierten Oligophenylenen entwickelt, bei dem ein unkomplizierter Aufbau mit allgemein verfügbaren Reagenzien und Katalysatoren unter milden Reaktionsbedingungen verwendet wird. Die Methode erweist sich als effektiv für eine breite Palette fluorierter Oligophenylene, die ansonsten über herkömmliche Synthesewege nur schwer zugänglich sind. Die wichtigsten Ergebnisse zeigen, dass die Position des Fluorsubstituenten einen entscheidenden Einfluss auf die Selektivität der Bromierung hat und die Bildung von dibromierten Produkten mit hoher Ausbeute und Regioselektion ermöglicht. Diese Technik bietet eine flexible Plattform für den Aufbau komplizierterer molekularer Gerüste und birgt ein erhebliches Potenzial für Anwendungen in der synthetischen und Materialchemie.

Schließlich gelang uns die Synthese von hochsymmetrischen, fluorierten Cyclometaphenylenen F_{16}[8]CMP F_{24}[12]CMP durch Yamamoto-Kopplung. Diese Forschungsarbeit bringt die Chemie der CMPs und Fluorarene voran und stellt gleichzeitig einen neuartigen Ansatz für die Entwicklung komplexer Nanoringe und Nanobelts dar.

VI. Experimental part

6.1. General Information

Solvents and chemicals

All chemicals and solvents were purchased in reagent grade from commercial suppliers (Acros®, Sigma-Aldrich® or Fluka®, Fluorochem®, Merck®, chemPur®) and used as received, unless otherwise specified. Solvents in HPLC grade were purchased from VWR® and Sigma-Aldrich®) was purchased from Acros®.

Nuclear magnetic resonance spectroscopy

NMR spectra were recorded on a Bruker Avance 400 operating at 400 MHz (^{1}H NMR), 100 MHz (^{13}C NMR) and 377 MHz (^{19}F NMR) at room temperature. The signals were referenced to residual solvent peaks (in parts per million (ppm) 1H: CDCl3, 7.26 ppm; CD2Cl2, 5.32 ppm; 13C: CDCl3, 77.0 ppm, CD2Cl2, 53.8 ppm). Coupling constants were assigned as observed. The obtained spectra were evaluated with the program MestReNova. Resonance peaks were indicated as “s” (singlet), “d” (doublet), “t” (triplet), “q” (quartet) and “m” (multiplet).

High-performance liquid chromatography

HPLC analyses were carried out using analytical Cosmosil PBr (4.6 x 250 mm) and purification using semi-preparative PBB-R (10 x 250 mm) column (UV-Vis detection).

Flash liquid chromatography

Automated flash-column chromatography (aFLC) was performed on Intershim® puriflash 430 with flash grade silica gel Kiesegel 60 (0.06 0.2 mm).

Thin layer chromatography

TLC was performed on silica-backed silica plates and visualized by UV-light (254 nm, 366 nm), layer thickness 0.25 mm, medium pore diameter 60 Å, Fluka.

Mass spectrometry

LIFDI MS stands for Liquid Injection Field Desorption/Ionization Mass Spectrometry (Thermo Fischer DFS). All spectra are reported as m/z.

Microwave assisted experiments

Microwave assisted experiments were carried out using Discover® SP Microwave Synthesizer, CEM and Biotage® initiator+ monomode microwave reactor, Biotage in the respective vials.

6.2. EXPERIMENTAL PROCEDURES

General Procedure 1.

To a solution of 2,2,6,6-Tetramethylpiperidine (2.42 g, 11,88 mL, 17.1 mmol, 2.2 equivalente, in THF (30 ml) at -78 °C was added n-BuLi (1.02 g, 24,8 mL, 2.5 M in hexanes, 16.0 mmol, 1.4 2 equiv) dropwise via a syringe and the orange suspension stirred for 30 minutes at -78 °C. 2,6-Difluorotoluene (4g, 11.4 mmol, 1 equiv) dissolved in THF (5 mL) was added dropwise and the suspension was stirred for a further 30 minutes at -78 °C. CuBr2 (13,8 g, 11.4 mmol, 2 equiv, was added under vigorous stirring and the resulting blue suspension was stirred for an additional 45 minutes at -78 °C. The dark green mixture was allowed to reach room temperature over a period of 3 h. A sat. aq. NH_4Cl-solution was added, layers were separated and the aqueous phase was extracted with CH_2Cl_2. The combined organic phases were washed with a sat. aq. NH_4Cl-solution and dried over Na_2SO_4, filtered and the solvent evaporated to dryness. Solvent evaporation under reduced pressure was followed by flash chromatography purification of the product (Hexane: Dichloromethane=20:1).

General Procedure 2.

The corresponding bromo-arene (1n mmol) and boronic acid (3 equiv. to halogene) were dissolved in 15ml of dioxane: H_2O (10:1) mixture containing potassium carbonate (755 mg, 3.82n mmol) and $Pd(PPh_3)_4$ (630 mg, 60%) as catalyst. The reaction mixture was stirred under reflux and argon atmosphere for 15 hours. After the completion of the reaction, the solvent was evaporated and the residue was purified by silica gel column chromatography eluting with (Hexane-Hexane: DCM 10:1) yielding the corresponding Fluorinated Oligophenylenes.

General Procedure 3.

A mixture of the corresponding Fluorinated Oligophenylenes. (0.26 g, 1 mmol) and iron powder (0.56 g, 10-30 mmol) were combined in CH_2Cl_2 (10 mL) at room temperature with stirring for 30 min. A solution of Br_2 (0.10 mL,2 mmol) in CH_2Cl_2 (10 mL) was slowly added drop-wise with vigorous stirring. After this addition, the reaction mixture was continuously stirred for 22h at room temperature. The mixture was quenched with Na2S2O3 (10%) and extracted with CH_2Cl_2 (20 mL 3). The combined organic extracts were washed with water and brine and evaporated to give pure corresponding Fluorinated Oligophenylenes as a white powder.

General Procedure 4.

A mixture of the corresponding Fluorinated Oligophenylenes. (0.26 g, 1 mmol) and iron powder (0.56 g, 2 mmol) were combined in CH2Cl2 (10 mL) at room temperature with stirring for 30 min. A solution of Br_2 (0.10 mL,10 mmol) in CH_2Cl_2 (10 mL) was slowly added drop-wise with vigorous stirring. After this addition, the reaction mixture was continuously stirred for 22h at room temperature. The mixture was quenched with Na_2S2O_3 (10%) and extracted with CH_2Cl_2 (20 mL 3). The combined organic extracts were washed with water and brine and evaporated to give pure corresponding Fluorinated Oligophenylenes as a white powder.

General Procedure 5.

A glass tube for microwave reactor was charged with 2 ml of HMPA, fluoroarene (0.03-0.1 mmol) and t-BuOK (66 mg, 3 equiv. to one fluorine). The tube was put in microwave reactor and stirred for 3 h at 120 °C. After cooling to room temperature, the mixture was filtrated through silica using hexane as a solvent (50/50 mixture of hexane/ethylacetate was used when the polar products were formed). The organic solvent was evaporated under the reduced pressure yielding the product.

General Procedure 6.

A glass tube for microwave reactor was charged with fluoroarene (0.1 mmol of difluorooligophenylene or 0.5 mmol of tetrafluoro oligophenylene or 0.33 mmol of hexafluorooligophenylene), Na2S (150 mg, 20 equiv), tetrabutylammonium bromide (120 mg, 4 equiv), and hexamethylphosphoramide (HMPA) (1 mL). The tube was put in a microwave reactor and stirred for 3 h at 180 °C. After cooling to room temperature, the mixture was purified via column chromatography using hexane−hexane/dichloromethane (DCM) (10:1) as an eluent. The organic solvent was evaporated under the reduced pressure, yielding the product.

- **Synthesis of 5,9-dibromodinaphtho[2,1-b:1',2'-d]furan 2.**

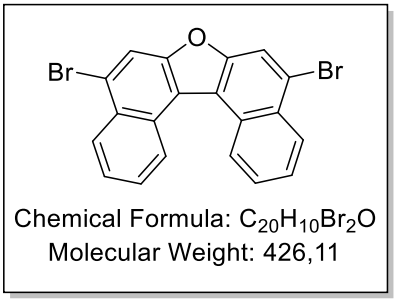

To a stirred solution of dinaphtho[2,1-b:1',2'-d]furan (100 mg, 0.37 mmol) in chloroform (10 mL) bromine (40 µl, 0.75 mmol) was added in the dark. The mixture was stirred overnight. After the completion of the reaction aqueous $NaHSO_3$ solution was added to quench the excess of bromine. The organic layer was separated and was dried over anhydrous Na_2SO_4, and concentrated to dryness to afford the crude compound, purification of the product was carried out by HPLC chromatography (PBr column, DCM:MeOH 70: 30 mixture as eluent). 5,9dibromodinaphtho[2,1-b:1',2'-d]furan as off-white solid in 82% (130 mg, 0.31 mmol). ^{1}H NMR (500 MHz, CDCl3) δ 9.10 (d, J = 8.4 Hz, 2H), 8.52 (dd, J = 8.4, 1.1 Hz, 2H), 8.19 (s, 2H), 7.80 (t, J = 4.8 Hz, 2H), 7.71 (t, J = 7.7 Hz, 2H). ^{13}C NMR (126 MHz, CDCl3) δ 153.5, 129.4, 128.8, 128.8, 127.1, 125.9, 125.7, 122.3, 119.2, 117.1.

- **Dimirization of 5,9-dibromodinaphtho[2,1-b:1',2'-d]furan 3.**

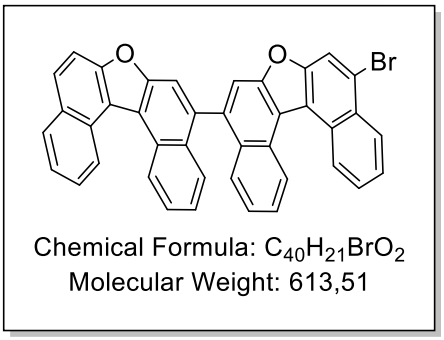

To a solution of 5,9-dibromodinaphtho[2,1-b:1',2'-d]furan (100mg, 1 equivalente, in THF (30 ml) at -78 °C was added n-BuLi (207 µl, 2.5 M in hexanes, 2.2 equiv) dropwise via a syringe and the suspension stirred for 30 minutes at -78 °C. $CuBr_2$ (53 mg, 1 equiv) was added under vigorous stirring and the resulting blue suspension was stirred for an additional 45 minutes at -78 °C. The dark green mixture was allowed to reach room temperature over a period of 3 h. A sat. aq. NH_4Cl-solution was added, layers were separated and the aqueous phase was extracted with CH_2Cl_2. The combined organic phases were washed with a sat. aq. NH4Cl-solution and dried over Na_2SO_4, filtered and the solvent evaporated to dryness. Solvent evaporation under reduced pressure was followed by purification with HPLC chromatography (PBr column, DCM:MeOH 70: 30 mixture as eluent). The compound 3 an off-white solid in 65% 94 mg. ^{1}H NMR (400 MHz, cdcl3) δ 9.18 (d, J = 8.4 Hz, 2H), 9.10 (d, J = 8.6 Hz, 3H), 8.52 (dd, J = 8.5, 0.9 Hz, 2H), 8.21 (s, 1H), 8.08 (d, J = 8.0 Hz, 2H), 8.00 (d, J = 8.9 Hz, 2H), 7.83 (d, J = 8.9 Hz, 2H), 7.81 – 7.75 (m, 3H), 7.75 – 7.67 (m, 2H), 7.61 (ddd, J = 8.0, 7.0, 1.1 Hz, 2H). ^{13}C NMR (101 MHz, cdcl3) δ 129.57 (s), 128.89 (s), 128.65 (s), 126.87 (s), 126.40 (s), 125.89 (s), 125.67 (s), 125.40 (s), 124.64 (s), 117.11 (s), 112.66 (s).

6.3. Synthesis of Fluorinated Oligophenylene precursors.

- **Homo-coupling of 2,6-Difluorotoluene.**

To a solution of 2,2,6,6-Tetramethylpiperidine (11,88 mL, 17.1 mmol, 2.2 equivalente, in THF (30 ml) at -78 °C was added n-BuLi (24,8 mL, 2.5 M in hexanes, 16.0 mmol, 2 equiv) dropwise via a syringe and the orange suspension stirred for 30 minutes at -78 °C. 2,6-Difluorotoluene (4g, 11.4 mmol, 1 equiv) dissolved in THF (5 mL) was added dropwise and the suspension was stirred for a further 30 minutes at -78 °C. CuBr2 (13,8 g, 11.4 mmol, 2 equiv, was added under vigorous stirring and the resulting blue suspension was stirred for an additional 45 minutes at -78 °C. The dark green mixture was allowed to reach room temperature over a period of 3 h. A

sat. aq. NH4Cl-solution was added, layers were separated and the aqueous phase was extracted with CH2Cl2. The combined organic phases were washed with a sat. aq. NH4Cl-solution and dried over Na2SO4, filtered and the solvent evaporated to dryness. Solvent evaporation under reduced pressure was followed by flash chromatography purification of the product (Hexane: Dichloromethane=20:1). 2,2',4,4'-tetrafluoro-3,3'-dimethyl-1,1'-biphenyl yield 2.9 g (37 %), 2,2",4,4',4",6'-hexafluoro-3,3",5'-trimethyl-1,1':3',1"-terphenyl yield 2.01 g (17 %), and 2,2"',4,4',4",4"',6',6"-octafluoro-3,3"',5'-trimethyl-1,1':3',1":3",1"'-quaterphenyl yield 1.10 g (7 %).

- **2,2',4,4'-tetrafluoro-3,3'-dimethyl-1,1'-biphenyl 5.**

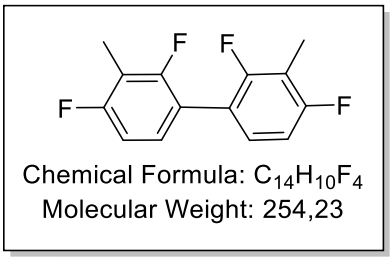

Chemical Formula: $C_{14}H_{10}F_4$
Molecular Weight: 254,23

^{1}H NMR (402 MHz, $CDCl_3$) δ 7.20 – 7.10 (m, 2H), 6.90 (t, J = 8.6 Hz, 1H), 2.33 – 2.21 (m, 6H). **^{19}F NMR** (378 MHz, $CDCl_3$) δ -114.44 (qd, J = 8.6, 1.8 Hz), -114.73 – -115.05 (m). **^{13}C NMR** (101 MHz, $CDCl_3$) δ 162.63 (d, J = 7.8 Hz), 160.19 (d, J = 7.6 Hz), 159.79 – 159.59 (m), 159.43 (s), 157.35 – 157.12 (m), 156.93 (s), 130.09 (s), 128.49 (dd, J = 9.5, 4.0 Hz), 118.82 (s), 118.45 (dd, J = 16.7, 3.8 Hz), 113.61 (t, J = 21.4 Hz), 110.67 (dd, J = 22.7, 3.7 Hz), 7.33 (dd, J = 21.6, 17.6 Hz).

LIFDI (m/z): $[M]^+$ calcd. for $C_{14}H_{10}F_4$, 254.0713; found, 254.0712

- **2,2'',4,4',4'',6'-hexafluoro-3,3'',5'-trimethyl-1,1':3',1''-terphenyl 6.**

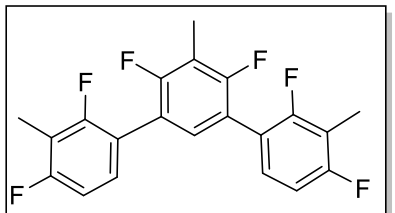

Chemical Formula: $C_{21}H_{14}F_6$
Molecular Weight: 380,33

^{1}H NMR (402 MHz, $CDCl_3$) δ 7.15 (dd, J = 15.6, 7.6 Hz, 3H), 6.90 (td, J = 8.6, 0.8 Hz, 2H), 2.33 – 2.21 (m, 9H). **^{19}F NMR** (378 MHz, $CDCl_3$) δ -114.49 (tdd, J = 6.5, 5.4, 1.8 Hz), -114.98 (dt, J = 14.1, 10.3 Hz), -115.06 – -115.22 (m).**^{13}C NMR** (101 MHz, $CDCl_3$) δ 162.61 (d, J = 7.4 Hz), 160.18 (d, J = 7.5 Hz), 159.53 (dd, J = 37.2, 8.8 Hz), 157.05 (dd, J = 39.5, 8.8 Hz), 130.10 (s), 128.50 (dd, J = 9.9, 4.7 Hz), 119.18 – 118.10 (m), 114.13 – 113.09 (m), 110.66 (dd, J = 22.7, 3.7 Hz), 7.39 (dt, J = 33.1, 4.1 Hz).

LIFDI (m/z): $[M]^+$ calcd. for $C_{21}H_{14}F_6$, 280.0994; found, 280.0991.

- **2,2''',4,4',4'',4''',6',6''-octafluoro-3,3''',5'-trimethyl-1,1':3',1'':3'',1'''-quaterphenyl 7.**

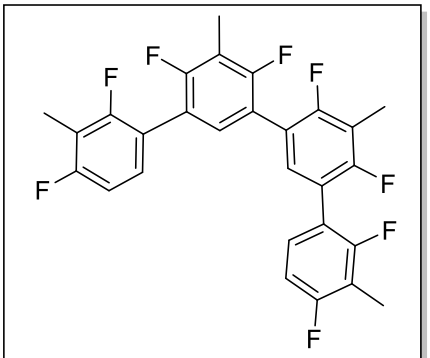

Chemical Formula: $C_{28}H_{18}F_8$
Molecular Weight: 506,44

^{1}H NMR (402 MHz, $CDCl_3$) δ 7.14 – 7.06 (m, 1H), 6.90 (t, J = 8.6 Hz, 1H), 2.24 (s, 3H). **^{19}F NMR** (378 MHz, $CDCl_3$) δ -114.76 – -114.87 (m), -115.21 (dd, J = 12.8, 9.3 Hz). **^{13}C NMR** (101 MHz, $CDCl_3$) δ 162.66 – 162.40 (m), 160.10 (d, J = 5.3 Hz), 159.67 (d, J = 8.4 Hz), 157.20 (d, J = 8.6 Hz), 128.46 (dt, J = 6.1, 2.8 Hz), 110.91 – 110.23 (m), 7.22 (t, J = 4.1 Hz).

LIFDI (m/z): [M]+ calcd. for $C_{28}H_{18}F_8$, 506.1275; found, 506.1276.

- **Synthesis of 3,3',4,4'-tetrafluoro-1,1'-biphenyl 8.**

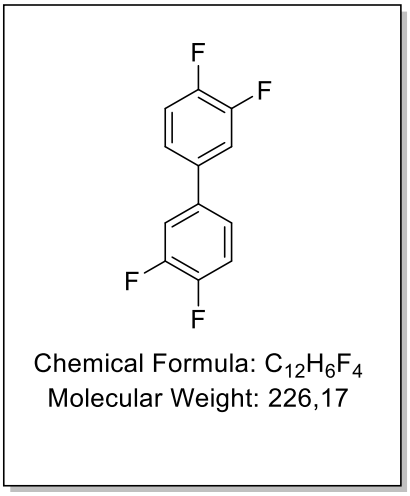

Chemical Formula: $C_{12}H_6F_4$
Molecular Weight: 226,17

The compound was synthesized according to General Procedure **2** using 1-bromo-3,4-difluorobenzene (2g). Yield 1.83 g (78 %). White solid.

^{1}H NMR (402 MHz, $CDCl_3$) δ 7.33 – 7.26 (m, 1H), 7.24 – 7.18 (m, 2H). **^{19}F NMR** (378 MHz, CDCl3) δ -136.82 – -137.11 (m), -139.07 – -139.36 (m). **^{13}C NMR** (101 MHz, $CDCl_3$) δ 151.74 (d, J = 12.8 Hz), 151.41 (d, J = 12.7 Hz), 149.28 (d, J = 12.8 Hz), 148.95 (d, J = 12.6 Hz), 136.20 (s), 133.61 (s), 128.79 – 128.30 (m), 122.89 (dd, J = 6.4, 3.5 Hz), 117.81 (d, J = 0.6 Hz), 117.64 (s), 116.02 (s), 115.84 (s).

LIFDI (m/z): [M]+ calcd. for $C_{12}H_6F_4$, 226.0400; found, 226.0777.

- **Synthesis of 3,3'',4,4',4'',5'-hexafluoro-1,1':2',1''-terphenyl 9.**

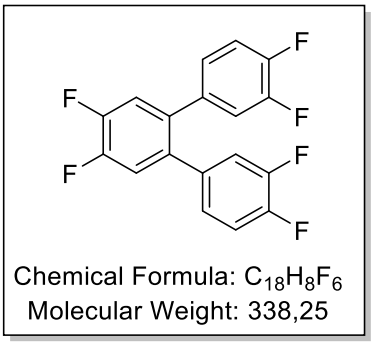

Chemical Formula: $C_{18}H_8F_6$
Molecular Weight: 338,25

The compound was synthesized according to General Procedure **2** using 1,2-dibromo-3,5-difluorobenzene (2g). Yield 1.80 g (72 %). White solid.

^{1}H NMR (402 MHz, $CDCl_3$) δ 7.18 (t, J = 9.3 Hz, 1H), 7.04 (dd, J = 18.3, 8.4 Hz, 1H), 6.87 (ddd, J = 22.9, 12.4, 8.7 Hz, 1H), 6.83 – 6.70 (m, 1H). **^{19}F NMR** (378 MHz, $CDCl_3$) δ -137.04 (ddd, J = 10.8, 9.6, 8.3 Hz), -138.22 (t, J = 9.4 Hz), -138.73 – -139.09 (m).**^{13}C NMR** (101 MHz, CDCl3) δ 151.34 – 150.73 (m), 148.93 – 148.09 (m), 135.88 (dd, J = 6.0, 4.2 Hz), 135.14 (s), 125.74 (dd, J = 6.2, 3.6 Hz), 119.57 – 118.92 (m), 118.52 (d, J = 17.8 Hz), 117.28 (d, J = 17.4 Hz).

LIFDI (m/z): [M]+ calcd. for $C_{18}H_8F_6$, 338.0524; found, 338.0524.

- **Synthesis of 2,2'-difluoro-1,1'-biphenyl 10.**

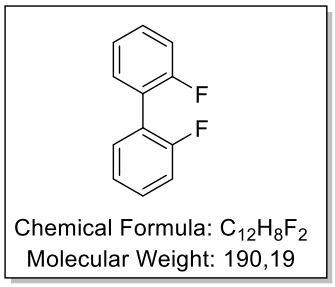

Chemical Formula: $C_{12}H_8F_2$
Molecular Weight: 190,19

The compound was synthesized according to the literature procedure[115].

- **Synthesis of 2,2',6,6'-tetrafluoro-1,1'-biphenyl 11.**

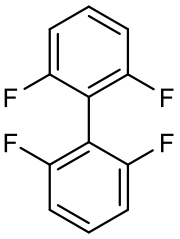

Chemical Formula: $C_{12}H_6F_4$
Molecular Weight: 226,17

The compound was synthesized according to the literature procedure[116].

- **Synthesis of 2,2',4,4'-tetrafluoro-1,1'-biphenyl 12.**

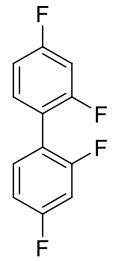

Chemical Formula: $C_{12}H_6F_4$
Molecular Weight: 226,17

The compound was synthesized according to the literature procedure[47].

- **Synthesis of 2,2'-difluoro-5,5'-dimethyl-1,1'-biphenyl 13.**

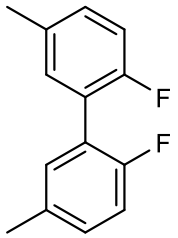

Chemical Formula: $C_{14}H_{12}F_2$
Molecular Weight: 218,25

The compound was synthesized according to the literature procedure[47].

- **Synthesis of 4,4'-difluoro-1,1'-biphenyl 14.**

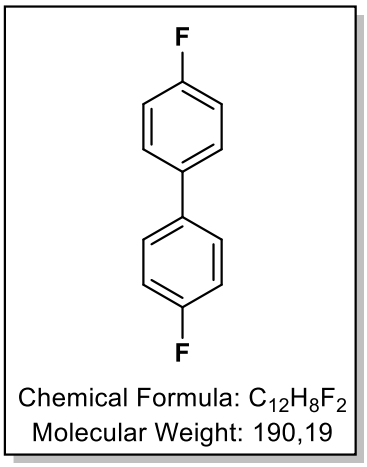

The compound was synthesized according to the literature procedure[117].

- **Synthesis of 2,2',3,3'-tetrafluoro-1,1'-biphenyl 15.**

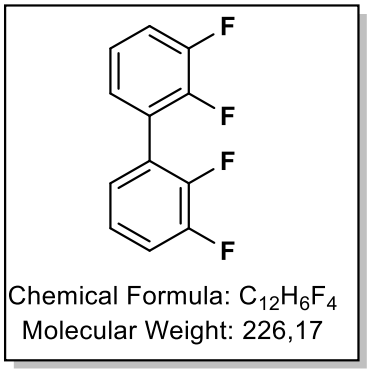

The compound was synthesized according to the literature procedure[111].

- **Synthesis of 2,2',5,5'-tetrafluoro-1,1'-biphenyl 16.**

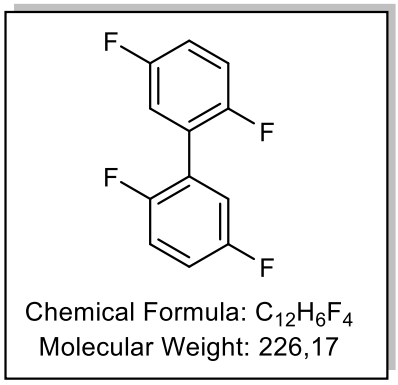

The compound was synthesized according to the literature procedure[47].

6.4. Bromination of Fluorinated Oligophenylene precursors.

- **Synthesis of 1,5-dibromo-2,4-difluoro-3-methylbenzene 4a.**

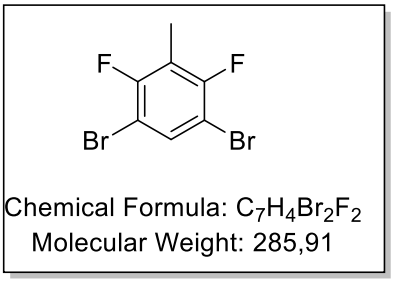

The compound was synthesized according to General Procedure **3** using 2,6-Difluorotoluene (100mg) and 10 equivalent of Iron. Yield 200 mg (90 %). White solid.

^{1}H NMR (402 MHz, $CDCl_3$) δ 7.57 (td, J = 7.2, 0.5 Hz, 1H), 2.32 – 2.17 (m, 3H). **^{19}F NMR** (378 MHz, $CDCl_3$) δ -106.85 – -107.01 (m). **^{13}C NMR** (101 MHz, $CDCl_3$) δ 158.18 (d, J = 8.0 Hz), 155.73 (d, J = 8.1 Hz), 132.66 (t, J = 1.2 Hz), 116.10 (t, J = 23.0 Hz), 104.58 – 103.38 (m), 8.29 (t, J = 3.2 Hz).

LIFDI (m/z): [M]+ calcd. for $C_7H_4F_2$, 285.8543; found, 285.8542.

- **Synthesis of 1,2,3-tribromo-4,6-difluoro-5-methylbenzene 4b.**

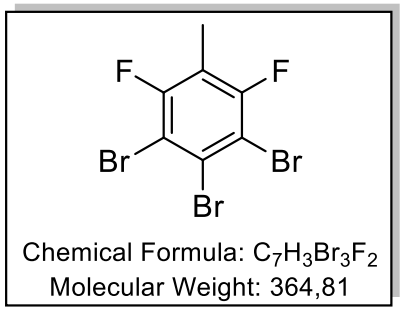

The compound was synthesized according to General Procedure **4** using 2,6-Difluorotoluene (100mg) and 2 equivalent of Iron. Yield 247 mg (87 %). White solid.

^{1}H NMR (402 MHz, $CDCl_3$) δ 2.22 (td, J = 2.1, 0.8 Hz, 1H). **^{19}F NMR** (378 MHz, $CDCl_3$) δ -98.67 – -98.76 (m). **^{13}C NMR** (101 MHz, $CDCl_3$) δ 158.48 (d, J = 9.6 Hz), 156.02 (d, J = 9.6 Hz), 125.54 (t, J = 1.6 Hz), 114.57 (t, J = 23.8 Hz), 109.05 – 108.24 (m), 8.49 (t, J = 3.0 Hz).

LIFDI (m/z): [M]+ calcd. for $C_7H_3Br_3F_2$, 363.7727; found, 363.7722.

- **Synthesis of 5,5'-dibromo-2,2',4,4'-tetrafluoro-3,3'-dimethyl-1,1'-biphenyl 5a.**

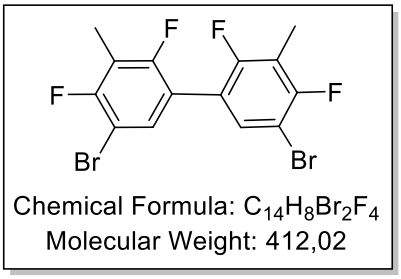

The compound was synthesized according to General Procedure **3** using 2,2',4,4'-tetrafluoro-3,3'-dimethyl-1,1'-biphenyl (**5**) (100mg) and 30 equivalent of Iron. Yield 147 mg (90 %). White solid.

^{1}H NMR (402 MHz, $CDCl_3$) δ 7.34 (s, 1H), 2.28 (s, 3H). **^{19}F NMR** (378 MHz, $CDCl_3$) δ -105.78 (s), -115.04 (s). **^{13}C NMR** (101 MHz, $CDCl_3$) δ 159.20 – 158.50 (m), 156.62 – 156.00 (m), 131.29 (s), 119.01 (s), 115.28 (s), 103.50 (d, J = 20.7 Hz), 7.93 (s).

LIFDI (m/z): [M]+ calcd. for $C_{14}H_8Br_2F_4$, 411.8902; found, 411.8899.

- **Synthesis of 5,5''-dibromo-2,2'',4,4',4'',6'-hexafluoro-3,3'',5'-trimethyl-1,1':3',1''-terphenyl 6a.**

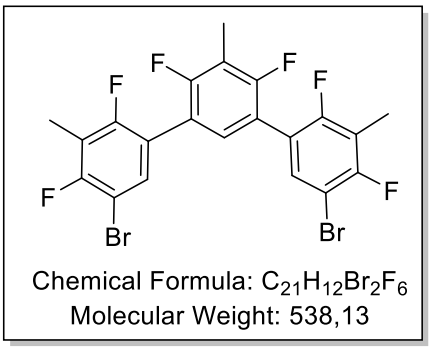

Chemical Formula: $C_{21}H_{12}Br_2F_6$
Molecular Weight: 538,13

The compound was synthesized according to General Procedure **3** using 2,2'',4,4',4'',6'-hexafluoro-3,3'',5'-trimethyl-1,1':3',1''-terphenyl (**6**) (100mg) and 20 equivalent of Iron. Yield 127 mg (90 %). White solid.

^{1}H NMR (402 MHz, $CDCl_3$) δ 7.39 (t, J = 7.5 Hz, 2H), 7.11 (t, J = 7.9 Hz, 1H), 2.29 (d, J = 1.8 Hz, 9H). **^{19}F NMR** (378 MHz, $CDCl_3$) δ -106.17 – -106.45 (m), -113.69 – -113.99 (m), -114.96 – -115.30 (m). **^{13}C NMR** (101 MHz, $CDCl_3$) δ 159.62 (s), 159.53 (s), 158.83 (s), 158.74 (s), 157.14 (s), 157.05 (s), 156.37 (d, J = 2.6 Hz), 156.29 (s), 131.39 (d, J = 3.2 Hz), 129.82 (s), 119.74 (d, J = 4.3 Hz), 119.56 (d, J = 4.2 Hz), 117.92 (d, J = 7.2 Hz), 117.74 (s), 115.60 – 114.74 (m), 114.21 (t, J = 22.0 Hz), 103.53 (d, J = 4.2 Hz), 103.31 (d, J = 4.2 Hz), 8.03 – 7.85 (m), 7.57 (t, J = 4.3 Hz).

HRMS (m/z): [M]+ calcd. for C21H12Br2F6, 537.9184; found, 537.9181.

- **Synthesis of 5,5'''-dibromo-2,2''',4,4',4'',4''',6',6''-octafluoro-3,3''',5',5''-tetramethyl-1,1':3',1'':3'',1'''-quaterphenyl 7a.**

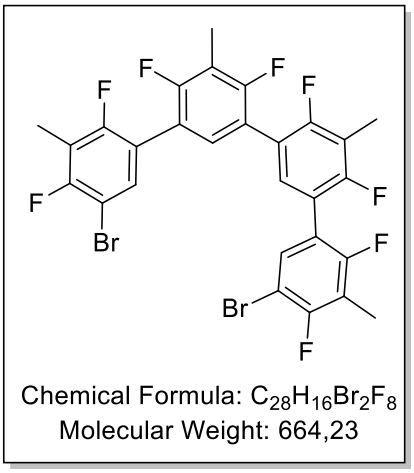

Chemical Formula: $C_{28}H_{16}Br_2F_8$
Molecular Weight: 664,23

The compound was synthesized according to General Procedure **3** using 2,2''',4,4',4'',4''',6',6''-octafluoro-3,3''',5'-trimethyl-1,1':3',1'':3'',1'''-quaterphenyl(**7**) (100g) and 10 equivalent of Iron. Yield 124 mg (98%). White solid.

^{1}H NMR (402 MHz, $CDCl_3$) δ 7.39 (t, J = 7.5 Hz, 1H), 7.14 (q, J = 7.9 Hz, 1H), 2.30 (d, J = 9.4 Hz, 6H).

^{19}F NMR (378 MHz, $CDCl_3$) δ -106.30 – -106.59 (m), -113.72 – -114.06 (m), -114.01 – -114.50 (m), -114.89 – -115.29 (m). **^{13}C NMR** (101 MHz, $CDCl_3$) δ 159.75 – 159.27 (m), 158.77 (dd, J = 8.0, 3.6 Hz), 157.31 – 156.81 (m), 156.51 – 156.15 (m), 131.42 (s), 129.93 (s), 119.77 (dd, J = 18.3, 4.1 Hz), 118.76 – 118.22 (m), 117.78 (d, J = 15.2 Hz), 115.59 – 114.75 (m), 114.13 (s), 103.39 (dd, J = 22.5, 4.2 Hz), 8.04 – 7.85 (m), 7.59 (s).

LIFDI (m/z): [M]+ calcd. for $C_{28}H_{16}Br_2F_8$, 663.9465; found, 663.9457.

- **Synthesis of 2,2'-dibromo-4,4',5,5'-tetrafluoro-1,1'-biphenyl 8a.**

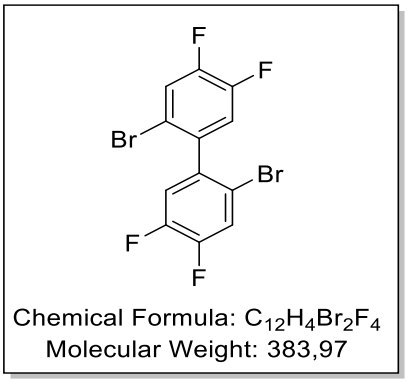

Chemical Formula: $C_{12}H_4Br_2F_4$
Molecular Weight: 383,97

The compound was synthesized according to General Procedure **3** using 3,3',4,4'-tetrafluoro-1,1'-biphenyl (**8**) (100mg) and 30 equivalent of Iron. Yield 129 mg (76%). White solid.

^{1}H NMR (402 MHz, $CDCl_3$) δ 7.49 (ddd, J = 10.1, 6.9, 3.2 Hz, 1H), 7.11 – 7.03 (m, 1H). **^{19}F NMR** (378 MHz, $CDCl_3$) δ -134.21 – -134.55 (m, 2F), -137.60 – -137.89 (m, 2F). **^{13}C NMR** (101 MHz, $CDCl_3$) δ 151.37 (s), 151.24 (s), 150.56 (s), 150.43 (s), 148.85 (s), 148.72 (s), 148.07 (s), 147.94 (s), 136.65 (d, J = 4.8 Hz), 121.82 (s), 121.62 (s), 119.64 (s), 119.46 (s), 117.35 (dd, J = 6.9, 3.5 Hz).

LIFDI (m/z): [M]+ calcd. for $C_{12}H_4Br_2F_4$, 383.8590; found, 383.8589.

- **Synthesis of 2,2'-dibromo-4,4',5,5'-tetrafluoro-1,1'-biphenyl 9a.**

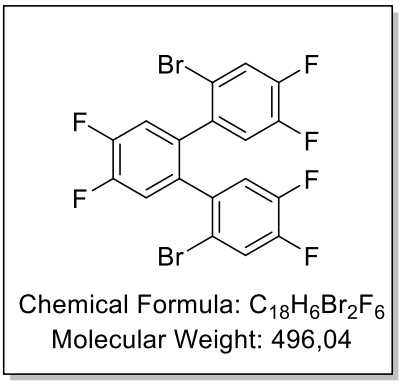

Chemical Formula: $C_{18}H_6Br_2F_6$
Molecular Weight: 496,04

The compound was synthesized according to General Procedure **3** using 3,3",4,4',4",5'-hexafluoro-1,1':2',1"-terphenyl (**9**) (100g) and 2 equivalent of Iron. Yield 122 mg (83%). White solid.

^{1}H NMR (402 MHz, $CDCl_3$) δ 7.37 (dd, J = 9.4, 7.5 Hz, 1H), 7.13 (t, J = 9.1 Hz, 1H), 7.08 – 6.97 (m, 1H). **^{19}F NMR** (378 MHz, $CDCl_3$) δ -134.45 (dt, J = 21.1, 8.8 Hz), -136.48 – -136.71 (m), -137.50 (ddd, J = 21.1, 10.2, 7.6 Hz). **^{13}C NMR** (101 MHz $CDCl_3$) δ 150.97 (d, J = 14.0 Hz), 150.19 (d, J = 12.6 Hz), 148.46 (d, J = 13.4 Hz), 147.71 (d, J = 12.5 Hz), 136.22 – 135.81 (m), 135.73 – 134.70 (m), 122.21 (d, J = 19.9 Hz), 121.44 (d, J = 20.0 Hz), 120.88 – 120.02 (m), 119.97 (s), 119.87 – 118.94 (m), 117.61 (s), 117.11 (dd, J = 7.2, 3.7 Hz).

LIFDI (m/z): [M]+ calcd. for $C_{18}H_6Br_2F_6$, 495.8714; found, 495.8718.

- **Synthesis of 5,5'-dibromo-2,2'-difluoro-1,1'-biphenyl 10a.**

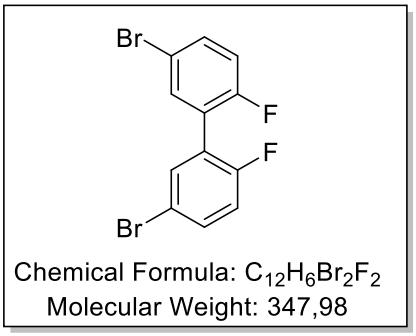

Chemical Formula: $C_{12}H_6Br_2F_2$
Molecular Weight: 347,98

The compound was synthesized according to General Procedure **3** using 2,2'-difluoro-1,1'-biphenyl (**10**) (100mg) and 30 equivalent of Iron. Yield 177 mg (97%). White solid.

^{1}H NMR (402 MHz, $CDCl_3$) δ 7.52 – 7.43 (m, 2H), 7.08 – 7.00 (m, 1H). **^{19}F NMR** (378 MHz, $CDCl_3$) δ -116.15 – -116.73 (m). **^{13}C NMR** (101 MHz, $CDCl_3$) δ 160.02 (d, J = 1.8 Hz), 157.53 (d, J = 1.8 Hz), 134.24 – 133.49 (m), 133.08 (dd, J = 11.1, 6.9 Hz), 117.89 – 117.28 (m), 116.57 (t, J = 1.8 Hz).

HRMS (m/z): [M]+ calcd. for C12H6Br2F2, 345.8795; found, 345.8775.

- **Synthesis of 4,4',5,5'-tetrabromo-2,2'-difluoro-1,1'-biphenyl 10b.**

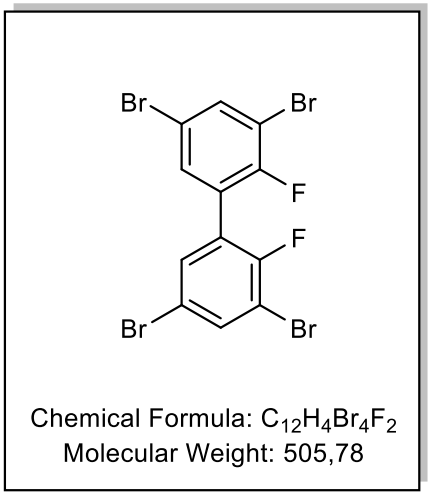

The compound was synthesized according to General Procedure **4** using 2,2'-difluoro-1,1'-biphenyl (**10**) (100mg) and 2 equivalent of Iron. Yield 181 g (68%). White solid.

^{1}H NMR (402 MHz, $CDCl_3$) δ 7.59 (dd, J = 4.5, 3.3 Hz, 1H), 7.48 – 7.44 (m, 1H). **^{19}F NMR** (378 MHz, $CDCl_3$) δ -113.69 – -113.91 (m).**^{13}C NMR** (101 MHz, $CDCl_3$) δ 159.35 (d, J = 1.9 Hz), 156.81 (d, J = 1.9 Hz), 134.92 (t, J = 2.6 Hz), 125.95 – 125.66 (m), 122.26 (dd, J = 10.5, 5.2 Hz), 121.47 (dt, J = 18.7, 10.4 Hz), 119.87 (t, J = 2.0 Hz).

LIFDI (m/z): [M]+ calcd. for $C_{12}H_4Br_4F_2$, 505.6967; found, 505.6969.

- **Synthesis of 3,3'-dibromo-2,2',6,6'-tetrafluoro-1,1'-biphenyl 11a.**

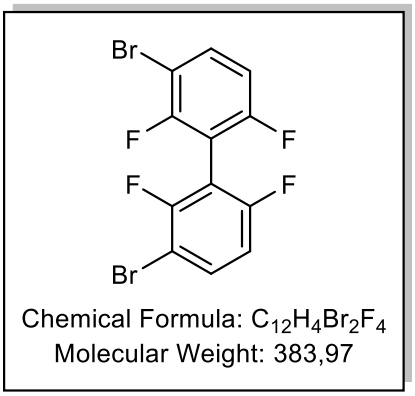

The compound was synthesized according to General Procedure **3** using 2,2',6,6'-tetrafluoro-1,1'-biphenyl (**11**) (100mg) and 30 equivalent of Iron. Yield 137 mg (81%). White solid.

^{1}H NMR (402 MHz, $CDCl_3$) δ 7.68 – 7.57 (m, 1H), 7.00 – 6.90 (m, 1H). **19F** NMR (378 MHz, $CDCl_3$) δ -100.43 – -103.12 (m), -109.75 – -111.59 (m). **^{13}C NMR** (101 MHz, $CDCl_3$) δ 160.67 (s), 158.18 (s), 157.86 (s), 155.38 (s), 134.75 – 134.12 (m), 112.63 (dd, J = 22.9, 4.1 Hz), 107.43 (s), 104.35 (s), 104.14 (s).

LIFDI (m/z): [M]+ calcd. for $C_{12}H_4Br_2F_4$, 383.8589; found, 383.8583.

- **Synthesis of 3,3',5-tribromo-2,2',6,6'-tetrafluoro-1,1'-biphenyl 11b.**

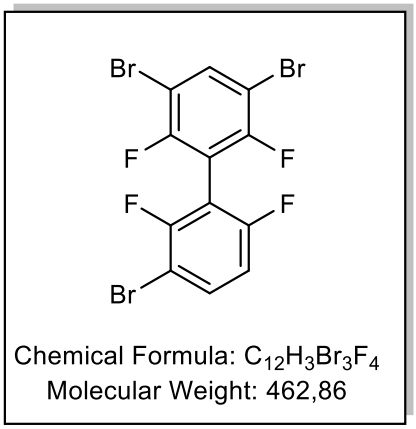

The compound was synthesized according to General Procedure **4** using 2,2',6,6'-tetrafluoro-1,1'-biphenyl (**11**) (100mg) and 2 equivalent of Iron. Yield 30 mg (15%). White solid.

^{1}H NMR (402 MHz, $CDCl_3$) δ 7.97 – 7.76 (m, 1H), 7.65 (ddd, J = 8.8, 7.7, 5.8 Hz, 1H), 6.97 (td, J = 9.0, 1.5 Hz, 1H). **^{19}F NMR** (378 MHz, $CDCl_3$) δ -101.30 – -101.58 (m), -102.20 (q, J = 7.6 Hz), -110.13 – -110.35 (m). **^{13}C NMR** (101 MHz, $CDCl_3$) δ 157.09 (s), 154.65 (s), 136.87 (s), 134.88 (dd, J = 9.5, 1.9 Hz), 112.75 (dd, J = 23.0, 4.1 Hz), 105.00 (s), 104.72 (s).

LIFDI (m/z): [M]+ calcd. for $C_{12}H_3Br_3F_4$, 462.7728; found, 462.7729.

- **Synthesis of 5,5'-dibromo-2,2',4,4'-tetrafluoro-1,1'-biphenyl 12a.**

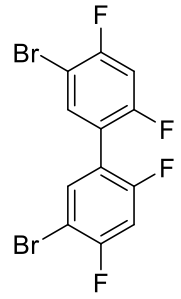

Chemical Formula: $C_{12}H_4Br_2F_4$
Molecular Weight: 383,97

The compound was synthesized according to General Procedure **3** using 2,2',4,4'-tetrafluoro-1,1'-biphenyl (**12**) (100mg) and 30 equivalent of Iron. Yield 119 mg (70%). White solid.

^{1}H NMR (402 MHz, $CDCl_3$) δ 7.53 (dt, J = 19.7, 7.7 Hz, 1H), 7.05 – 6.96 (m, 1H). **^{19}F NMR** (378 MHz, $CDCl_3$) δ -101.84 – -102.10 (m), -110.74 – -111.04 (m).**^{13}C NMR** (101 MHz, $CDCl_3$) δ 160.34 (dd, J = 34.5, 11.4 Hz), 158.42 – 157.22 (m), 134.94 (d, J = 2.5 Hz), 119.15 (d, J = 9.2 Hz), 106.04 – 104.86 (m), 104.02 (d, J = 21.4 Hz).

LIFDI (m/z): [M]+ calcd. for $C_{12}H_4Br_2F_4$, 383.8590; found, 385.8589.

- **Synthesis of 3,3'-dibromo-2,2'-difluoro-5,5'-dimethyl-1,1'-biphenyl 13a.**

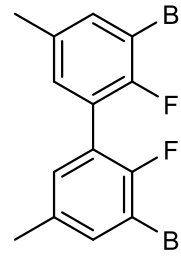

Chemical Formula: $C_{14}H_{10}Br_2F_2$
Molecular Weight: 376,04

The compound was synthesized according to General Procedure **3** using 2,2'-difluoro-5,5'-dimethyl-1,1'-biphenyl (**13**) (100mg) and 30 equivalent of Iron. Yield 124 mg (73%). White solid.

^{1}H NMR (402 MHz, $CDCl_3$) δ 7.35 (dd, J = 5.6, 3.5 Hz, 1H), 7.21 – 7.17 (m, 1H), 2.38 (s, 3H). **^{19}F NMR** (378 MHz, $CDCl_3$) δ -117.08 – -117.15 (m).**^{13}C NMR** (101 MHz, $CDCl_3$) δ 158.69 (d, J = 1.6 Hz), 156.20 (d, J = 1.7 Hz), 133.80 (t, J = 1.9 Hz), 132.73 (s), 132.43 (t, J = 2.6 Hz), 124.66 – 124.36 (m), 121.67 (dd, J = 10.0, 4.6 Hz), 120.11 – 119.47 (m), 119.17 (s), 118.92 (s), 22.04 (d, J = 7.3 Hz).

LIFDI (m/z): [M]+ calcd. for $C_{14}H_{10}Br_2F_2$, 375.9091; found, 375.9087.

- **Synthesis of 2,2',4,4',5,5'-hexabromo-6,6'-difluoro-3,3'-dimethyl-1,1'-biphenyl 13b.**

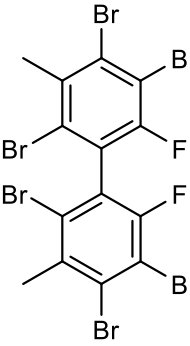

Chemical Formula: $C_{14}H_6Br_6F_2$
Molecular Weight: 691,62

The compound was synthesized according to General Procedure **4** using2,2'-difluoro-5,5'-dimethyl-1,1'-biphenyl (**13**) (100mg) and 2 equivalent of Iron. Yield 270 mg (85%). White solid.

^{1}H NMR (402 MHz, $CDCl_3$) δ 2.74 (s, 1H). **^{19}F NMR** (378 MHz, $CDCl_3$) δ -95.46 (s). **^{13}C NMR** (101 MHz, $CDCl_3$) δ 155.79 (s), 153.32 (s), 136.13 (d, J = 3.8 Hz), 129.22 (s), 125.47 (s), 124.64 (d, J = 19.8 Hz), 113.37 (s), 113.14 (s), 26.10 (s).

LIFDI (m/z): [M]+ calcd. for $C_{14}H_6Br_6F_2$, 691.5471; found, 691.5458.

- **Synthesis of 4,4'-dibromo-2,2',5,5'-tetrafluoro-1,1'-biphenyl 16a.**

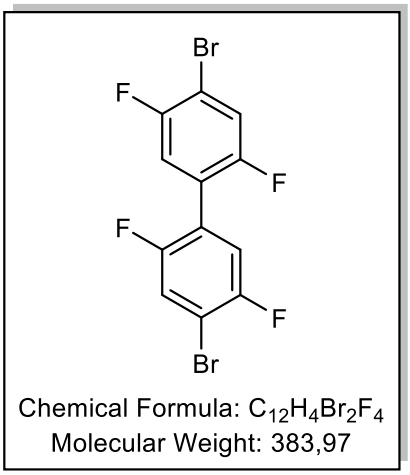

Chemical Formula: $C_{12}H_4Br_2F_4$
Molecular Weight: 383,97

The compound was synthesized according to General Procedure **3** using 2,2',5,5'-tetrafluoro-1,1'-biphenyl (**16**) (100mg) and 2 equivalent of Iron. Yield 157 mg (93%). White solid.

^{1}H NMR (402 MHz, $CDCl_3$) δ 7.38 (ddd, J = 10.7, 7.8, 5.1 Hz, 1H), 7.19 – 7.10 (m, 1H). **^{19}F NMR** (378 MHz, $CDCl_3$) δ -112.40 – -112.72 (m), -117.90 – -118.27 (m).**^{13}C NMR** (101 MHz, $CDCl_3$) δ 156.61 (d, J = 2.8 Hz), 156.31 (dd, J = 2.8, 1.6 Hz), 154.19 (d, J = 2.9 Hz), 153.82 (dd, J = 3.0, 1.6 Hz), 122.39 – 121.78 (m), 121.29 – 120.66 (m), 117.95 (dt, J = 25.6, 3.2 Hz), 110.13 – 109.60 (m).

LIFDI (m/z): [M]+ calcd. for $C_{12}H_4Br_2F_4$, 383.8591; found, 383.8584.

- **Synthesis of 2,4'-dibromo-3',5-difluoro-1,1'-biphenyl 17a.**

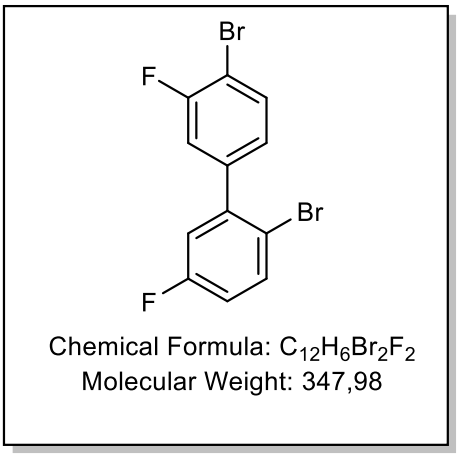

Chemical Formula: $C_{12}H_6Br_2F_2$
Molecular Weight: 347,98

The compound was synthesized according to General Procedure **3** using 3,3'-difluoro-1,1'-biphenyl(**17**) (100mg) and 30 equivalent of Iron. Yield 162 mg (89%). White solid.

^{1}H NMR (402 MHz, $CDCl_3$) δ 7.65 – 7.55 (m, 2H), 7.31 – 7.25 (m, 1H), 7.22 – 7.17 (m, 1H), 7.03 – 6.91 (m, 2H). **^{19}F NMR** (378 MHz, $CDCl_3$) δ -106.24 – -106.52 (m), -114.06 – -114.68 (m). **^{13}C NMR** (101 MHz, $CDCl_3$) δ 162.70 (s), 160.61 (s), 160.25 (s), 158.16 (s), 134.13 – 133.84 (m), 123.54 (d, J = 3.5 Hz), 118.06 (s), 117.83 (s), 117.47 (d, J = 3.4 Hz), 117.10 (s), 116.88 (s), 114.96 (s), 114.73 (s), 109.04 (s), 108.83 (s).

LIFDI (m/z): [M]+ calcd. for $C_{12}H_6Br_2F_2$, 347.8777; found, 347.8774.

6.5. Synthesis of F_{16}[8]CMP and F_{24}[12]CMP.

2,2'-Bipyridine (4.40 equiv.) and 1,5-cyclooctadiene (COD) (8 equiv.) were dissolved in dry, degassed THF in a flame-driedflask under glove box conditions. Then $Ni(COD)_2$ (4.40 equiv.) was added, generating a purple solution. **7a** (1.00 equiv.) was dissolved in dry THF and added dropwise at a rate of approx.1 drop per second. The flask was stirred for 1 hours at 60 oC under the exclusion of light. The mixture was filtered through a silica plug and eluted with THF before the solvent was removed under reduced pressure. The crude product was purified by HPLC (DCM/MeOH 3:7) yielding F_{16}[8]CMP 1% and trace of F_{24}[12]CMP.

- **F_{16}[8]CMP 18.**

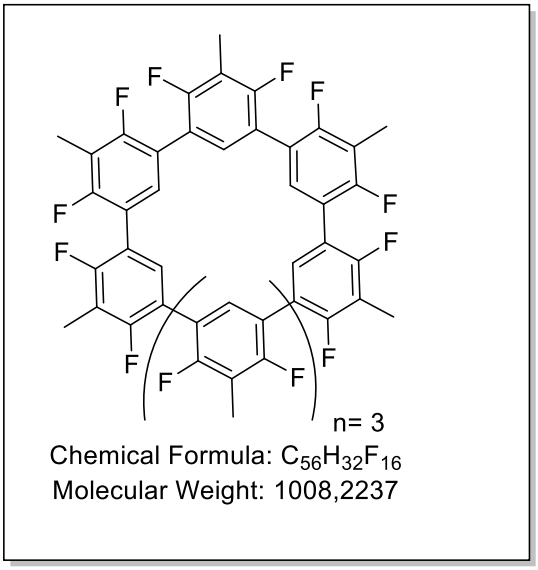

^{1}H NMR (400 MHz, $CDCl_3$) δ 7.02 (tt, J = 13.3, 6.8 Hz, 1H), 2.24 (s, 3H). **^{19}F NMR** (378 MHz, $CDCl_3$) δ -113.50 (t, *J* = 312.9 Hz). **^{13}C NMR** (101 MHz, $CDCl_3$) δ 129.64 (s), 119.30 (s), 114.14 (s), 113.93 (s), 7.79 (s).
LIFDI (m/z): [M]+ calcd. for $C_{56}H_{32}F_{16}$, 1008.2243; found, 1008.2237.

- **F_{24}[12]CMP 19.**

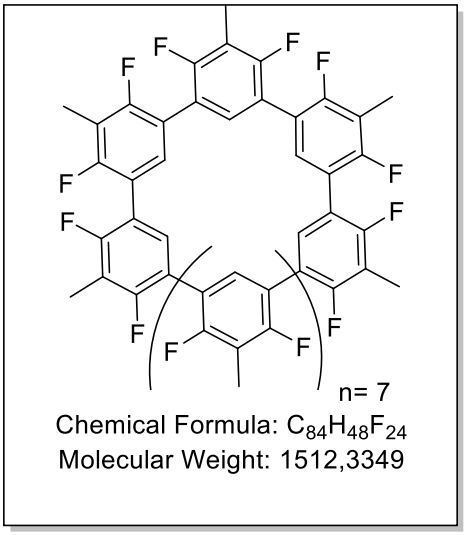

LIFDI (m/z): [M]+ calcd. for $C_{84}H_{48}F_{24}$, 1512.3367; found, 1512.3349.

6.6. LooP reaction of 2,2',4,4'-tetrafluoro-3,3'-dimethyl-1,1'-biphenyl 5.

A glass tube for microwave reactor was charged with 2 ml of HMPA, **5** (25mg, 1 equiv) and t-BuOK (66 mg, 3 equiv. to one fluorine). The tube was put in microwave reactor and stirred for 3 h at 120 °C. After cooling to room temperature, the mixture was filtrated through silica using hexane as a solvent (50/50 mixture of hexane/ethylacetate was used when the polar products were formed). The organic solvent was evaporated under the reduced pressure yielding 14 mg (63%).

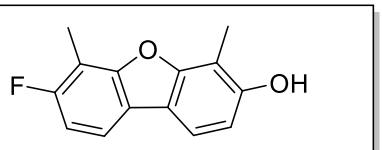

Chemical Formula: $C_{14}H_{11}FO_2$
Molecular Weight: 230,24

^{1}H NMR (600 MHz, $CDCl_3$) δ 7.57 – 7.50 (m, 2H), 6.99 (dd, J = 9.6, 8.7 Hz, 1H), 6.80 (d, J = 8.2 Hz, 1H), 2.50 – 2.45 (m, 6H). **^{19}F NMR** (564 MHz, $CDCl_3$) δ -121.69 – -121.90 (m). **^{13}C NMR** (151 MHz, $CDCl_3$) δ 160.66 (s), 159.06 (s), 156.87 (d, J = 2.1 Hz), 155.76 (d, J = 10.5 Hz), 153.01 (s), 117.55 (s), 116.92 (d, J = 10.2 Hz), 111.11 (s), 9.30 – 6.20 (m).

LIFDI (m/z): [M]+ calcd. for $C_{14}H_{11}F_1O_2$, 347.0737; found, 347.0770.

6.7. Extending Fluorinated Oligophenylenes.

- **Synthesis of 2,2'',4',6'-tetrafluoro-5'-methyl-1,1':3',1''-terphenyl 23.**

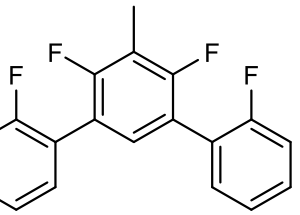

Chemical Formula: $C_{19}H_{12}F_4$
Molecular Weight: 316,30

The 1,5-dibromo-2,4-difluoro-3-methylbenzene (250mg, 1 equiv) and (2-fluorophenyl)boronic acid (6 equiv) were dissolved in 15ml of dioxane: H_2O (10:1) mixture containing potassium carbonate (725 mg, 6 equiv) and Pd(PPh3)4 (607 mg, 60%) as catalyst. The reaction mixture was stirred under reflux and argon atmosphere for 15 hours. After the completion of the reaction, the solvent was evaporated and the residue was purified by silica gel column chromatography eluting with (Hexane-Hexane: DCM 10:1) to afford the product as a white solid (249 mg, 90 %). **^{1}H NMR** (402 MHz, CD_2Cl_2) δ 7.44 (tdd, J = 7.4, 6.4, 1.7 Hz, 4H), 7.35 – 7.19 (m, 5H), 2.38 (t, J = 2.0 Hz, 3H). **^{19}F NMR** (378 MHz, CD_2Cl_2) δ -115.04 – -115.22 (m), -115.22 – -115.37 (m). **^{13}C NMR** (101 MHz, CD_2Cl_2) δ 161.13 (s), 159.51 (dd, J = 8.6, 2.9 Hz), 158.67 (s), 157.02 (dd, J = 9.1, 3.0 Hz), 131.73 – 131.48 (m), 130.40 – 129.62 (m), 124.24 (d, J = 3.6 Hz), 122.91 (d, J = 15.1 Hz), 119.45 – 119.04 (m), 115.78 (s), 115.57 (s), 114.08 (s), 113.86 (s), 113.65 (s), 7.29 (t, J = 4.3 Hz).

LIFDI (m/z): [M]+ calcd. for $C_{19}H_{12}F_4$, 316.0869; found, 316.0867.

- **Synthesis of 2,2'-(4,6-difluoro-5-methyl-1,3-phenylene)bis(1-fluoronaphthalene) 25.**

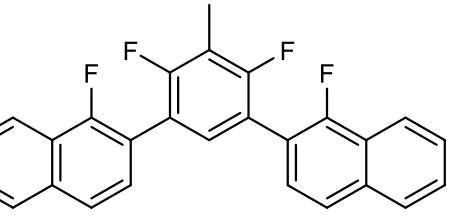

Chemical Formula: $C_{27}H_{16}F_4$
Molecular Weight: 416,42

The compound was synthesized according to General Procedure **2** using 1,5-dibromo-2,4-difluoro-3-methylbenzene (250 mg). Yield 316 g (87 %). White solid.

^{1}H NMR (402 MHz, $CDCl_3$) δ 8.24 – 8.14 (m, 2H), 7.88 (d, J = 7.6 Hz, 2H), 7.70 (d, J = 8.5 Hz, 2H), 7.63 – 7.53 (m, 4H), 7.53 – 7.40 (m, 3H), 2.39 (s, 3H). **^{19}F NMR** (378 MHz, $CDCl_3$) δ -114.22 – -114.95 (m), -124.09 – -124.71 (m). **^{13}C NMR** (101 MHz, $CDCl_3$) δ 159.58 (d, J = 9.0 Hz), 157.10 (d, J = 9.0 Hz), 156.61 (s), 154.10 (s), 134.52 (d, J = 5.0 Hz), 130.71 (s), 127.93 (d, J = 3.3 Hz), 127.42 (d, J = 2.9 Hz),

127.13 (s), 126.60 (d, J = 1.8 Hz), 123.62 (dd, J = 21.2, 10.8 Hz), 120.95 (d, J = 6.0 Hz), 119.56 – 119.15 (m), 116.98 (d, J = 14.5 Hz), 114.25 (s), 114.03 (s), 113.81 (s), 7.70 (t, J = 4.4 Hz).

LIFDI (m/z): [M]+ calcd. for $C_{27}H_{16}F_4$, 416.1182; found, 416.1179.

- **Synthesis of 2,2''',4',4'',6',6''-hexafluoro-5',5''-dimethyl-1,1':3',1'':3'',1'''-quaterphenyl 26.**

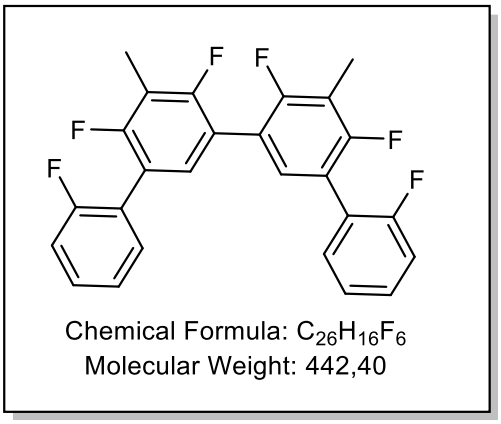

The compound was synthesized according to General Procedure **2** 5,5'-dibromo-2,2',4,4'-tetrafluoro-3,3'-dimethyl-1,1'-biphenyl (250 mg). Yield 223 mg (83 %). White solid.

^{1}H NMR (402 MHz, CD_2Cl_2) δ 7.41 (s, 2H), 7.31 – 7.14 (m, 3H), 2.33 (s, 3H). **^{19}F NMR** (378 MHz, CD_2Cl_2) δ -115.09 – -115.64 (m). **^{13}C NMR** (101 MHz, CD_2Cl_2) δ 161.01 (s), 159.49 (s), 158.54 (s), 156.99 (s), 131.52 (s), 130.49 – 129.83 (m), 124.20 (d, J = 3.5 Hz), 122.76 (d, J = 15.2 Hz), 115.73 (s), 115.51 (s), 7.30 (s).

LIFDI (m/z): [M]+ calcd. for $C_{26}H_{16}F_6$, 442.1150; found, 442.1147.

- **Synthesis of 2,2'-(4,4',6,6'-tetrafluoro-5,5'-dimethyl-[1,1'-biphenyl]-3,3'-diyl)bis(1-fluoronaphthalene) 27.**

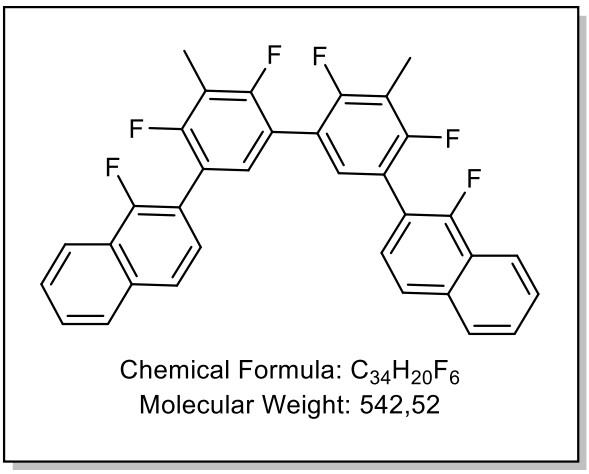

The compound was synthesized according to General Procedure **2** 5,5'-dibromo-2,2',4,4'-tetrafluoro-3,3'-dimethyl-1,1'-biphenyl (250 mg). Yield 240 mg (73 %). White solid.

^{1}H NMR (402 MHz, $CDCl_3$) δ 8.20 – 8.12 (m, 1H), 7.87 (d, J = 7.6 Hz, 1H), 7.68 (d, J = 8.5 Hz, 1H), 7.60 – 7.52 (m, 2H), 7.46 (t, J = 7.7 Hz, 1H), 7.37 (t, J = 8.2 Hz, 1H), 2.37 (s, 3H). **^{19}F NMR** (378 MHz, $CDCl_3$) δ -114.34 (dd, J = 9.2, 8.1 Hz), -114.67 – -114.88 (m), -124.37 (dd, J = 17.3, 7.0 Hz). **^{13}C NMR** (101 MHz, $CDCl_3$) δ 159.67 – 159.31 (m), 157.06 – 156.84 (m), 156.58 (s), 154.06 (s), 134.51 (d, J = 5.0 Hz), 130.44 (s), 127.86 (d, J = 1.8 Hz), 127.40 (d, J = 2.9 Hz), 127.13 (s), 126.59 (d, J = 1.8 Hz), 123.59 (dd, J = 18.6, 10.7 Hz), 120.93 (d, J = 6.0 Hz), 119.36 (d, J = 19.1 Hz), 118.84 – 118.64 (m), 116.85 (d, J = 14.5 Hz), 113.99 (s), 7.67 (s).

LIFDI (m/z): [M]+ calcd. for $C_{34}H_{20}F_6$, 542.1463; found, 542.1461.

- **Synthesis of 2,2'''',4',4'',4''',6',6'',6'''-octafluoro-5',5'',5'''-trimethyl-1,1':3',1'':3'',1''':3''',1''''-quinquephenyl 28.**

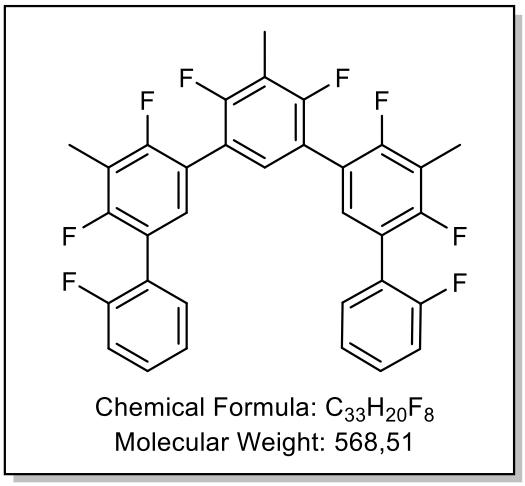

The compound was synthesized according to General Procedure **2** 5,5''-dibromo-2,2'',4,4',4'',6'-hexafluoro-3,3'',5'-trimethyl-1,1':3',1''-terphenyl (250 mg). Yield 214 mg (81 %). White solid.

^{1}H NMR (402 MHz, CD_2Cl_2) δ 7.40 (dd, J = 13.4, 6.4 Hz, 3H), 7.32 – 7.14 (m, 5H), 2.34 (d, J = 4.2 Hz, 6H). **^{19}F NMR** (378 MHz, CD_2Cl_2) δ -114.90 – -115.53 (m). **^{13}C NMR** (101 MHz, CD_2Cl_2) δ 161.02 (s), 159.50 (d, J = 9.1 Hz), 158.55 (d, J = 4.6 Hz), 157.02 (d, J = 9.0 Hz), 131.53 (s), 130.53 – 129.83 (m), 129.71 (s), 124.19 (d, J = 3.5 Hz), 122.75 (d, J = 15.4 Hz), 119.25 (dd, J = 17.0, 4.1 Hz), 118.57 (td, J = 17.0, 5.8 Hz), 115.72 (s), 115.50 (s), 113.92 (td, J = 21.9, 8.4 Hz), 7.28 (t, J = 4.3 Hz).

- **Synthesis of 2,2'-(4,4',4'',6,6',6''-hexafluoro-5,5',5''-trimethyl-[1,1':3',1''-terphenyl]-3,3''-diyl)bis(1-fluoronaphthalene) 29.**

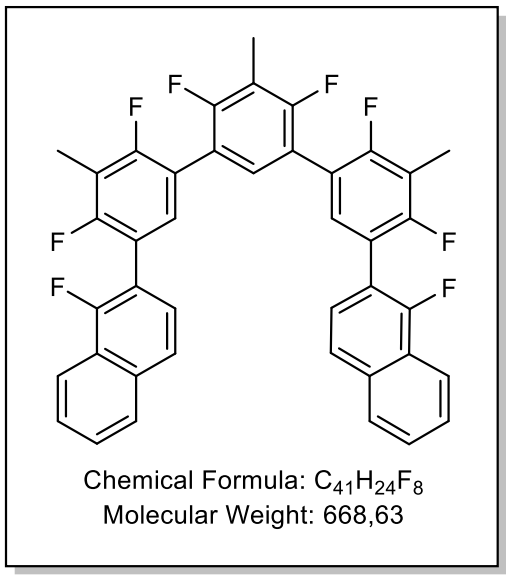

The compound was synthesized according to General Procedure **2** 5,5''-dibromo-2,2'',4,4',4'',6'-hexafluoro-3,3'',5'-trimethyl-1,1':3',1''-terphenyl (250 mg). Yield 195 mg (63 %). White solid.

^{1}H NMR (502 MHz, $CDCl_3$) δ 8.20 – 8.15 (m, 4H), 7.88 (d, J = 7.6 Hz, 4H), 7.69 (d, J = 8.5 Hz, 4H), 7.60 – 7.54 (m, 8H), 7.47 (t, J = 7.6 Hz, 4H), 7.37 (t, J = 8.0 Hz, 4H), 7.31 (t, J = 7.9 Hz, 2H), 2.37 (s, 17H). **^{19}F NMR** (473 MHz, $CDCl_3$) δ -114.14 – -114.35 (m), -114.40 – -114.57 (m), -114.74 (d, J = 5.0 Hz), -124.34 (dd, J = 17.3, 6.9 Hz). **^{13}C NMR** (126 MHz, $CDCl_3$) δ 159.31 (dd, J = 26.5, 8.2 Hz), 157.34 (dd, J = 24.5, 8.5 Hz), 156.34 (s), 154.32 (s), 134.52 (d, J = 4.9 Hz), 130.43 (s), 130.23 (s), 127.87 (s), 127.41 (d, J = 2.8 Hz), 127.15 (s), 126.61 (d, J = 1.7 Hz), 123.60 (dd, J = 22.5, 10.7 Hz), 120.93 (d, J = 5.9 Hz), 119.40 (dd, J = 17.3, 4.0 Hz), 118.93 – 118.42 (m), 116.84 (d, J = 14.5 Hz), 114.18 (s), 114.11 – 113.76 (m), 7.66 (t, J = 4.2 Hz).

LIFDI (m/z): [M]+ calcd. for $C_{41}H_{24}F_8$, 668.1744; found, 668.1734.

- **Synthesis of 2,2'-(4,4',4'',4''',6,6',6'',6'''-octafluoro-5,5',5'',5'''-tetramethyl-[1,1':3',1'':3'',1'''-quaterphenyl]-3,3'''-diyl)bis(1-fluorophenyl) 30.**

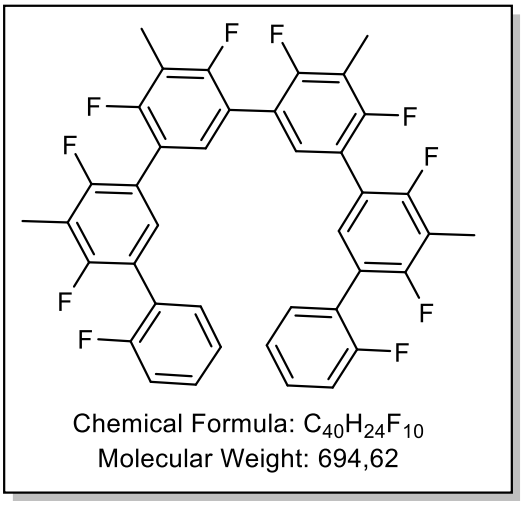

The compound was synthesized according to General Procedure **2** 5,5'''-dibromo 2,2''',4,4',4'',4''',6',6''-octafluoro-3,3''',5',5''-tetramethyl-1,1':3',1'':3'',1'''-quaterphenyl (250 mg). Yield 170 mg (65 %). White solid.

^{1}H NMR (402 MHz, CD_2Cl_2) δ 7.43 – 7.35 (m, 1H), 7.29 – 7.12 (m, 2H), 2.31 (d, J = 2.0 Hz, 3H). **^{19}F NMR** (378 MHz, cd2cl2) δ -115.03 – -115.32 (m), -115.34 – -115.56 (m). **^{13}C NMR** (101 MHz, cd2cl2) δ 131.51 (s), 130.21 – 129.83 (m), 124.18 (d, J = 3.6 Hz), 115.71 (s), 115.49 (s), 113.85 (s), 7.29 (s).

LIFDI (m/z): [M]+ calcd. for $C_{40}H_{24}F_{10}$, 694.1712; found, 694.1711.

- **Synthesis of 2,2'-(4,4',4'',4''',6,6',6'',6'''-octafluoro-5,5',5'',5'''-tetramethyl-[1,1':3',1'':3'',1'''-quaterphenyl]-3,3'''-diyl)bis(1-fluoronaphthalene) 31.**

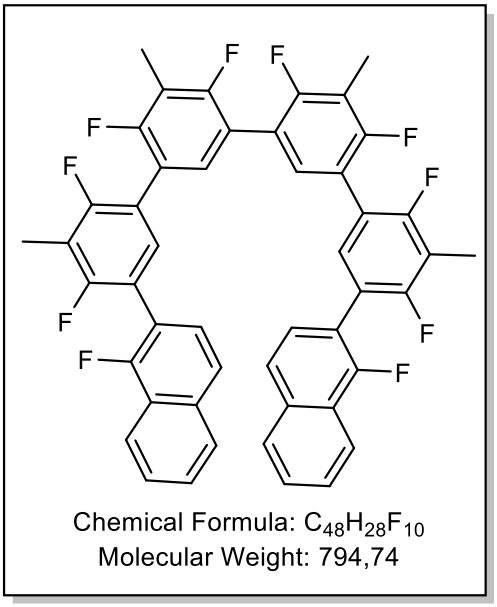

The compound was synthesized according to General Procedure **2** 5,5'''-dibromo-2,2''',4,4',4'',4''',6',6''-octafluoro-3,3''',5',5''-tetramethyl-1,1':3',1'':3'',1'''-quaterphenyl (250 mg). Yield 170 mg (57 %). White solid.

^{1}H NMR (402 MHz, $CDCl_3$) δ 8.17 – 8.10 (m, 1H), 7.90 – 7.82 (m, 1H), 7.66 (d, J = 8.5 Hz, 1H), 7.60 – 7.51 (m, 2H), 7.43 (t, J = 7.7 Hz, 1H), 7.32 (t, J = 8.0 Hz, 1H), 7.24 (s, 1H), 2.33 (d, J = 4.8 Hz, 6H). **^{19}F NMR** (378 MHz, $CDCl_3$) δ -114.19 – -114.38 (m), -114.50 (d, J = 26.5 Hz), -114.70 – -114.92 (m), -124.39 (dd, J = 17.2, 6.8 Hz). **^{13}C NMR** (101 MHz, $CDCl_3$) δ 160.41 – 157.39 (m), 157.79 – 155.25 (m), 154.37 – 153.18 (m), 134.49 (d, J = 5.1 Hz), 130.38 (s), 130.16 (s), 127.83 (s), 127.39 (d, J = 2.9 Hz), 127.14 (s), 126.60 (s), 123.57 (dd, J = 18.0, 10.7 Hz), 120.91 (d, J = 6.0 Hz), 118.64 (s), 113.96 (s), 7.64 (s).

LIFDI (m/z): [M]+ calcd. for $C_{48}H_{28}F_{10}$, 794.2025; found, 794.2019.

6.8. Synthesis of 4,4'-difluoro-3,3'-bis(2''',4,4',4'',4''',6,6',6''-octafluoro-5'''-(1-fluoronaphthalen-2-yl)-3''',5,5',5''-tetramethyl-[1,1':3',1'':3'',1'''-quaterphenyl]-3-yl)-1,1'-binaphthalene 32.

A solution of **31** (0.1 mmol) in dichloromethane (10 mL) containing two to three drops of Trifluoromethanesulfonic acid at 0 ºC was treated with DDQ (2 equivalent per C-C bond formation), and the solution immediately took on a darkgreen coloration. The progress of the reaction was monitored by TLC . After completion of the reaction, it was quenched with a saturated aqueous solution of $NaHCO_3$ (20 mL). The dichloromethane layer was separated and washed with water and brine solution and dried over anhydrous $MgSO_4$ and filtered. Removal of the solvent in vacuo afforded the crude product was by purified by flash chromatography Hex/DCM 90/10. resulting compound **32** in 30% yield.

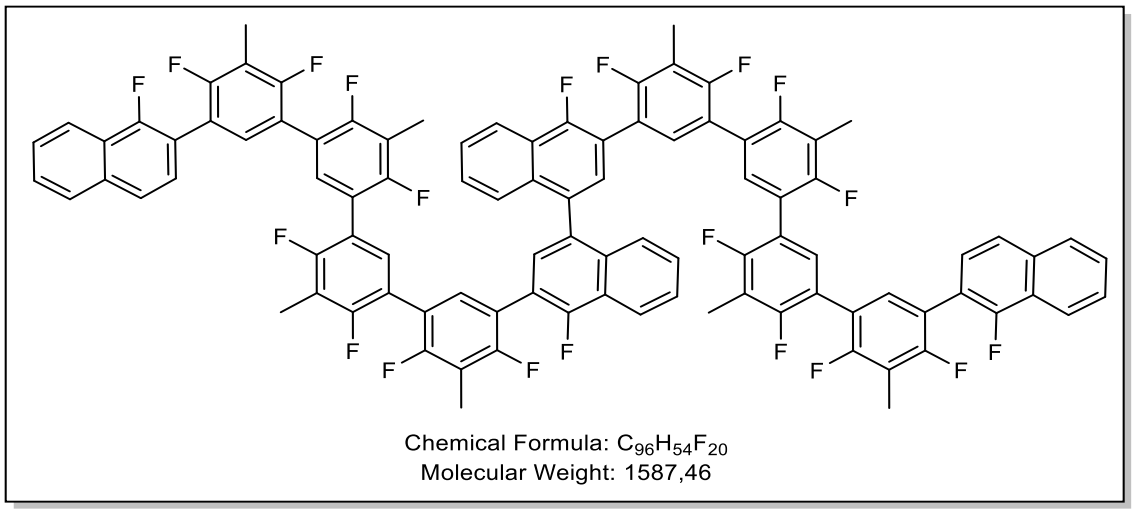

^{1}H NMR (600 MHz, CD_2Cl_2) δ 8.24 (t, J = 9.4 Hz, 3H), 7.60 (dt, J = 8.5, 2.8 Hz, 3H), 7.49 (t, J = 6.1 Hz, 3H), 7.47 – 7.39 (m, 6H), 7.36 (t, J = 7.7 Hz, 1H), 7.30 (t, J = 7.6 Hz, 2H), 7.22 (s, 3H), 2.36 – 2.23 (m, 18H). **^{19}F NMR** (564 MHz, CD_2Cl_2) δ -111.82 – -116.80 (m), -122.09 – -126.08 (m). **^{13}C NMR** (151 MHz, CD_2Cl_2) δ 159.55 – 158.73 (m), 157.59 – 156.96 (m), 155.99 (d, J = 2.6 Hz), 154.30 (d, J = 2.2 Hz), 134.28 – 132.97 (m), 130.87 – 129.09 (m), 127.85 – 127.04 (m), 127.04 – 126.43 (m), 126.43 – 125.82 (m), 124.12 – 122.95 (m), 121.59 – 120.50 (m), 119.89 – 117.90 (m), 116.31 (dd, J = 14.9, 3.7 Hz), 114.56 – 113.53 (m), 8.23 – 6.33 (m).

LIFDI (m/z): [M]+ calcd. for $C_{96}H_{54}F_{20}$, 1587.3779; found, 1587.3767.

6.9. LOOP reactions.

- **LOOP Reaction of 23 using t-BuOK.**

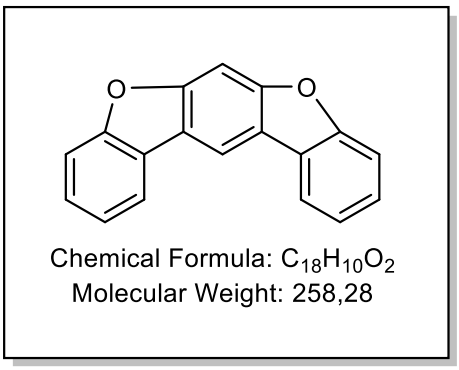

The compound was synthesized according to General Procedure **5** using 2,2",4',6'-tetrafluoro-5'-methyl-1,1':3',1"-terphenyl (20mg). Yield 10.4 mg (64 %). White solid.

^{1}H NMR (600 MHz, $CDCl_3$) δ 8.44 (s, 1H), 8.03 (d, J = 7.6 Hz, 2H), 7.72 (s, 1H), 7.58 (d, J = 8.1 Hz, 2H), 7.45 (t, J = 7.7 Hz, 2H), 7.37 (t, J = 7.4 Hz, 2H). **^{13}C NMR** (151 MHz, CHLOROFORM-D) δ 156.97 (d, J = 2.5 Hz), 156.14 (d, J = 10.2 Hz), 126.73 (s), 122.95 (s), 120.36 (s), 111.66 (s), 111.49 (s), 95.49 (s).

LIFDI (m/z): [M]+ calcd. for $C_{18}H_{10}O_2$, 258.0675; found, 258.0674.

- **LOOP Reaction of 23 using t-BuOK.**

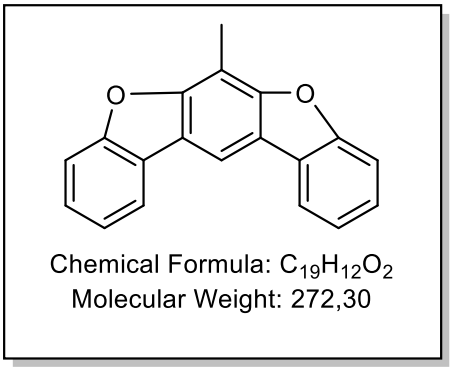

The compound was synthesized according to General Procedure **5** using 2,2",4',6'-tetrafluoro-5'-methyl-1,1':3',1"-terphenyl (20 mg). Yield 5 mg (31 %). White solid.

^{1}H NMR (600 MHz, $CDCl_3$) δ 8.27 (s, 1H), 8.01 (d, J = 7.5 Hz, 2H), 7.59 (d, J = 8.1 Hz, 2H), 7.45 – 7.42 (m, 2H), 7.36 (dd, J = 11.0, 3.8 Hz, 2H), 2.80 (s, 3H). **^{13}C NMR** (151 MHz, CHLOROFORM-D) δ 156.90 (d, J = 4.0 Hz), 154.89 (d, J = 4.6 Hz), 126.48 (s), 122.77 (s), 120.43 (s), 111.61 (s), 108.38 (d, J = 19.4 Hz), 9.04 (d, J = 2.0 Hz).

LIFDI (m/z): [M]+ calcd. for $C_{19}H_{11}O_2$, 271.0753; found, 271.0752.

- **LOOP Reaction of 23 using Na_2S/ TBAB.**

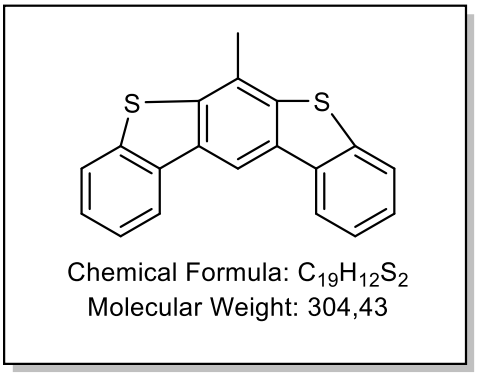

The compound was synthesized according to General Procedure **6** using 2,2",4',6'-tetrafluoro-5'-methyl-1,1':3',1"-terphenyl (15 mg). Yield 15 mg (78 %). White solid.

^{1}H NMR (600 MHz, $CDCl_3$) δ 8.67 (s, 1H), 8.25 – 8.21 (m, 2H), 7.86 (td, J = 7.3, 2.2 Hz, 2H), 7.53 – 7.44 (m, 4H), 2.74 (s, 3H). ^{13}C NMR (151 MHz, $CDCl_3$) δ 139.14 (s), 138.35 (s), 136.13 (s), 133.39 (s), 126.66 (s), 125.24 (s), 124.44 (d, J = 11.6 Hz), 123.08 – 122.73 (m), 121.50 (s), 111.54 (s),19.30 (s).

LIFDI (m/z): [M]+ calcd. for $C_{19}H_{12}S_2$, 304.0330; found, 304.0362

- **LOOP Reaction of 25 using t-BuOK.**

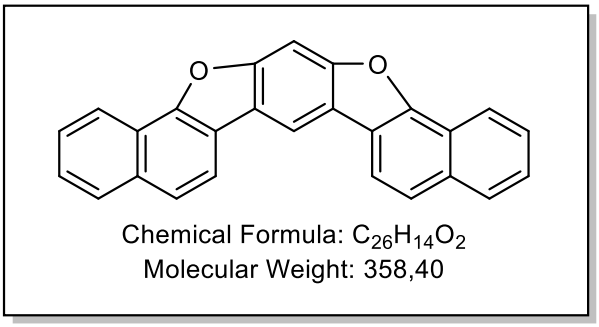

The compound was synthesized according to General Procedure **5** using 2,2'-(4,6-difluoro-5-methyl-1,3-phenylene)bis(1-fluoronaphthalene) (20 mg). Yield 14.8 mg (86 %). White solid.

^{1}H NMR (402 MHz, $CDCl_3$) δ 8.55 (s, 1H), 8.48 (d, *J* = 8.2 Hz, 2H), 8.15 – 8.10 (m, 2H), 8.02 (d, *J* = 9.5 Hz, 3H), 7.84 (d, *J* = 8.4 Hz, 2H), 7.67 (t, *J* = 7.5 Hz, 2H), 7.57 (t, *J* = 7.5 Hz, 2H).

- **LOOP Reaction of 25 using Na_2S/ TBAB.**

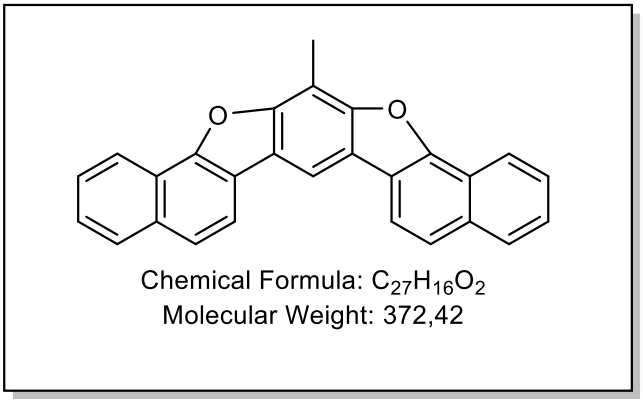

The compound was synthesized according to General Procedure **5** using 2,2'-(4,6-difluoro-5-methyl-1,3-phenylene)bis(1-fluoronaphthalene) (20 mg). Yield 1 mg (6 %). White solid.

^{1}H NMR (402 MHz, $CDCl_3$) δ 8.54 (dd, *J* = 12.8, 8.4 Hz, 3H), 8.38 (s, 1H), 8.11 (d, *J* = 8.4 Hz, 2H), 8.01 (dd, *J* = 7.9, 4.1 Hz, 2H), 7.83 (t, *J* = 9.1 Hz, 2H), 7.71 – 7.63 (m, 2H), 7.57 (dd, *J* = 13.4, 5.3 Hz, 2H), 3.04 – 2.99 (m, 3H).

- **LOOP Reaction of 23 using t-BuOK.**

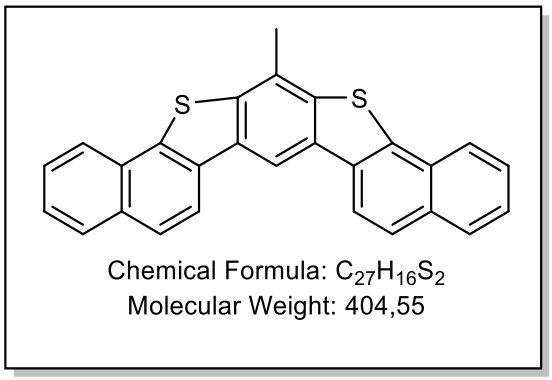

The compound was synthesized according to General Procedure **6** using 2,2'-(4,6-difluoro-5-methyl-1,3-phenylene)bis(1-fluoronaphthalene) (20 mg). Yield 10.8 mg (56 %). White solid.

^{1}H NMR (402 MHz, $CDCl_3$) δ 8.88 (s, 1H), 8.34 (d, *J* = 8.6 Hz, 2H), 8.19 (d, *J* = 8.0 Hz, 2H), 8.01 (d, *J* = 8.1 Hz, 2H), 7.94 (d, *J* = 8.6 Hz, 2H), 7.65 (t, *J* = 7.4 Hz, 2H), 7.58 (t, *J* = 7.4 Hz, 2H), 2.97 (s, 3H).

VII. BIBLIOGRAPHY.

[1] I. Meric, M. Y. Han, A. F. Young, B. Ozyilmaz, P. Kim, K. L. Shepard, *Nature Nanotech* **2008**, *3*, 654–659.

[2] *Quelques propriétés typiques des corps solides* **1935**, *tome 5, no 3*, 177–222.

[3] U. K. Sur, *International Journal of Electrochemistry* **2012**, *2012*, 1–12.

[4] A. B. Kuzmenko, E. Van Heumen, F. Carbone, D. Van Der Marel, *Phys. Rev. Lett.* **2008**, *100*, 117401.

[5] C. Lee, X. Wei, J. W. Kysar, J. Hone, *Science* **2008**, *321*, 385–388.

[6] E. Ivanov, R. Kotsilkova, H. Xia, Y. Chen, R. K. Donato, K. Donato, A. P. Godoy, R. Di Maio, C. Silvestre, S. Cimmino, V. Angelov, *Applied Sciences* **2019**, *9*, 1209.

[7] A. A. Balandin, *Nature Mater* **2011**, *10*, 569–581.

[8] Y.-M. Lin, C. Dimitrakopoulos, K. A. Jenkins, D. B. Farmer, H.-Y. Chiu, A. Grill, Ph. Avouris, *Science* **2010**, *327*, 662–662.

[9] J. Wu, W. Pisula, K. Müllen, *Chem. Rev.* **2007**, *107*, 718–747.

[10] X. Wang, L. Zhi, K. Müllen, *Nano Lett.* **2008**, *8*, 323–327.

[11] K. Kim, J.-Y. Choi, T. Kim, S.-H. Cho, H.-J. Chung, *Nature* **2011**, *479*, 338–344.

[12] D. Akinwande, L. Tao, Q. Yu, X. Lou, P. Peng, D. Kuzum, *IEEE Nanotechnology Mag.* **2015**, *9*, 6–14.

[13] L. Huang, M. Zhang, C. Li, G. Shi, *J. Phys. Chem. Lett.* **2015**, *6*, 2806–2815.

[14] S. Zhu, T. Li, *ACS Nano* **2014**, *8*, 2864–2872.

[15] S. S. Varghese, S. Lonkar, K. K. Singh, S. Swaminathan, A. Abdala, *Sensors and Actuators B: Chemical* **2015**, *218*, 160–183.

[16] C. S. Boland, U. Khan, C. Backes, A. O'Neill, J. McCauley, S. Duane, R. Shanker, Y. Liu, I. Jurewicz, A. B. Dalton, J. N. Coleman, *ACS Nano* **2014**, *8*, 8819–8830.

[17] N. S. Green, M. L. Norton, *Analytica Chimica Acta* **2015**, *853*, 127–142.

[18] X. Feng, W. Pisula, K. Müllen, *Pure and Applied Chemistry* **2009**, *81*, 2203–2224.

[19] M. Müller, C. Kübel, F. Morgenroth, V. S. Iyer, K. Müllen, *Carbon* **1998**, *36*, 827–831.

[20] G. Klärner, M. Müller, F. Morgenroth, M. Wehmeier, T. Soczka-Guth, K. Müllen, *Synthetic Metals* **1997**, *84*, 297–301.

[21] Q. Ai, K. Jarolimek, S. Mazza, J. E. Anthony, C. Risko, *Chem. Mater.* **2018**, *30*, 947–957.

[22] A. A. Balandin, S. Ghosh, W. Bao, I. Calizo, D. Teweldebrhan, F. Miao, C. N. Lau, *Nano Lett.* **2008**, *8*, 902–907.

[23] K. Ho, M. Boutchich, C. Su, R. Moreddu, E. S. R. Marianathan, L. Montes, C. Lai, *Advanced Materials* **2015**, *27*, 6519–6525.

[24] K. Harigaya, Y. Kobayashi, K. Takai, J. r me Ravier, T. Enoki, *J. Phys.: Condens. Matter* **2002**, *14*, L605–L611.

[25] L. Chen, Y. Hernandez, X. Feng, K. Müllen, *Angew Chem Int Ed* **2012**, *51*, 7640–7654.

[26] J. Zhao, C. He, R. Yang, Z. Shi, M. Cheng, W. Yang, G. Xie, D. Wang, D. Shi, G. Zhang, *Appl. Phys. Lett.* **2012**, *101*, 063112.

[27] L. Zhi, K. Müllen, *J. Mater. Chem.* **2008**, *18*, 1472.

[28] Z. Liu, S. Fu, X. Liu, A. Narita, P. Samorì, M. Bonn, H. I. Wang, *Advanced Science* **2022**, *9*, 2106055.

[29] Y. Gu, Z. Qiu, K. Müllen, *J. Am. Chem. Soc.* **2022**, *144*, 11499–11524.

[30] D. Zanetti, O. Matuszewska, G. Giorgianni, C. Pezzetta, N. Demitri, D. Bonifazi, *JACS Au* **2023**, *3*, 3045–3054.

[31] W. Matsuoka, H. Ito, D. Sarlah, K. Itami, *Nat Commun* **2021**, *12*, 3940.

[32] D. P. Das, K. M. Parida, *Journal of Molecular Catalysis A: Chemical* **2006**, *253*, 70–78.

[33] G. W. Gribble, *Chem. Soc. Rev.* **1999**, *28*, 335–346.

[34] Alison. Butler, J. V. Walker, *Chem. Rev.* **1993**, *93*, 1937–1944.

[35] Norio. Miyaura, Akira. Suzuki, *Chem. Rev.* **1995**, *95*, 2457–2483.

[36] K. Sonogashira, Y. Tohda, N. Hagihara, *TetrahedronLetters,* **1975**, *50*, pp 4467-4470,.
[37] R. F. Heck, J. P. Nolley, *J. Org. Chem.* **1972**, *37*, 2320–2322.
[38] D. Milstein, J. K. Stille, *J. Am. Chem. Soc.* **1978**, *100*, 3636–3638.
[39] A. S. Guram, S. L. Buchwald, *J. Am. Chem. Soc.* **1994**, *116*, 7901–7902.
[40] E. R. Darzi, B. M. White, L. K. Loventhal, L. N. Zakharov, R. Jasti, *J. Am. Chem. Soc.* **2017**, *139*, 3106–3114.
[41] E. C. Rüdiger, S. Koser, F. Rominger, J. Freudenberg, U. H. F. Bunz, *Chemistry A European J* **2018**, *24*, 9919–9927.
[42] J. Cai, P. Ruffieux, R. Jaafar, M. Bieri, T. Braun, S. Blankenburg, M. Muoth, A. P. Seitsonen, M. Saleh, X. Feng, K. Müllen, R. Fasel, *Nature* **2010**, *466*, 470–473.
[43] K. Smith, G. A. El-Hiti, M. E. W. Hammond, D. Bahzad, Z. Li, C. Siquet, *J. Chem. Soc., Perkin Trans. 1* **2000**, 2745–2752.
[44] Q. Fan, L. Yan, M. W. Tripp, O. Krejčí, S. Dimosthenous, S. R. Kachel, M. Chen, A. S. Foster, U. Koert, P. Liljeroth, J. M. Gottfried, *Science* **2021**, *372*, 852–856.
[45] M. Kolmer, R. Zuzak, A. K. Steiner, L. Zajac, M. Engelund, S. Godlewski, M. Szymonski, K. Amsharov, *Science* **2019**, *363*, 57–60.
[46] M. Kolmer, A.-K. Steiner, I. Izydorczyk, W. Ko, M. Engelund, M. Szymonski, A.-P. Li, K. Amsharov, *Science* **2020**, *369*, 571–575.
[47] M. Feofanov, V. Akhmetov, R. Takayama, K. Amsharov, *Angewandte Chemie* **2021**, *133*, 5259–5263.
[48] M. Feofanov, V. Akhmetov, R. Takayama, K. Amsharov, *Org. Biomol. Chem.* **2021**, *19*, 7172–7175.
[49] A.-K. Steiner, D. I. Sharapa, S. I. Troyanov, J. Nuss, K. Amsharov, *Chemistry – A European Journal* **2021**, *27*, 6223–6229.
[50] F. Ullmann, J. Bielecki, *Ber. Dtsch. Chem. Ges.* **1901**, *34*, 2174–2185.
[51] S. Iijima, *Nature* **1991**, *354*, 56–58.
[52] P. Avouris, M. Freitag, V. Perebeinos, *Nature Photon* **2008**, *2*, 341–350.
[53] V. Sgobba, D. M. Guldi, *Chem. Soc. Rev.* **2009**, *38*, 165–184.
[54] D. A. Heller, S. Baik, T. E. Eurell, M. S. Strano, *Advanced Materials* **2005**, *17*, 2793–2799.
[55] M. Zhang, S. Fang, A. A. Zakhidov, S. B. Lee, A. E. Aliev, C. D. Williams, K. R. Atkinson, R. H. Baughman, *Science* **2005**, *309*, 1215–1219.
[56] R. Jasti, J. Bhattacharjee, J. B. Neaton, C. R. Bertozzi, *J. Am. Chem. Soc.* **2008**, *130*, 17646–17647.
[57] H. Takaba, H. Omachi, Y. Yamamoto, J. Bouffard, K. Itami, *Angew Chem Int Ed* **2009**, *48*, 6112–6116.
[58] S. Yamago, Y. Watanabe, T. Iwamoto, *Angew Chem Int Ed* **2010**, *49*, 757–759.
[59] T. Iwamoto, Y. Watanabe, Y. Sakamoto, T. Suzuki, S. Yamago, *J. Am. Chem. Soc.* **2011**, *133*, 8354–8361.
[60] H. A. Staab, F. Binnig, *Chem. Ber.* **1967**, *100*, 293–305.
[61] D. J. Cram, T. Kaneda, R. C. Helgeson, S. B. Brown, C. B. Knobler, E. Maverick, K. N. Trueblood, *J. Am. Chem. Soc.* **1985**, *107*, 3645–3657.
[62] D. J. Cram, R. A. Carmack, R. C. Helgeson, *J. Am. Chem. Soc.* **1988**, *110*, 571–577.
[63] W. Pisula, M. Kastler, C. Yang, V. Enkelmann, K. Müllen, *Chemistry An Asian Journal* **2007**, *2*, 51–56.
[64] J. M. W. Chan, T. M. Swager, *Tetrahedron Letters* **2008**, *49*, 4912–4914.
[65] R. Scholl, J. Mansfeld, *Ber. Dtsch. Chem. Ges.* **1910**, *43*, 1734–1746.
[66] G. Baddeley, *J. Chem. Soc.* **1950**, *0*, 994–997.
[67] B. T. King, J. Kroulík, C. R. Robertson, P. Rempala, C. L. Hilton, J. D. Korinek, L. M. Gortari, *J. Org. Chem.* **2007**, *72*, 2279–2288.
[68] P. Rempala, J. Kroulík, B. T. King, *J. Am. Chem. Soc.* **2004**, *126*, 15002–15003.
[69] L. Zhai, R. Shukla, S. H. Wadumethrige, R. Rathore, *J. Org. Chem.* **2010**, *75*, 4748–4760.

[70] Jones. J. Kenner, *Journal of the Chemical Society (Resumed),* **1933**, 363-368.
[71] L. Zhai, R. Shukla, R. Rathore, *Org. Lett.* **2009**, *11*, 3474–3477.
[72] Rooney, J. J., and R. C. Pink., *Proc. Chem. Soc.* **1961**.
[73] G. A. Clowes, *J. Chem. Soc., C* **1968**, 2519.
[74] Z. Huang, *Sci. Bull.* **2015**, *60(16):*, 1391–1394.
[75] A. McKillop, A. G. Turrell, D. W. Young, E. C. Taylor, *J. Am. Chem. Soc.* **1980**, *102,* 6504–6512.
[76] J. Doussot, A. Guy, C. Ferroud, *Tetrahedron Letters* **2000**, *41*, 2545–2547.
[77] B. Feringa, H. Wynberg', *BIOORGANIC CHEMISTRY* **1978**, *7*, 397–408.
[78] K. Wang, M. Lu, A. Yu, X. Zhu, Q. Wang, *J. Org. Chem.* **2009**, *74*, 935–938.
[79] M. Wang, Y. Hu, Z. Li, M. Wu, Z. Liu, B. Su, A. Yu, Y. Liu, Q. Wang, *New York* **2010**.
[80] I. M. Matheson (Née Davidson), O. C. Musgrave, C. J. Webster, *Chem. Commun. (London)* **1965**, *0*, 278–279.
[81] J. A. Ashenhurst, *Chem. Soc. Rev.* **2010**, *39*, 540–548.
[82] Peter. Kovacic, M. B. Jones, *Chem. Rev.* **1987**, *87*, 357–379.
[83] A. Kirste, G. Schnakenburg, F. Stecker, A. Fischer, S. R. Waldvogel, *Angewandte Chemie* **2010**, *122*, 983–987.
[84] M. Müller, C. Kübel, K. Müllen, *Chem. Eur. J.* **1998**, *4*, 2099–2109.
[85] H. Arslan, F. J. Uribe-Romo, B. J. Smith, W. R. Dichtel, *Chem. Sci.* **2013**, *4*, 3973.
[86] J. Liu, A. Narita, S. Osella, W. Zhang, D. Schollmeyer, D. Beljonne, X. Feng, K. Müllen, *J. Am. Chem. Soc.* **2016**, *138*, 2602–2608.
[87] A. Tsumura, H. Koezuka, T. Ando, *Appl. Phys. Lett.* **1986**, *49*, 1210.
[88] H. E. Katz, *J. Mater. Chem.,* **1997**, *7(3)*, 369–376.
[89] C. D. Dimitrakopoulos, P. R. L. Malenfant, *Adv. Mater.* **2002**, *14*, 2.
[90] H. Sirringhaus, P. J. Brown, R. H. Friend, M. M. Nielsen, K. Bechgaard, B. M. W. Langeveld-Voss, A. J. H. Spiering, R. A. J. Janssen, E. W. Meijer, P. Herwig, D. M. de Leeuw, **1999**.
[91] A. Dodabalapur, A. J. Lovinger, *Appl. Phys. Lett.* **1996**, *69*, 4108.
[92] K. Xiao, Y. Liu, T. Qi, W. Zhang, F. Wang, J. Gao, W. Qiu, Y. Ma, G. Cui, S. Chen, X. Zhan, G. Yu, J. Qin, W. Hu, D. Zhu, *J. AM. CHEM. SOC.* **2005**, *127*, 13281–13286.
[93] H. Ebata, E. Miyazaki, T. Yamamoto, K. Takimiya, *Org. Lett.,* **2007**, *Vol. 9*, No. 22,.
[94] J. G. Laquindanum, H. E. Katz, A. J. Lovinger, *J. Am. Chem. Soc.* **1998**, *Vol. 120*, No. 4.
[95] X. M. Hong, H. E. Katz, A. J. Lovinger, B.-C. Wang, K. Raghavachari, *Chem. Mater.* **2001**, *13*, 4686–4691.
[96] M. Mushrush, A. Facchetti, M. Lefenfeld, H. E. Katz, T. J. Marks, *J. AM. CHEM. SOC.* **2003**, *125*, 9414–9423.
[97] A. Facchetti, J. Letizia, M.-H. Yoon, M. Mushrush, H. E. Katz, T. J. Marks, *Chem. Mater.* **2004**, *16*, 4715–4727.
[98] H. Sirringhaus, K. Mullenb, *J. Mater. Chem.,* **1999**, *9*, 2095–2101.
[99] P. Gao, D. Beckmann, H. N. Tsao, X. Feng, V. Enkelmann, M. Baumgarten, W. Pisula, K. Mullen, *Adv. Mater.* **2009**, *21*, 213–216.
[100] P. Gao, D. Beckmann, H. N. Tsao, X. Feng, V. Enkelmann, W. Pisulaz, *Chem. Commun.,* **2008**, 1548–1550.
[101] P. Gao, X. Feng, X. Yang, V. Enkelmann, M. Baumgarten, K. Mullen, *J. Org. Chem.* **2008**, *73*, 9207–9213.
[102] P. Gao, D. Cho, X. Yang, V. Enkelmann, M. Baumgarten, K. Müllen, *Chem. Eur. J.* **2010**, *16*, 5119–5128.
[103] M. Feofanov, V. Akhmetov, R. Takayama, K. Y. Amsharov, *J. Org. Chem.* **2021**, *86*, 14759–14766.
[104] H. Shudo, P. Wiesener, E. Kolodzeiski, K. Mizukami, D. Imoto, H. Mönig, S. Amirjalayer, H. Sakamoto, H. Klaasen, B. J. Ravoo, N. Kimizuka, A. Yagi, K. Itami, *Nat Commun* **2025**, *16*, 1074.
[105] M. Parisien, D. Valette, K. Fagnou, *J. Org. Chem. ,* **2005**, *70,* 7578–7584.
[106] T. Okazaki, M. Nakagawa, T. Futemma, T. Kitagawa, *J. Phys. Org. Chem.* **2015**.
[107] C. S. Nervig, P. J. Waller, D. Kalyani, *Org. Lett.,* **2012**, *Vol. 14,* No. 18,.

[108] P. C. Solórzano, F. Brigante, A. B. Pierini, L. B. Jimenez, *J. Org. Chem.* **2018**.
[109] H. Tsuji, E. Nakamura, *Acc. Chem. Res.* **2017**.
[110] T. Okamoto, H. Dosei, M. Mitani, Y. Murata, H. Ishii, K. Nakamura, M. Yamagishi, M. Yano, J. Takeya, *Asian J. Org. Chem.* **2018**, *7*, 2309–2314.
[111] M. S. Sundar et al., *Tetrahedron: Asymmetry* **2016**, *27*, 777–781.
[112] M. A. Truong, K. Nakano, *Beilstein J. Org. Chem.* **2016**.
[113] A. Vladimir et al., *RSC Adv.* **2020**, *10*, 10879.
[114] Rapson, W. S.; Shuttleworth, R. G.; van, Niekerk, J. N, W S Rapson, *J. Chem. Soc.* **1943**, 326−327.
[115] A.-K. Steiner, K. Y. Amsharov, *Angewandte Chemie International Edition* **2017**, *56*, 14732–14736.
[116] D. Bulfield, S. M. Huber, *J. Org. Chem.* **2017**, *82*, 13188–13203.
[117] R. Erami, D. Díaz-García, S. Prashar, A. Rodríguez-Diéguez, M. Fajardo, M. Amirnasr, S. Gómez-Ruiz, *Catalysts* **2017**, *7*, 76.
[118] H. Shudo, M. Kuwayama, Y. Segawa, A. Yagi, K. Itami, *Chem. Commun.* **2023**, *59*, 13494–13497.
[119] B. Kurscheid, L. Belkoura, B. Hoge, *Organometallics* **2012**, *31*, 1329–1334.

VIII. Appendix – Spectra (NMR, MS).

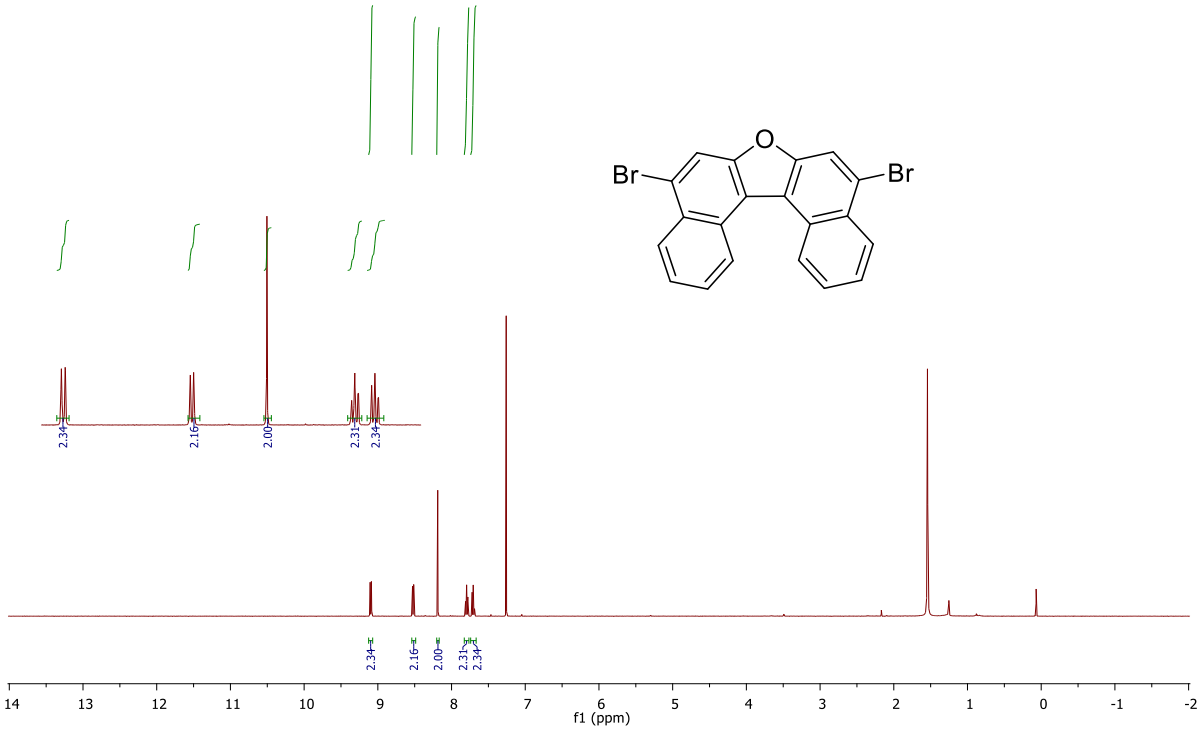

Figure A1. ^{1}H NMR (400 MHz, $CDCl_3$) of 2.

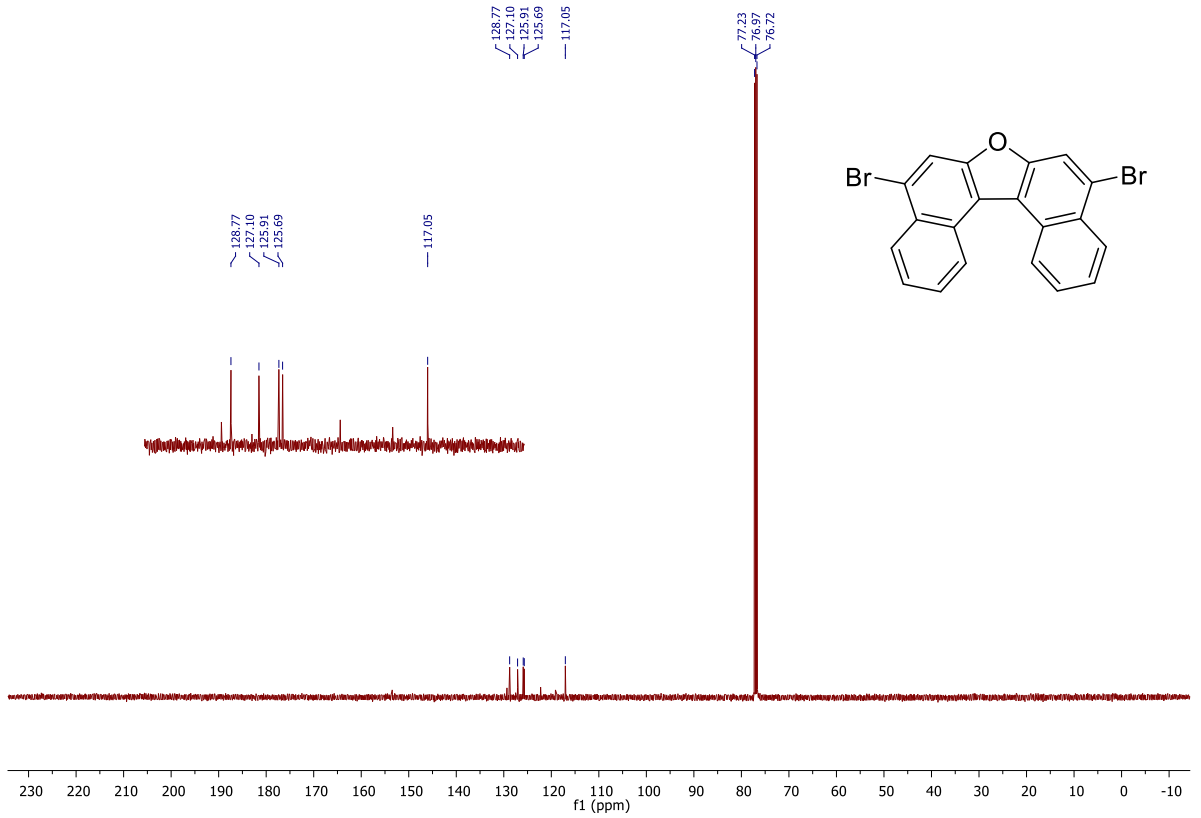

Figure A2. ^{13}C NMR (101 MHz, $CDCl_3$) of 2.

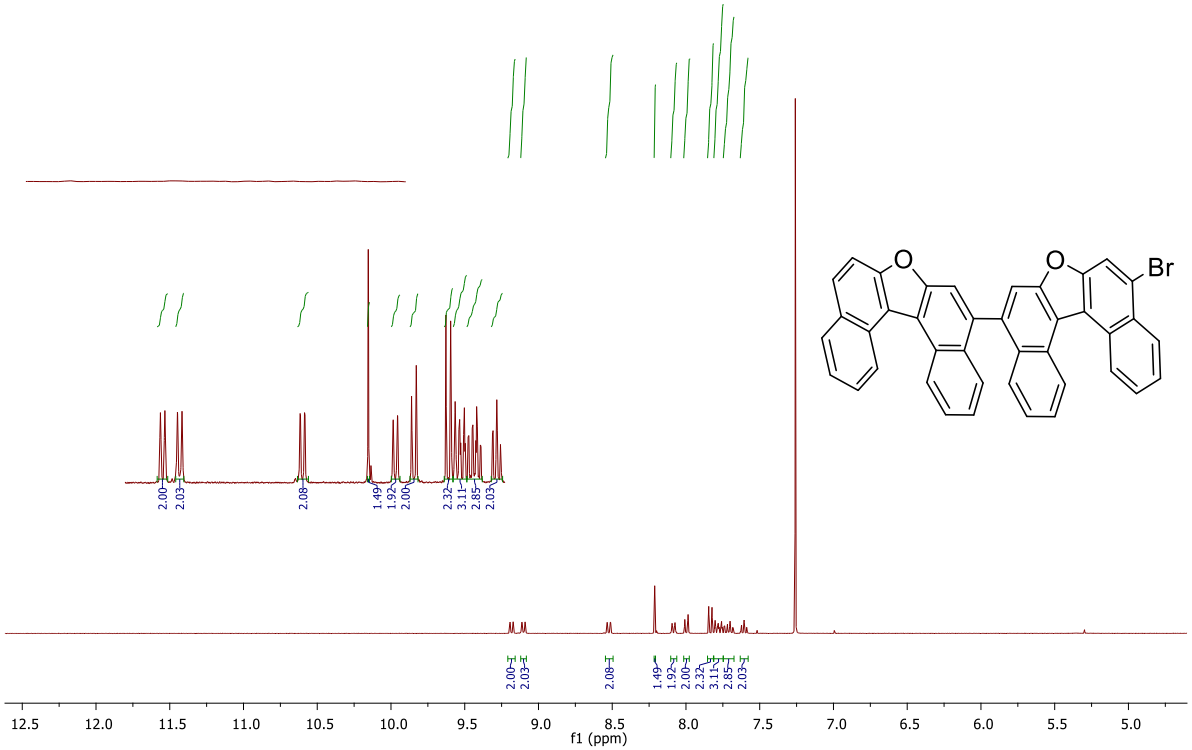

Figure A3. ^{1}H NMR (400 MHz, $CDCl_3$) of 3.

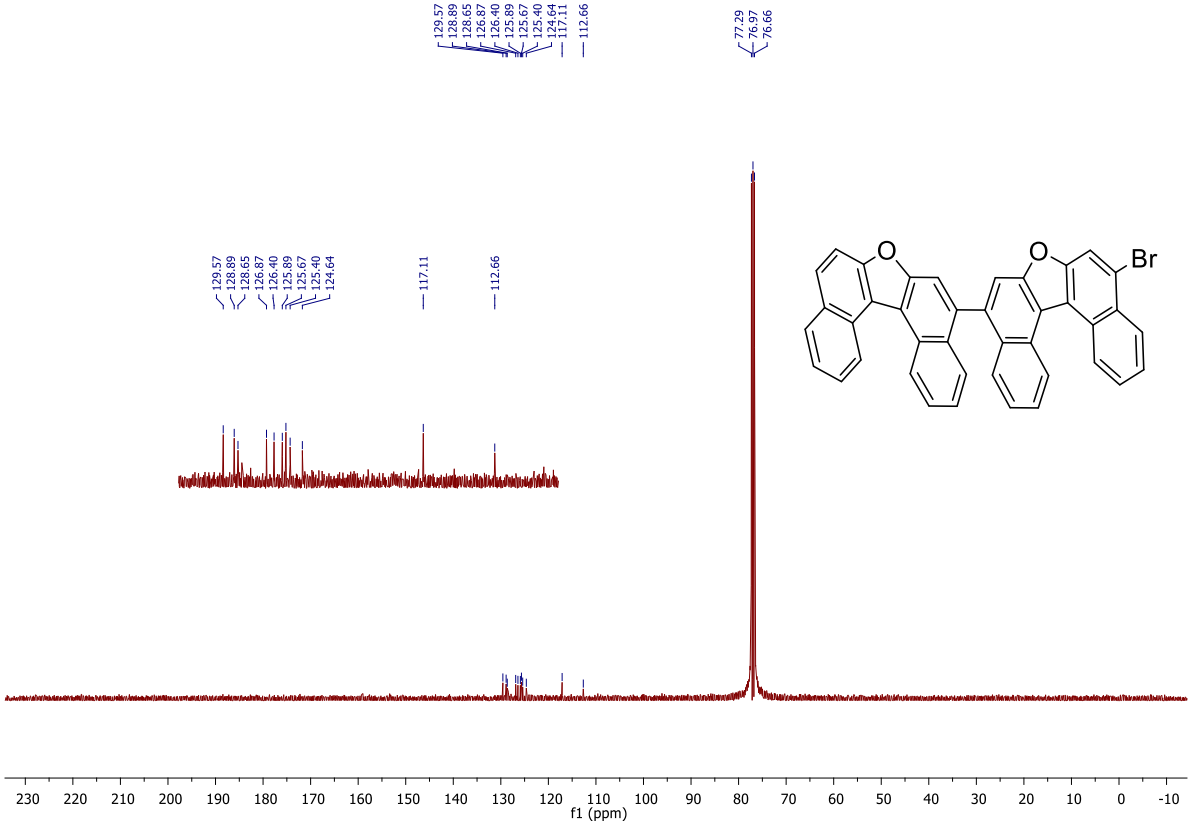

Figure A4. ^{13}C NMR (101 MHz, $CDCl_3$) of 3.

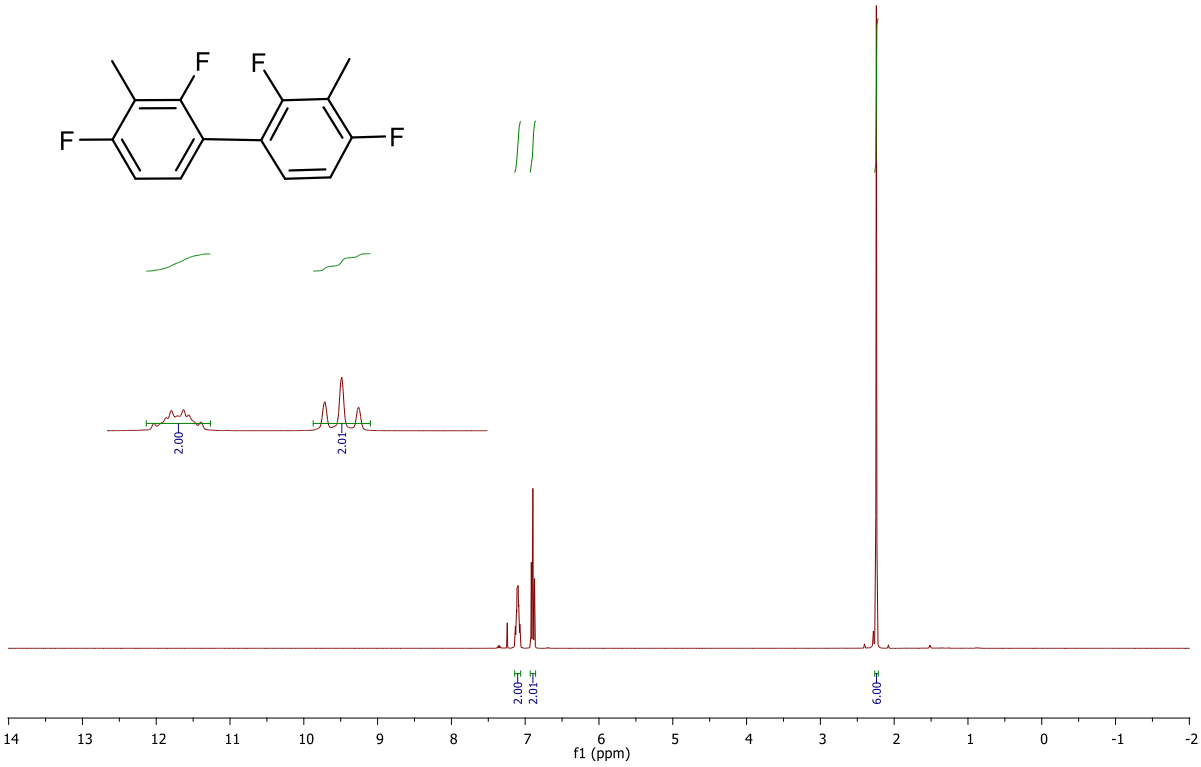

Figure A5. ^{1}H NMR (400 MHz, $CDCl_3$) of 5.

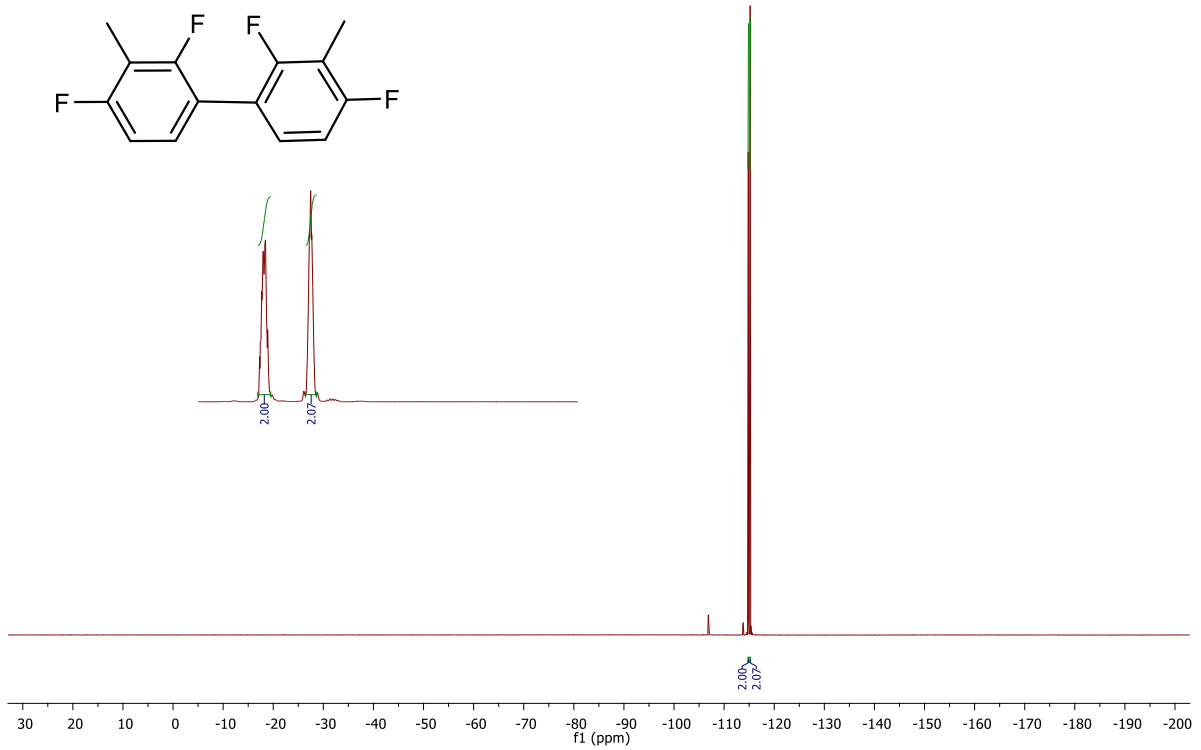

Figure A6. ^{19}F NMR (376 MHz, $CDCl_3$) of 5.

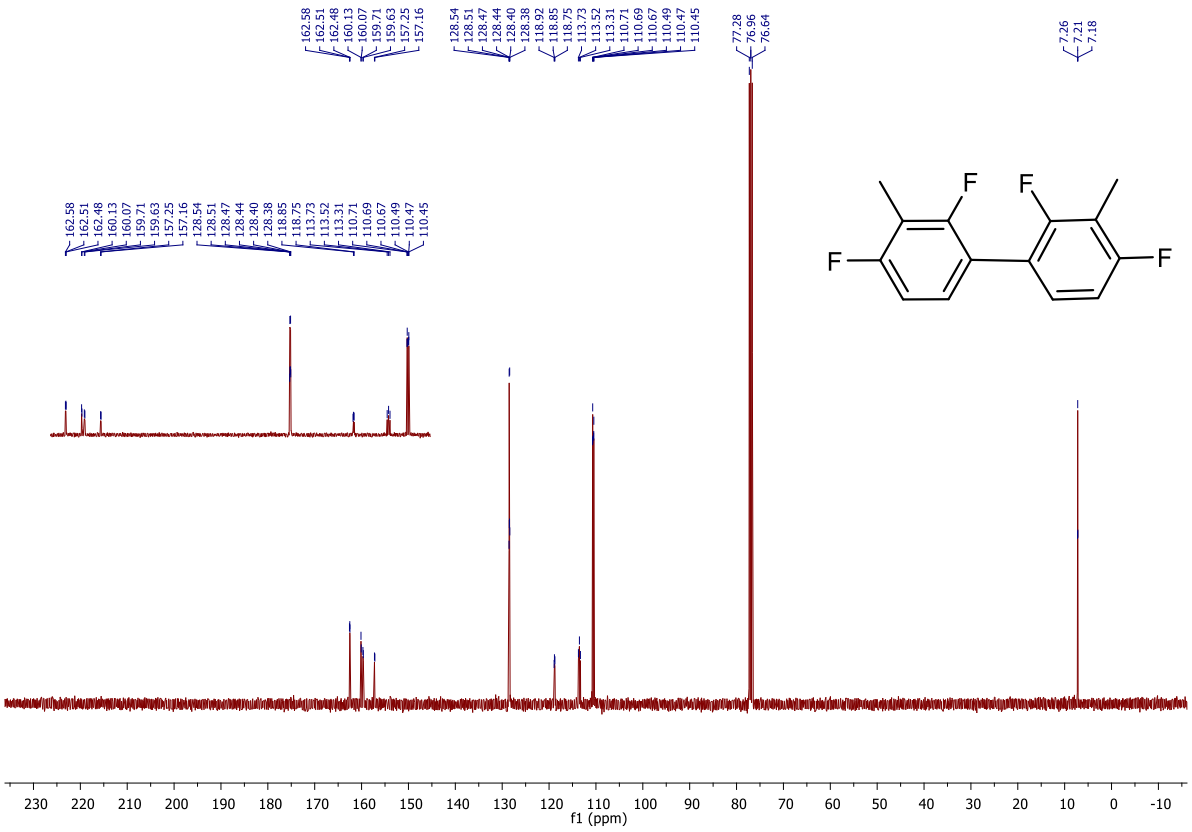

Figure A7. ^{13}C NMR (101 MHz, $CDCl_3$) of 5.

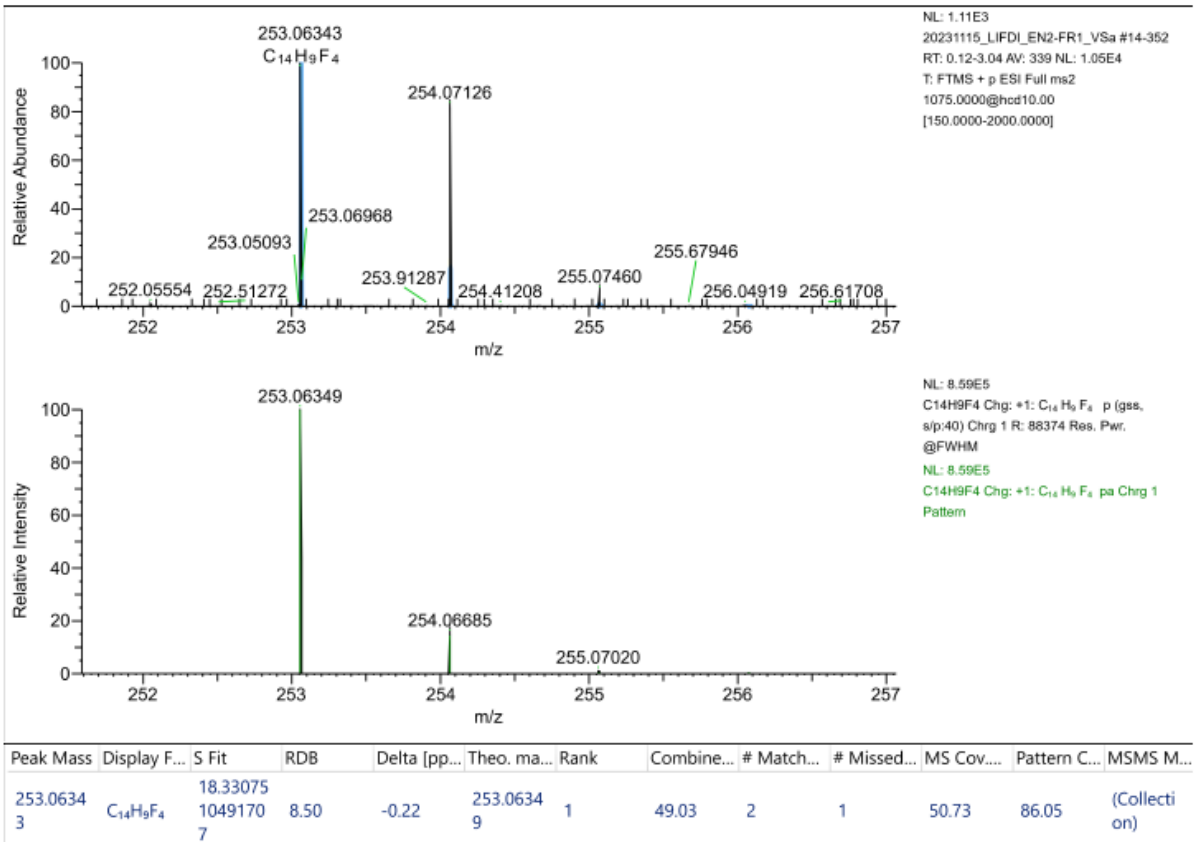

Peak Mass	Display F...	S Fit	RDB	Delta [pp...	Theo. ma...	Rank	Combine...	# Match...	# Missed...	MS Cov....	Pattern C...	MSMS M...
253.06343	$C_{14}H_9F_4$	18.33075 1049170 7	8.50	-0.22	253.06349	1	49.03	2	1	50.73	86.05	(Collection)

Figure A8. HRMS (LIFDI) of 5.

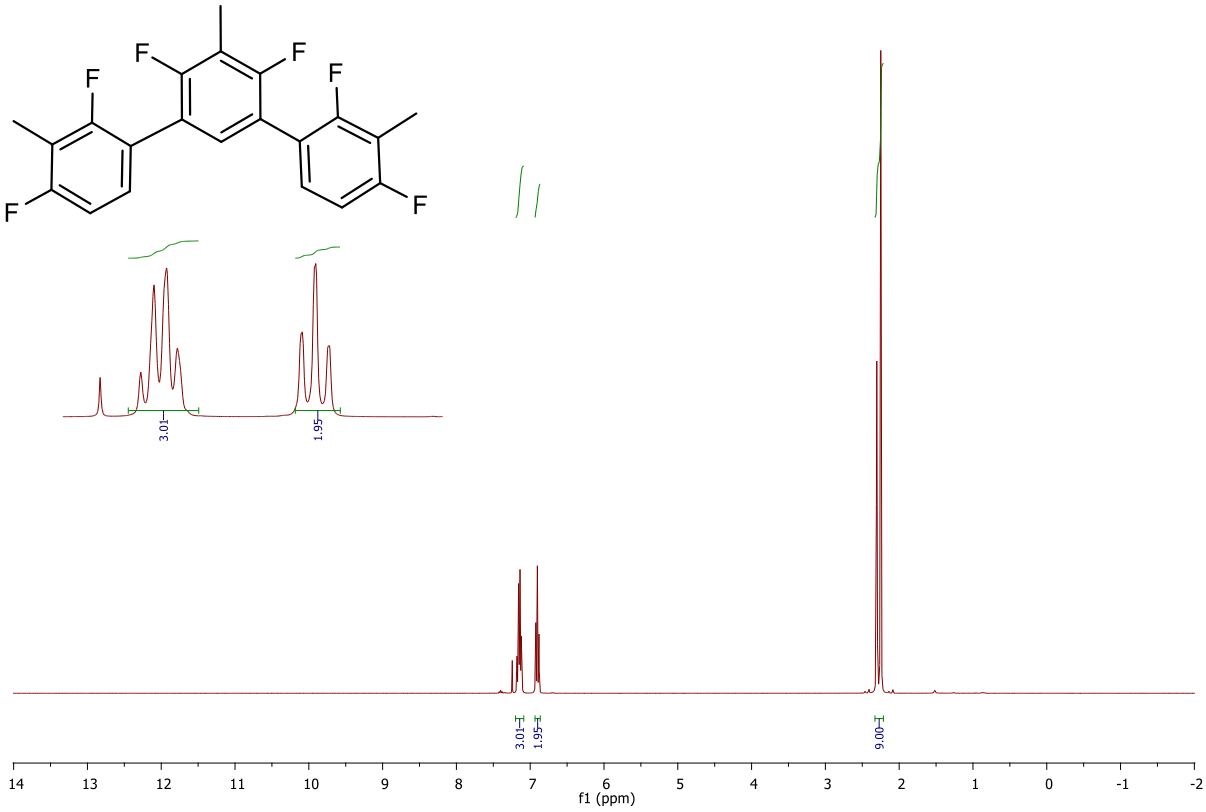

Figure A9. ^{1}H NMR (400 MHz, $CDCl_3$) of 6.

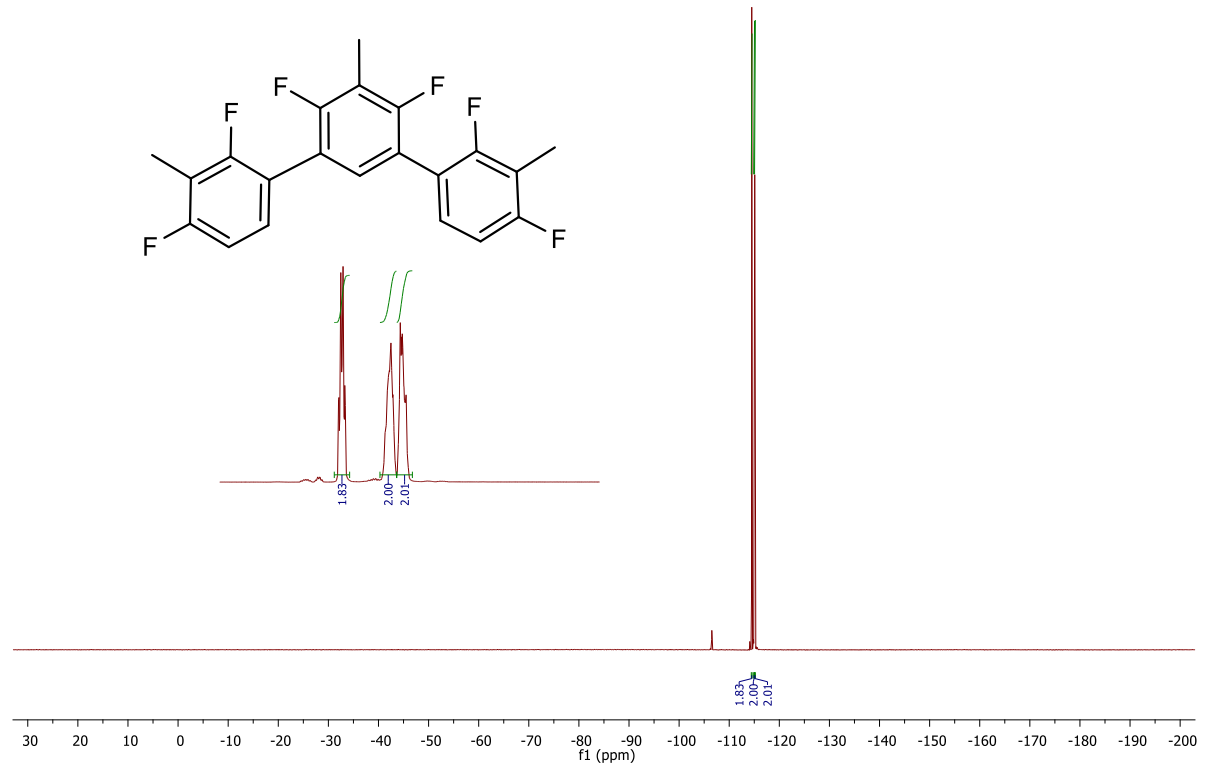

Figure A10. ^{19}F NMR (376 MHz, $CDCl_3$) of 6.

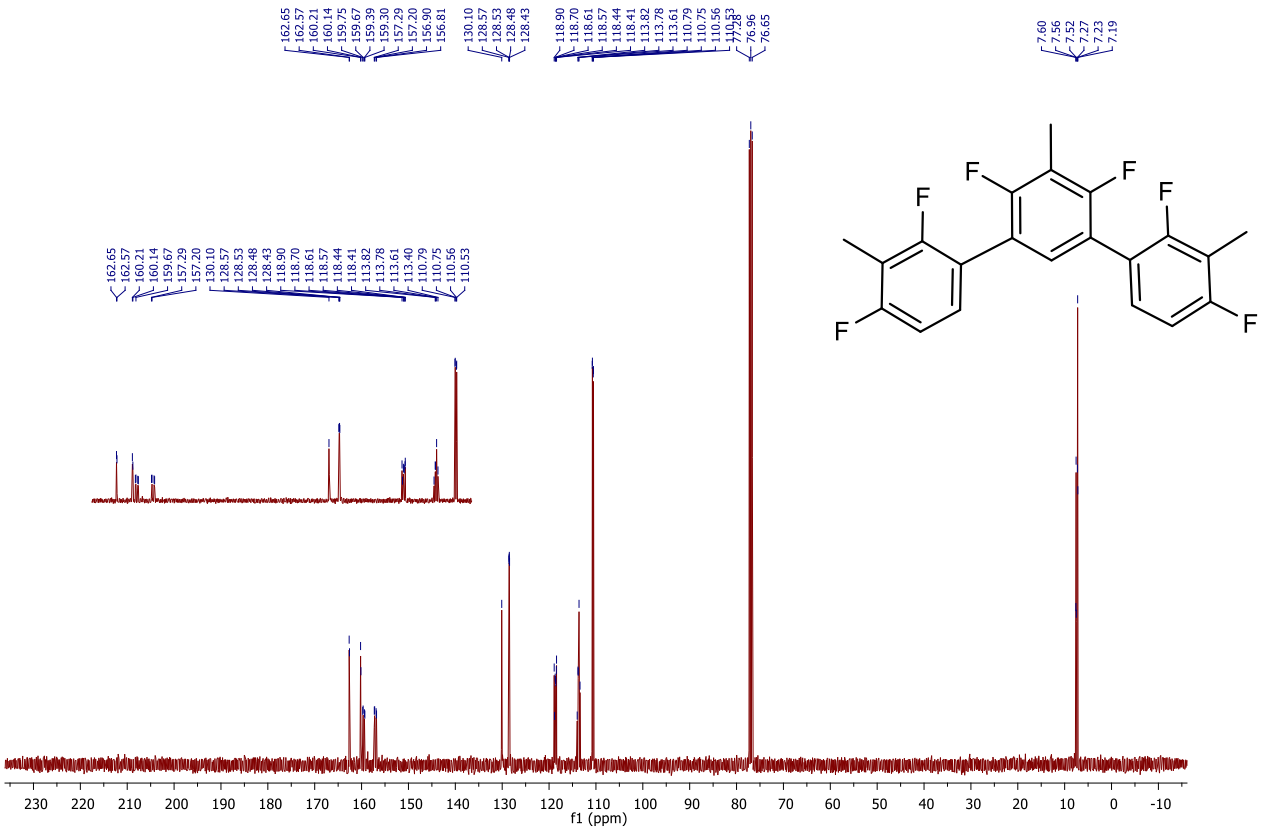

Figure A11. 13C NMR (101 MHz, CD2Cl2) of 6.

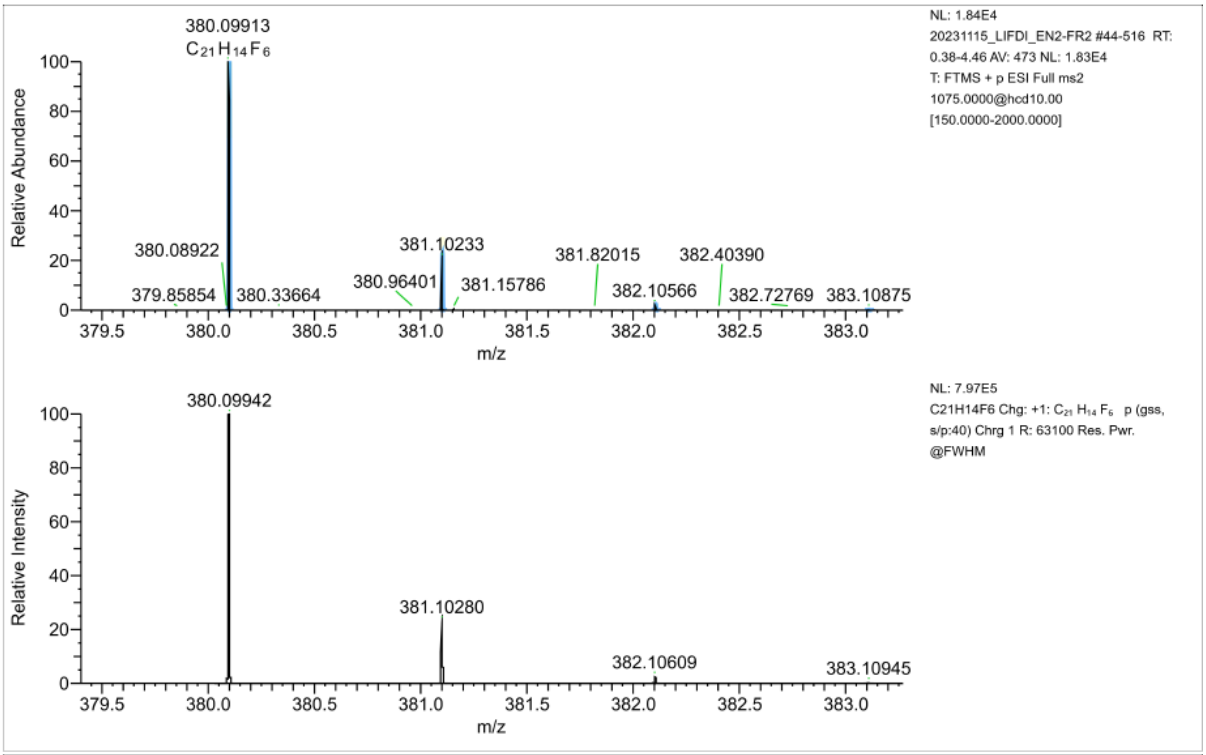

Peak Mass	Display F...	S Fit	RDB	Delta [pp...	Theo. ma...	Rank	Combine...	# Match...	# Missed...	MS Cov....	Pattern C...	MSMS M...
380.09913	$C_{21}H_{14}F_6$	46.740760103026 4	12.00	-0.78	380.09942	1	96.35	4	0	99.1	99.87	(Collection)

Figure A12. HRMS (LIFDI) of 6.

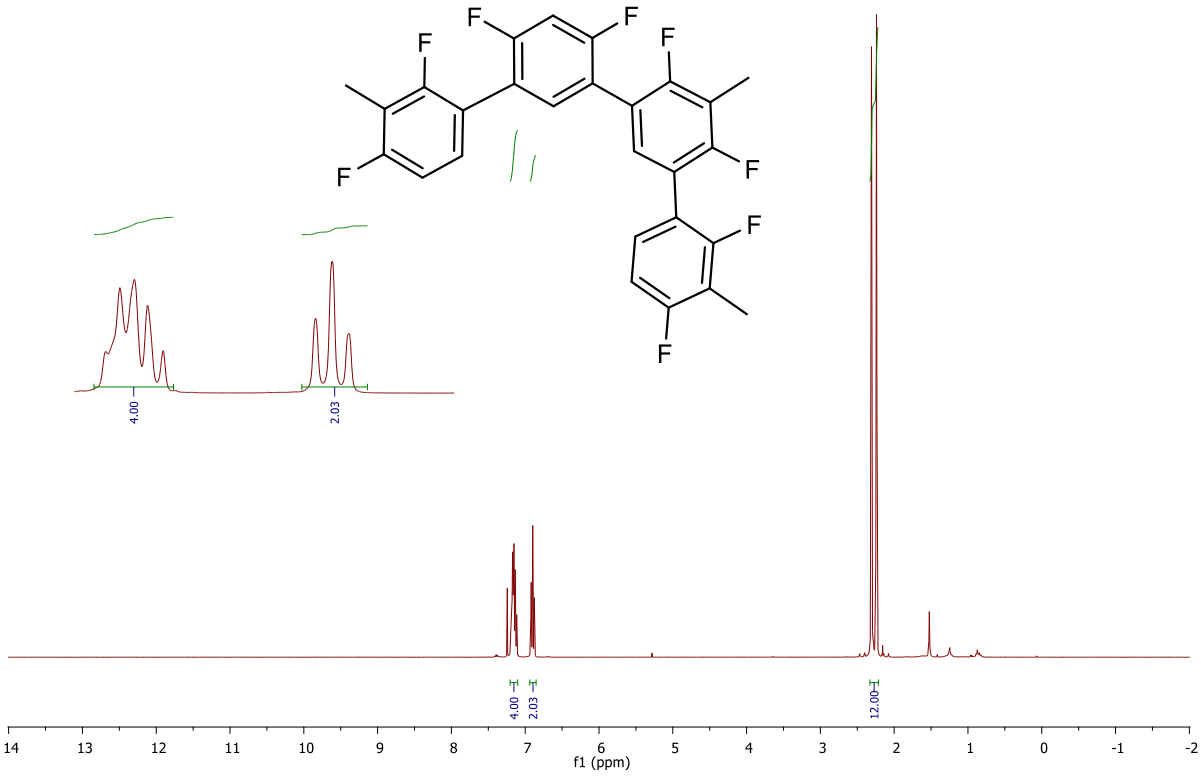

Figure A13. ^{1}H NMR (400 MHz, $CDCl_3$) of 7.

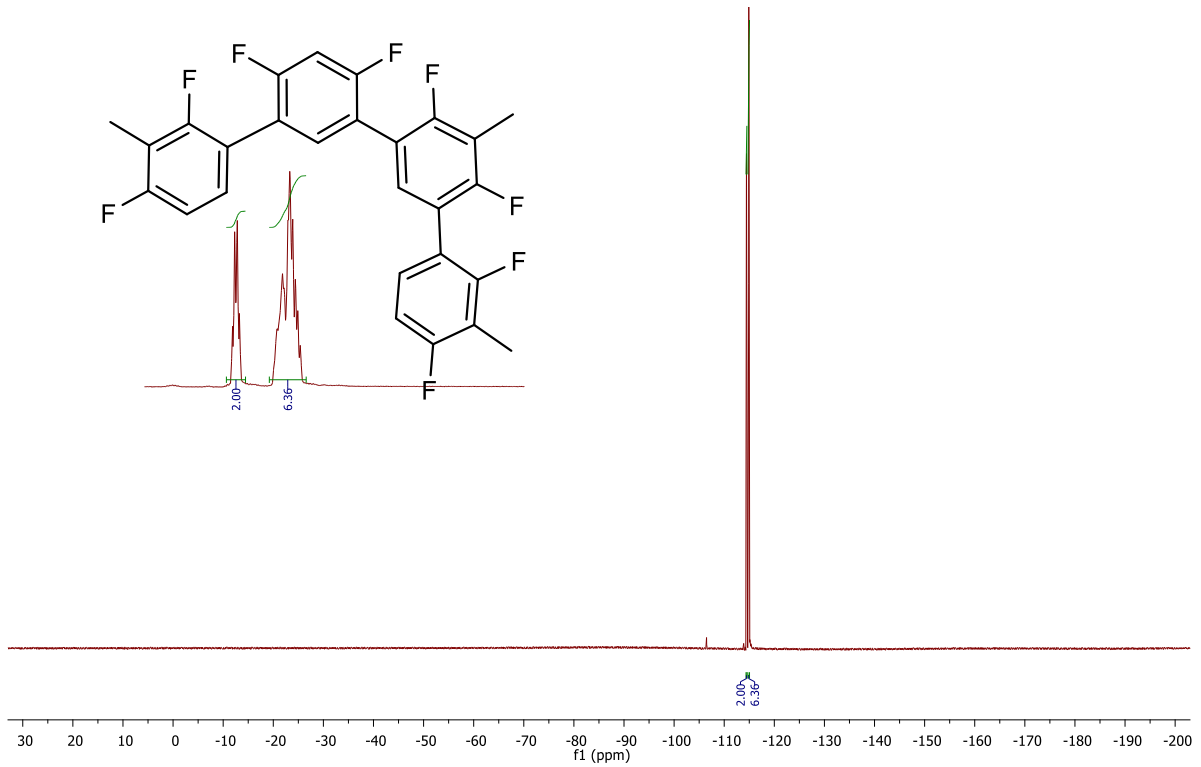

Figure A14. ^{19}F NMR (376 MHz, $CDCl_3$) of 7.

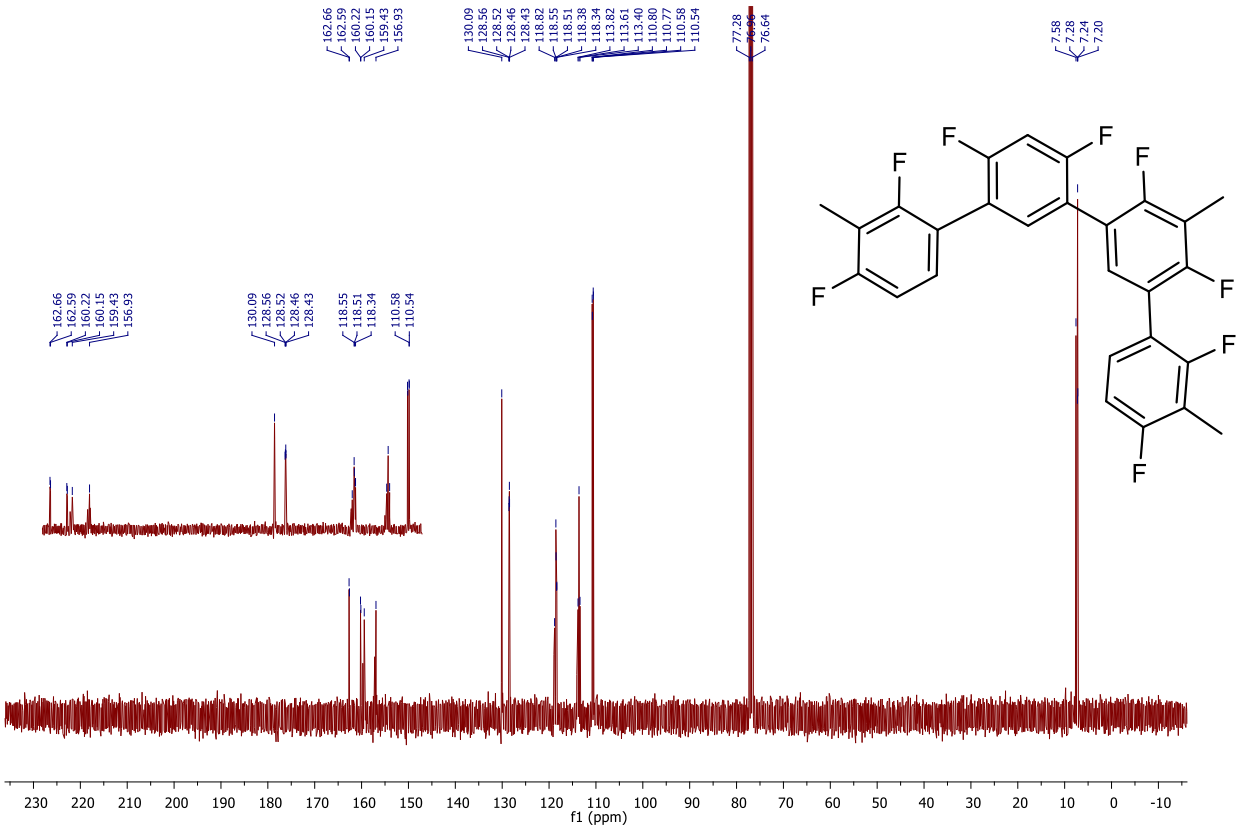

Figure A15. ^{13}C NMR (101 MHz, $CDCl_3$) of 7.

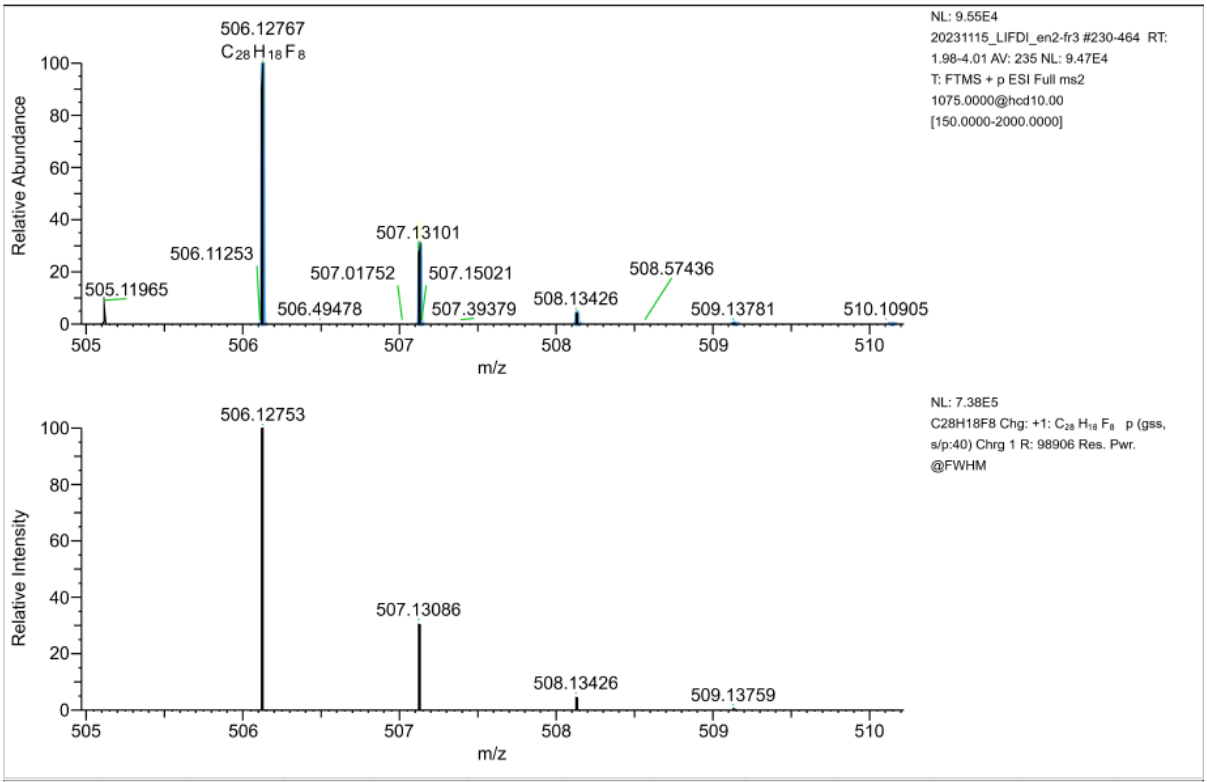

Peak Mass	Display F...	S Fit	RDB	Delta [pp...	Theo. ma...	Rank	Combine...	# Match...	# Missed...	MS Cov....	Pattern C...	MSMS M...
506.1276 7	$C_{28}H_{18}F_8$	49.66397 5433541	16.00	0.28	506.1275 3	1	97.1	4	0	99.74	99.69	(Collecti on)

Figure A16. HRMS (LIFDI) of 7.

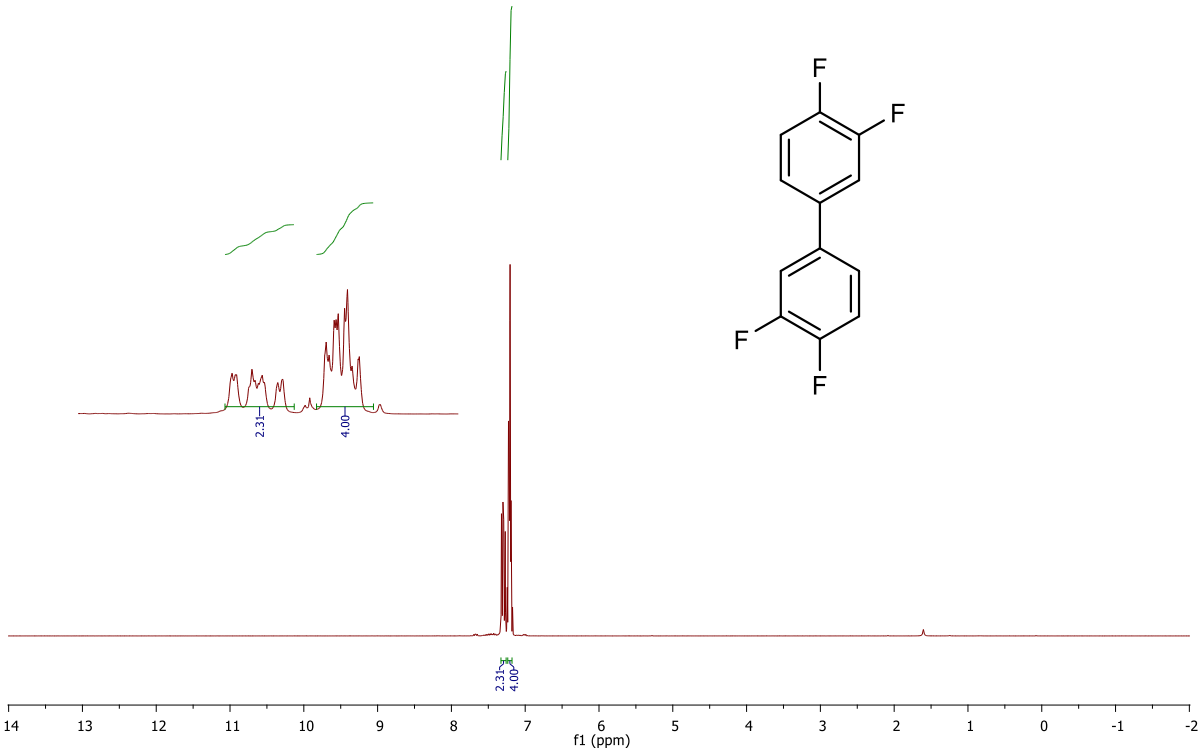

Figure A17. ^{1}H NMR (400 MHz, $CDCl_3$) of 8.

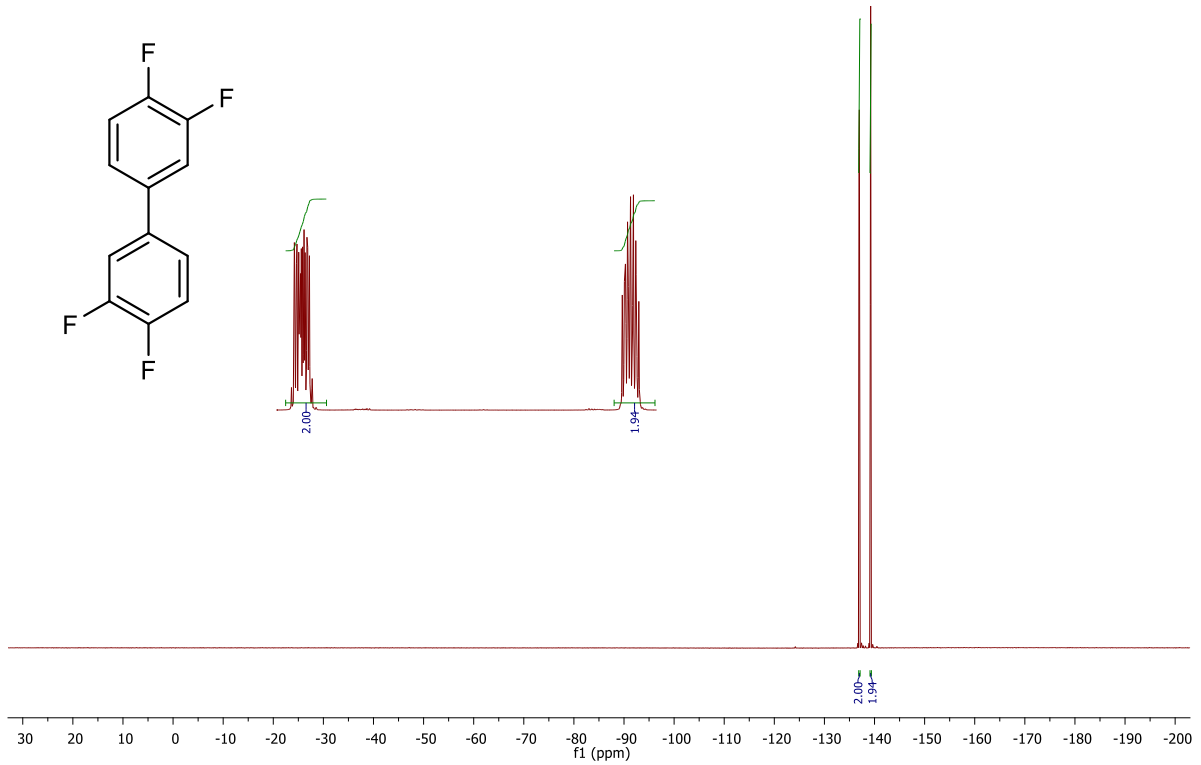

Figure A18. ^{19}F NMR (376 MHz, $CDCl_3$) of 8.

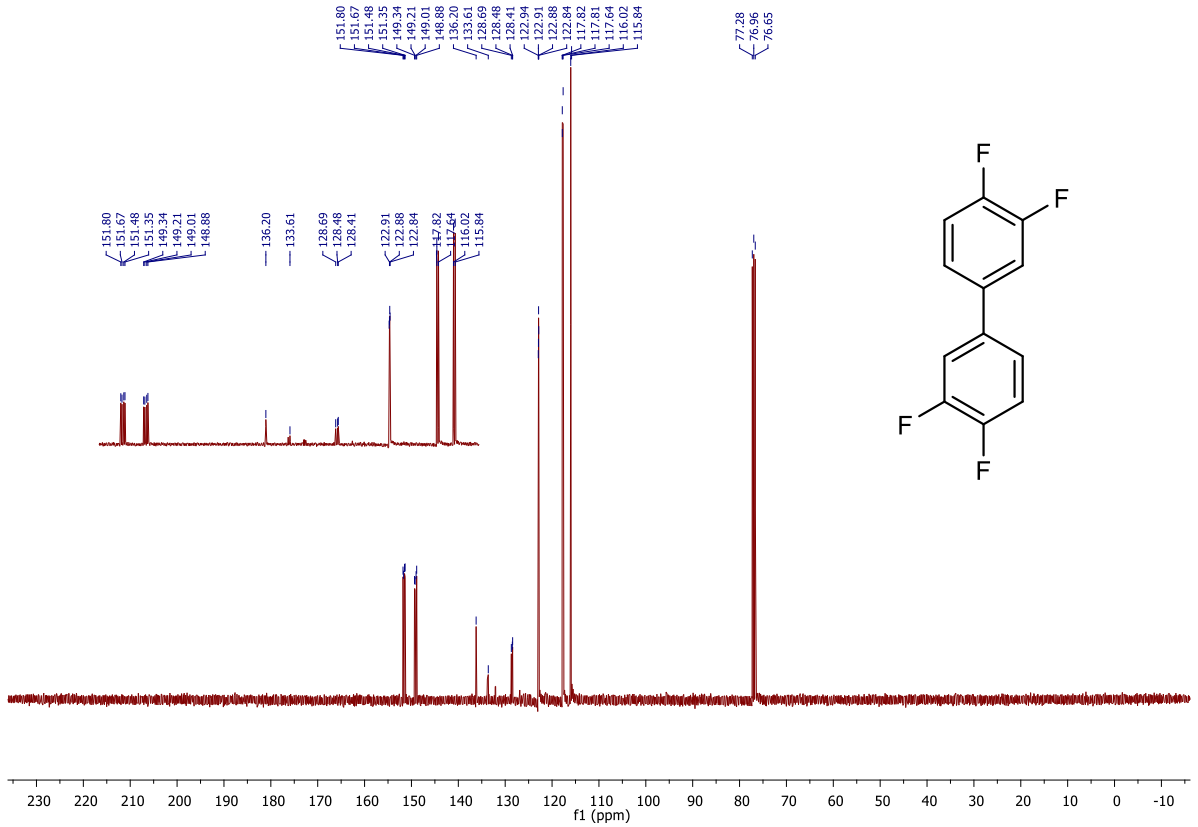

Figure A19. ^{13}C NMR (101 MHz, $CDCl_3$) of 8.

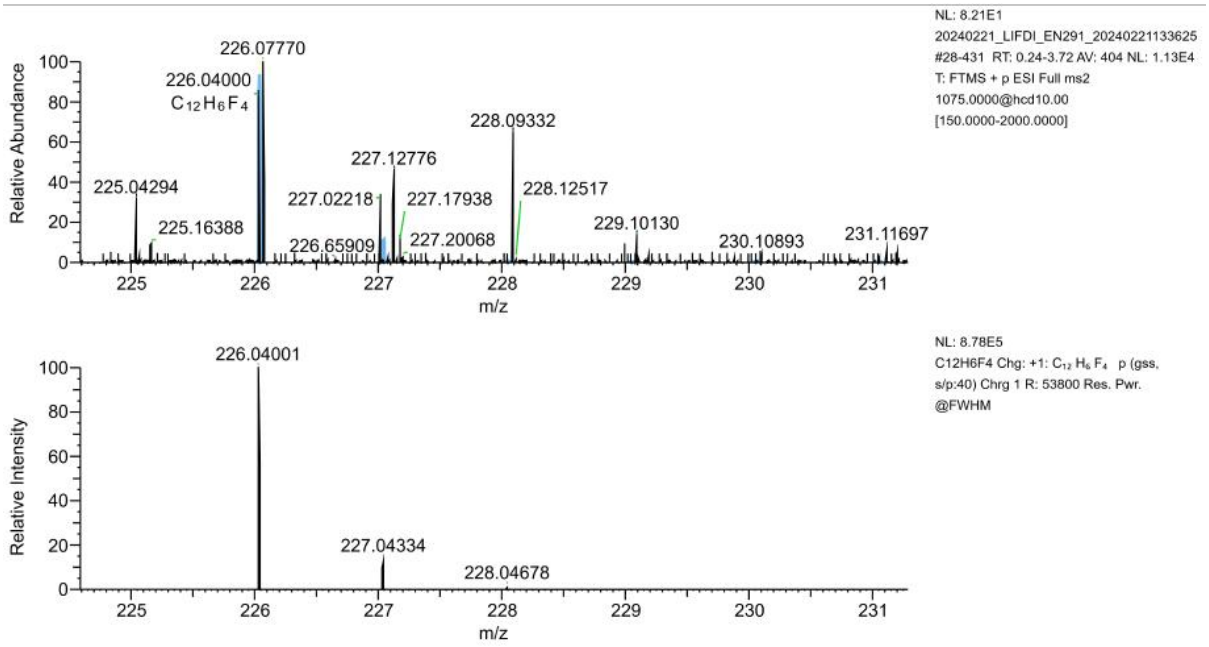

Peak Mass	Display F...	S Fit	RDB	Delta [pp...	Theo. ma...	Rank	Combine...	# Match...	# Missed...	MS Cov....	Pattern C...	MSMS M..
226.04000	$C_{12}H_6F_4$	29.284068625050 3	8.00	-0.09	226.04001	1	32.96	2	0	33.17	88.52	(Collection)

Figure A20. HRMS (LIFDI) of 8.

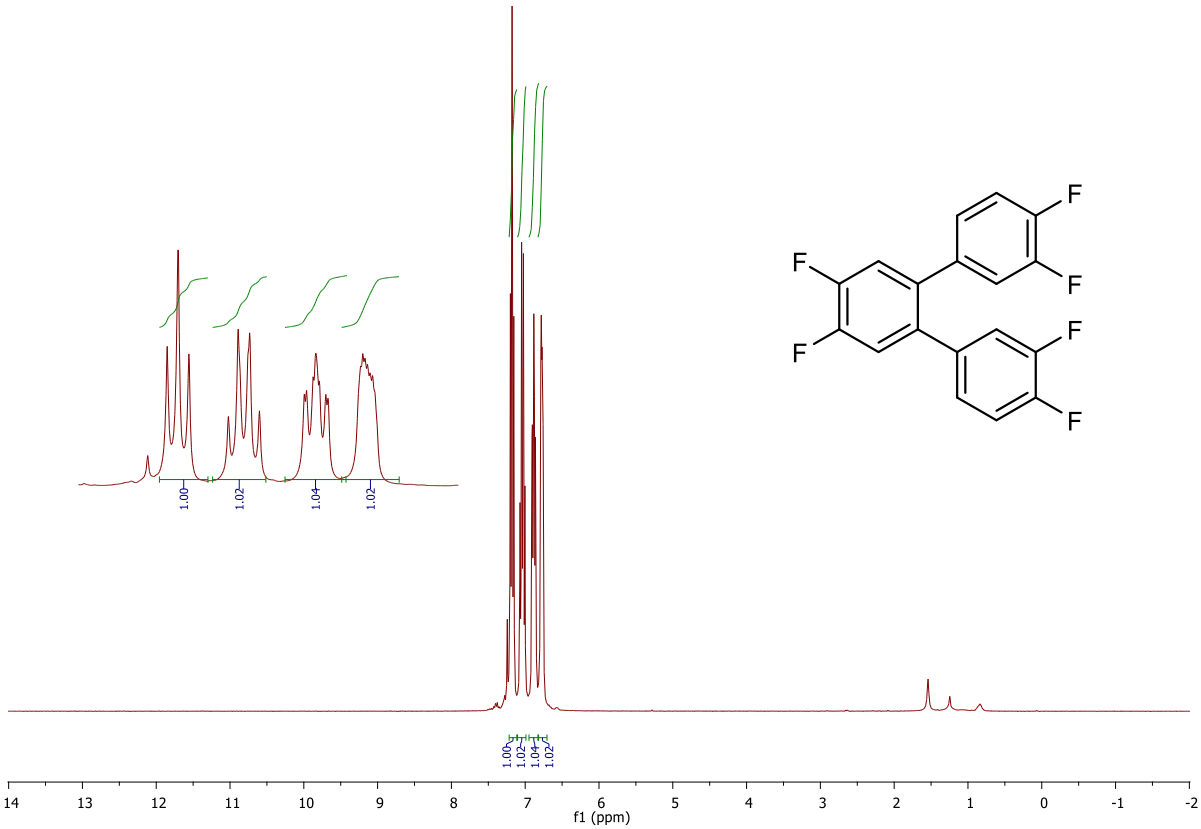

Figure A21. ^{1}H NMR (400 MHz, $CDCl_3$) of 9.

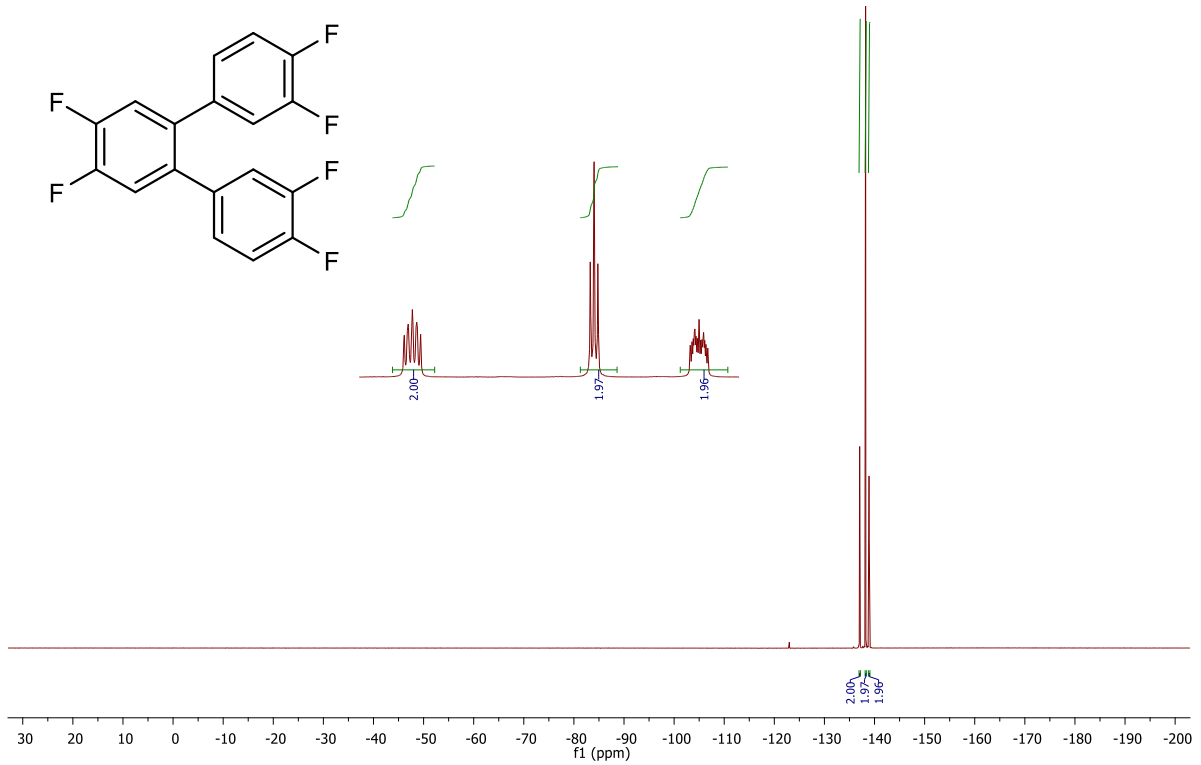

Figure A22. ^{19}F NMR (376 MHz, $CDCl_3$) of 9.

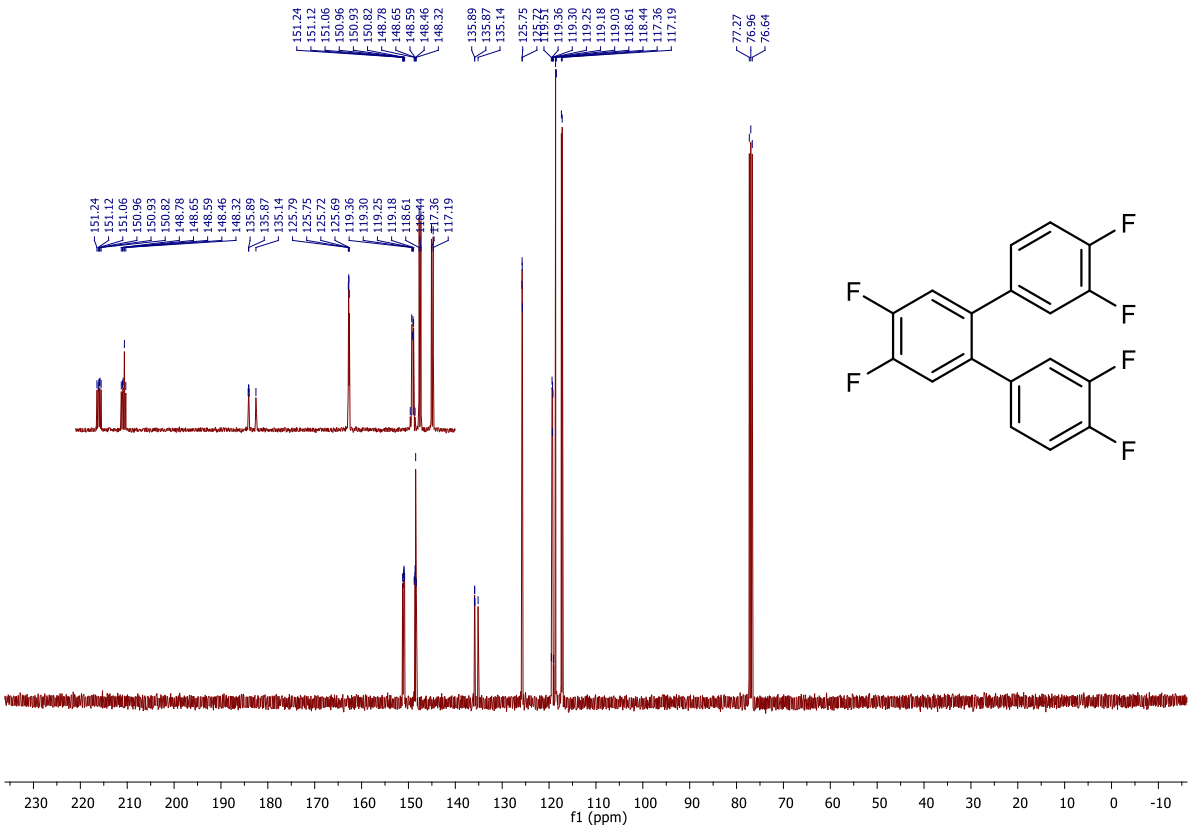

Figure A23. ^{13}C NMR (101 MHz, $CDCl_3$) of 9.

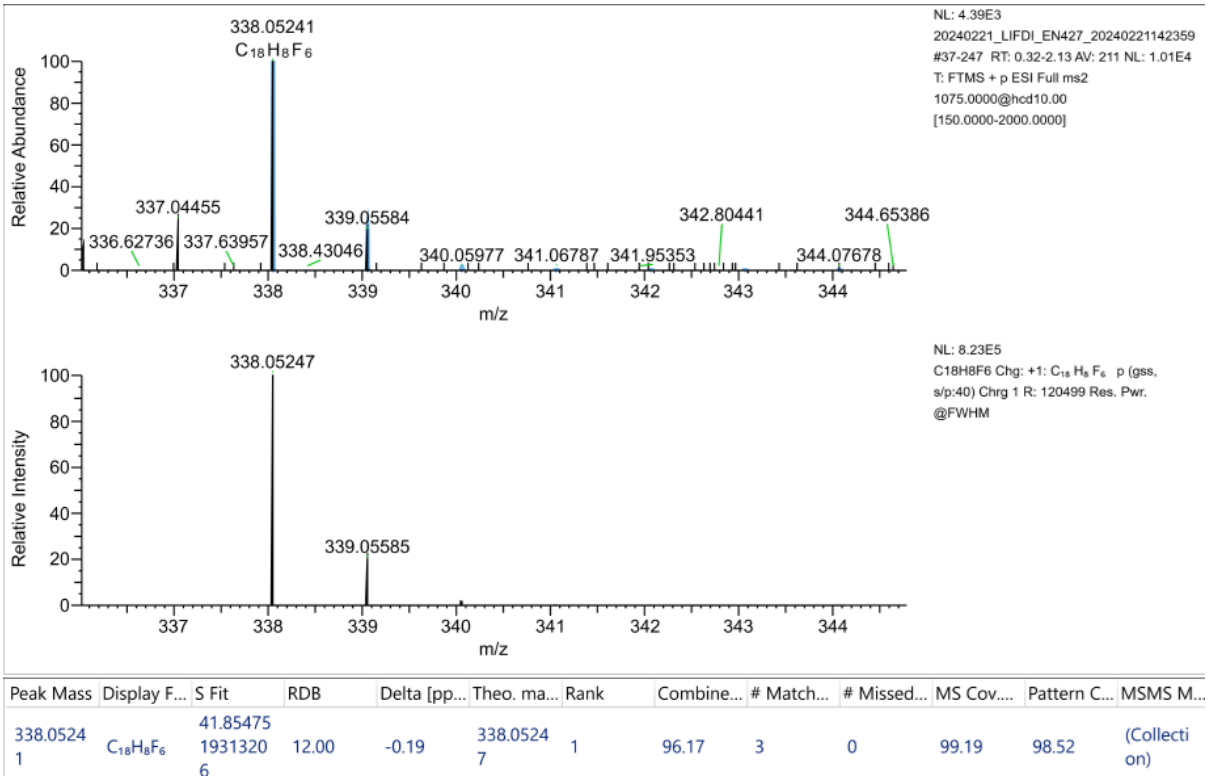

Peak Mass	Display F...	S Fit	RDB	Delta [pp...	Theo. ma...	Rank	Combine...	# Match...	# Missed...	MS Cov....	Pattern C...	MSMS M...
338.05241	$C_{18}H_8F_6$	41.854751931320 6	12.00	-0.19	338.05247	1	96.17	3	0	99.19	98.52	(Collection)

Figure A24. HRMS (LIFDI) of 9.

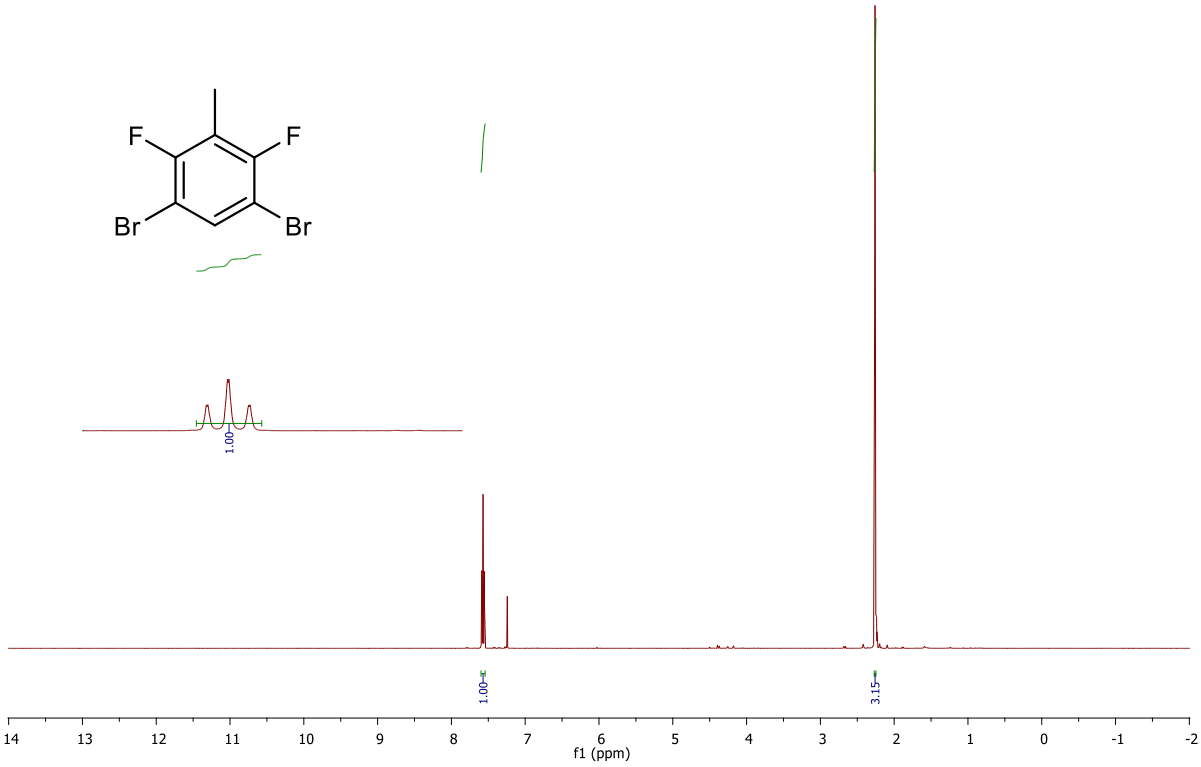

Figure A25. ^{1}H NMR (400 MHz, $CDCl_3$) of 4a.

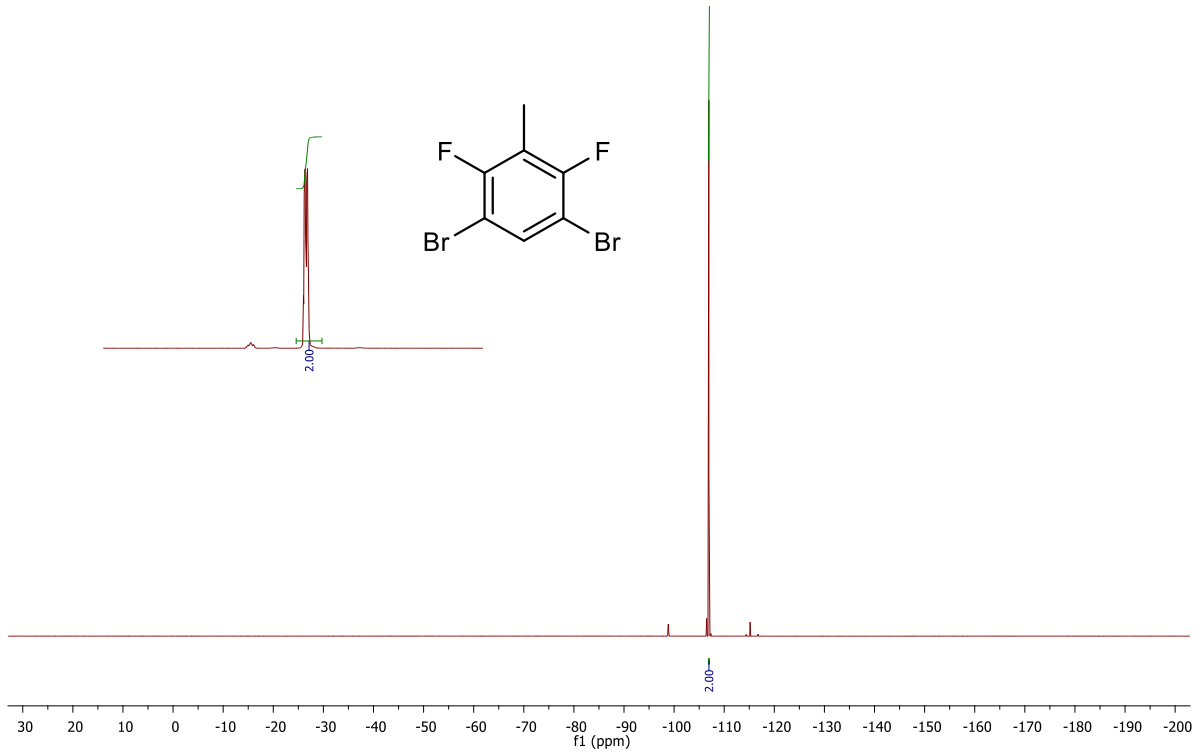

Figure A26. ^{19}F NMR (376 MHz, $CDCl_3$) of 4a.

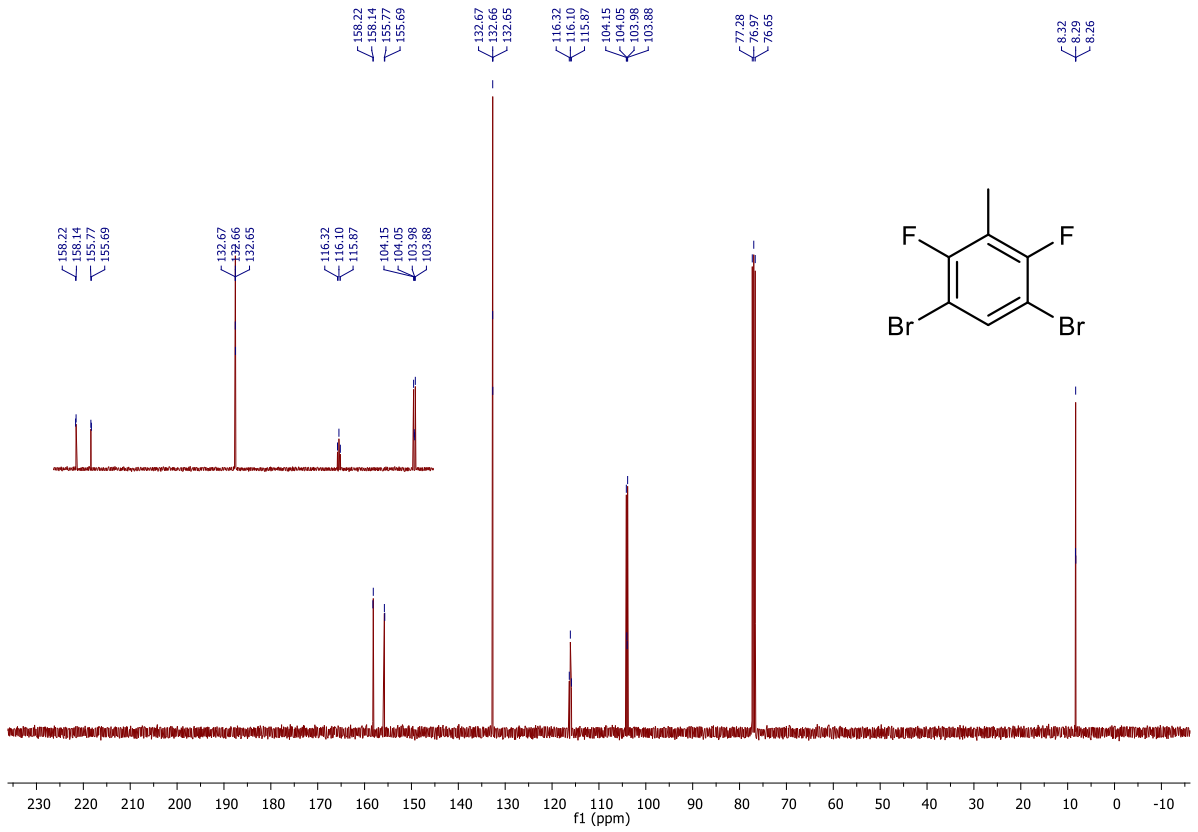

Figure A27. ^{13}C NMR (101 MHz, $CDCl_3$) of 4a.

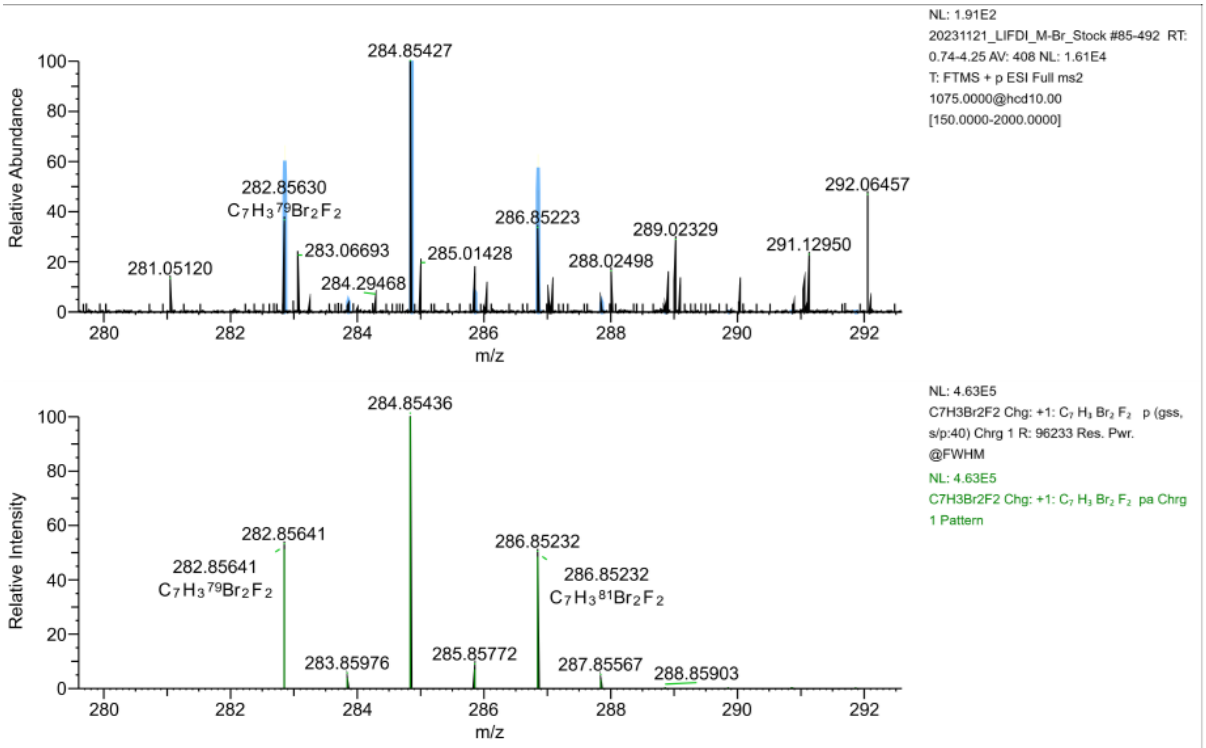

Peak Mass	Display F...	S Fit	RDB	Delta [pp...	Theo. ma...	Rank	Combine...	# Match...	# Missed...	MS Cov....	Pattern C...	MSMS M...
282.85630	$C_7H_3{}^{79}Br_2F_2$	18.307304620460 7	4.50	-0.37	282.85641	1	31.91	3	0	32.66	49.99	(Collection)

Figure A28. HRMS (LIFDI) of 4a.

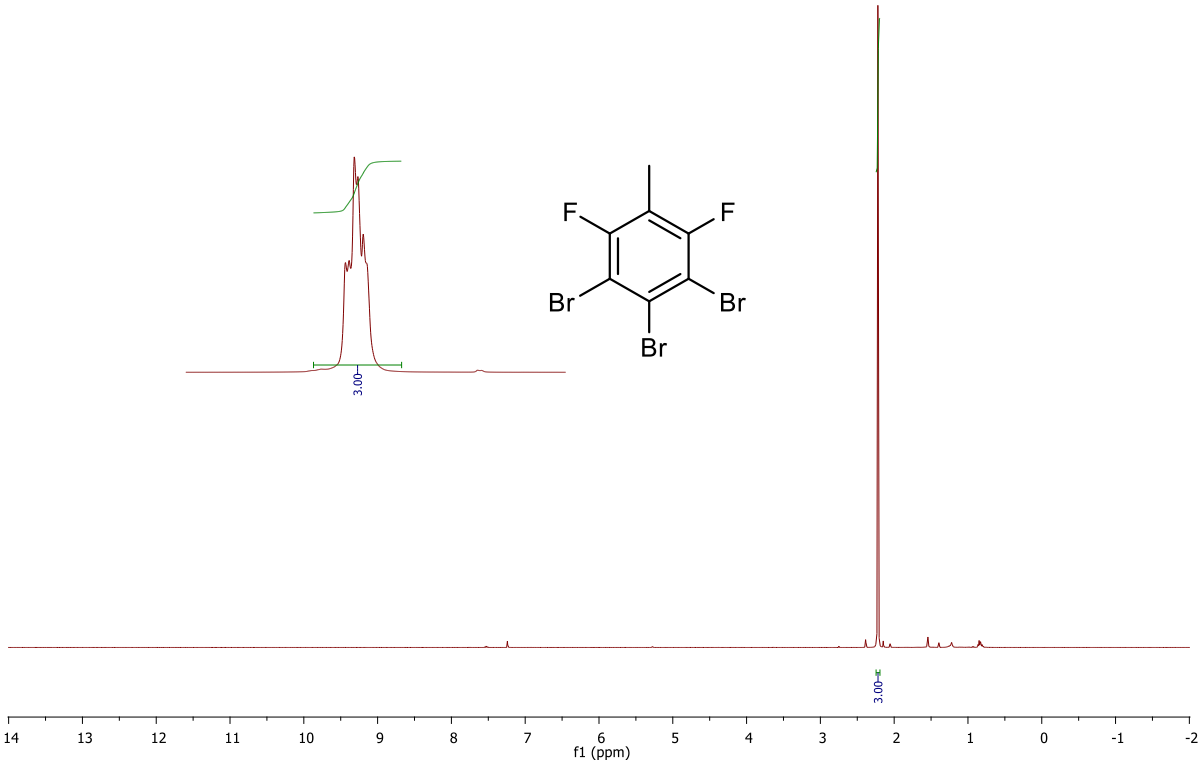

Figure A29. ^{1}H NMR (400 MHz, $CDCl_3$) of 4b.

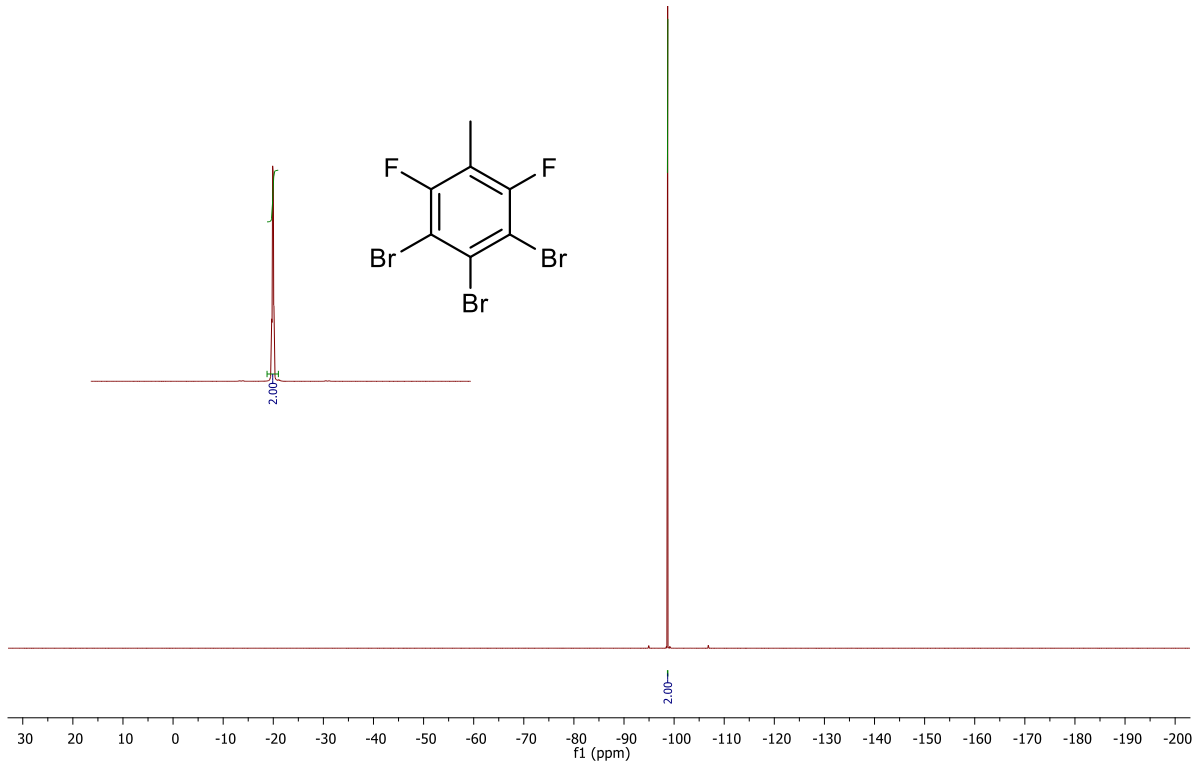

Figure A30. ^{19}F NMR (376 MHz, $CDCl_3$) of 4b.

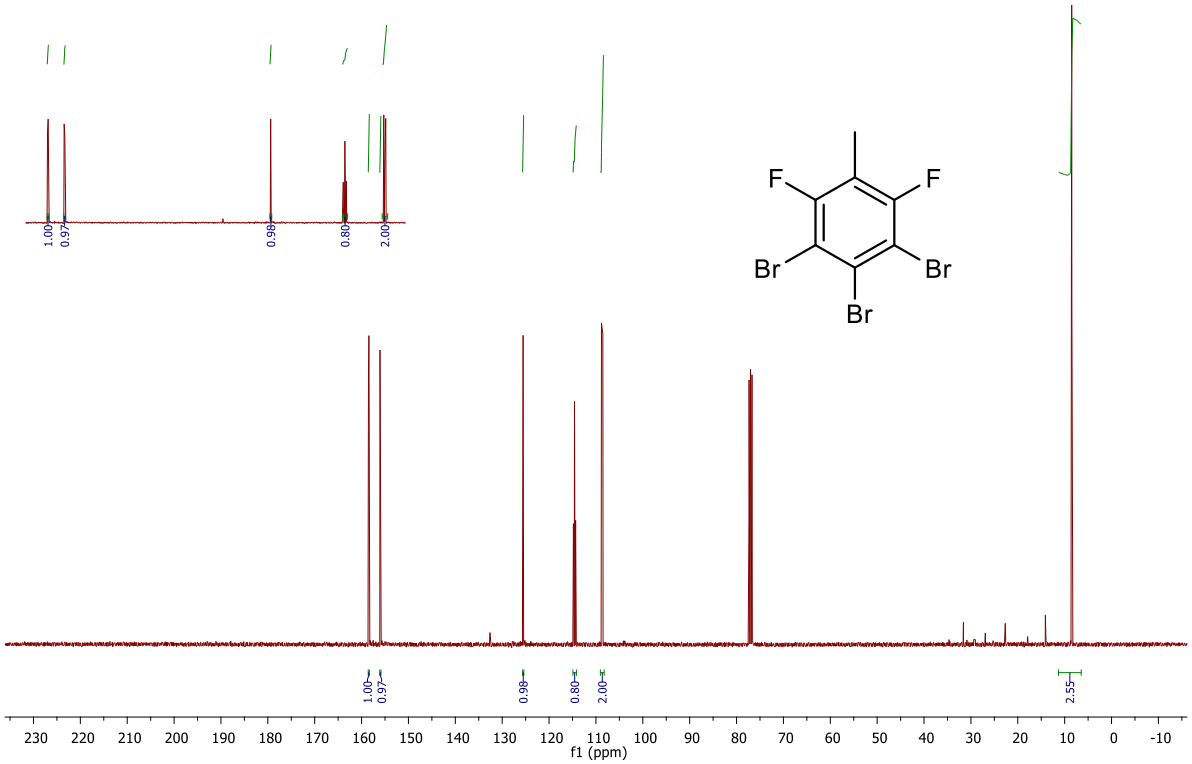

Figure A31. ^{13}C NMR (101 MHz, $CDCl_3$) of 4b.

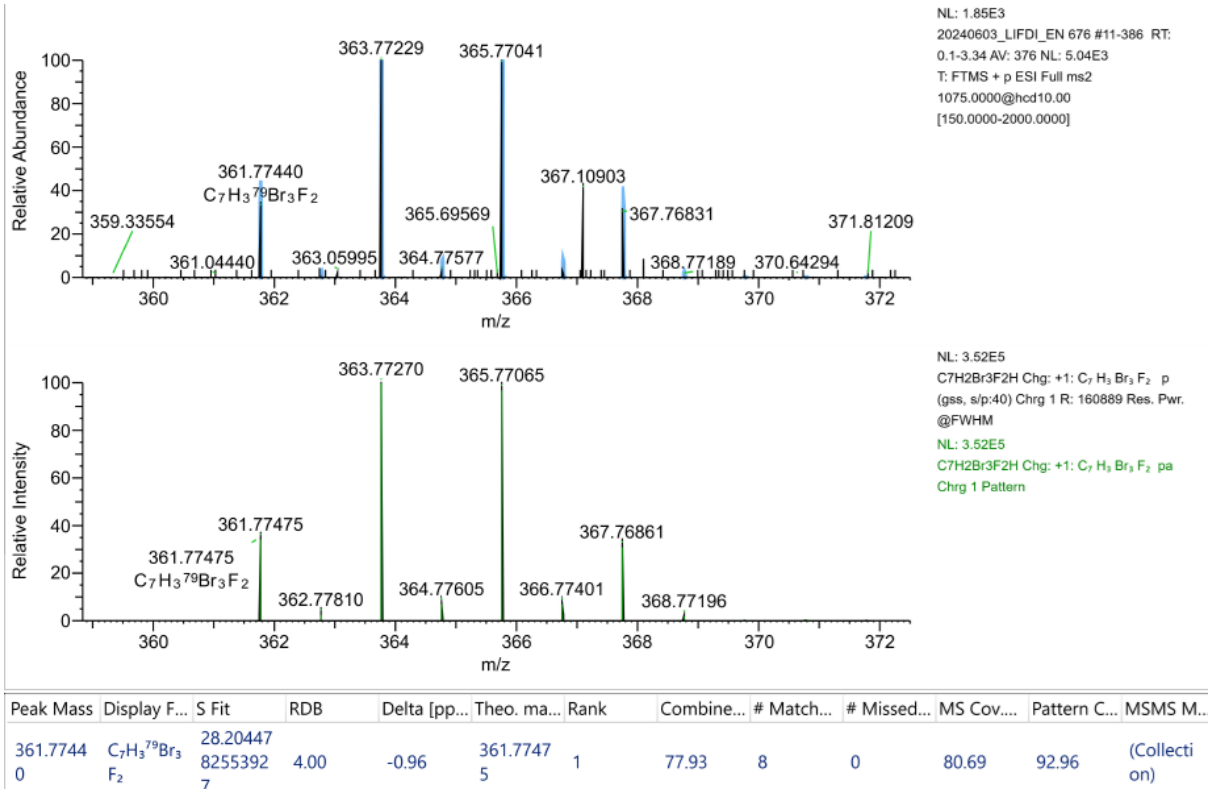

Peak Mass	Display F...	S Fit	RDB	Delta [pp...	Theo. ma...	Rank	Combine...	# Match...	# Missed...	MS Cov....	Pattern C...	MSMS M..
361.77440	$C_7H_3{}^{79}Br_3F_2$	28.204478255392 7	4.00	-0.96	361.77475	1	77.93	8	0	80.69	92.96	(Collection)

Figure A32. HRMS (LIFDI) of 4b.

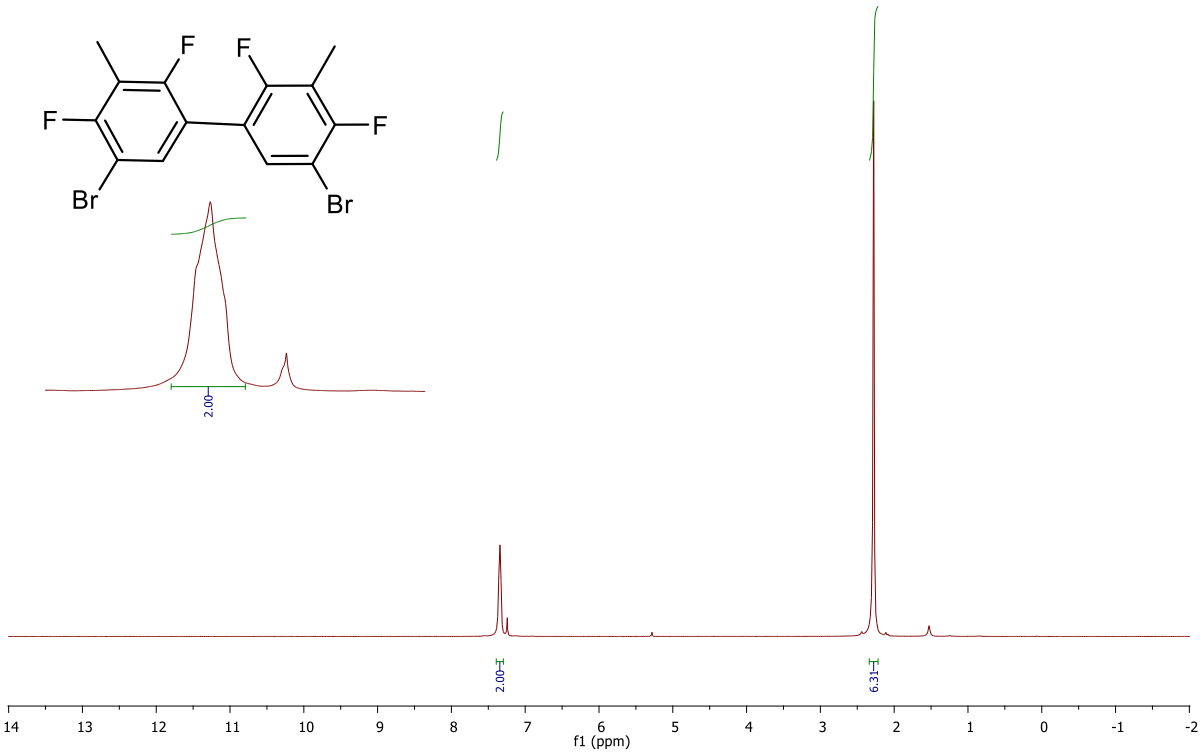

Figure A33. ^{1}H NMR (400 MHz, $CDCl_3$) of 5a.

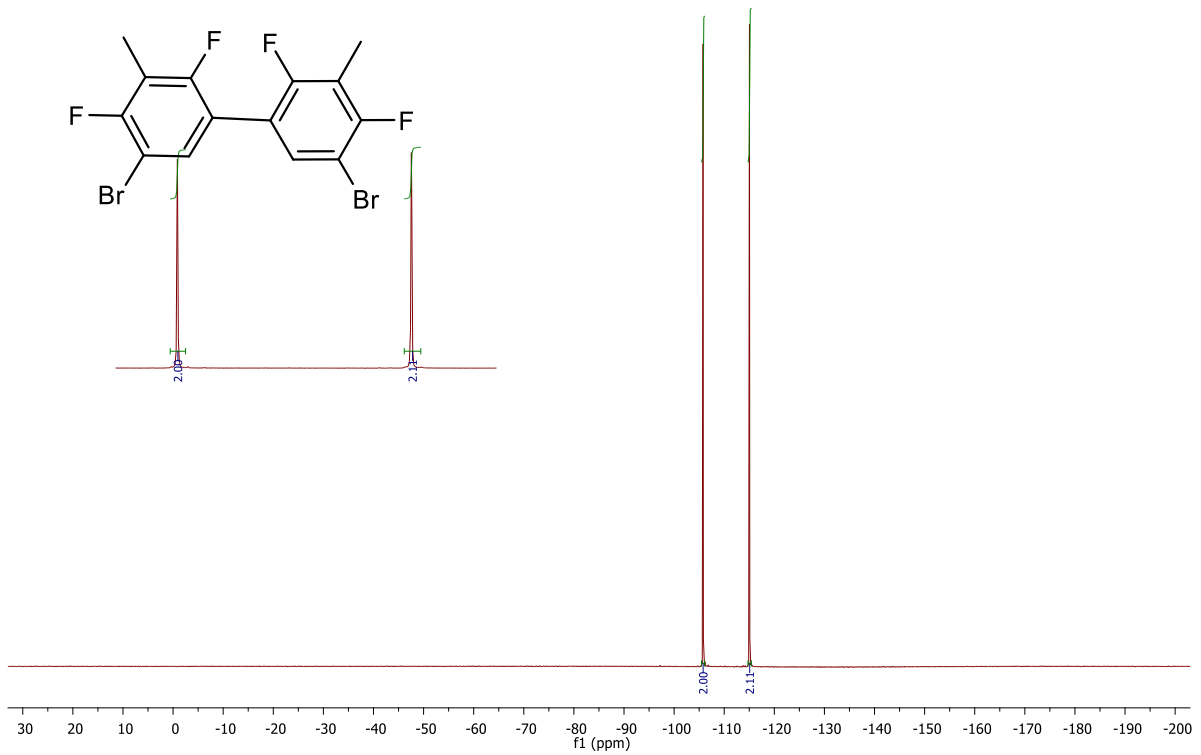

Figure A34. ^{19}F NMR (376 MHz, $CDCl_3$) of 5a.

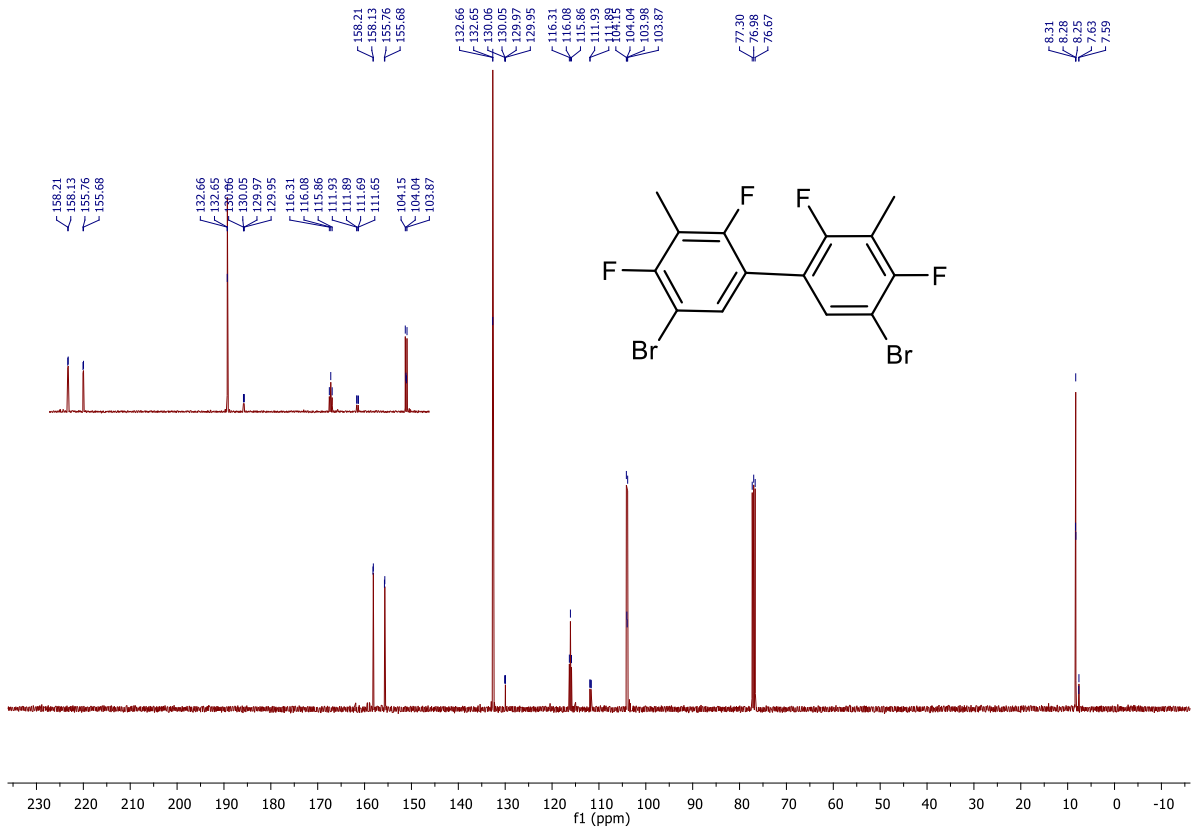

Figure A35. ^{13}C NMR (101 MHz, $CDCl_3$) of 5a.

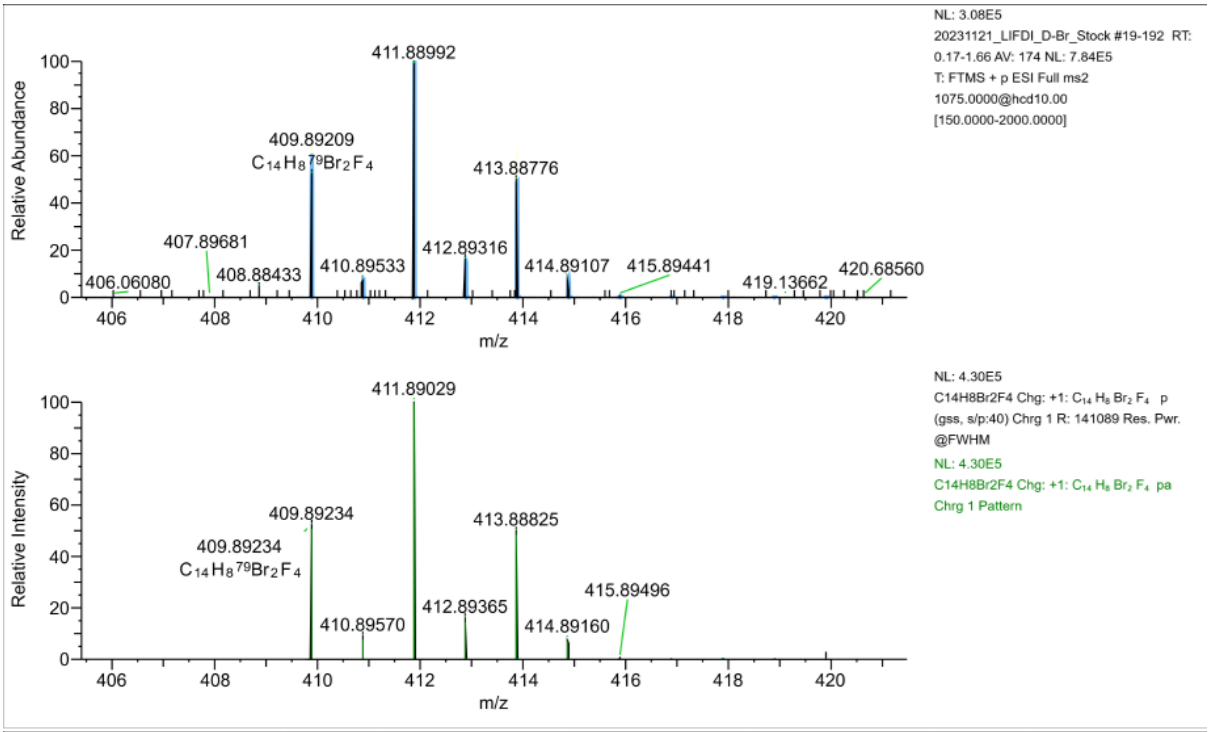

Peak Mass	Display F...	S Fit	RDB	Delta [pp...	Theo. ma...	Rank	Combine...	# Match...	# Missed...	MS Cov....	Pattern C...	MSMS M...
409.89209	$C_{14}H_8{}^{79}Br_2F_4$	50.49751 0711373 9	8.00	-0.61	409.89234	1	93.74	7	2	96.14	99.31	(Collection)

Figure A36. HRMS (LIFDI) of 5a.

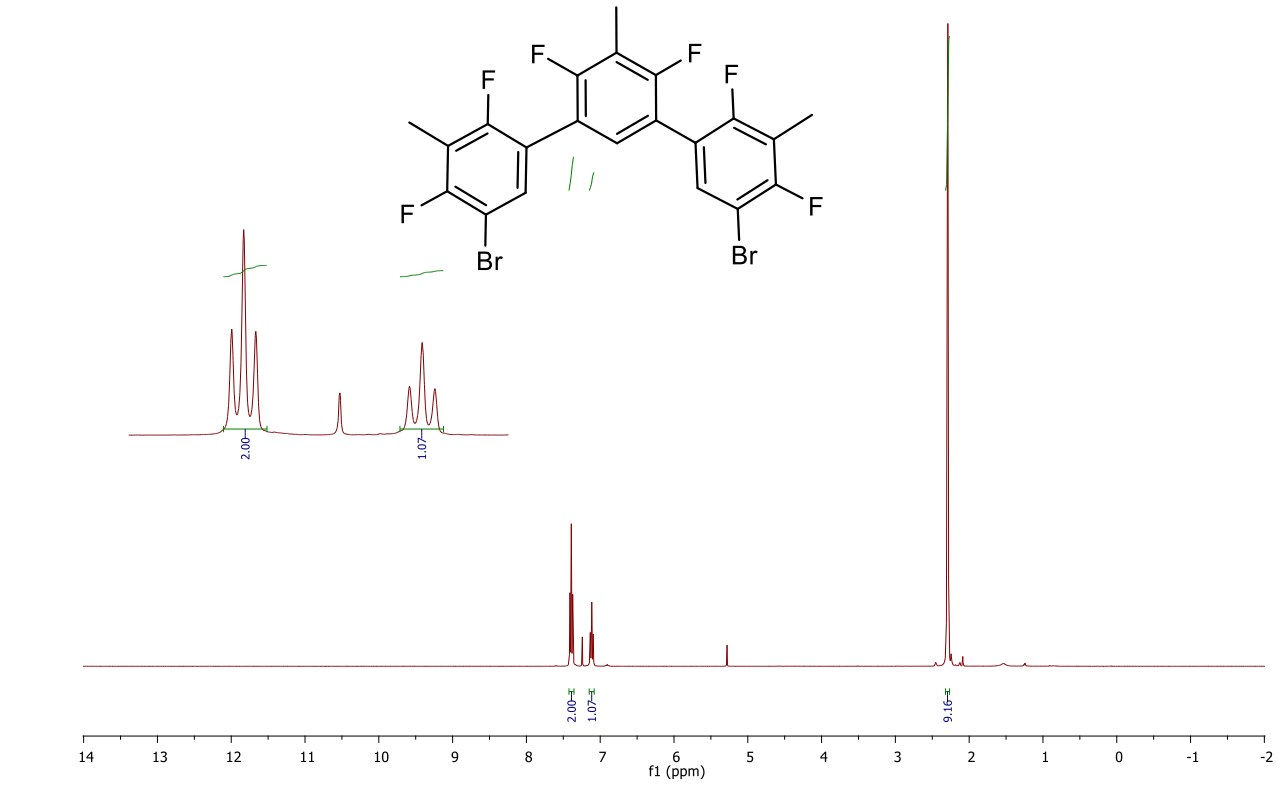

Figure A37. ^{1}H NMR (400 MHz, $CDCl_3$) of 6a.

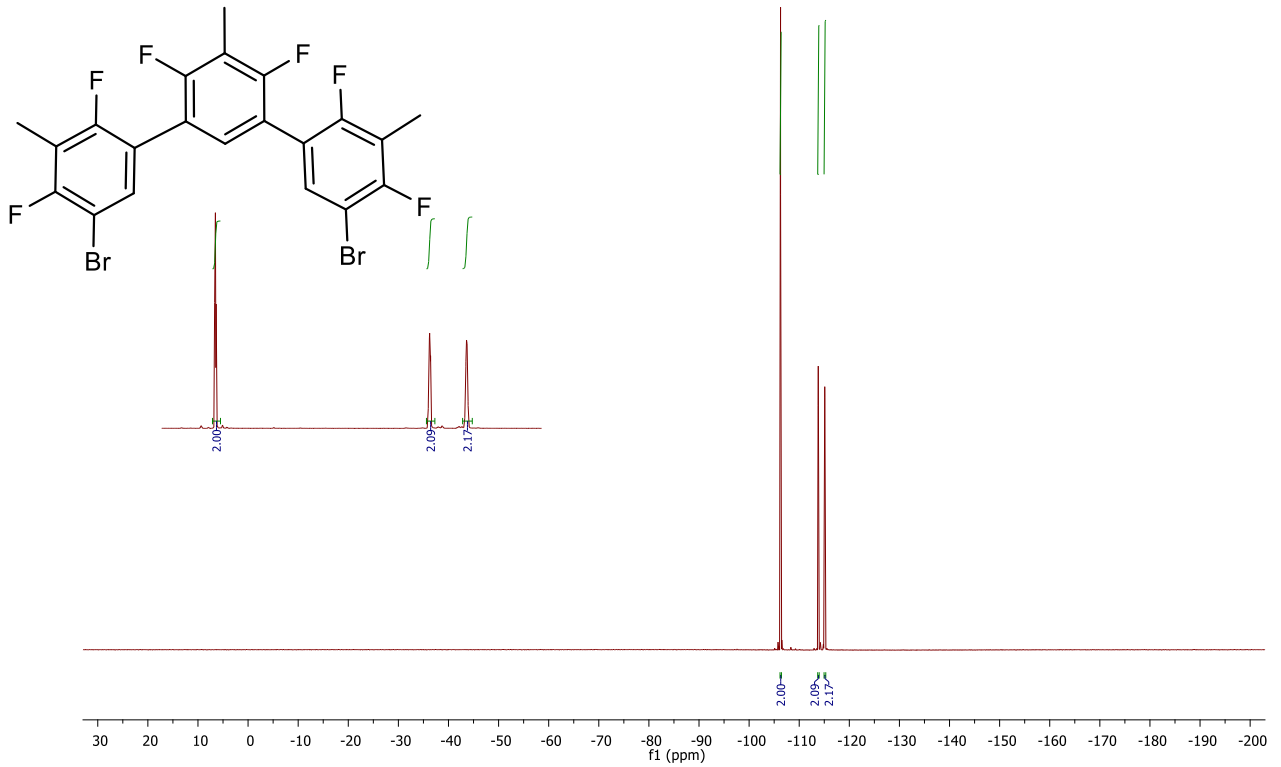

Figure A38. ^{19}F NMR (376 MHz, $CDCl_3$) of 6a.

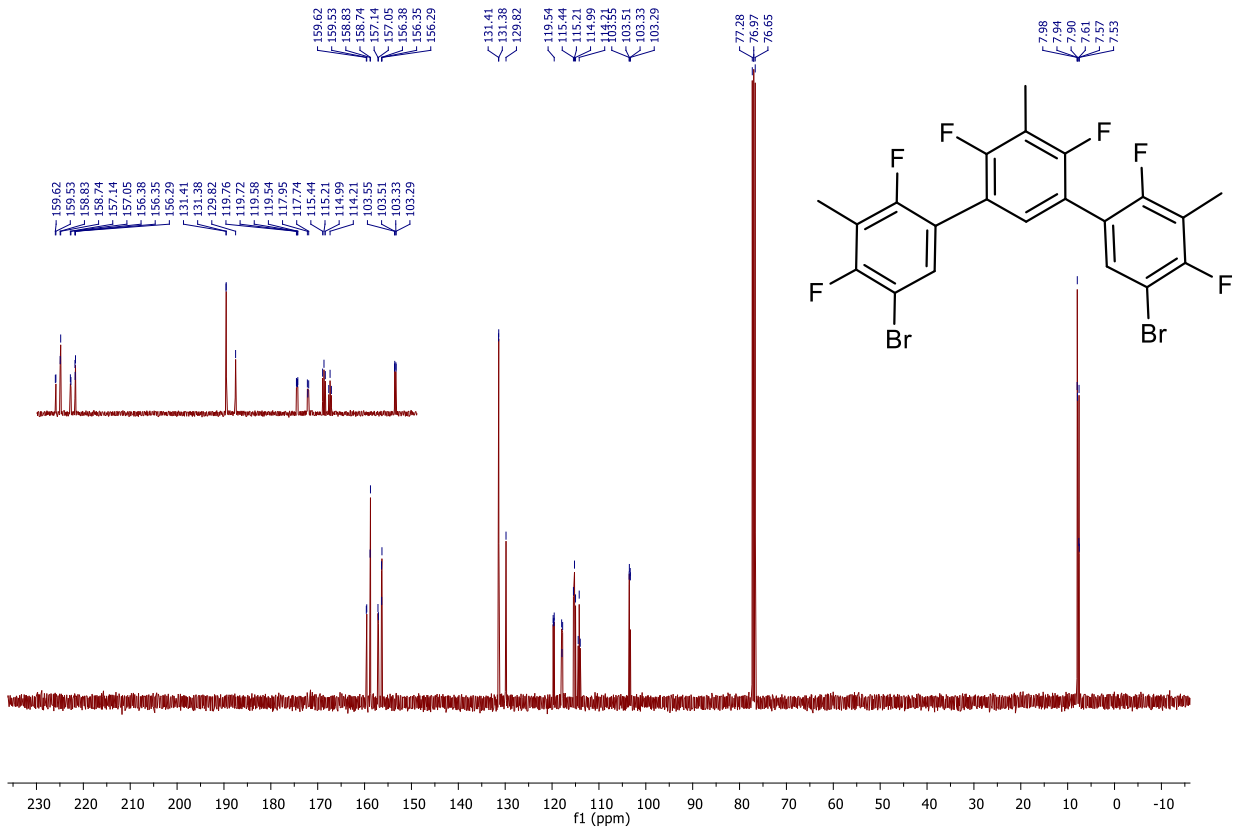

Figure A39. ^{13}C NMR (101 MHz, $CDCl_3$) of 6a.

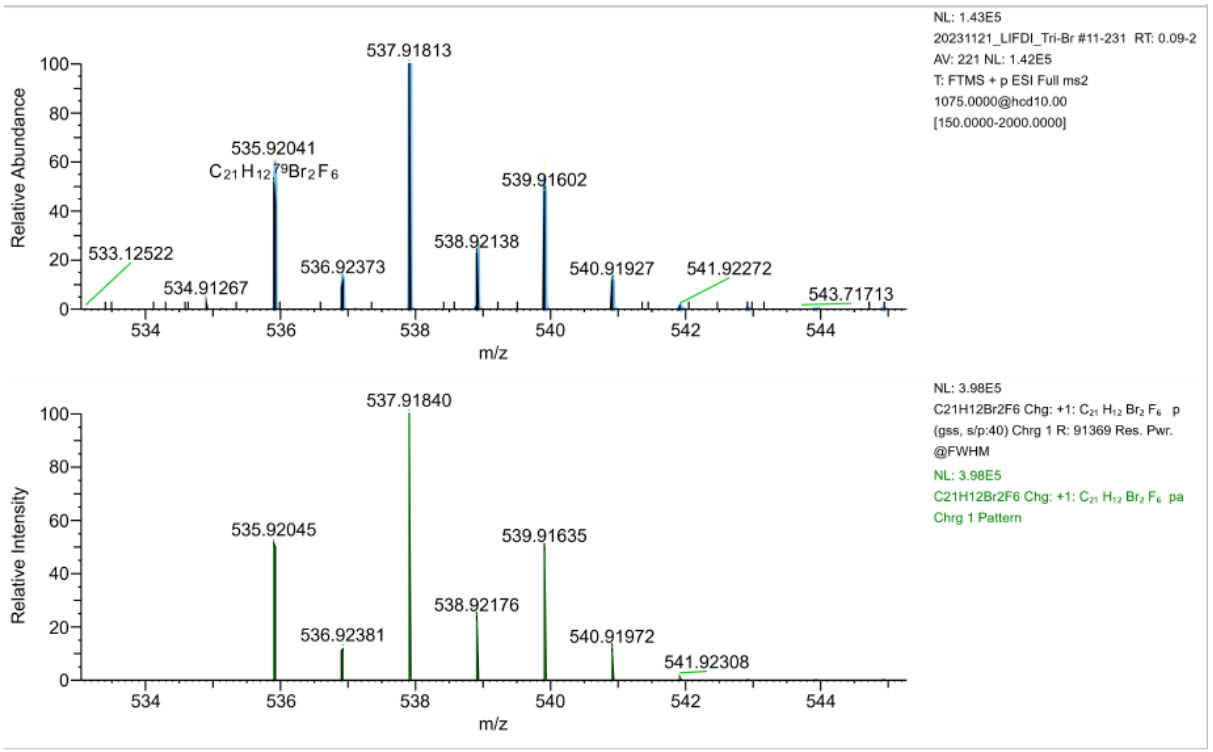

Peak Mass	Display F...	S Fit	RDB	Delta [pp...	Theo. ma...	Rank	Combine...	# Match...	# Missed...	MS Cov....	Pattern C...	MSMS M...
535.92041	$C_{21}H_{12}{}^{79}Br_2F_6$	86.56834 5184364 c	12.00	-0.07	535.92045	1	96.16	7	0	96.7	100	(Collection)

Figure A40. HRMS (LIFDI) of 6a.

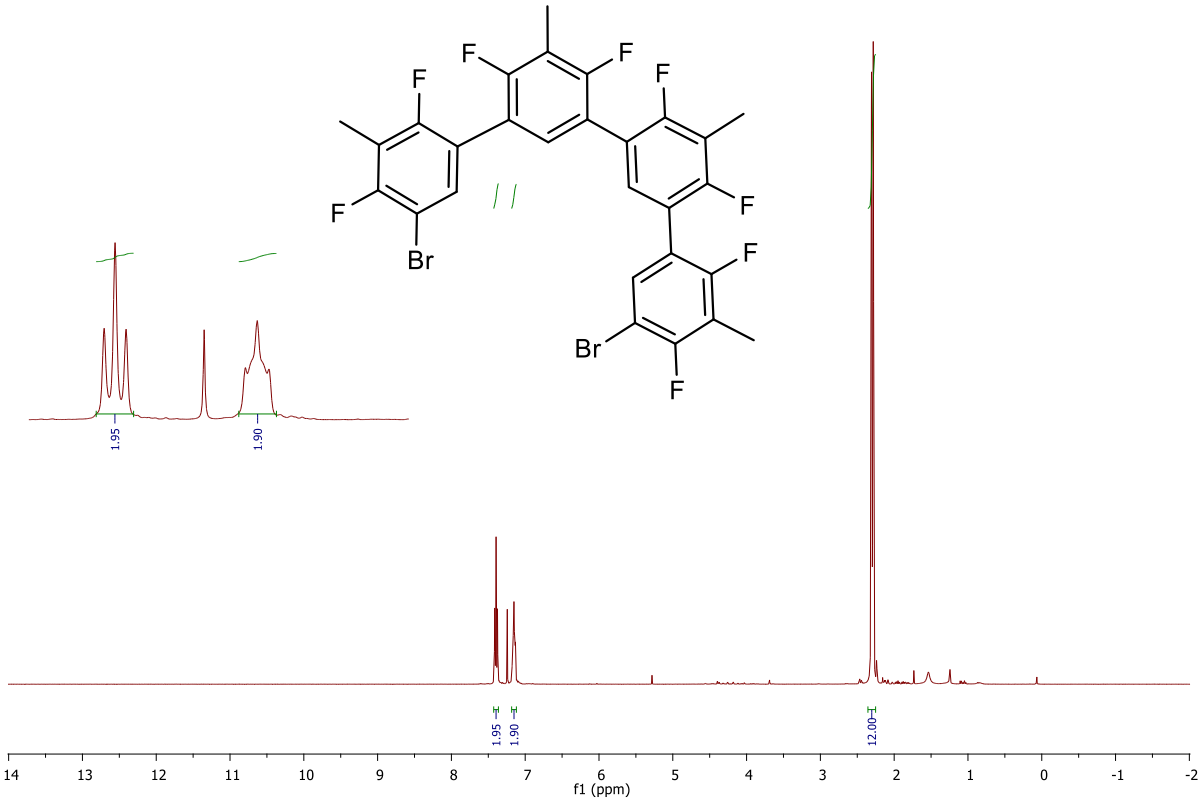

Figure A41. ^{1}H NMR (400 MHz, $CDCl_3$) of 7a.

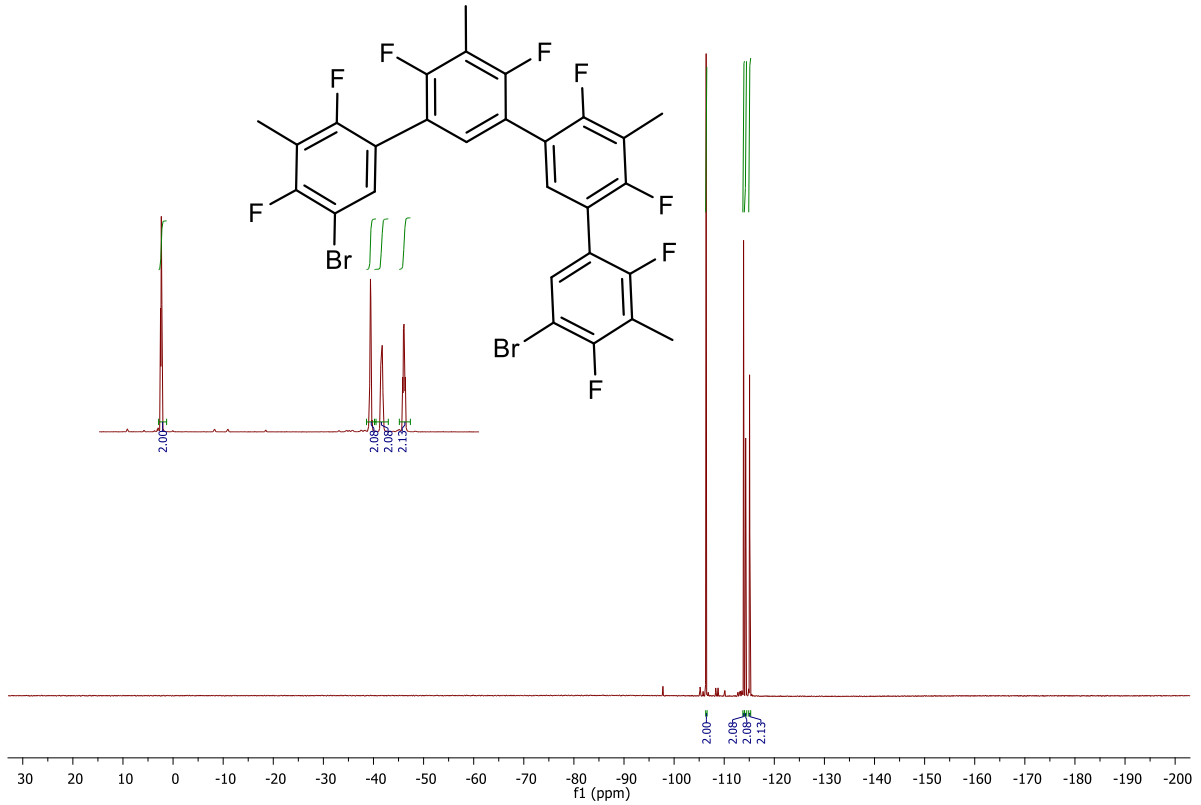

Figure A42. ^{19}F NMR (376 MHz, $CDCl_3$) of 7a.

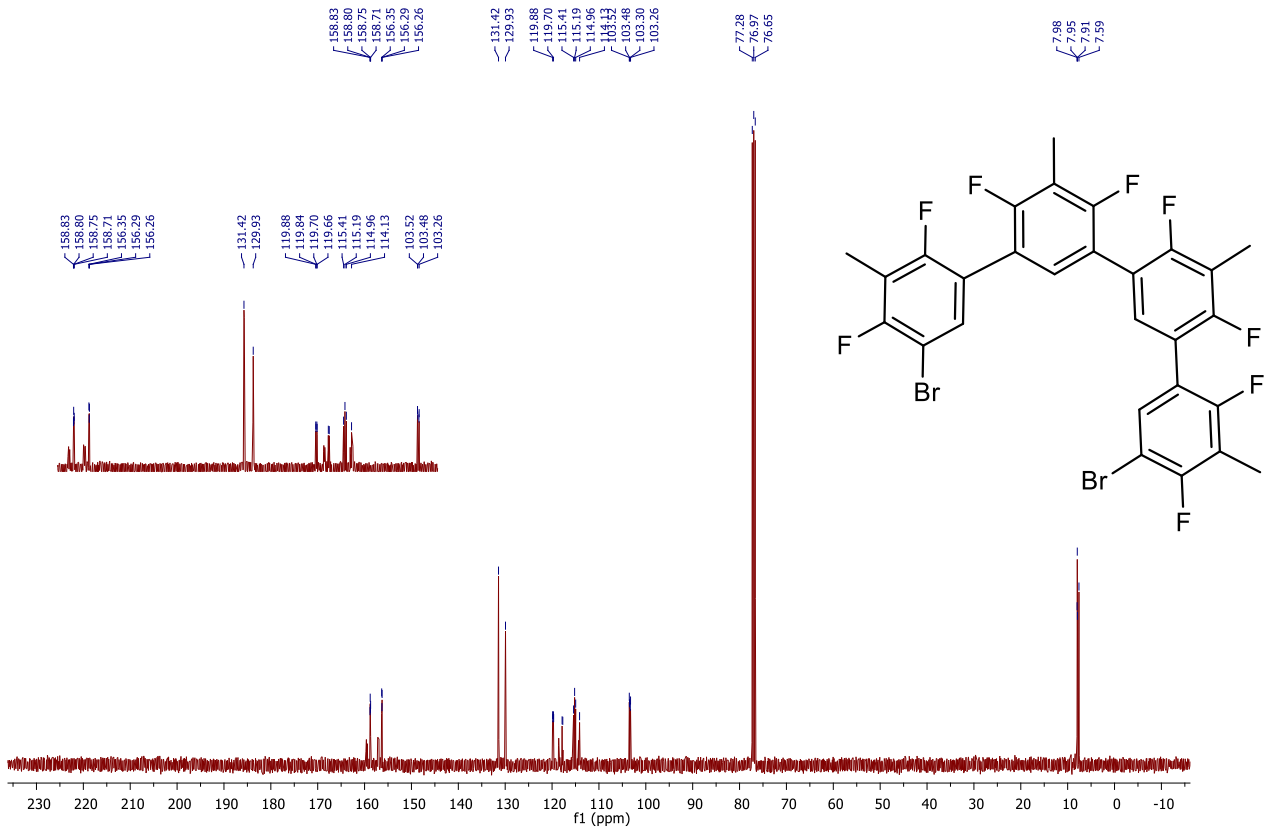

Figure A43. ^{13}C NMR (101 MHz, $CDCl_3$) of 7a.

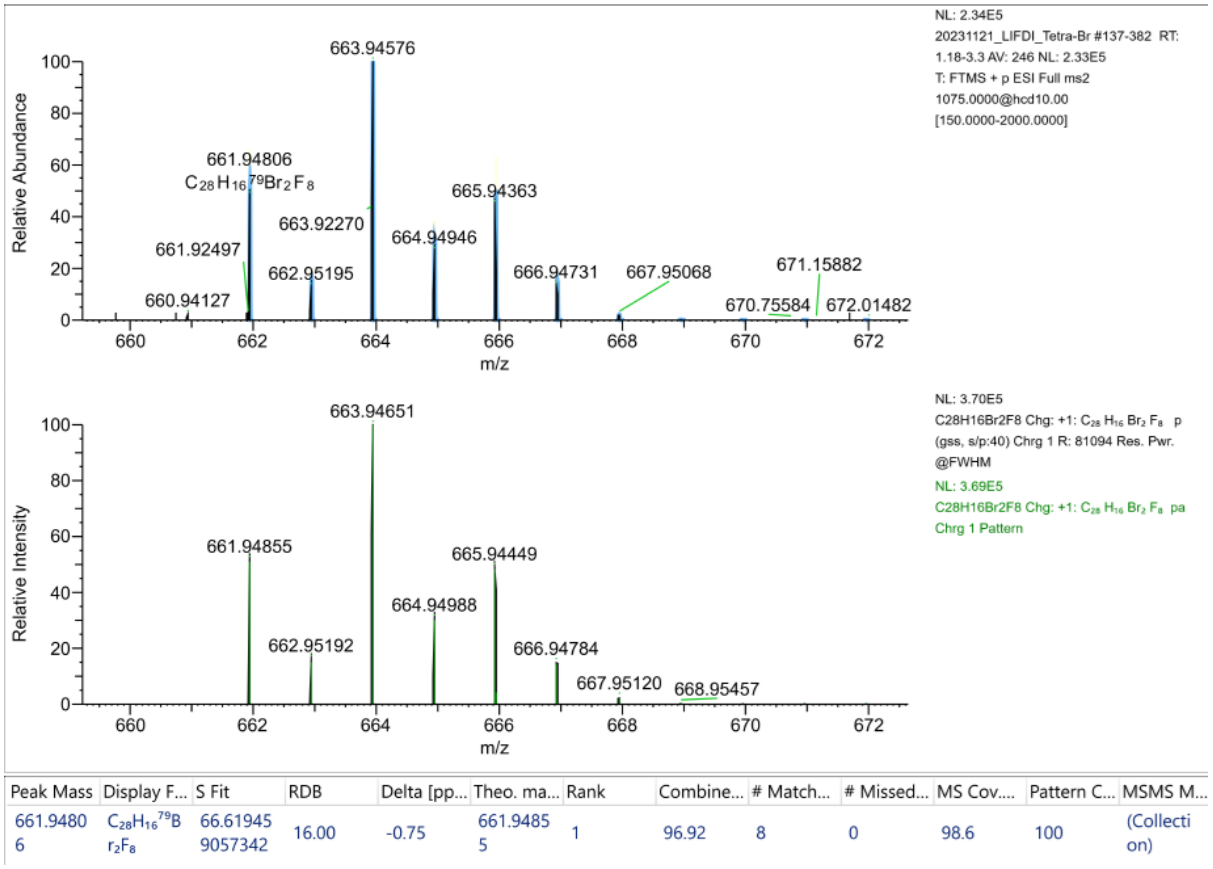

Peak Mass	Display F...	S Fit	RDB	Delta [pp...	Theo. ma...	Rank	Combine...	# Match...	# Missed...	MS Cov....	Pattern C...	MSMS M...
661.94806	$C_{28}H_{16}{}^{79}Br_2F_8$	66.619459057342	16.00	-0.75	661.94855	1	96.92	8	0	98.6	100	(Collection)

Figure A44. HRMS (LIFDI) of 7a.

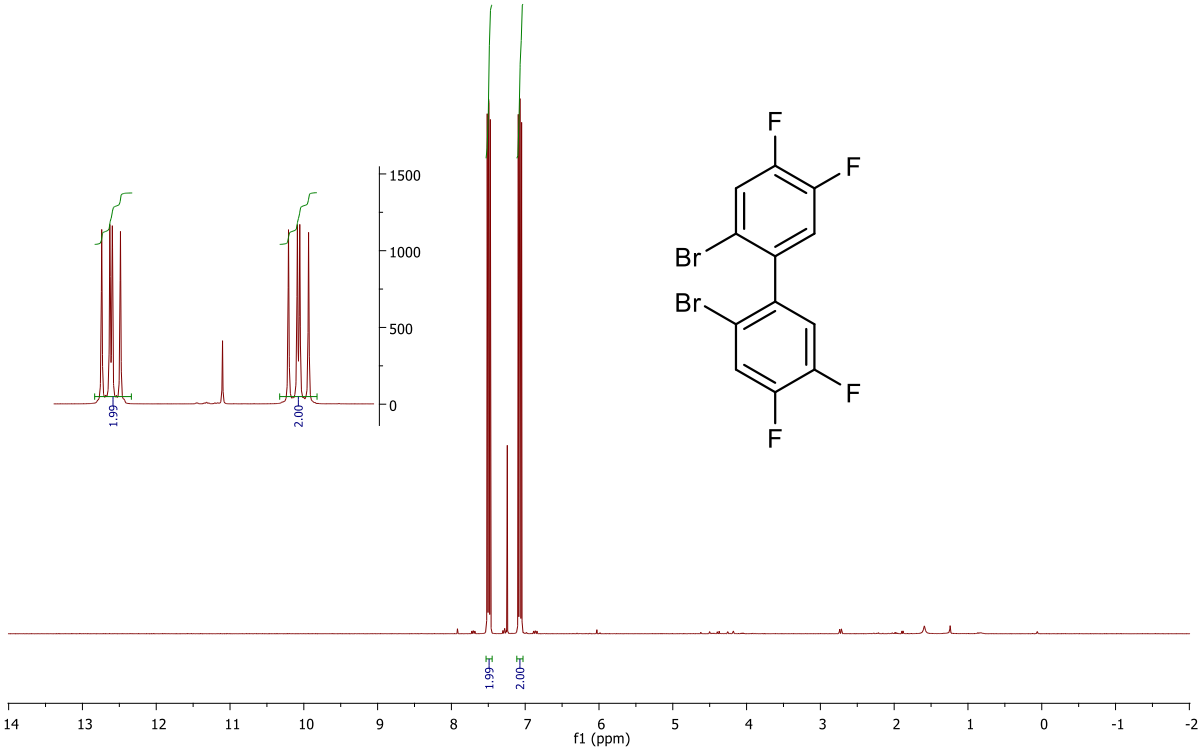

Figure A45. ^{1}H NMR (400 MHz, $CDCl_3$) of 8a.

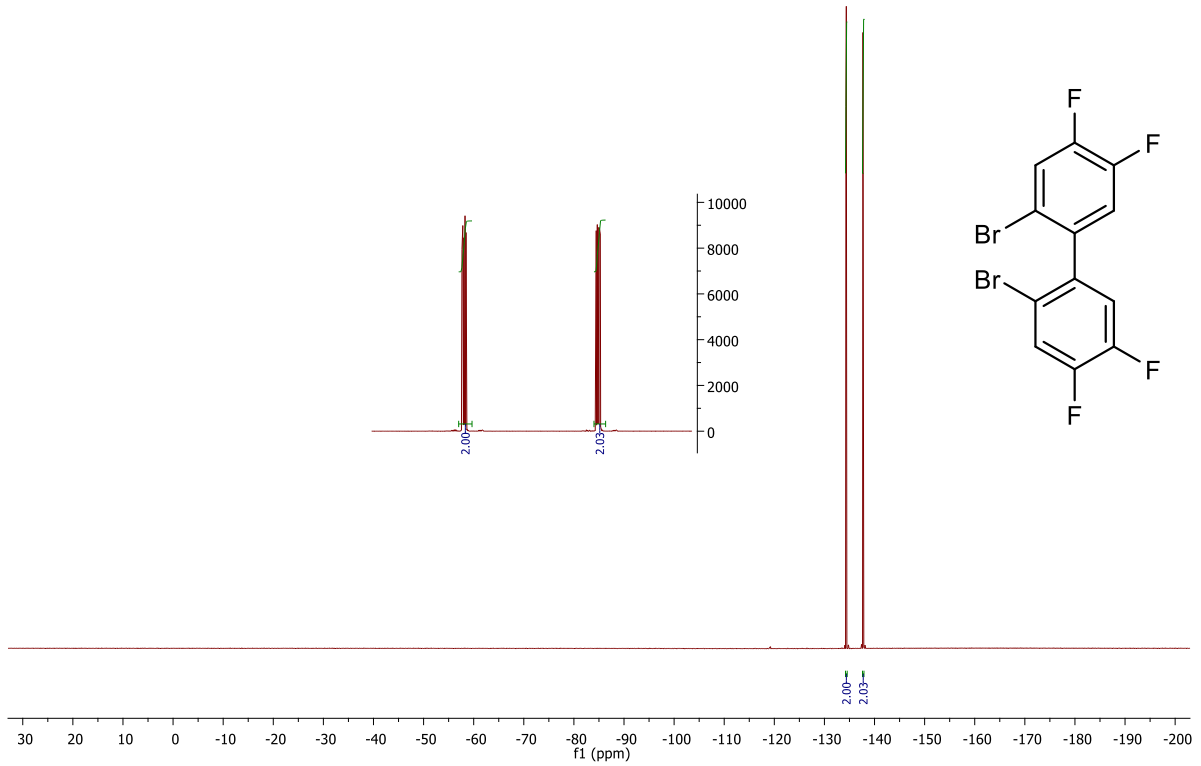

Figure A46. ^{19}F NMR (376 MHz, $CDCl_3$) of 8a.

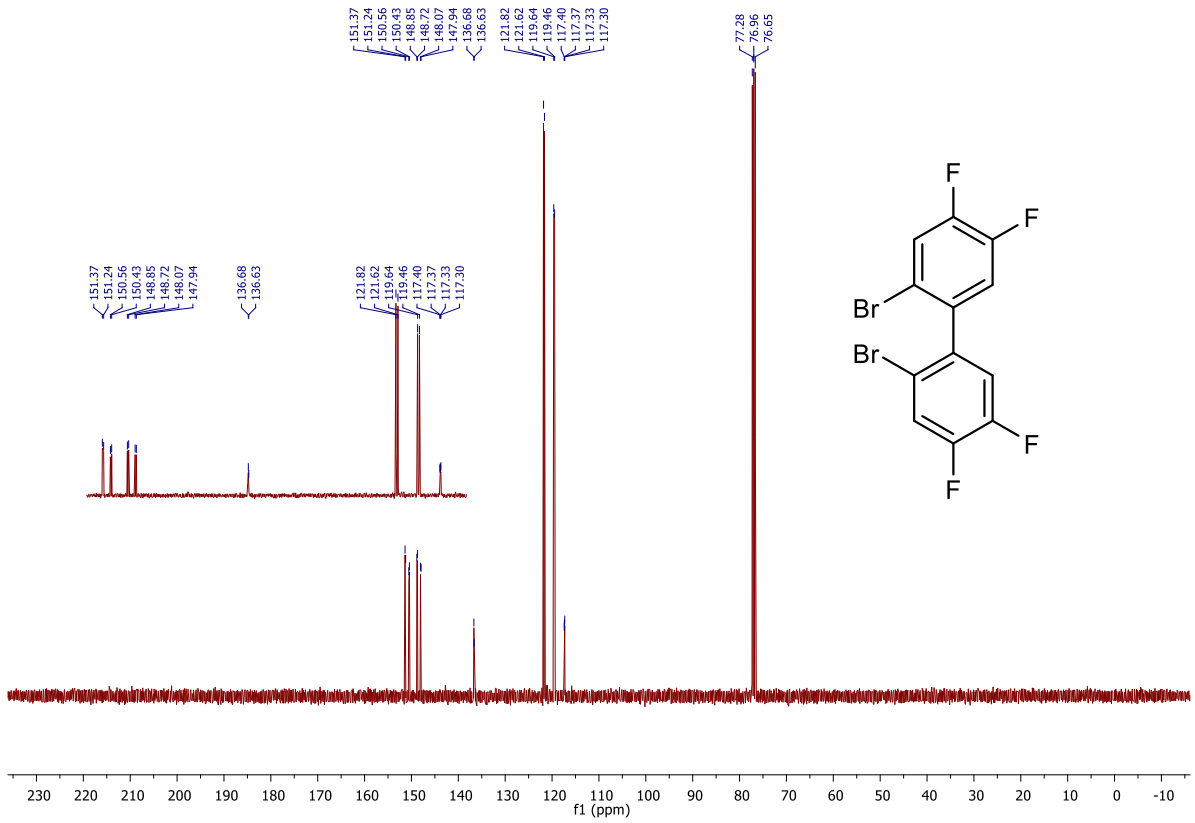

Figure A47. ^{13}C NMR (101 MHz, $CDCl_3$) of 8a.

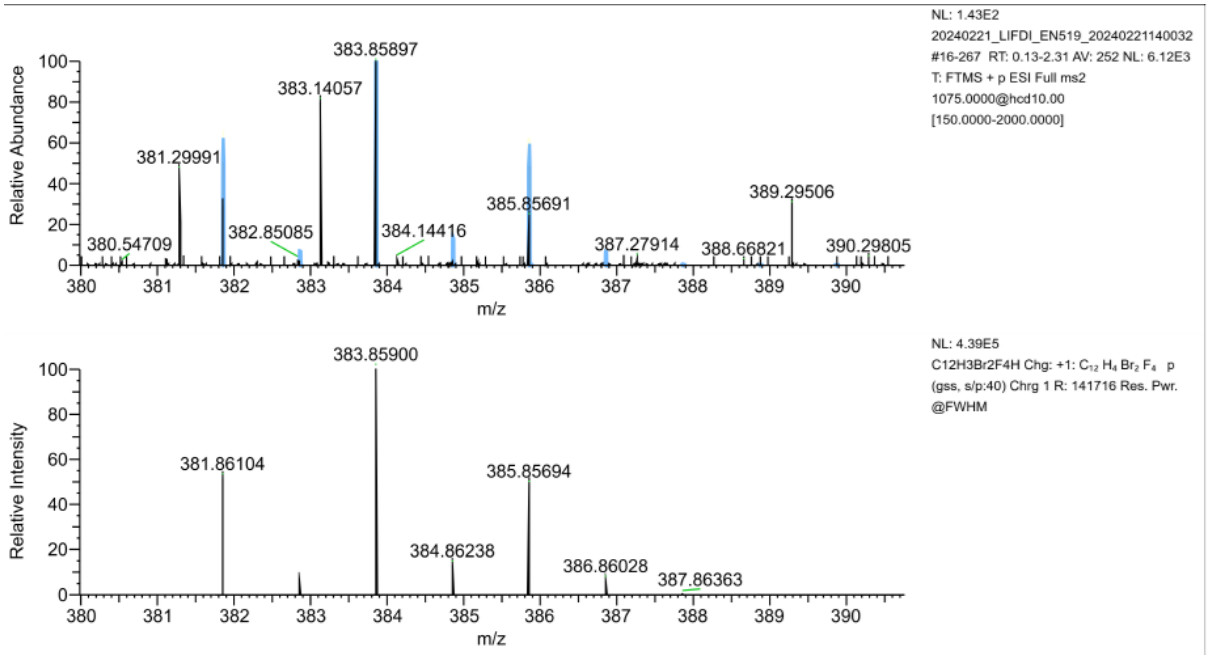

Peak Mass	Display F...	S Fit	RDB	Delta [pp...	Theo. ma...	Rank	Combine...	# Match...	# Missed...	MS Cov....	Pattern C...	MSMS M...
381.8610 3	$C_{12}H_4{}^{79}Br_2F_4$	18.34847 7386225 6	8.00	-0.02	381.8610 4	1	34.98	3	0	35.9	49.99	(Collecti on)

Figure A48. HRMS (LIFDI) of 8a.

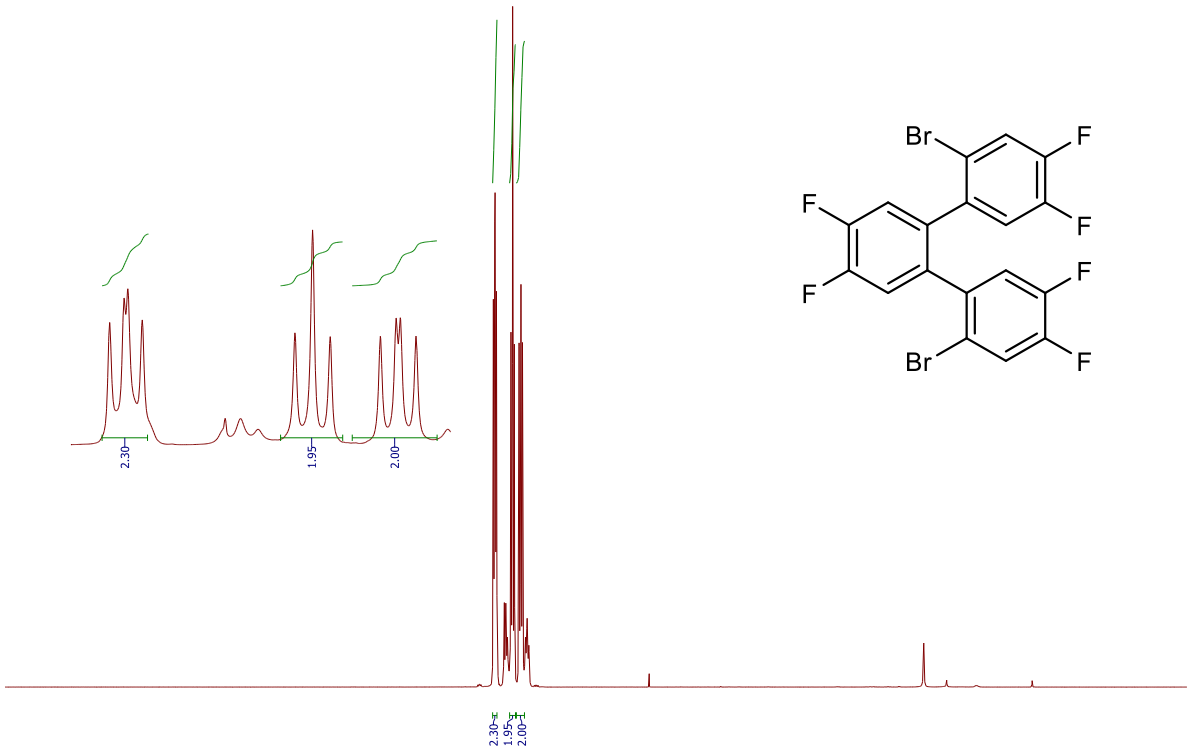

Figure A49. ^{1}H NMR (400 MHz, $CDCl_3$) of 9a.

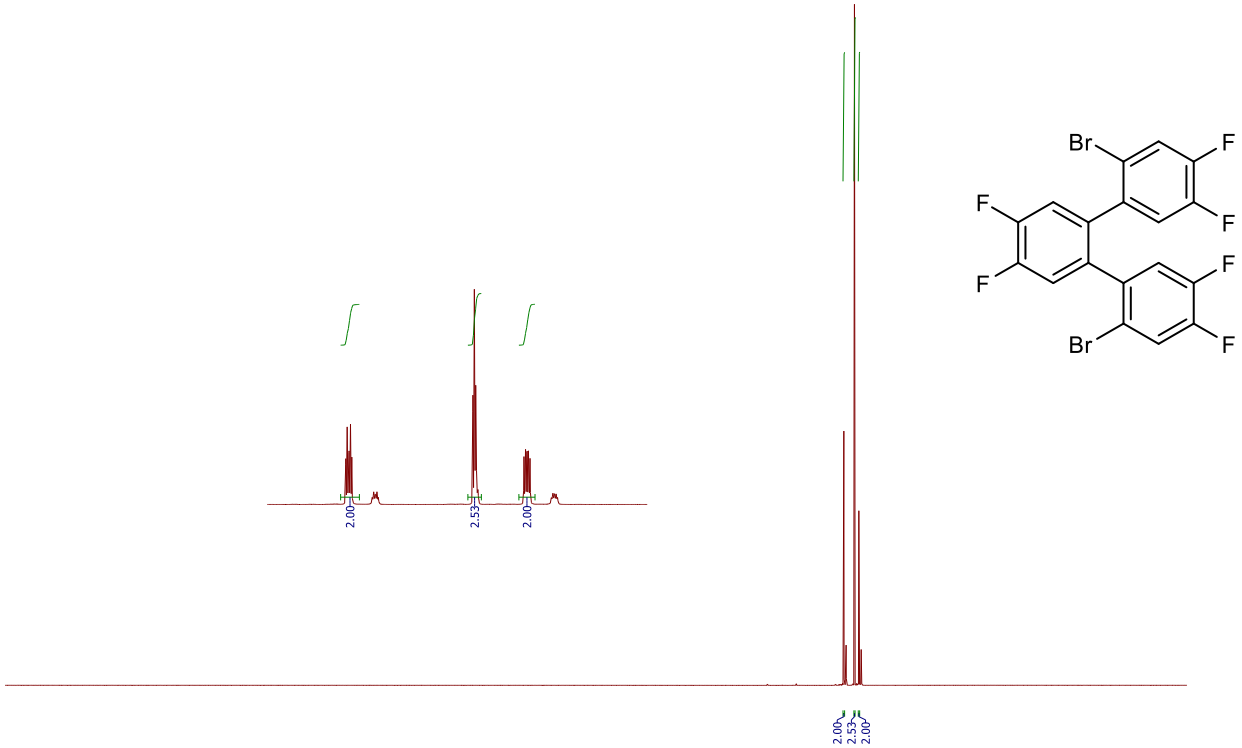

Figure A50. ^{19}F NMR (376 MHz, $CDCl_3$) of 9a.

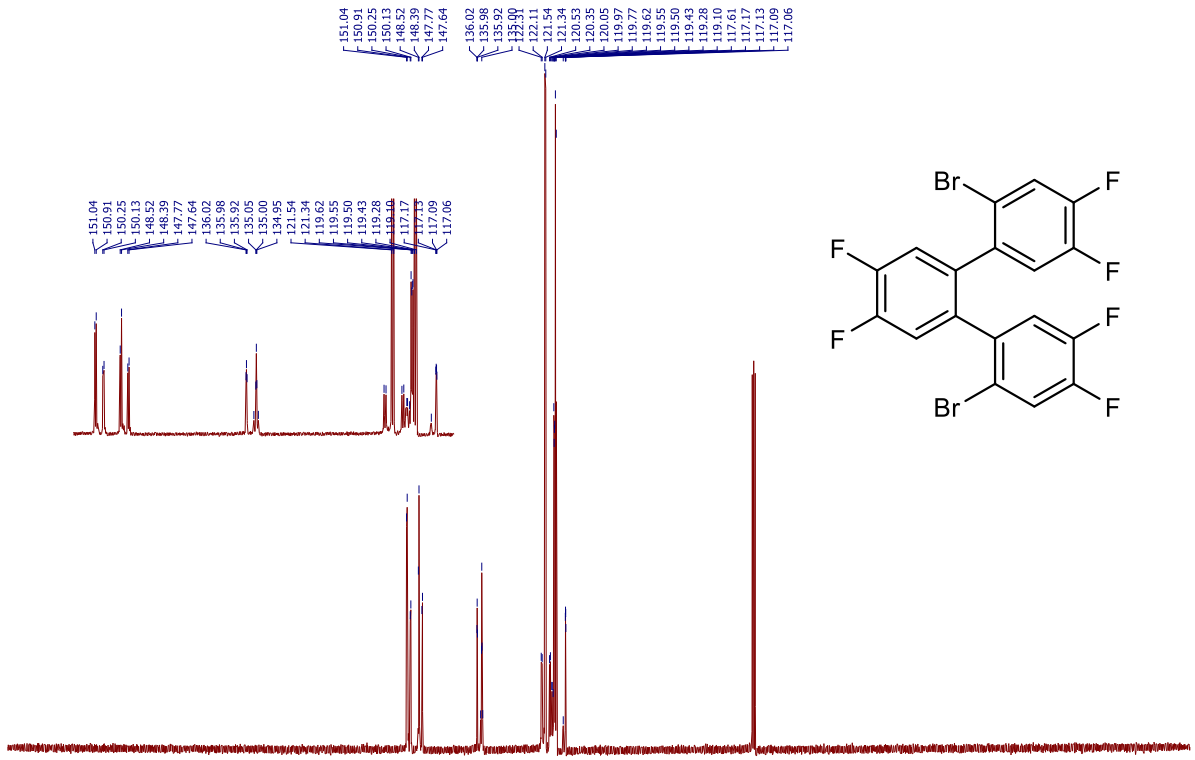

Figure A51. ^{13}C NMR (101 MHz, $CDCl_3$) of 9a.

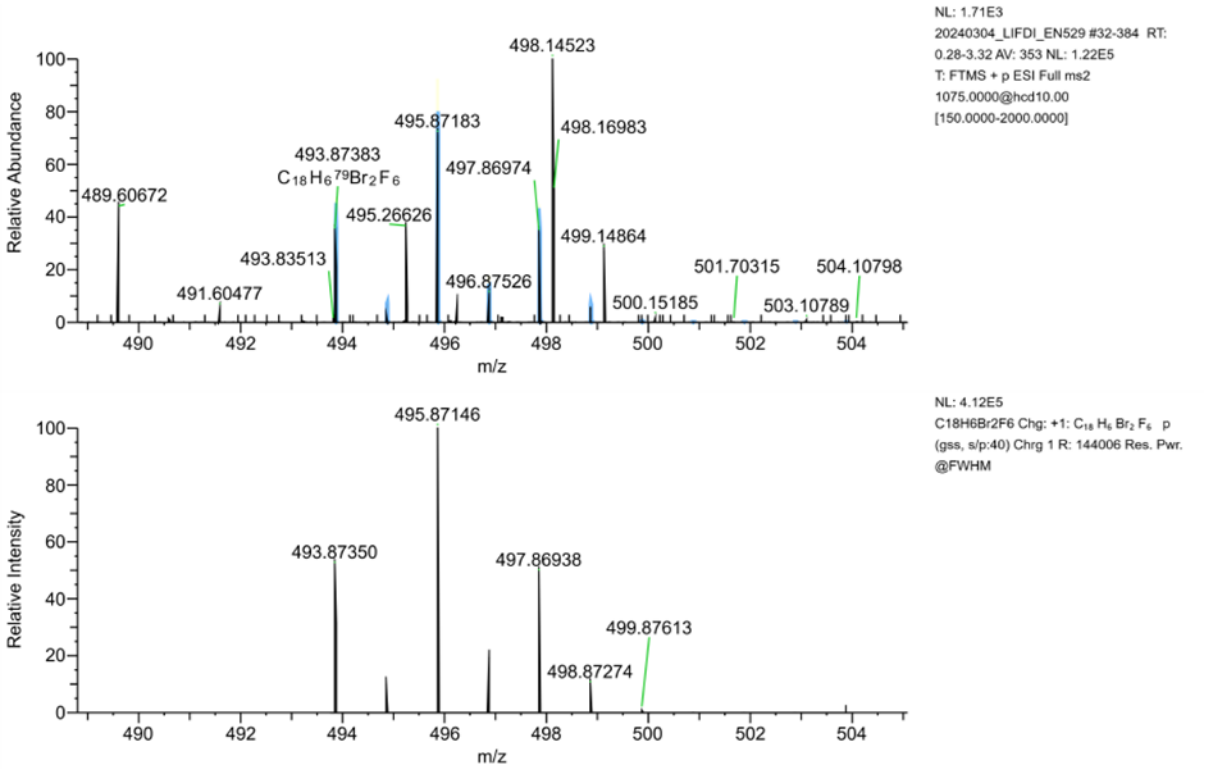

Peak Mass	Display F...	S Fit	RDB	Delta [pp...	Theo. ma...	Rank	Combine...	# Match...	# Missed...	MS Cov....	Pattern C...	MSMS M..
493.87383	$C_{18}H_6{}^{79}Br_2F_6$	29.71023 0077634 8	12.00	0.68	493.87350	1	47.93	6	1	48.94	91.16	(Collection)

Figure A52. HRMS (LIFDI) of 9a.

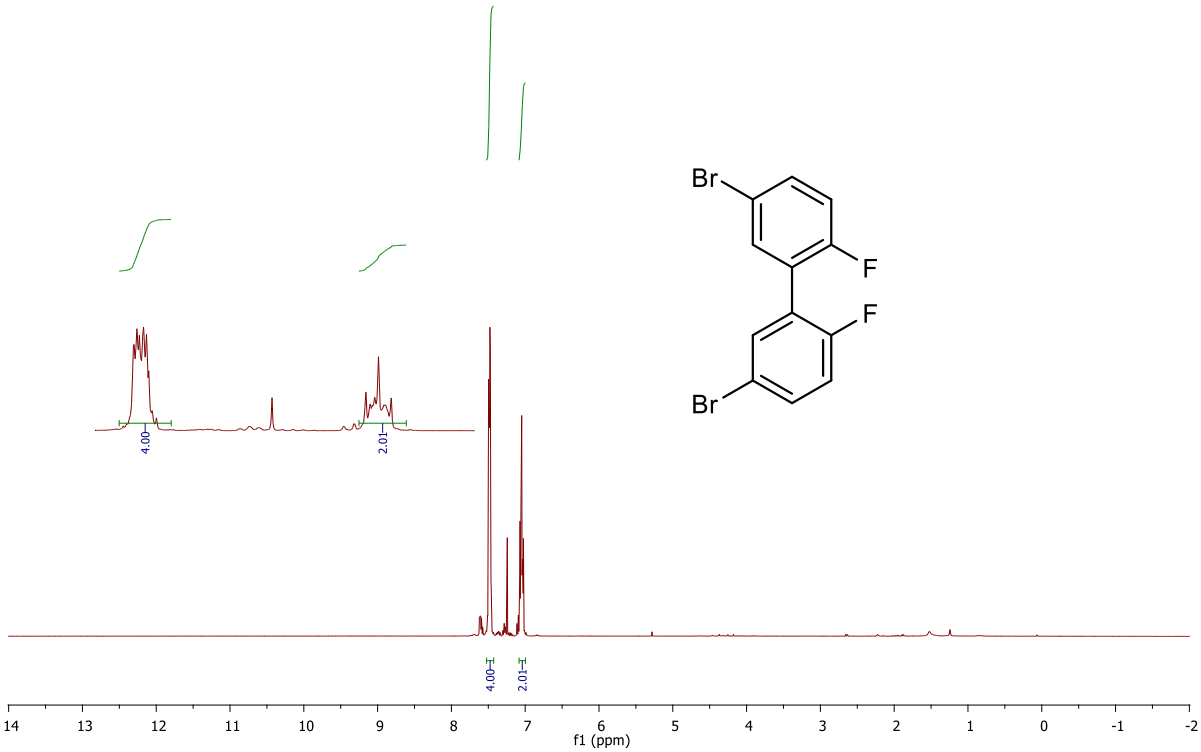

Figure A53. ^{1}H NMR (400 MHz, $CDCl_3$) of 10a.

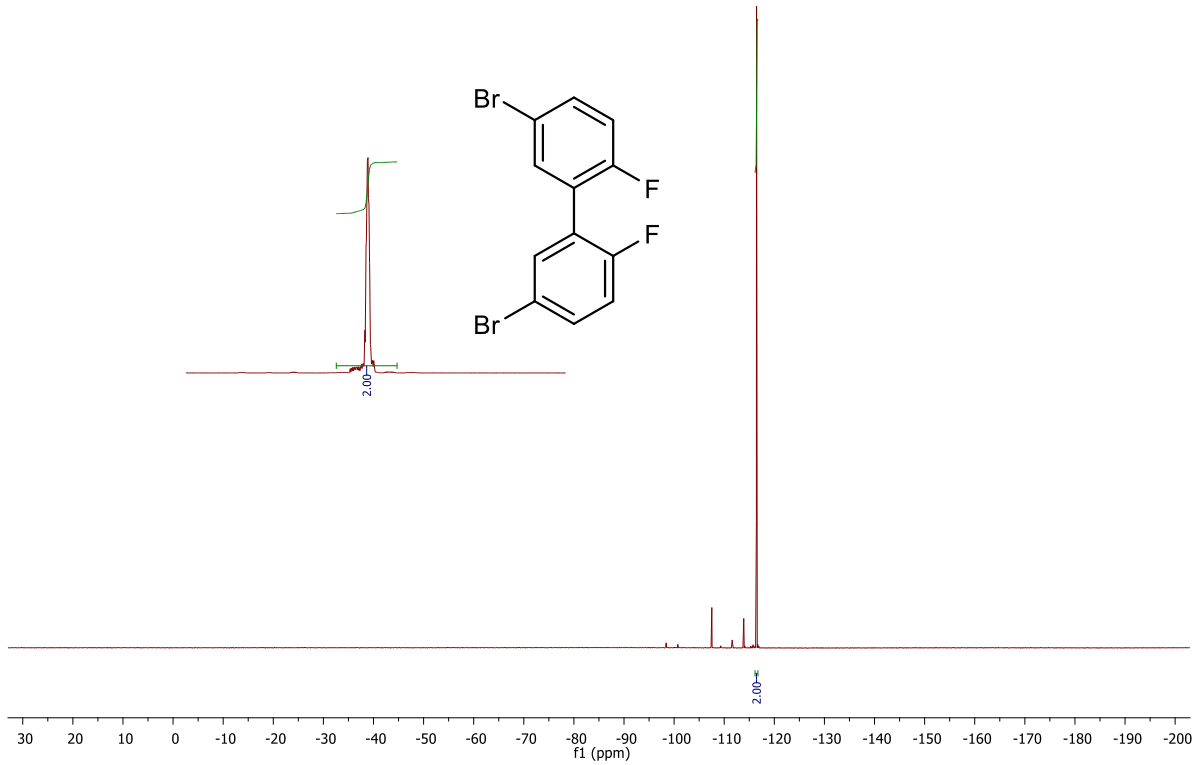

Figure A54. ^{19}F NMR (376 MHz, $CDCl_3$) of 10a.

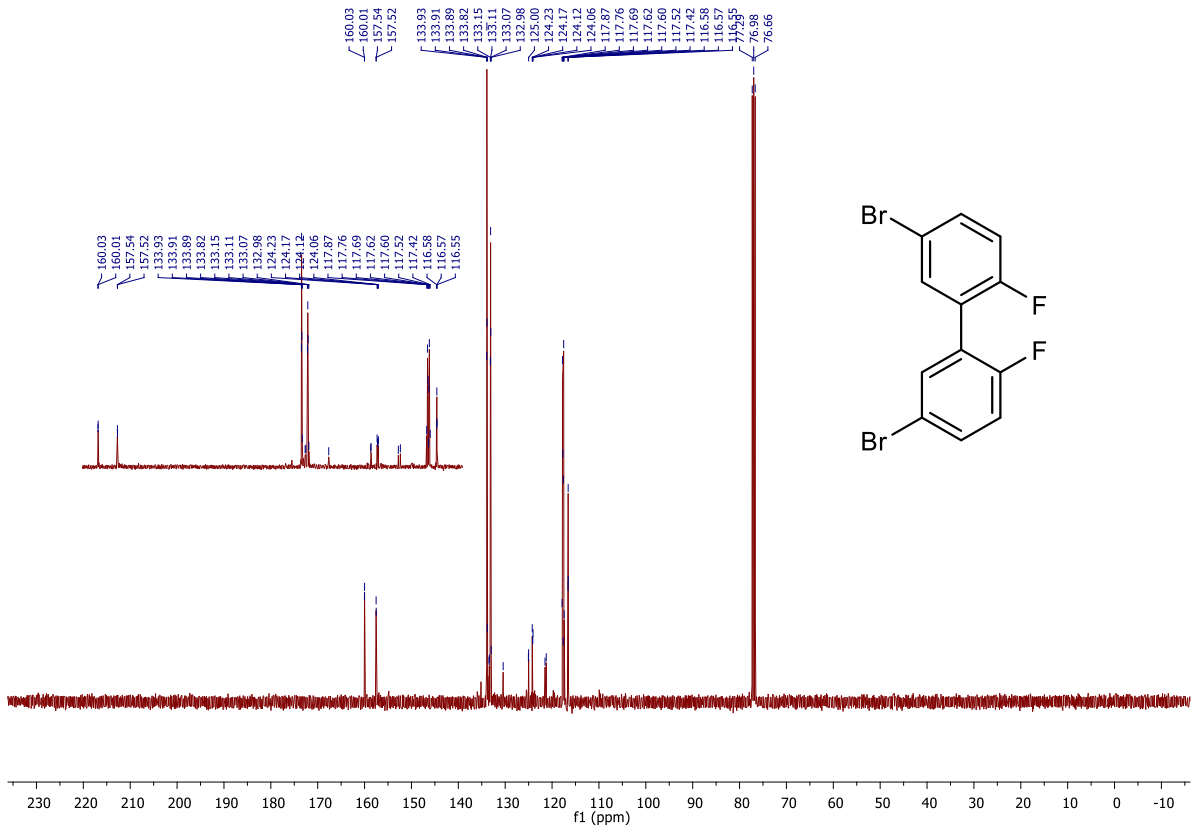

Figure A55. ^{13}C NMR (101 MHz, $CDCl_3$) of 10a.

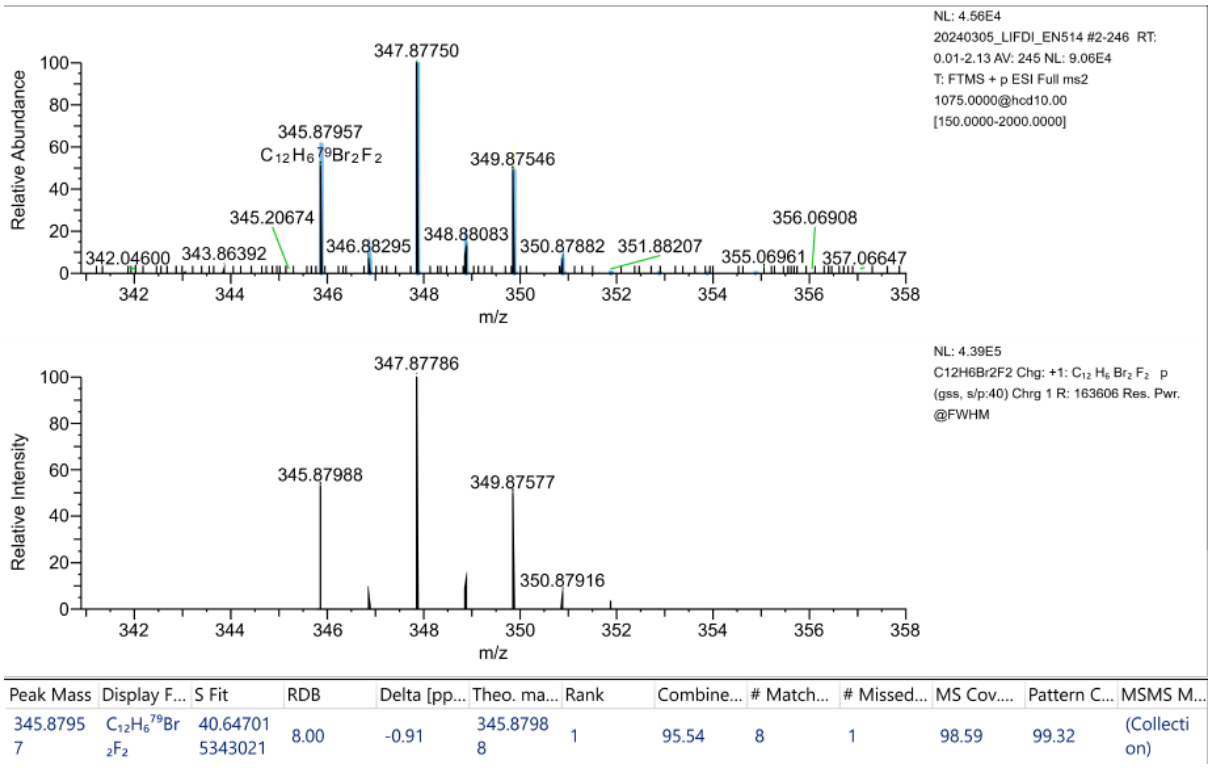

Peak Mass	Display F...	S Fit	RDB	Delta [pp...	Theo. ma...	Rank	Combine...	# Match...	# Missed...	MS Cov....	Pattern C...	MSMS M...
345.87957	$C_{12}H_6{}^{79}Br_2F_2$	40.64701 5343021	8.00	-0.91	345.87988	1	95.54	8	1	98.59	99.32	(Collection)

Figure A56. HRMS (LIFDI) of 10a.

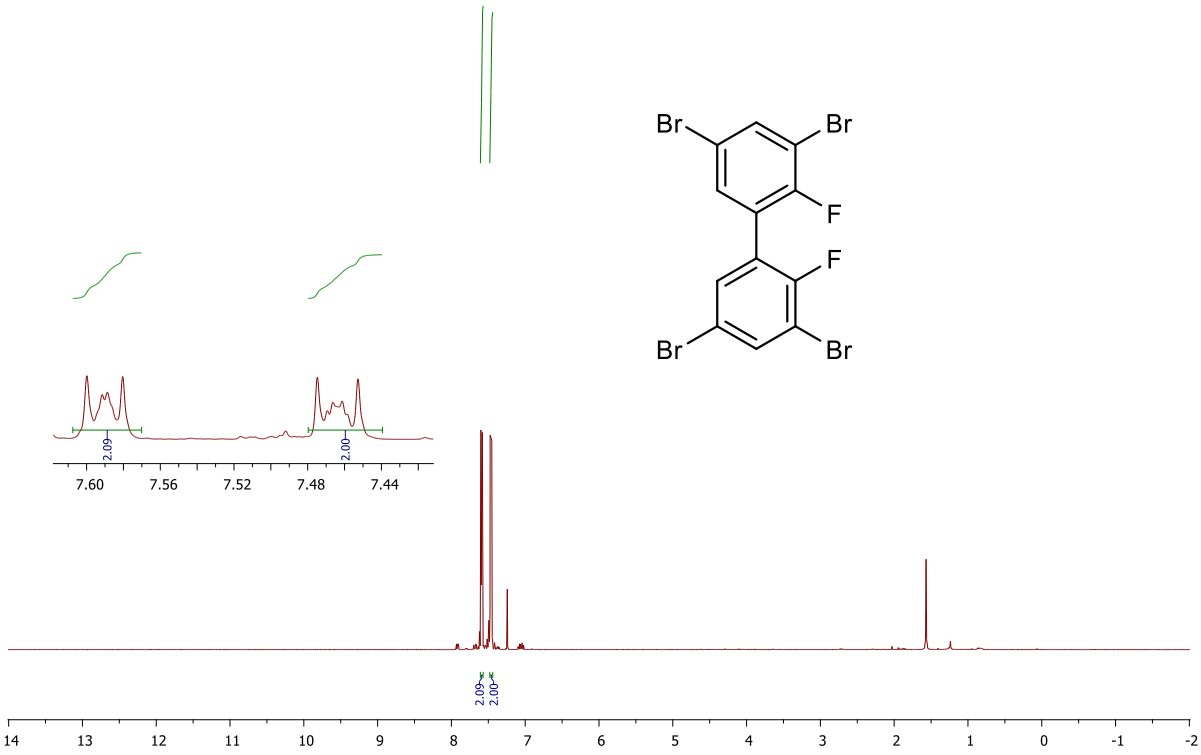

Figure A57. ^{1}H NMR (400 MHz, $CDCl_3$) of 10b.

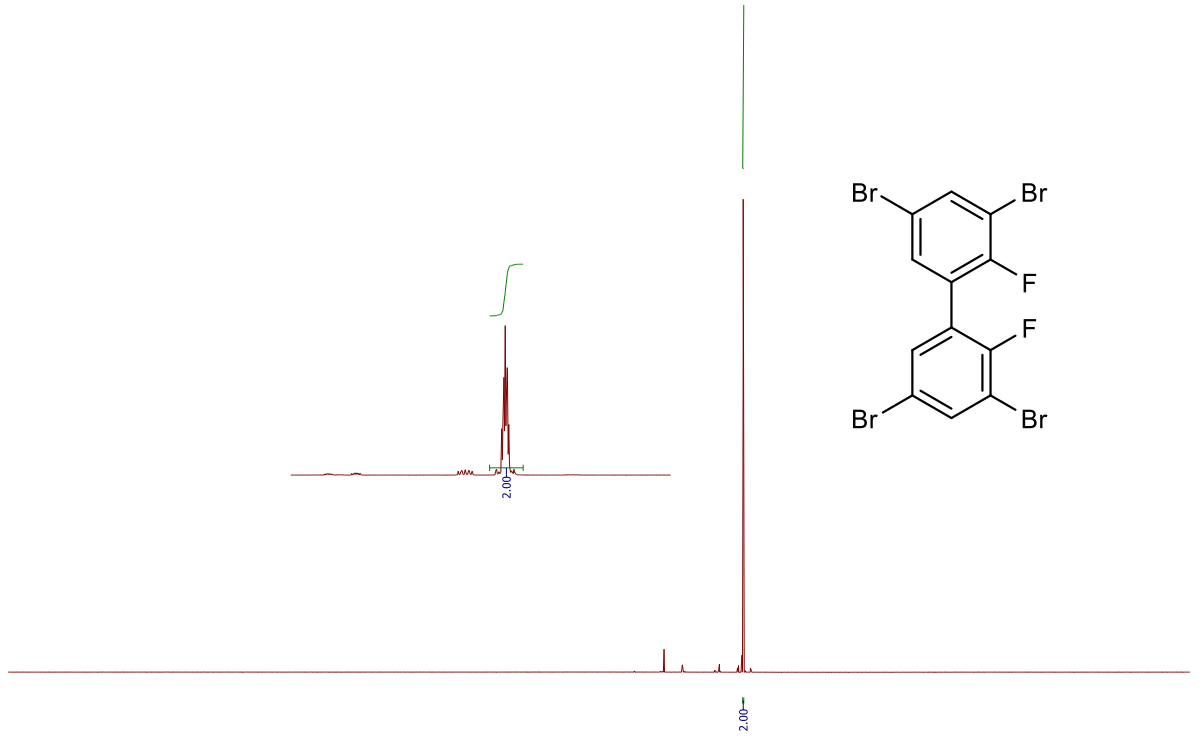

Figure A58. ^{19}F NMR (376 MHz, $CDCl_3$) of 10b.

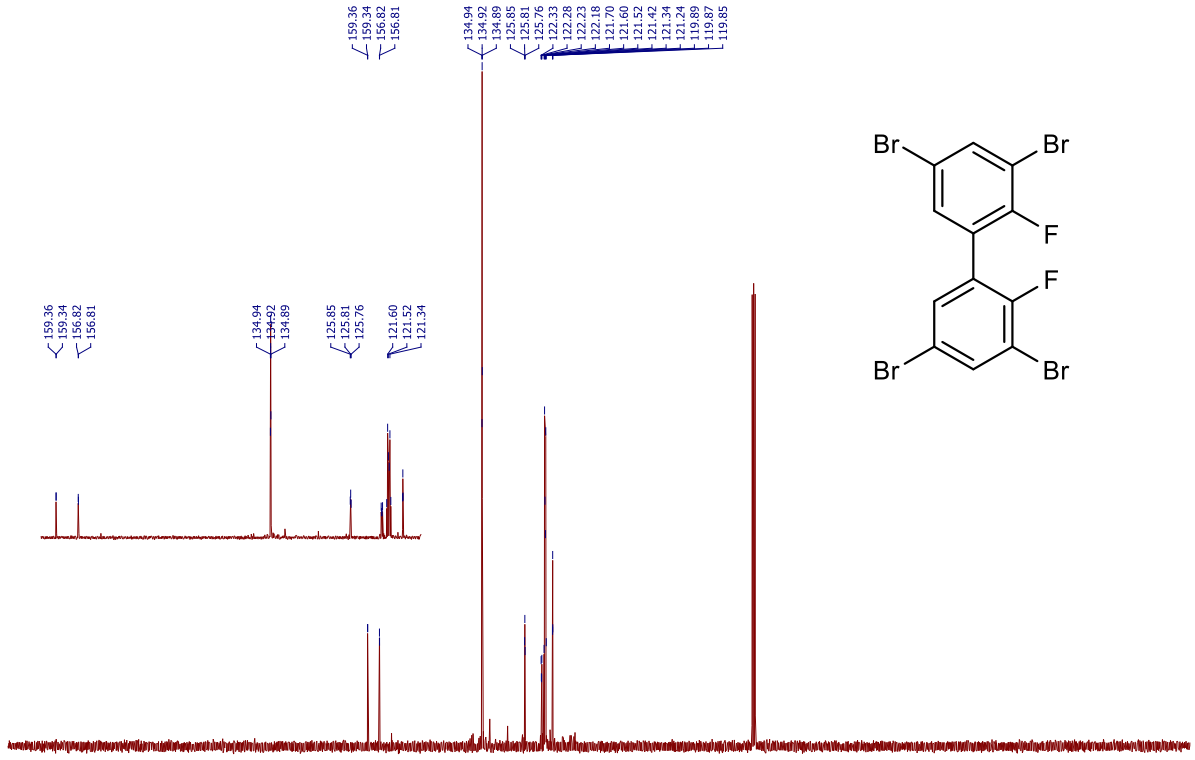

Figure A59. ^{13}C NMR (101 MHz, $CDCl_3$) of 10b.

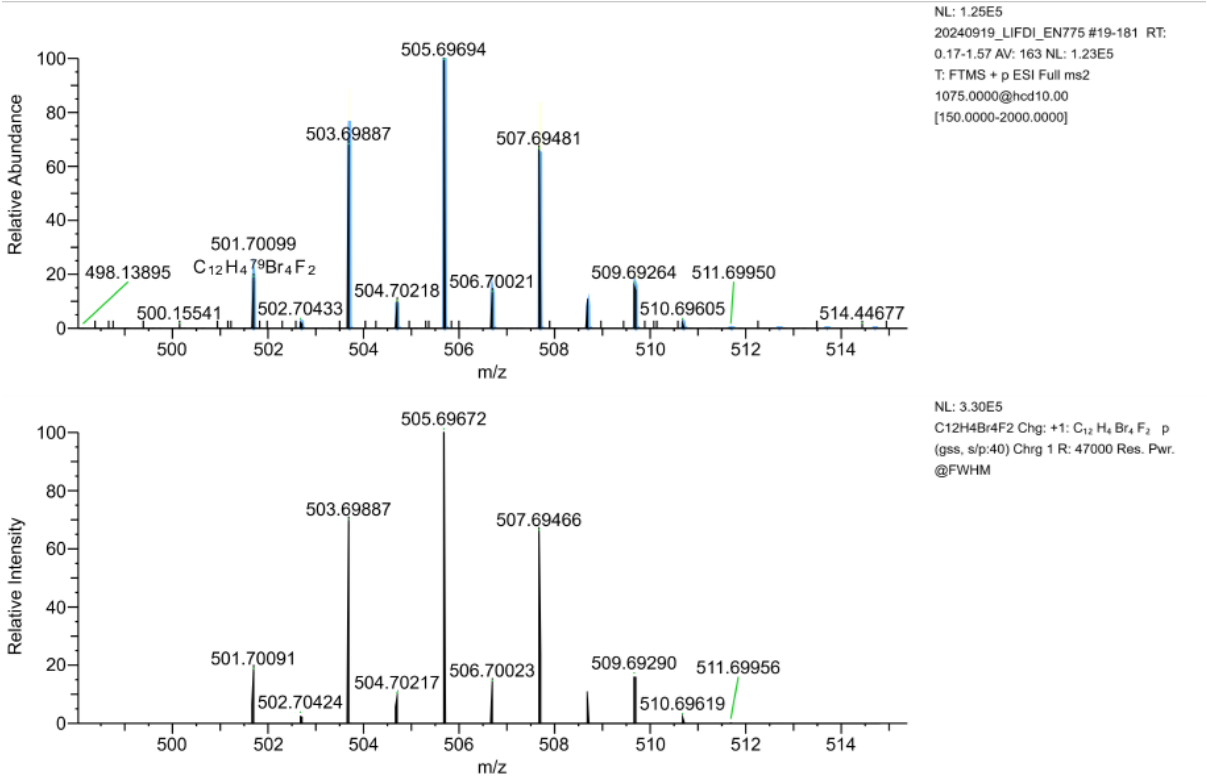

Peak Mass	Display F...	S Fit	RDB	Delta [pp...	Theo. ma...	Rank	Combine...	# Match...	# Missed...	MS Cov....	Pattern C...	MSMS M..
501.70099	$C_{12}H_4{}^{79}Br_4F_2$	58.72479 4711218	8.00	0.15	501.70091	1	97.76	11	1	99.93	99.79	(Collection)

Figure A60. HRMS (LIFDI) of 10b.

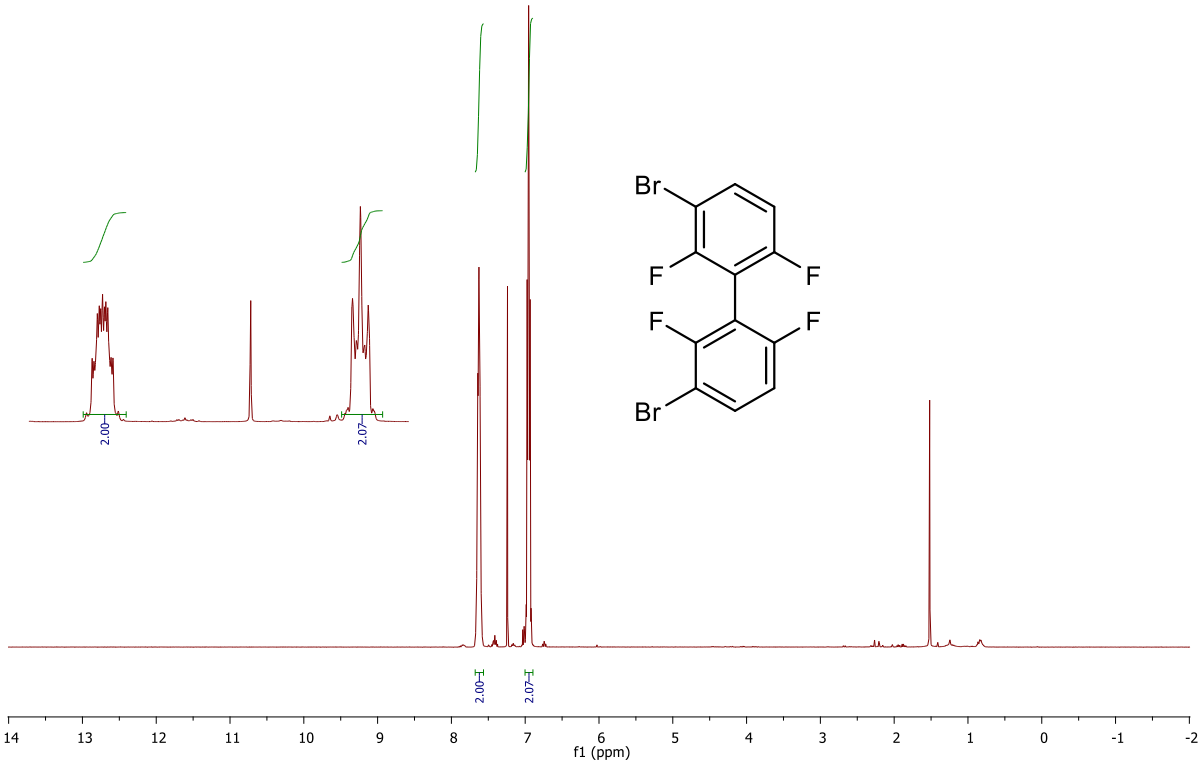

Figure A61. ^{1}H NMR (400 MHz, $CDCl_3$) of 11a.

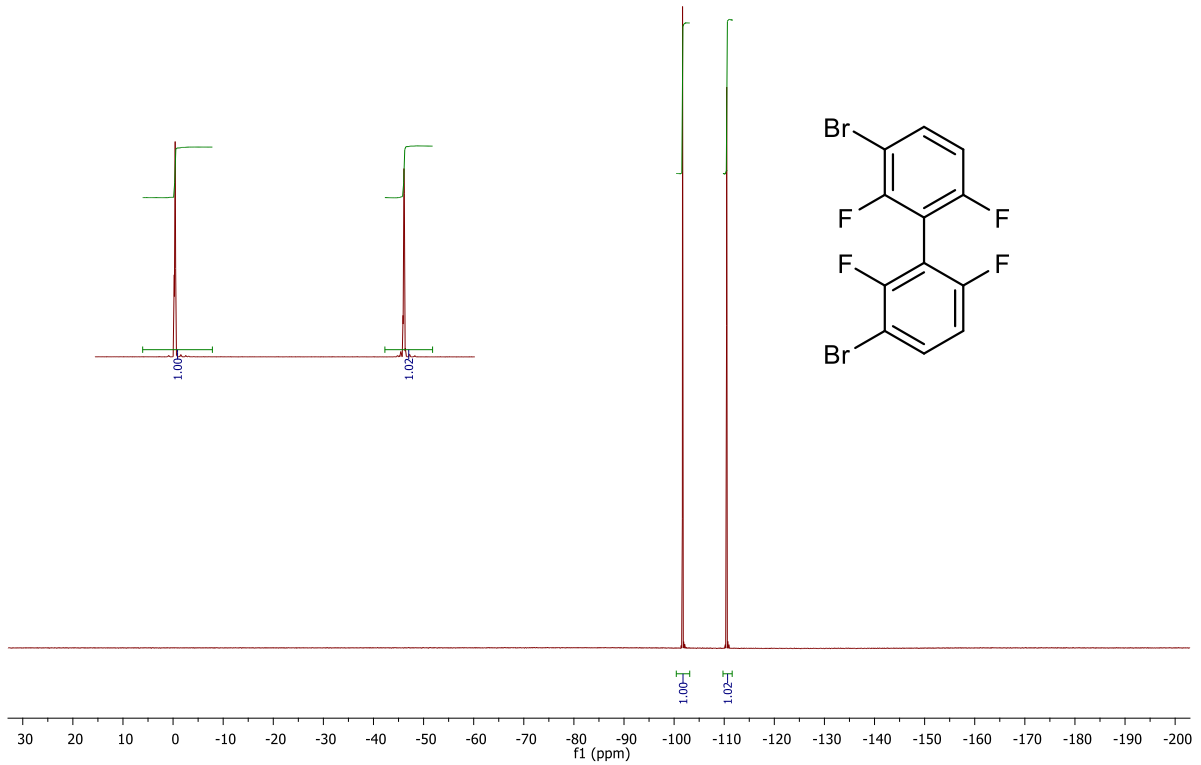

Figure A62. ^{19}F NMR (376 MHz, $CDCl_3$) of 11a.

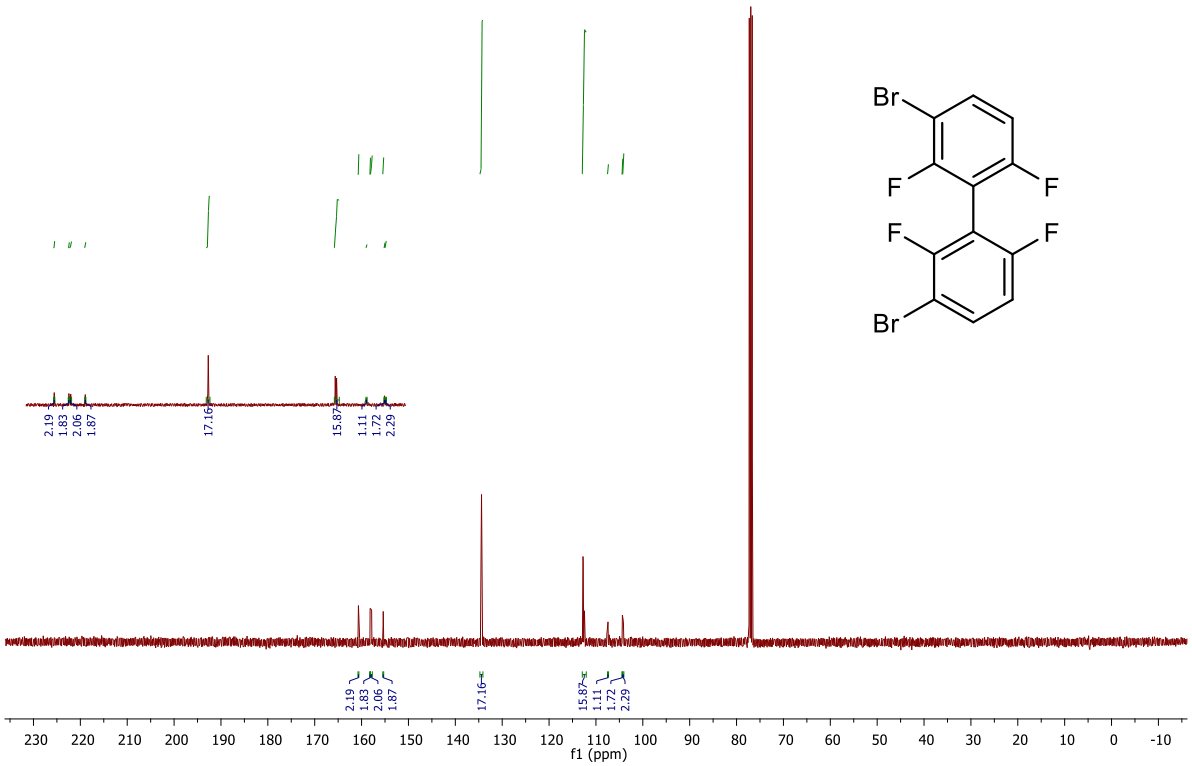

Figure A63. ^{13}C NMR (101 MHz, $CDCl_3$) of 11a.

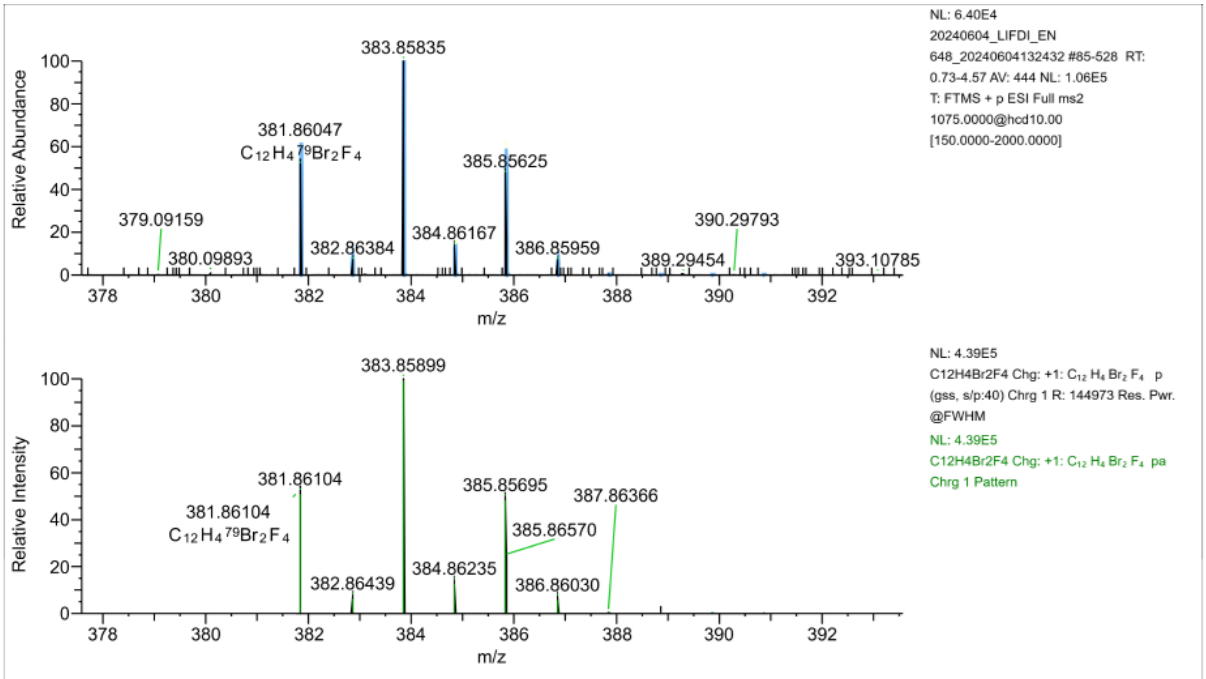

Peak Mass	Display F...	S Fit	RDB	Delta [pp...	Theo. ma...	Rank	Combine...	# Match...	# Missed...	MS Cov....	Pattern C...	MSMS M...
381.86047	$C_{12}H_4{}^{79}Br_2F_4$	44.79239 1839421 3	8.00	-1.50	381.86104	1	96.6	8	1	99.48	99.49	(Collection)

Figure A64. HRMS (LIFDI) of 11a.

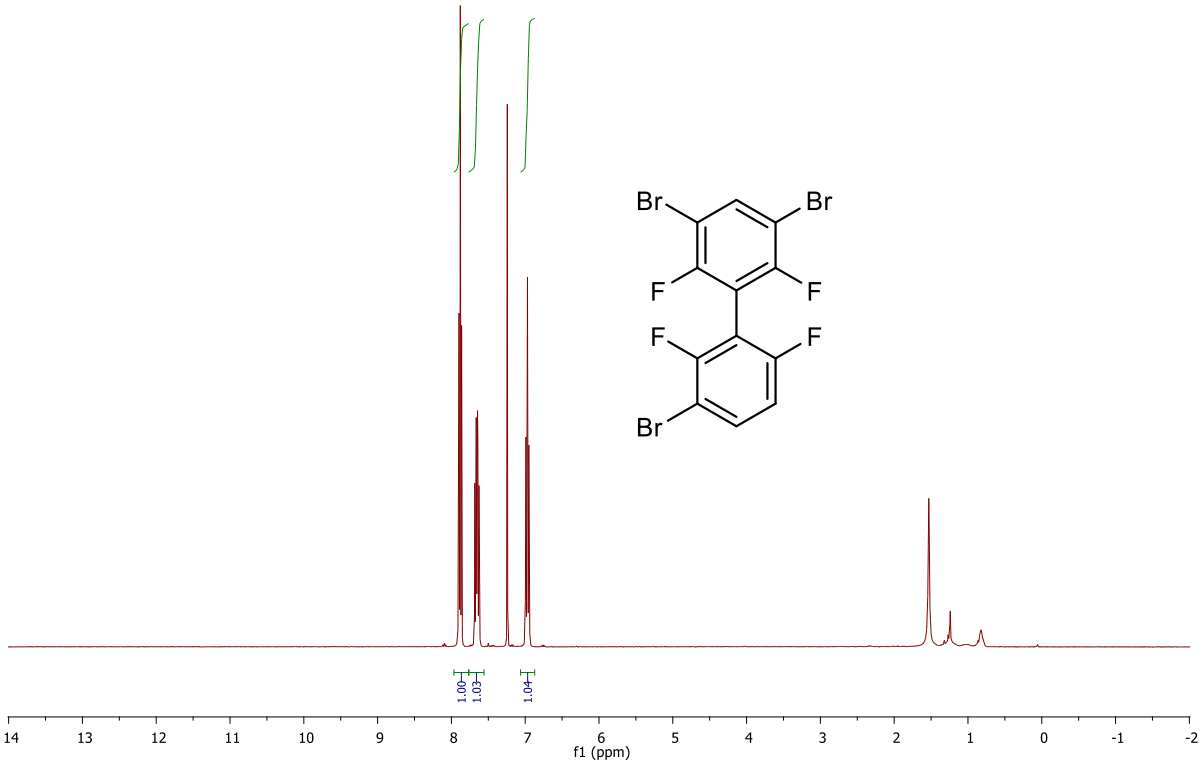

Figure A65. ^{1}H NMR (400 MHz, $CDCl_3$) of 11b.

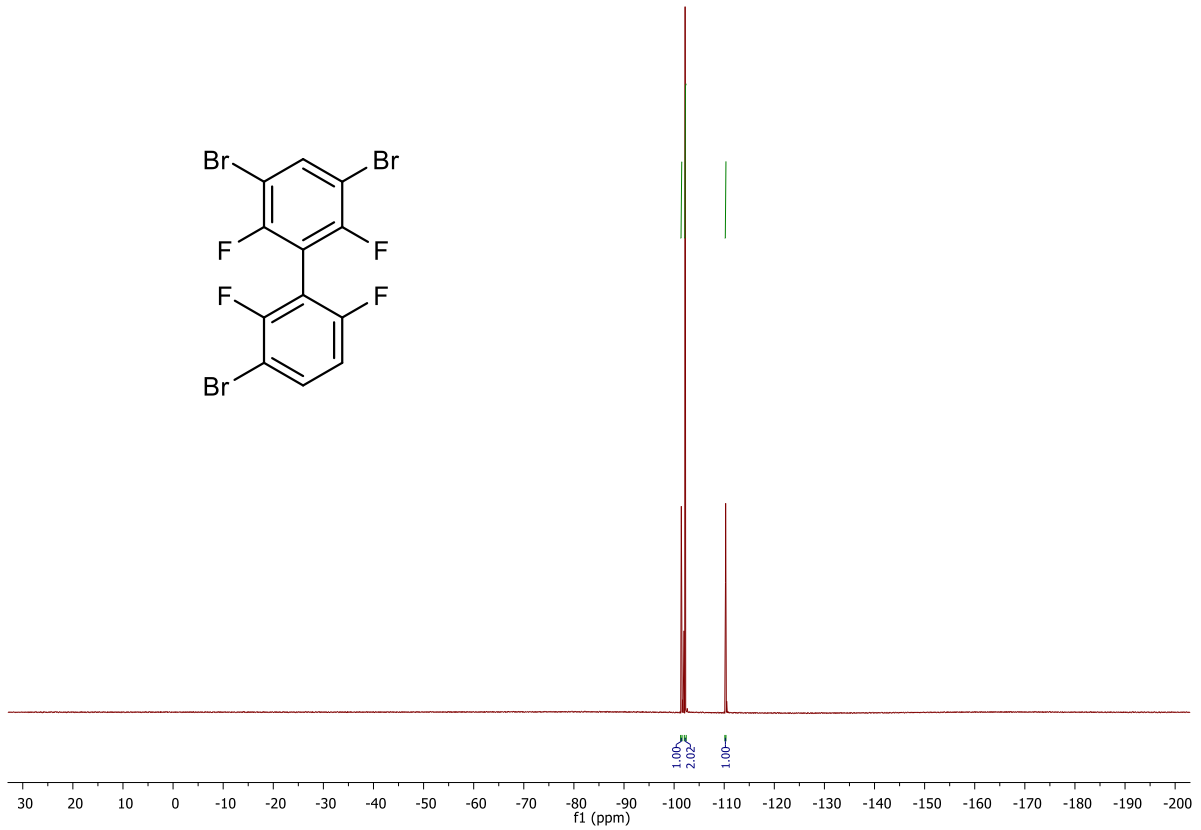

Figure A66. ^{19}F NMR (376 MHz, $CDCl_3$) of 11b.

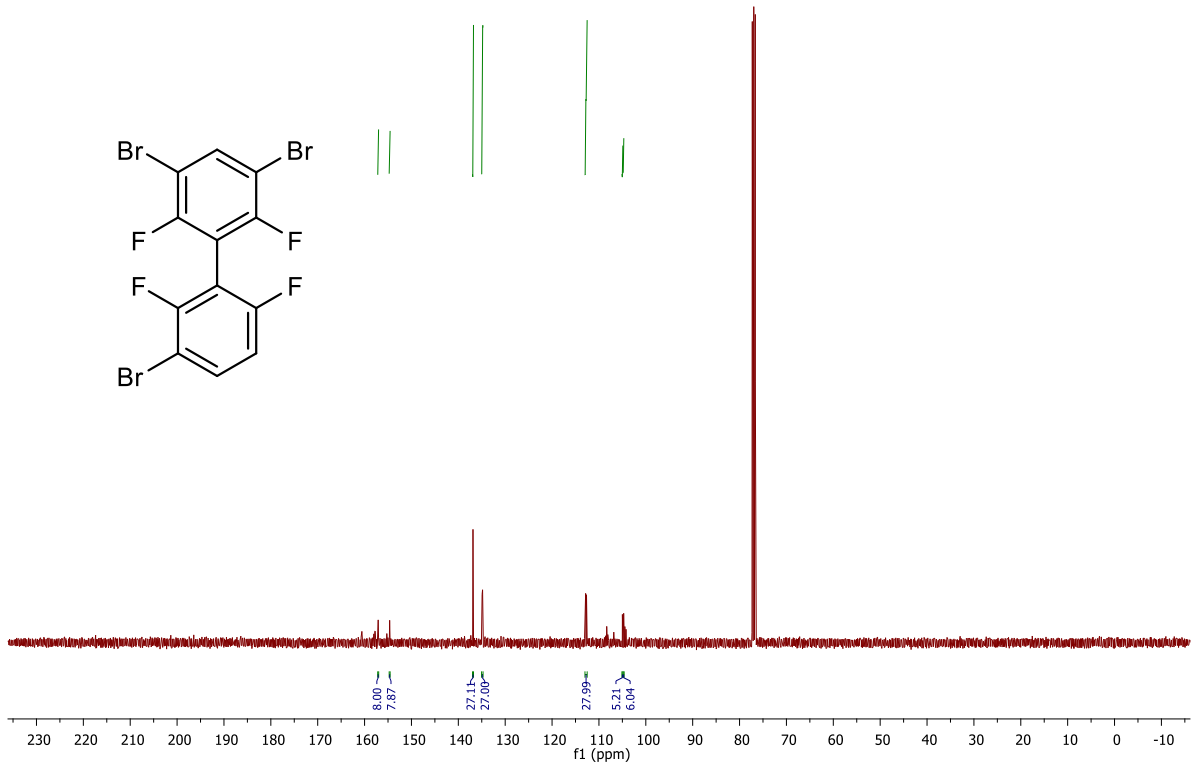

Figure A67. ^{13}C NMR (101 MHz, $CDCl_3$) of 11b.

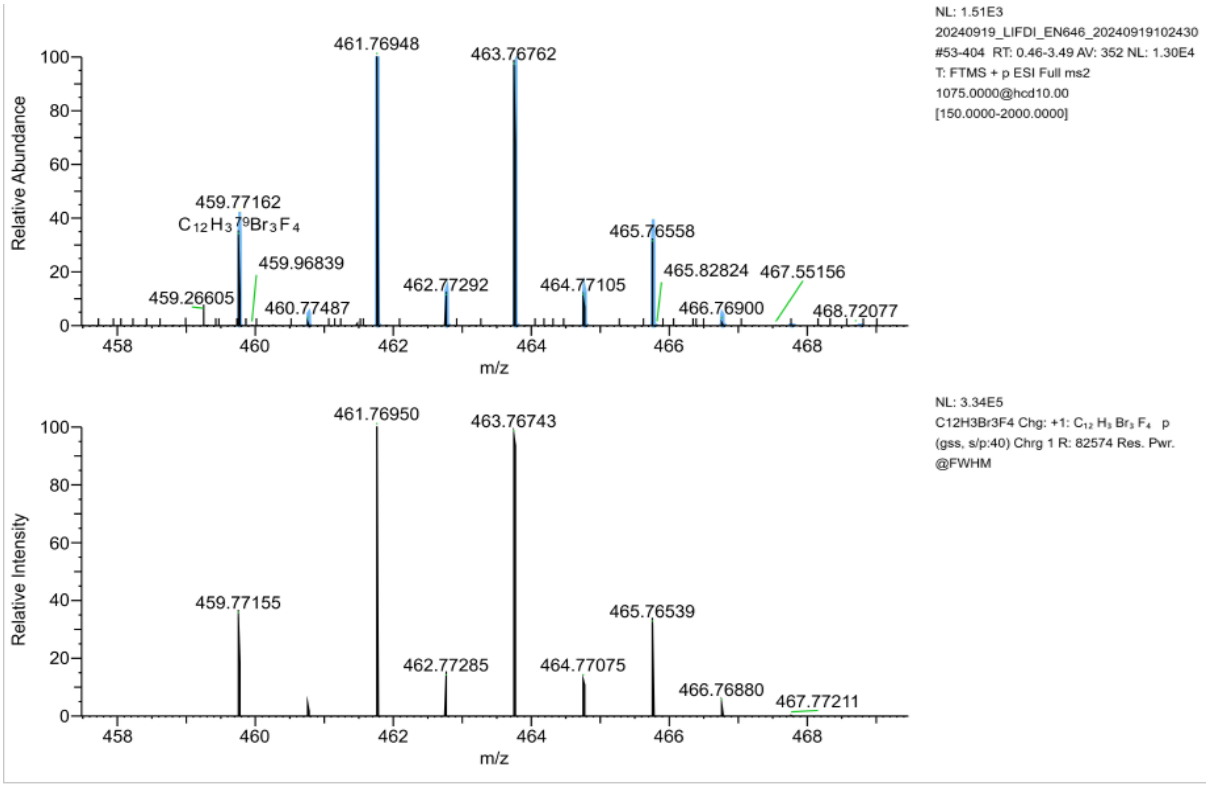

Peak Mass	Display F...	S Fit	RDB	Delta [pp...	Theo. ma...	Rank	Combine...	# Match...	# Missed...	MS Cov....	Pattern C...	MSMS M...
459.77162	$C_{12}H_3{}^{79}Br_3F_4$	44.53326 6051848 4	8.00	0.14	459.77155	1	94.23	8	0	96.99	97.13	(Collection)

Figure A68. HRMS (LIFDI) of 11b.

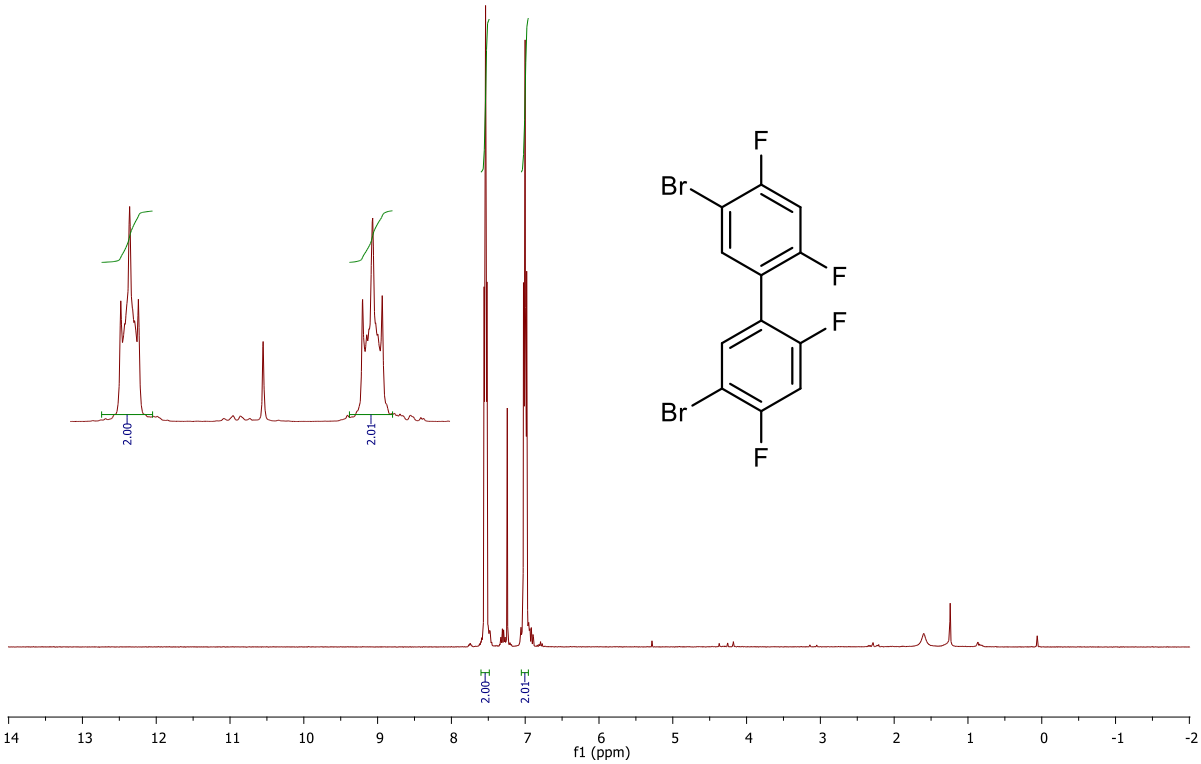

Figure A69. ^{1}H NMR (400 MHz, $CDCl_3$) of 12a.

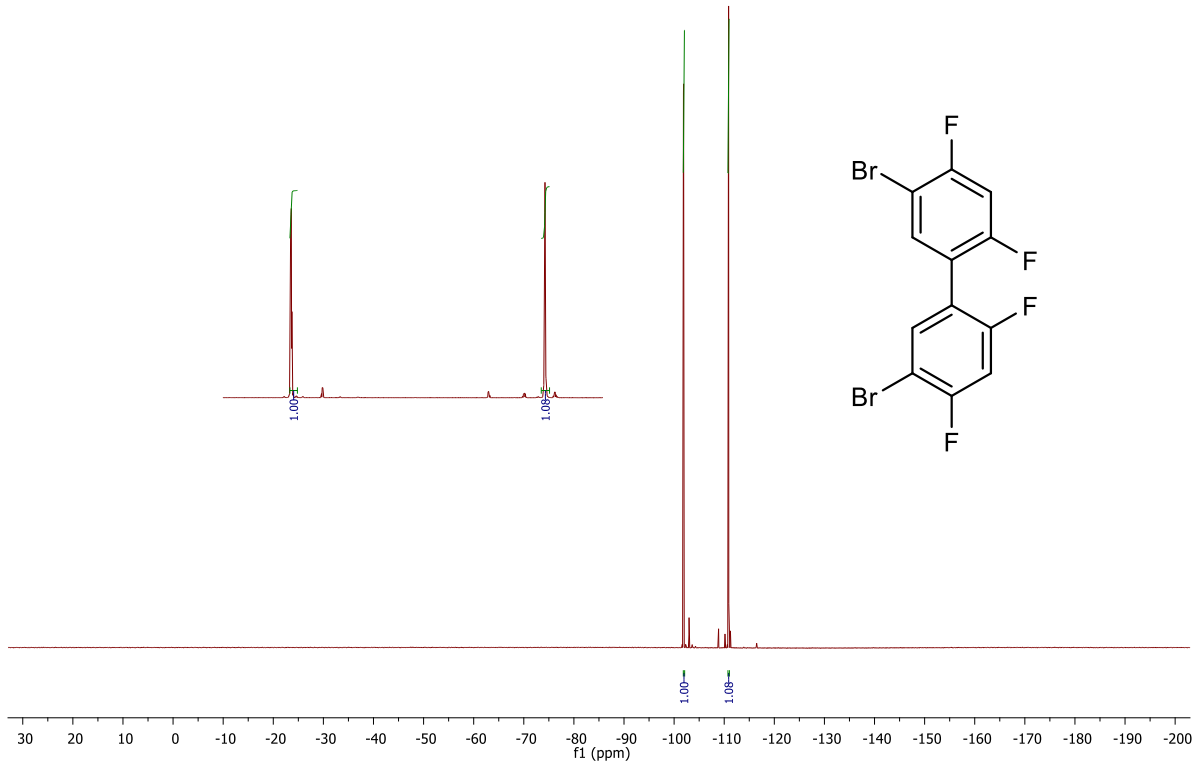

Figure A70. ^{19}F NMR (376 MHz, $CDCl_3$) of 12a.

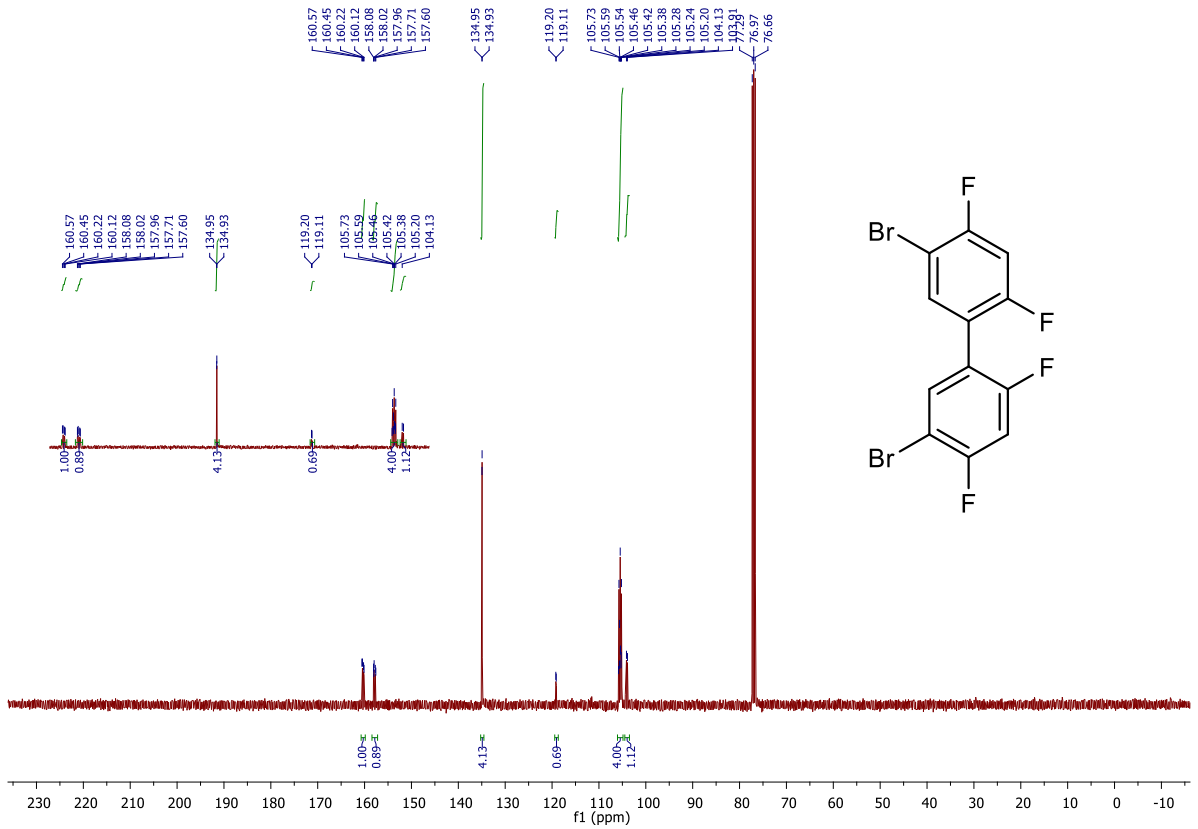

Figure A71. ^{13}C NMR (101 MHz, $CDCl_3$) of 12a.

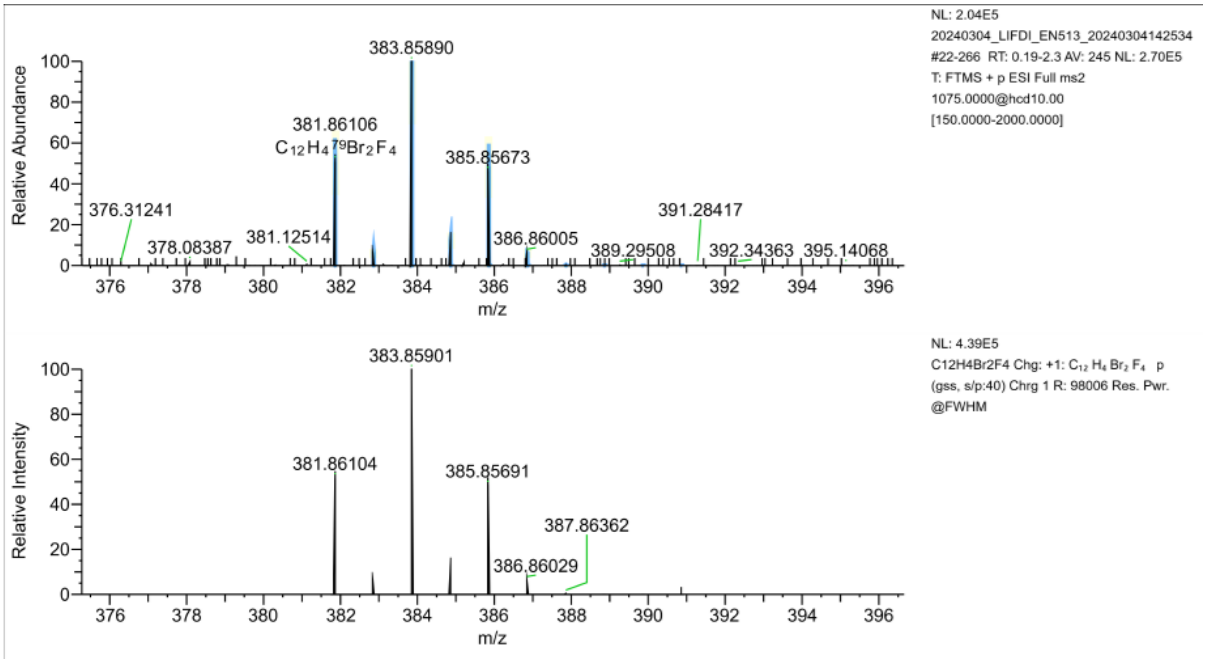

Peak Mass	Display F...	S Fit	RDB	Delta [pp...	Theo. ma...	Rank	Combine...	# Match...	# Missed...	MS Cov....	Pattern C...	MSMS M...
381.86106	$C_{12}H_4{}^{79}Br_2F_4$	50.30151 9832040 1	8.00	0.05	381.86104	1	95.99	9	0	98.53	99.49	(Collection)

Figure A72. HRMS (LIFDI) of 12a.

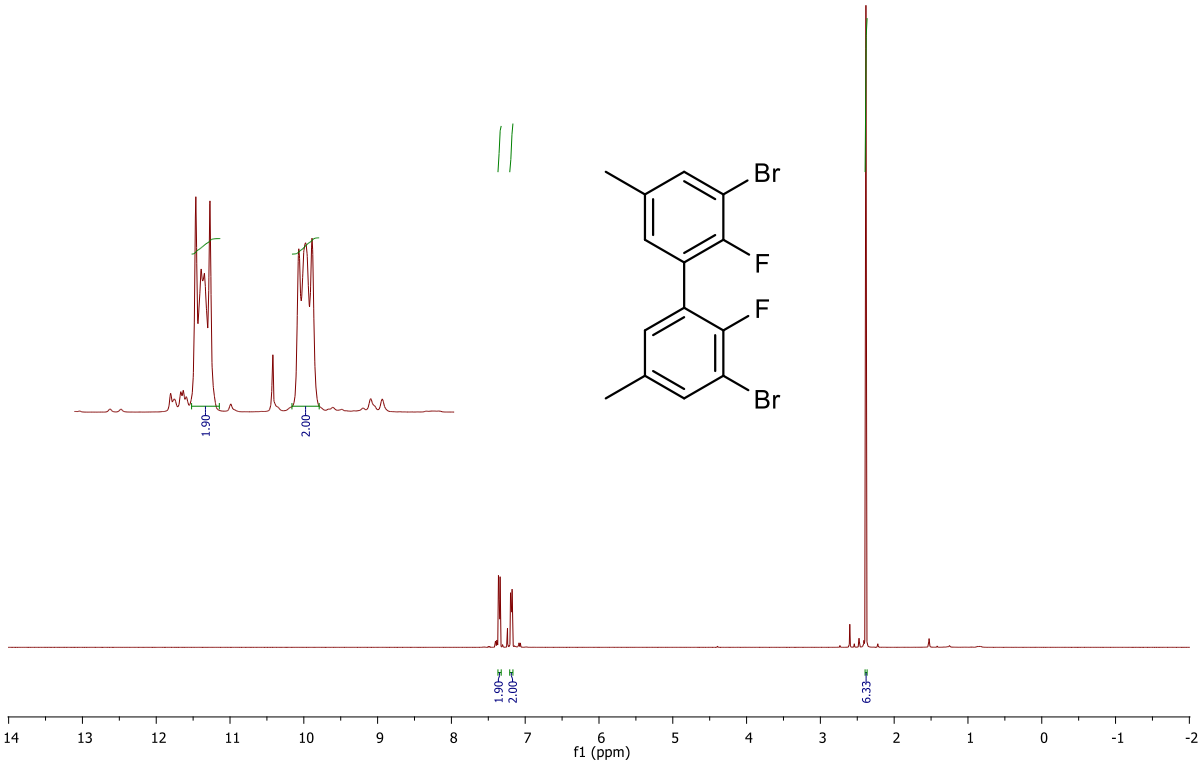

Figure A73. ^{1}H NMR (400 MHz, $CDCl_3$) of 13a.

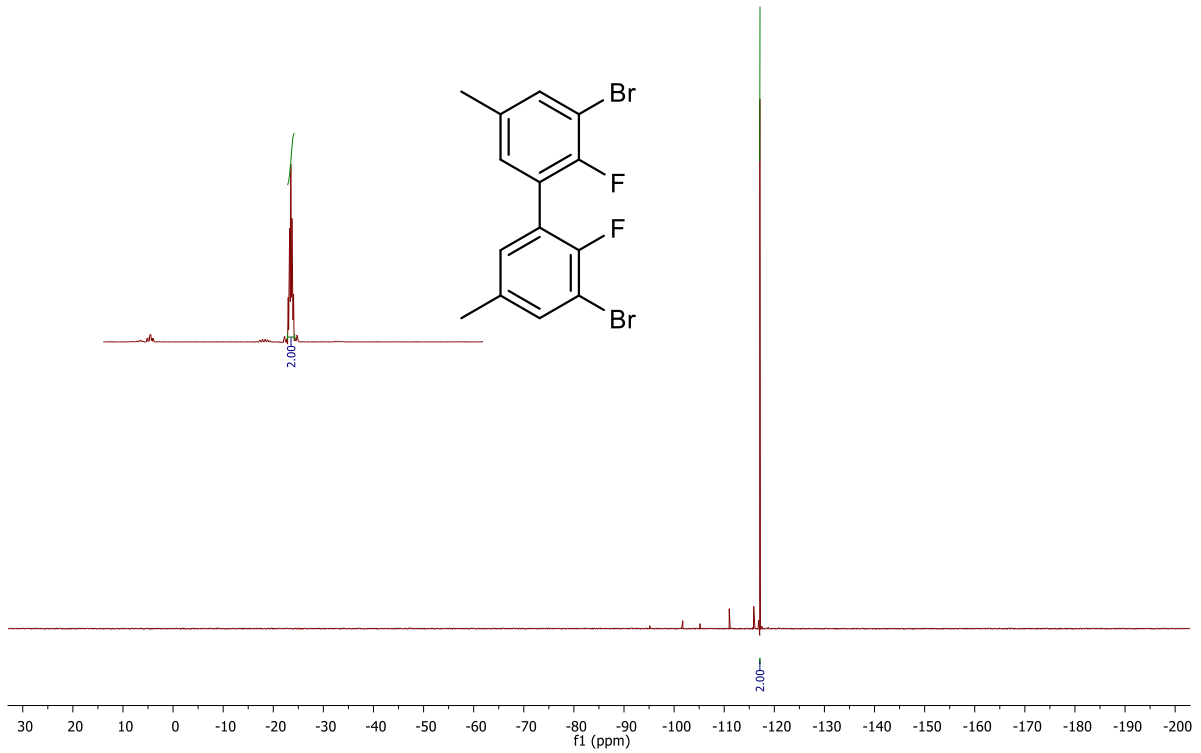

Figure A74. ^{19}F NMR (376 MHz, $CDCl_3$) of 13a.

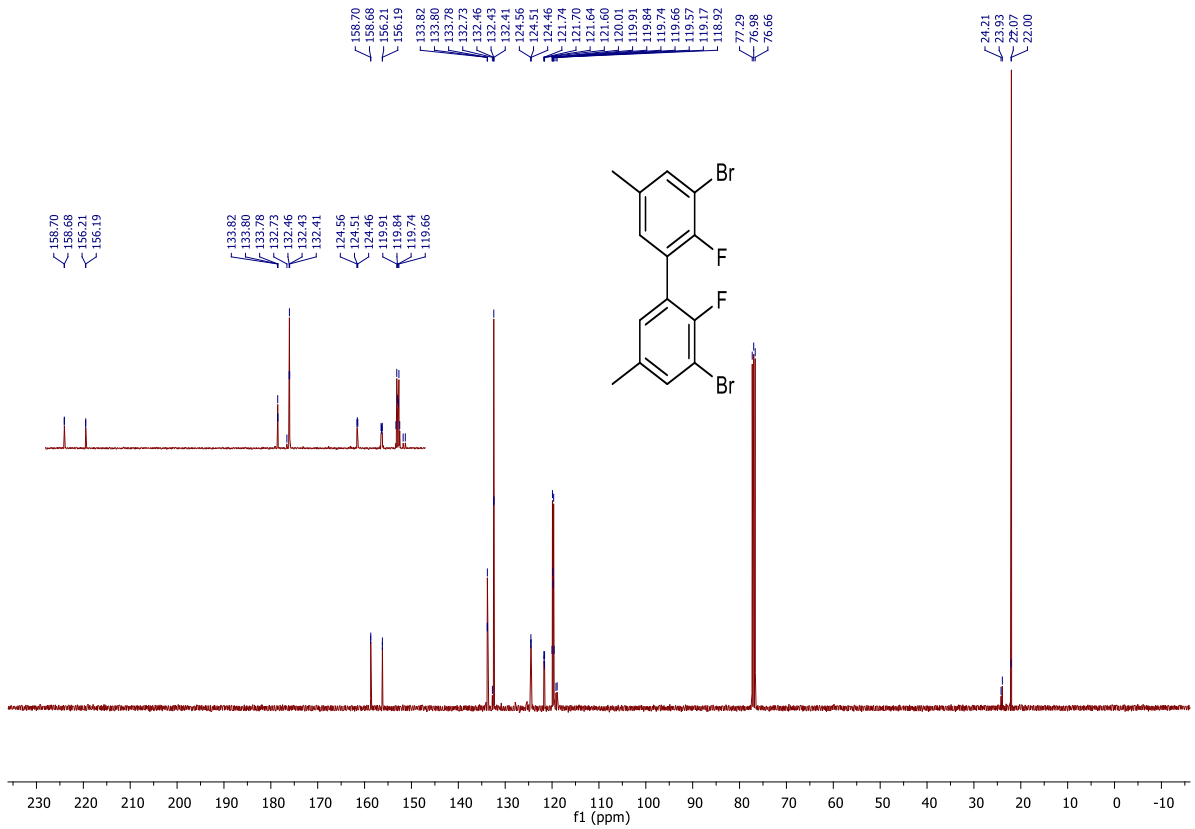

Figure A75. ^{13}C NMR (101 MHz, $CDCl_3$) of 13a.

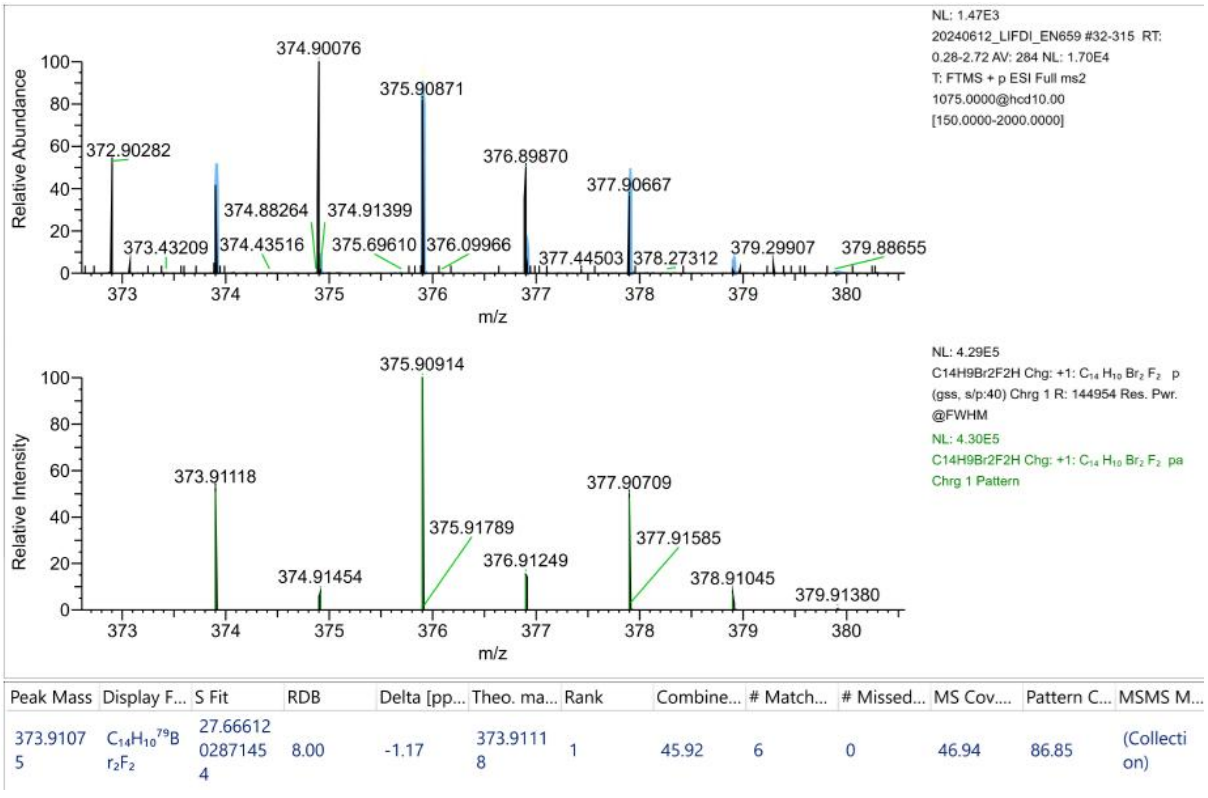

Peak Mass	Display F...	S Fit	RDB	Delta [pp...	Theo. ma...	Rank	Combine...	# Match...	# Missed...	MS Cov....	Pattern C...	MSMS M...
373.91075	$C_{14}H_{10}{}^{79}Br_2F_2$	27.666120287145 4	8.00	-1.17	373.91118	1	45.92	6	0	46.94	86.85	(Collection)

Figure A76. HRMS (LIFDI) of 13a.

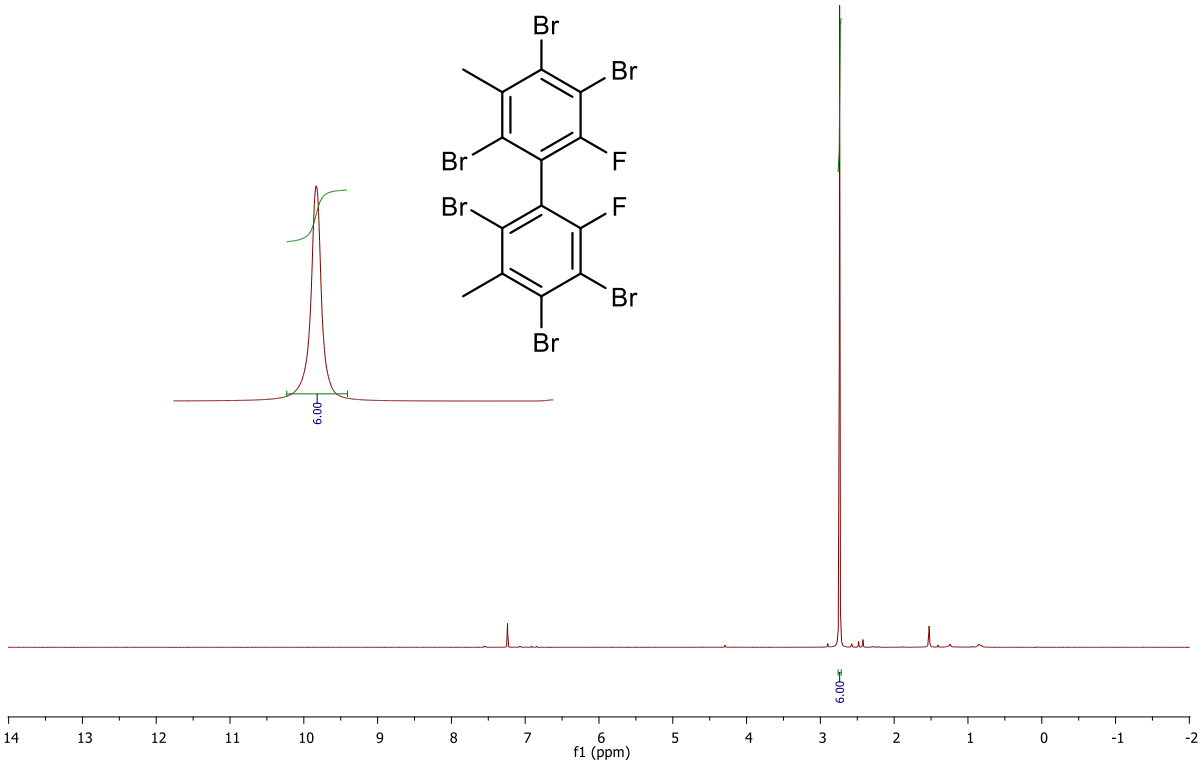

Figure A77. ^{1}H NMR (400 MHz, $CDCl_3$) of 13b.

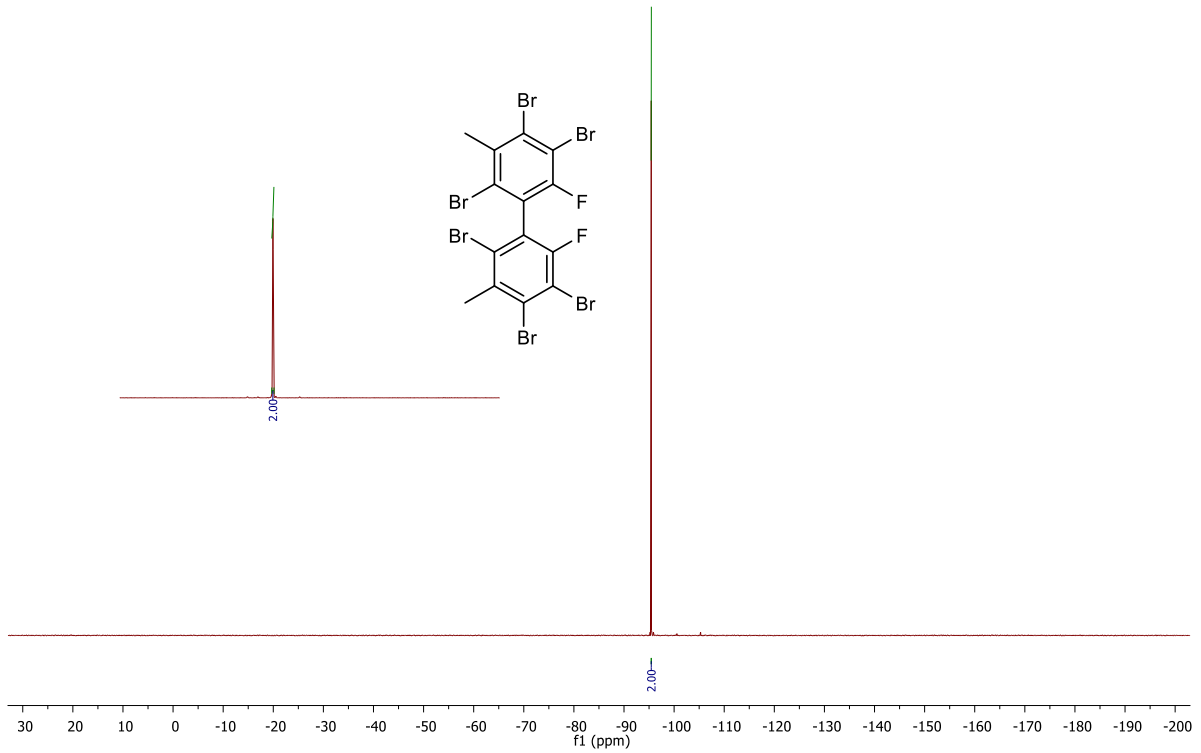

Figure A78. ^{19}F NMR (376 MHz, $CDCl_3$) of 13b.

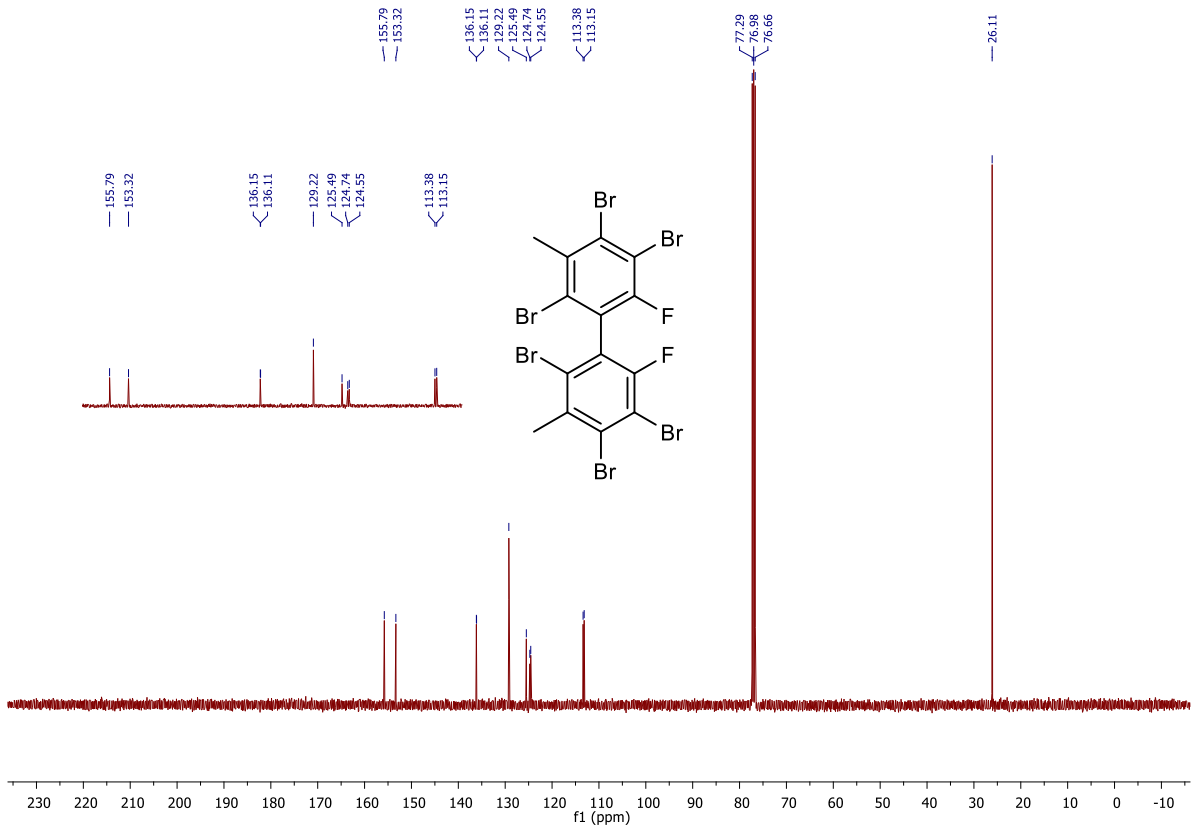

Figure A79. ^{13}C NMR (101 MHz, $CDCl_3$) of 13b.

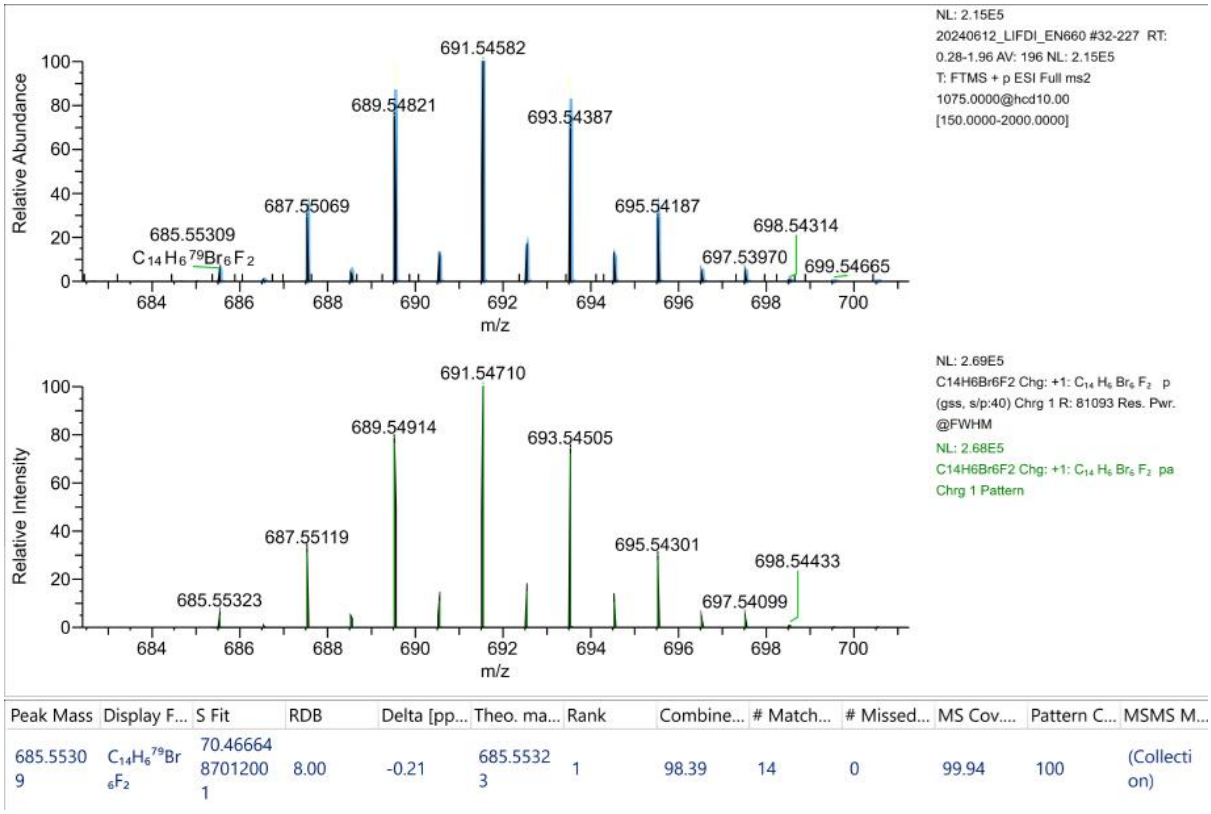

Peak Mass	Display F...	S Fit	RDB	Delta [pp...	Theo. ma...	Rank	Combine...	# Match...	# Missed...	MS Cov....	Pattern C...	MSMS M...
685.55309	$C_{14}H_6{}^{79}Br_6F_2$	70.466648701201	8.00	-0.21	685.55323	1	98.39	14	0	99.94	100	(Collection)

Figure A80. HRMS (LIFDI) of 13b.

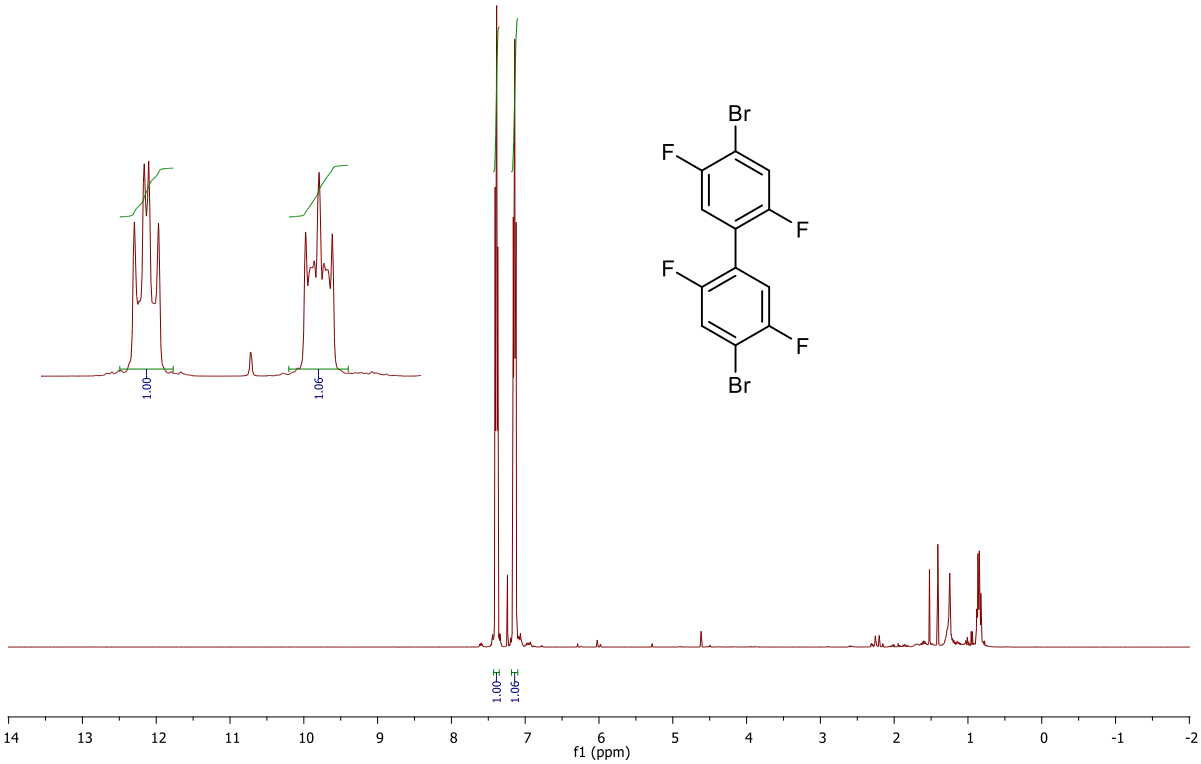

Figure A81. ^{1}H NMR (400 MHz, $CDCl_3$) of 16a.

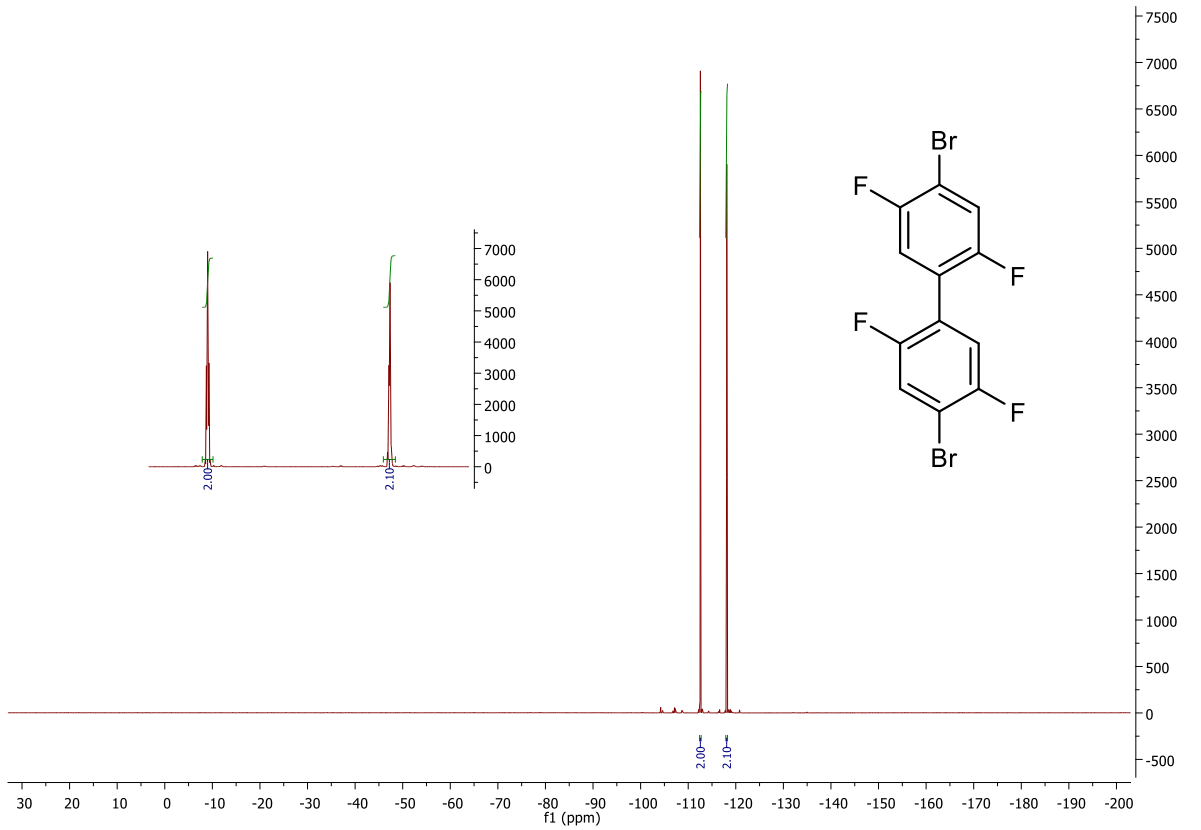

Figure A82. ^{19}F NMR (376 MHz, $CDCl_3$) of 16a.

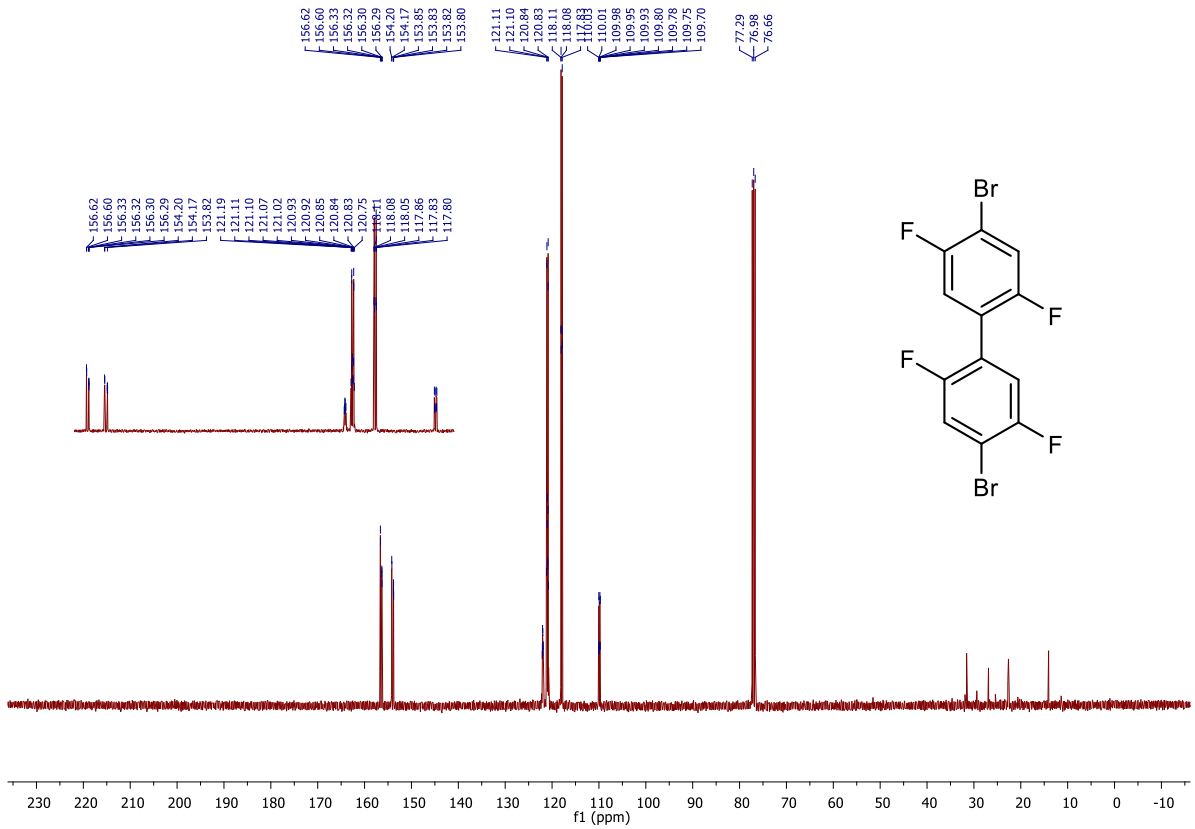

Figure A83. ^{13}C NMR (101 MHz, $CDCl_3$) of 16a.

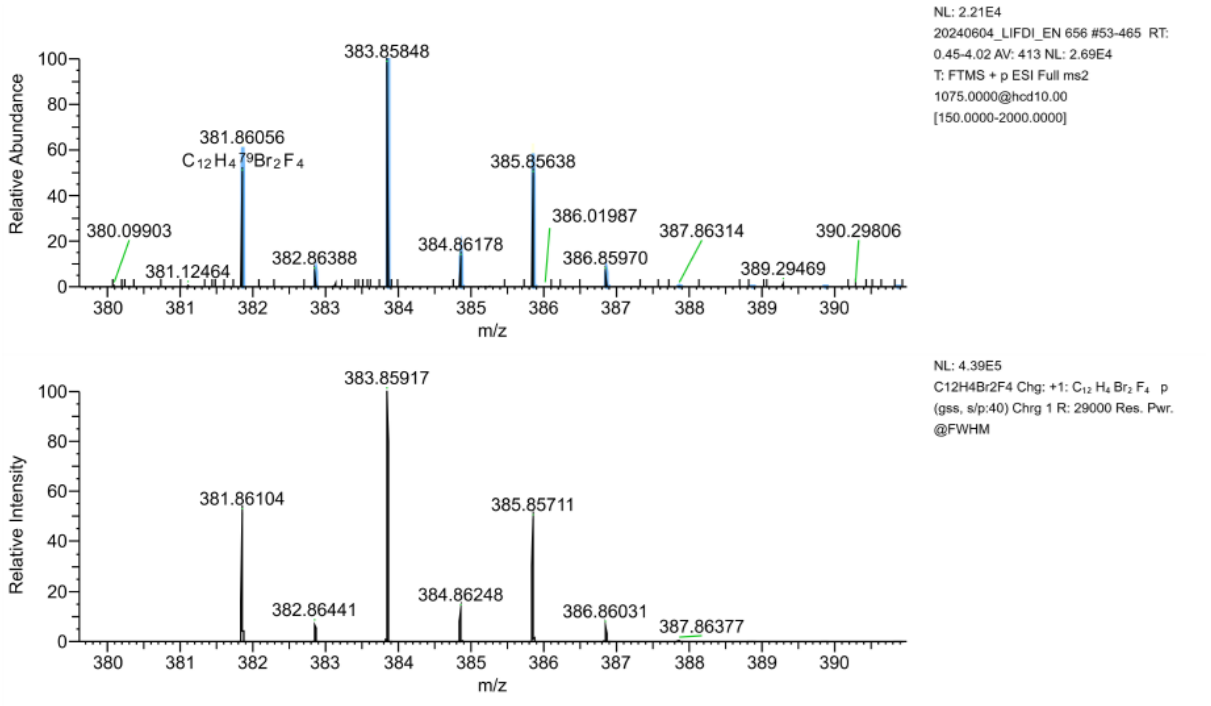

Peak Mass	Display F...	S Fit	RDB	Delta [pp...	Theo. ma...	Rank	Combine...	# Match...	# Missed...	MS Cov....	Pattern C...	MSMS M...
381.86056	$C_{12}H_4{}^{79}Br_2F_4$	39.65789 25361484	8.00	-1.27	381.86104	1	95.43	8	1	98.53	99.32	(Collection)

Figure A84. HRMS (LIFDI) of 16a.

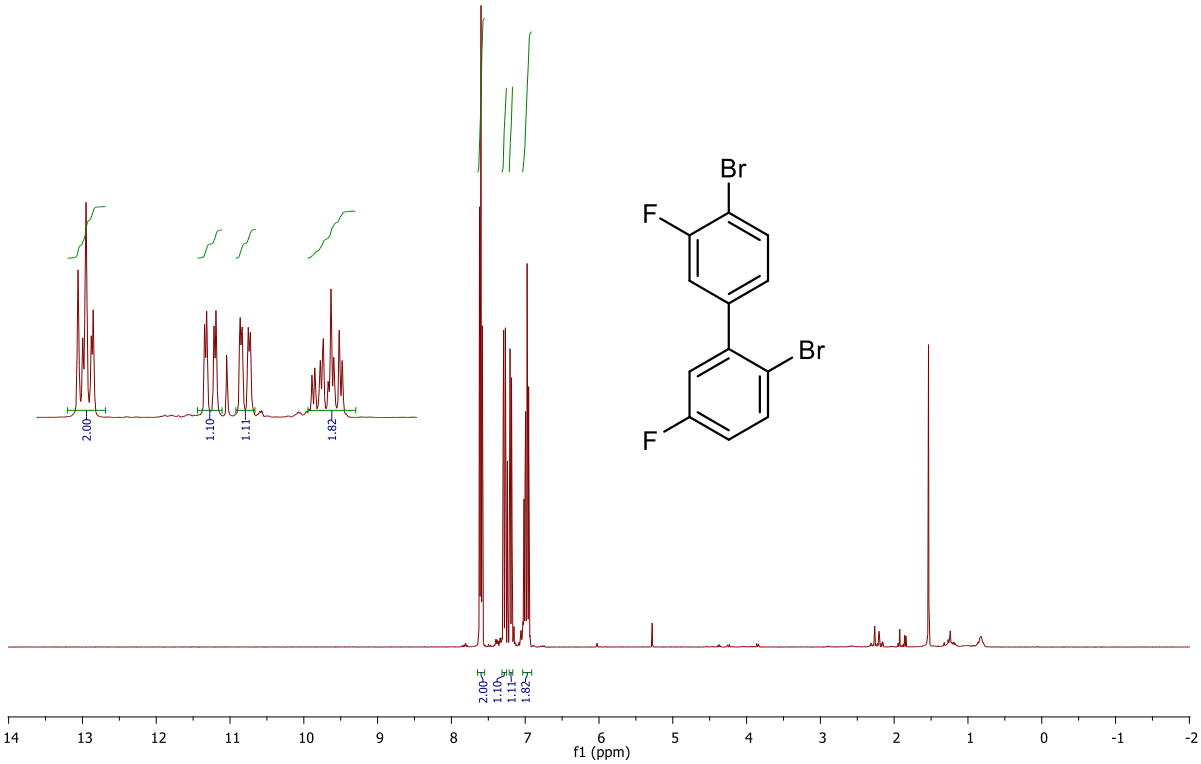

Figure A85. ^{1}H NMR (400 MHz, $CDCl_3$) of 17a.

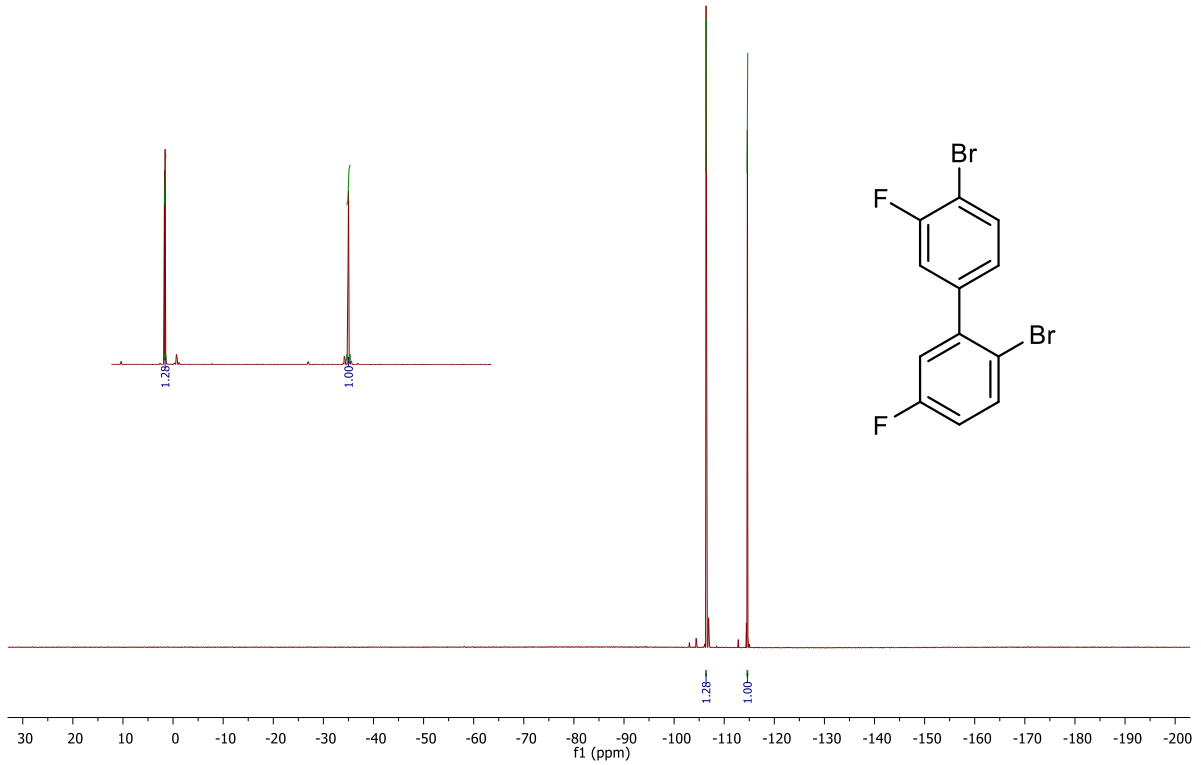

Figure A86. ^{19}F NMR (376 MHz, $CDCl_3$) of 17a.

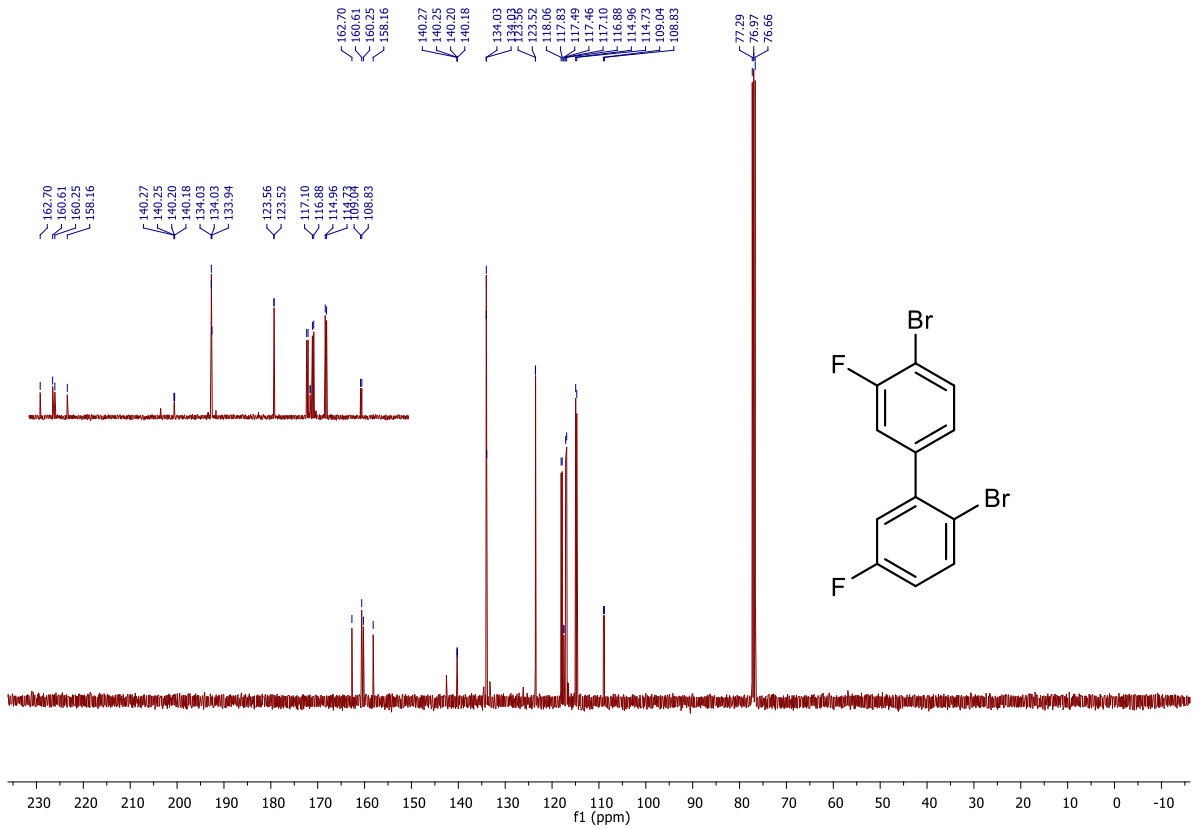

Figure A87. ^{13}C NMR (101 MHz, $CDCl_3$) of 17a.

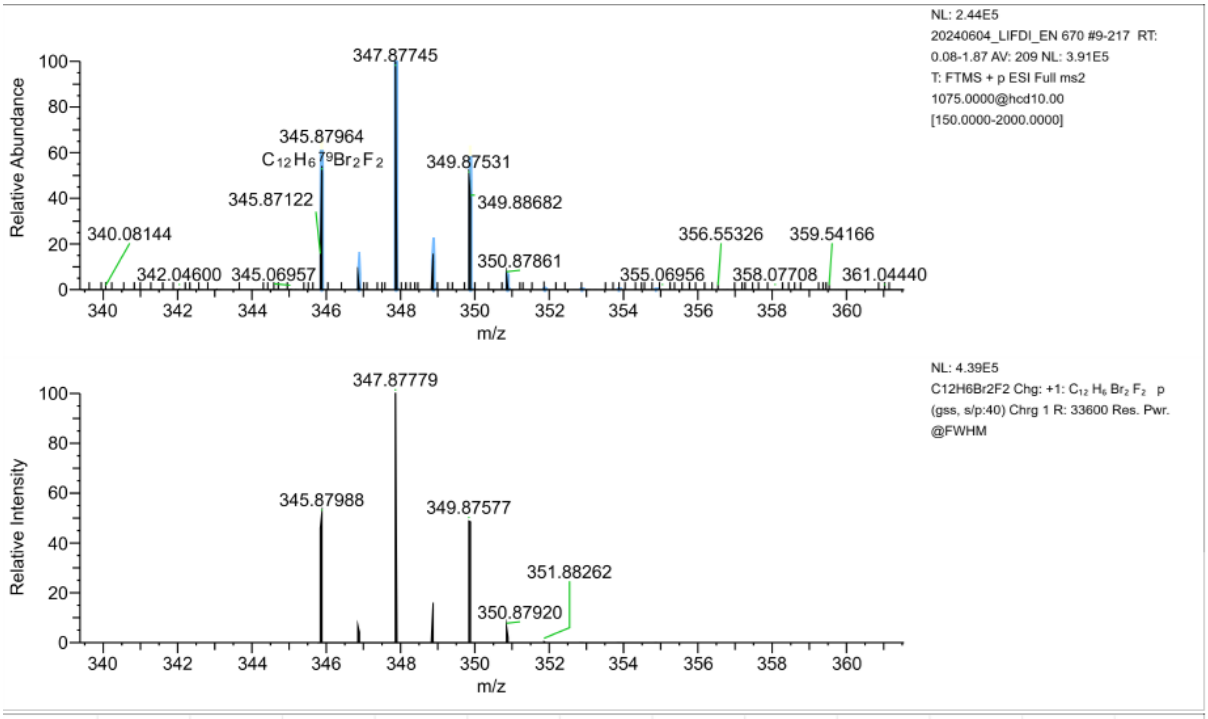

Peak Mass	Display F...	S Fit	RDB	Delta [pp...	Theo. ma...	Rank	Combine...	# Match...	# Missed...	MS Cov....	Pattern C...	MSMS M...
345.87964	$C_{12}H_6{}^{79}Br_2F_2$	49.82570 3473425 6	8.00	-0.72	345.87988	1	97.22	9	0	99.85	99.49	(Collection)

Figure A88. HRMS (LIFDI) of 14a.

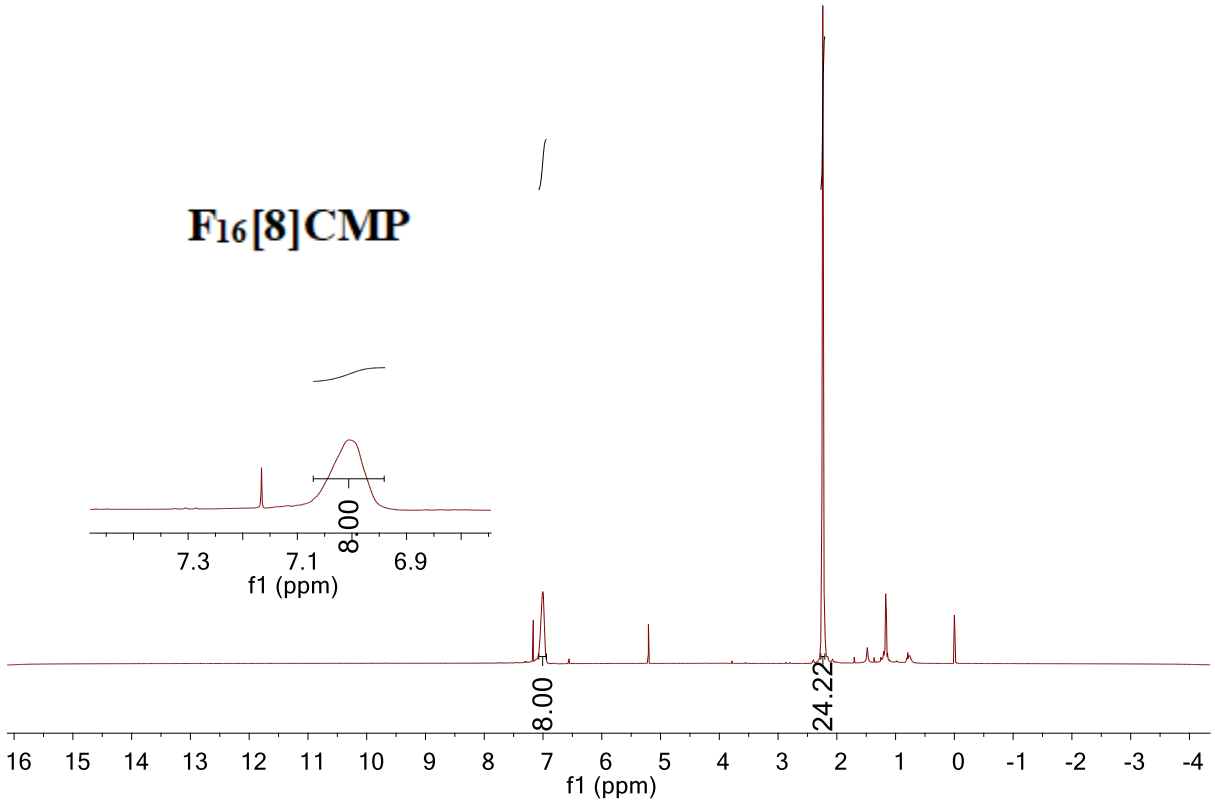

Figure A89. ^{1}H NMR (400 MHz, $CDCl_3$) of F_{16}[8]CMP.

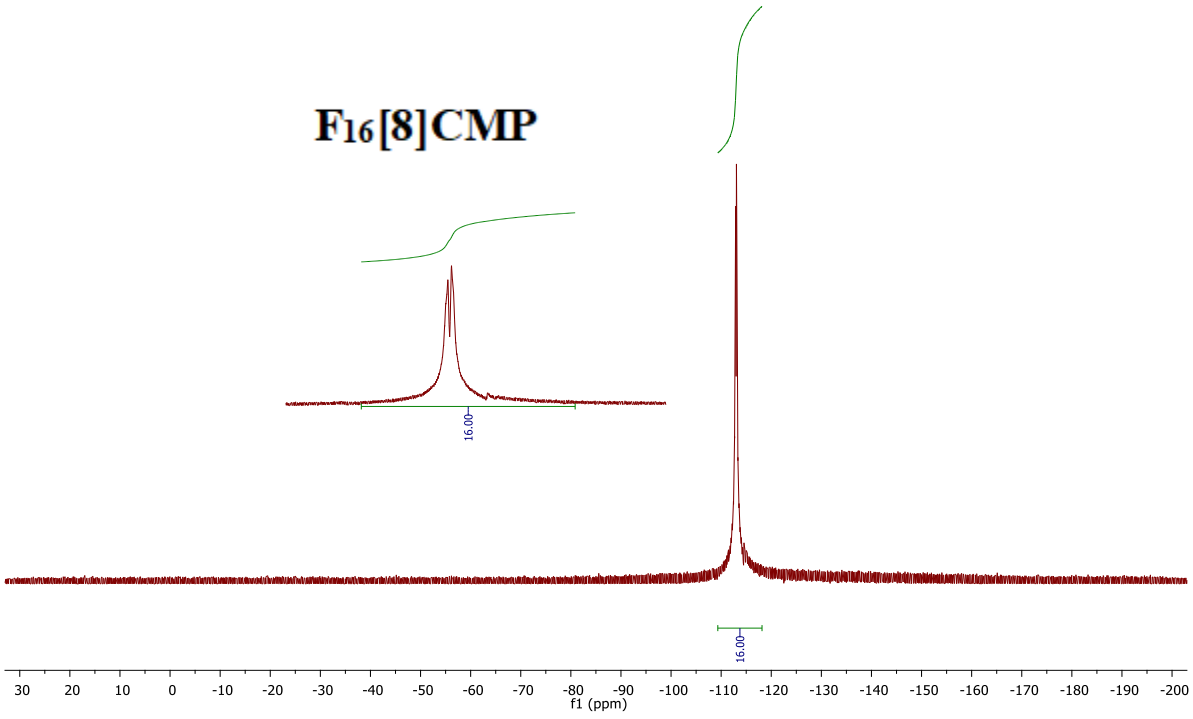

Figure A90. ^{19}F NMR (101 MHz, $CDCl_3$) of F_{16}[8]CMP.

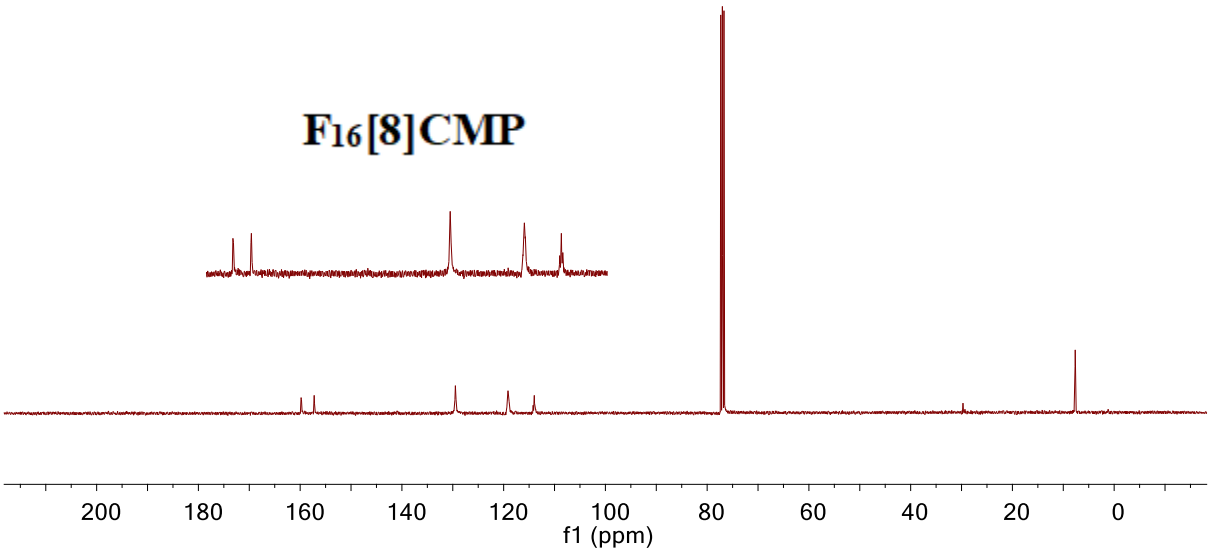

Figure A91. ^{13}C NMR (101 MHz, $CDCl_3$) of F_{16}[8]CMP.

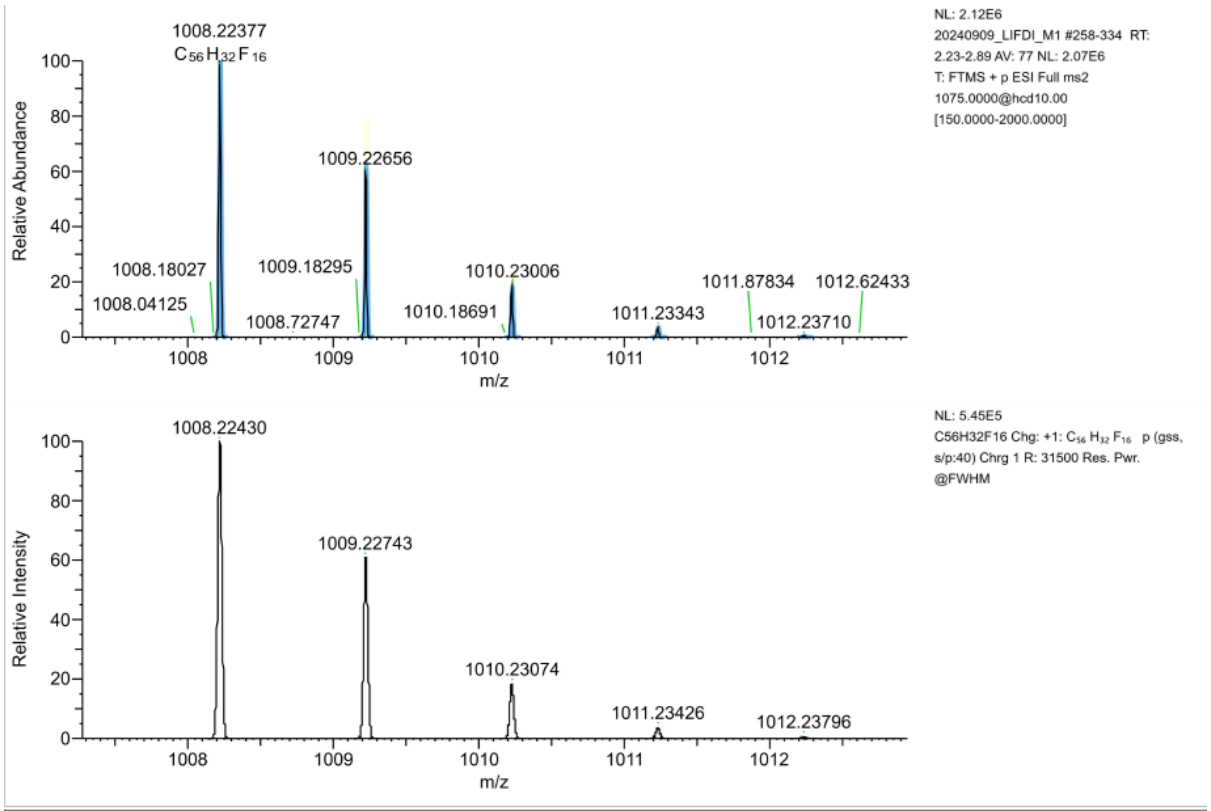

Peak Mass	Display F...	S Fit	RDB	Delta [pp...	Theo. ma...	Rank	Combine...	# Match...	# Missed...	MS Cov....	Pattern C...	MSMS M...
1008.22377	$C_{56}H_{32}F_{16}$	86.314713384932 6	33.00	-0.53	1008.22430	1	99.24	5	0	99.96	100	(Collection)

Figure A92. HRMS (LIFDI) of F_{16}[8]CMP.

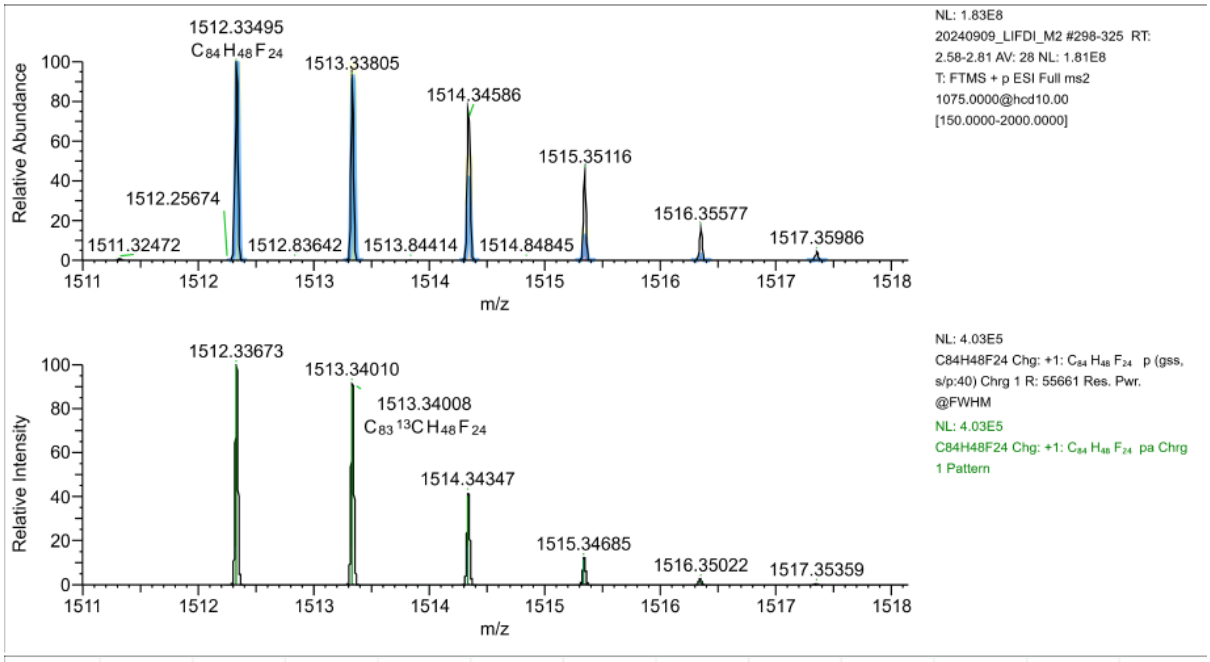

Peak Mass	Display F...	S Fit	RDB	Delta [pp...	Theo. ma...	Rank	Combine...	# Match...	# Missed...	MS Cov....	Pattern C...	MSMS M...
1512.33495	$C_{84}H_{48}F_{24}$	17.693557879273 7	49.00	-1.18	1512.33673	1	55.25	3	3	57.33	77.15	(Collection)

Figure A93. HRMS (LIFDI) of F_{24}[12]CMP.

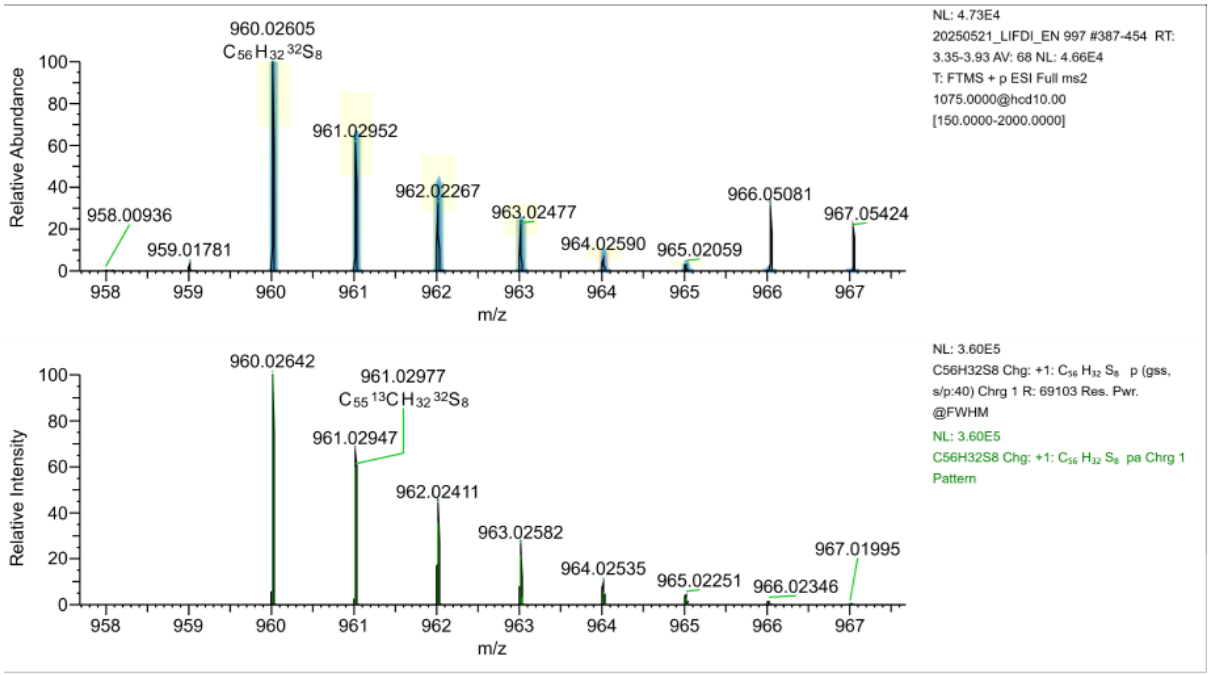

Peak Mass	Display F...	S Fit	RDB	Delta [pp...	Theo. ma...	Rank	Combine...	# Match...	# Missed...	MS Cov....	Pattern C...	MSMS M...
960.02605	$C_{56}H_{32}{}^{32}S_8$	25.906867517877 2	41.00	-0.38	960.02642	1	73.71	9	0	76.36	95.36	(Collection)

Figure A94. HRMS (LIFDI) of F_{16}[8-S]CMP.

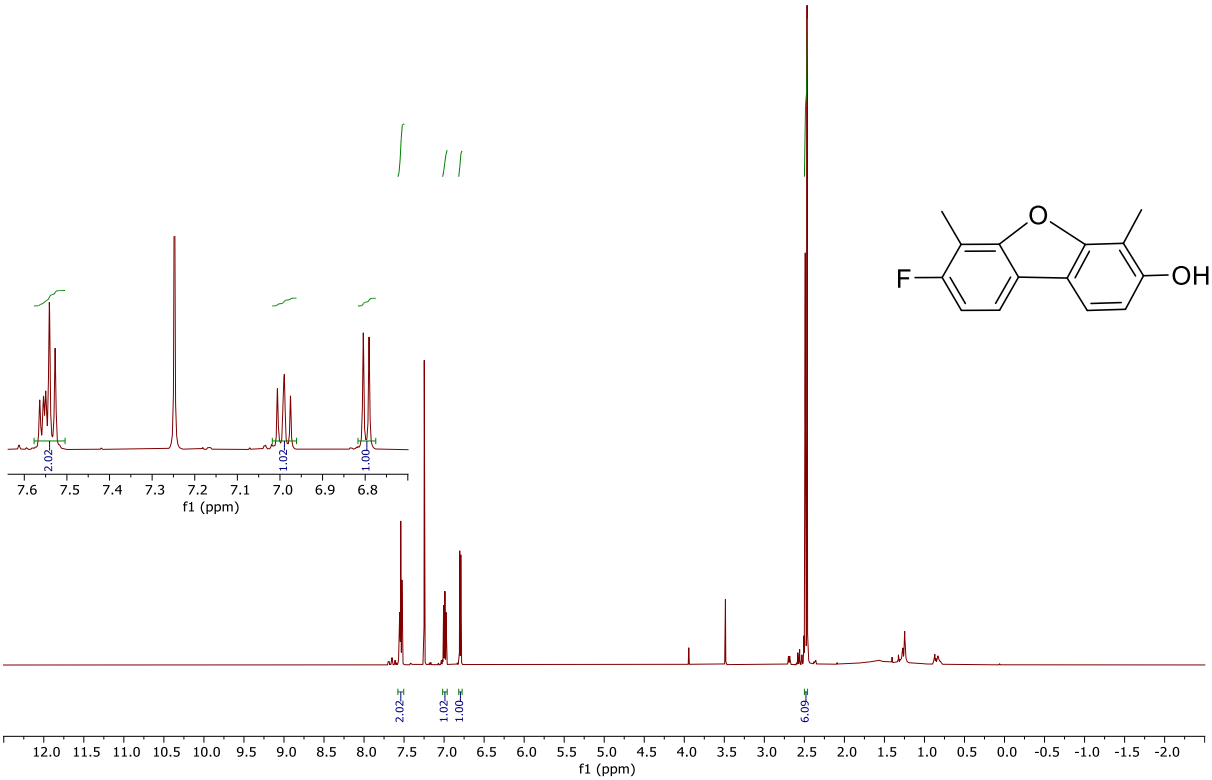

Figure A95. ^{1}H NMR (400 MHz, $CDCl_3$) of 21.

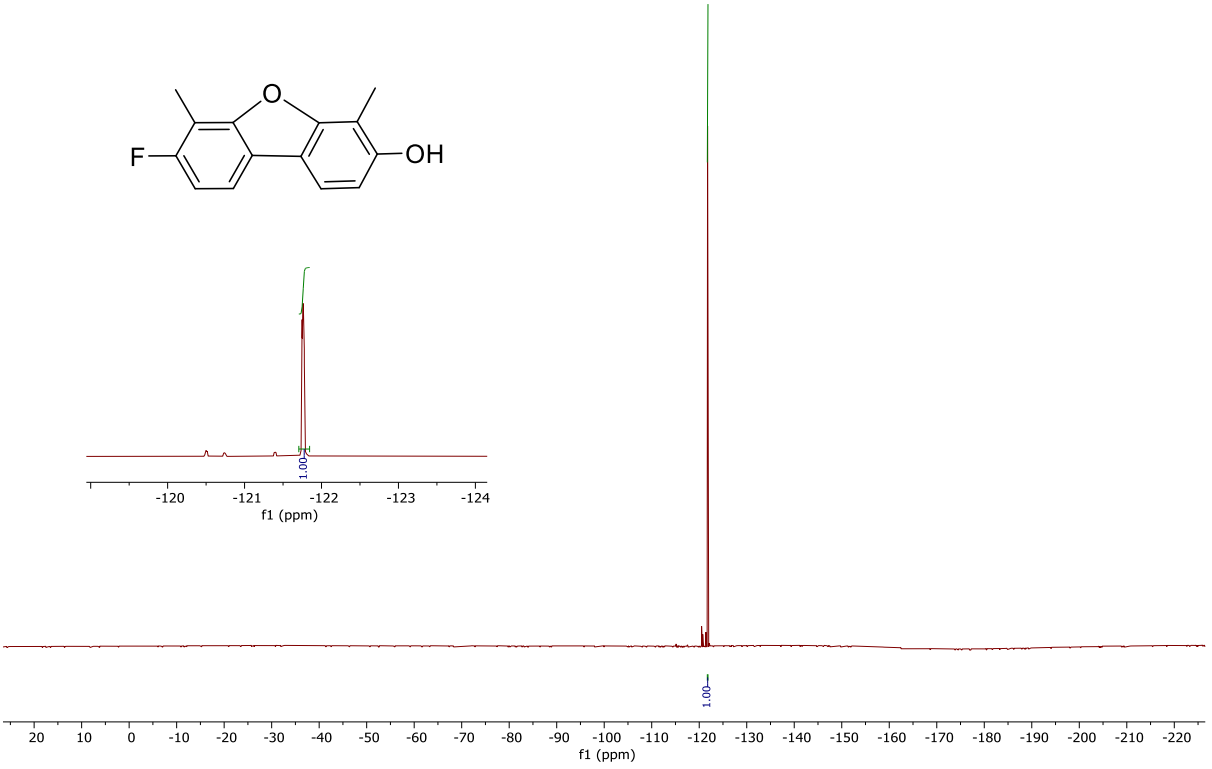

Figure A96. ^{19}F NMR (376 MHz, $CDCl_3$) of 21.

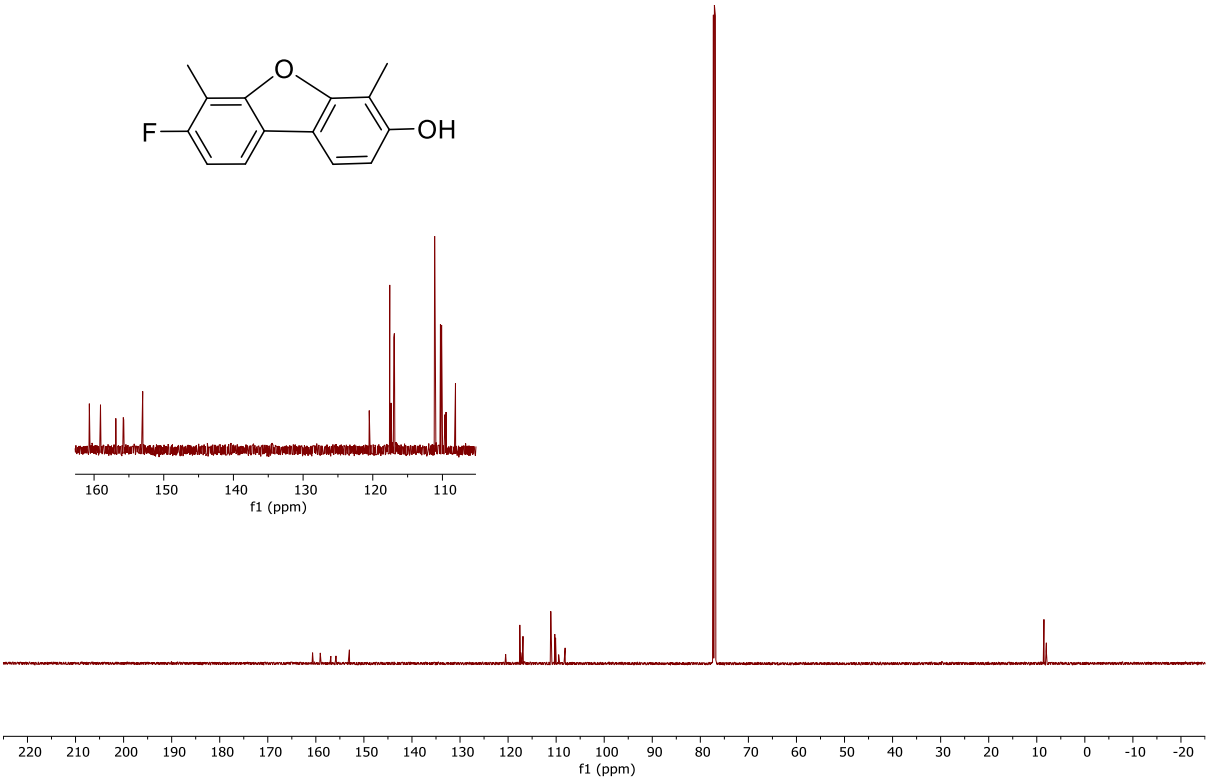

Figure A97. ^{13}C NMR (101 MHz, $CDCl_3$) of 21.

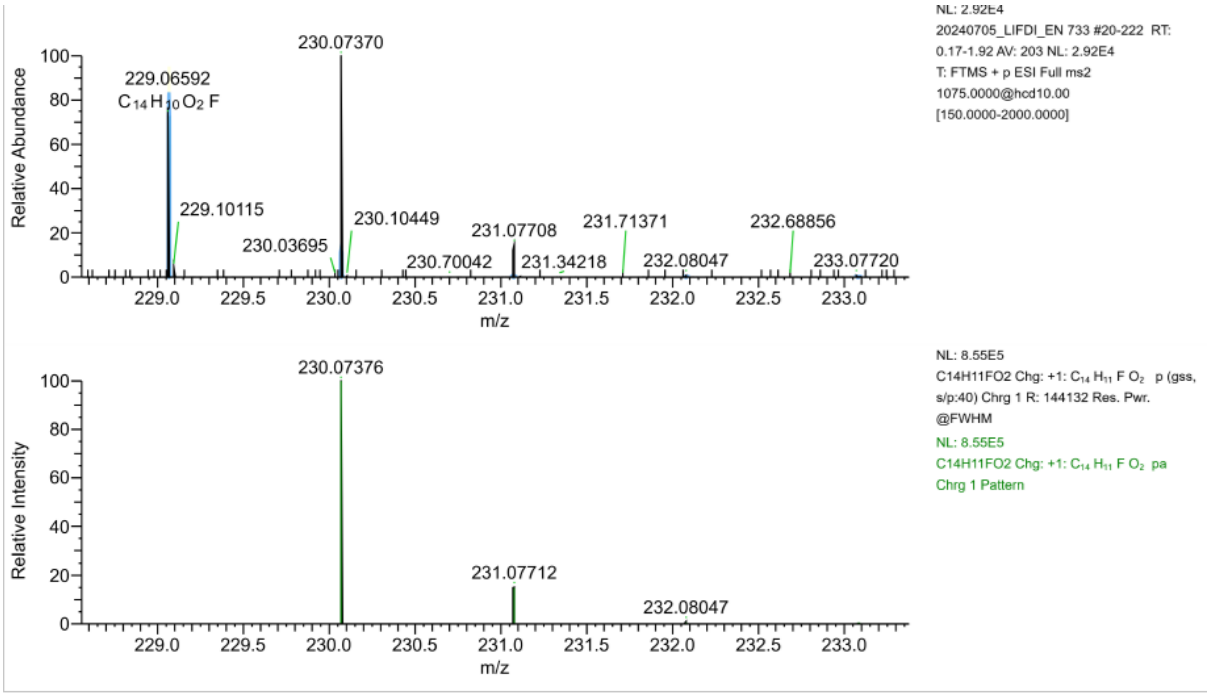

Peak Mass	Display F...	S Fit	RDB	Delta [pp...	Theo. ma...	Rank	Combine...	# Match...	# Missed...	MS Cov....	Pattern C...	MSMS M..
229.06592	$C_{14}H_{10}O_2F$	20.656514072489	9.50	-0.05	229.06593	1	42.13	4	1	43.32	98.63	(Collection)

Figure A98. HRMS (LIFDI) of 21.

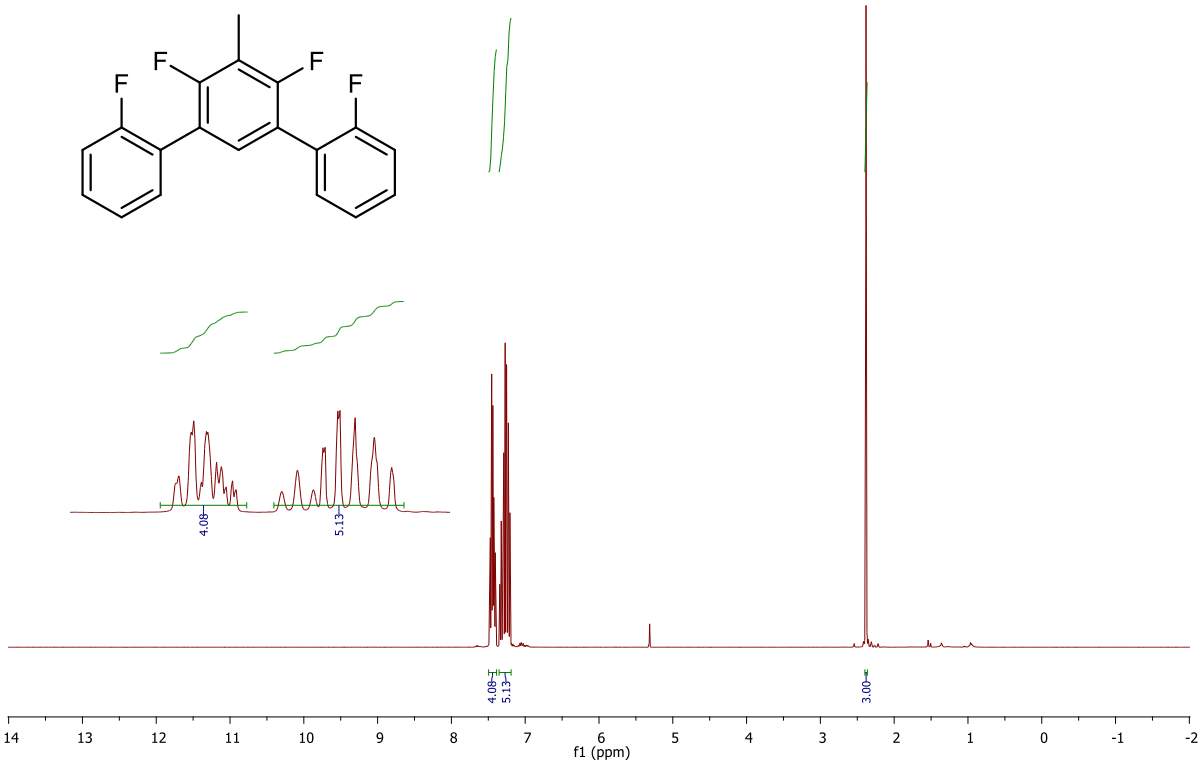

Figure A99. ^{1}H NMR (400 MHz, $CDCl_3$) of 23.

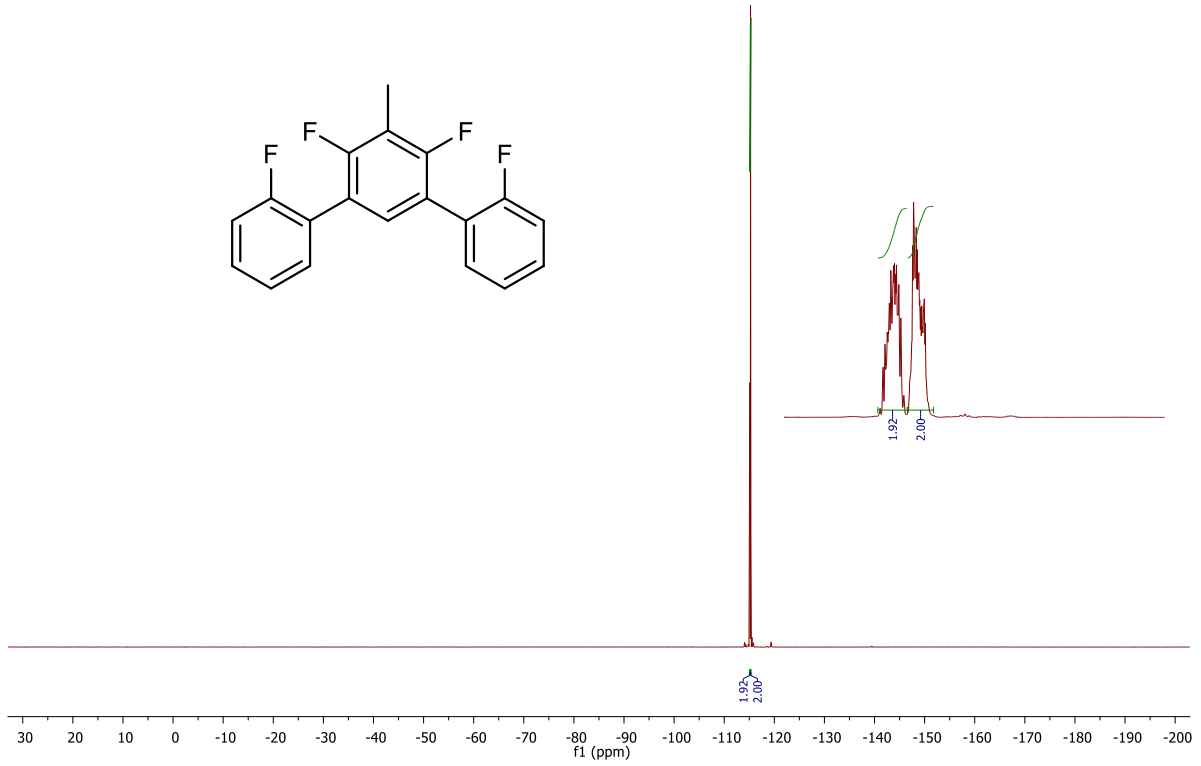

Figure A100. ^{19}F NMR (376 MHz, $CDCl_3$) of 23.

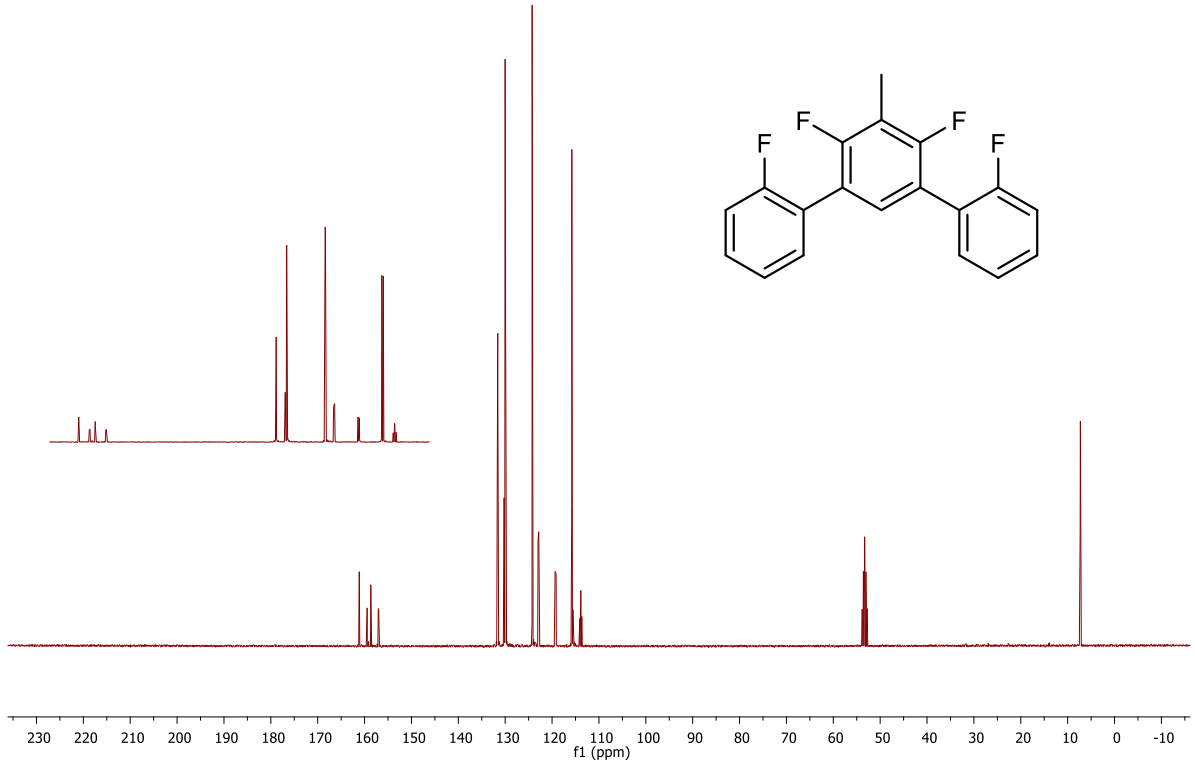

Figure A101. ^{13}C NMR (101 MHz, $CDCl_3$) of 23.

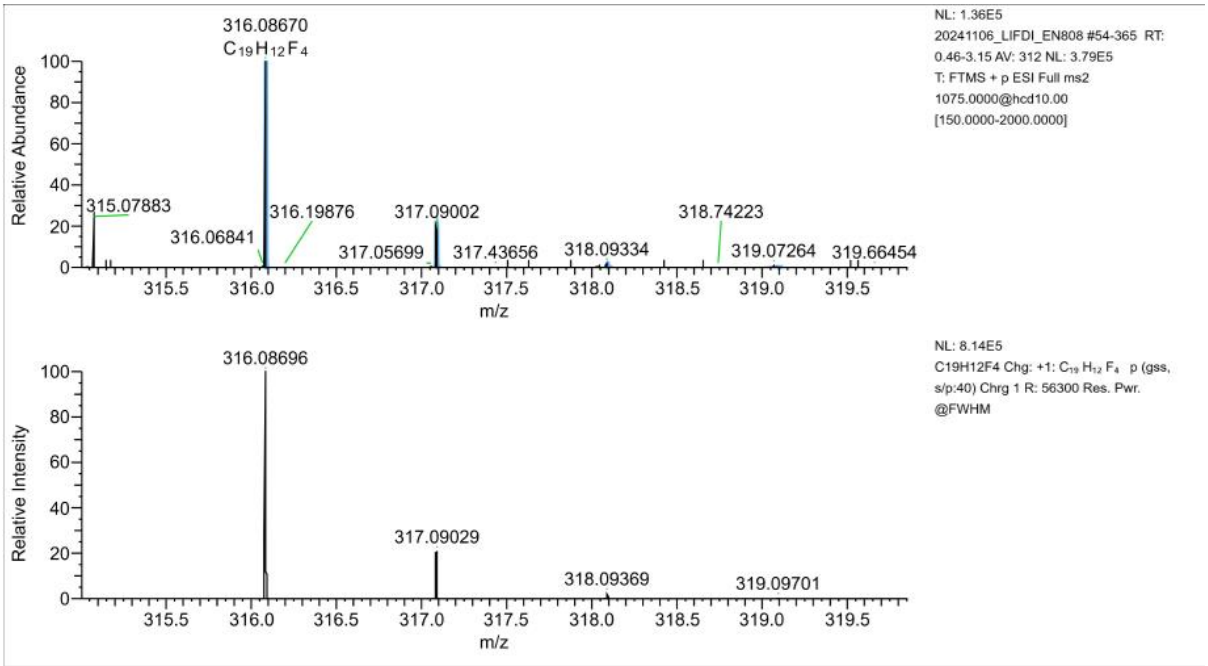

Peak Mass	Display F...	S Fit	RDB	Delta [pp...	Theo. ma...	Rank	Combine...	# Match...	# Missed...	MS Cov....	Pattern C...	MSMS M...
316.08670	$C_{19}H_{12}F_4$	48.14367 1917086 4	12.00	-0.83	316.08696	1	93.81	4	0	96.35	99.9	(Collection)

Figure A102. HRMS (LIFDI) of 23.

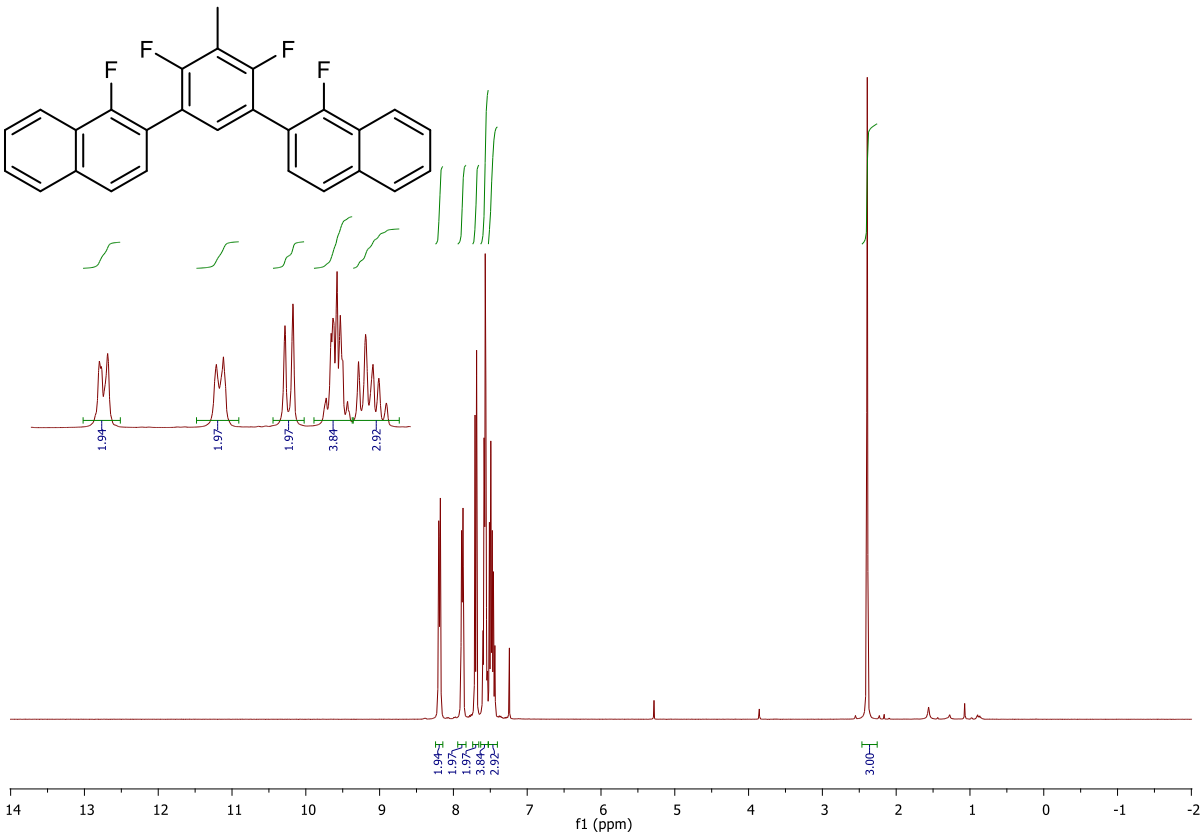

Figure A103. ^{1}H NMR (400 MHz, $CDCl_3$) of 25.

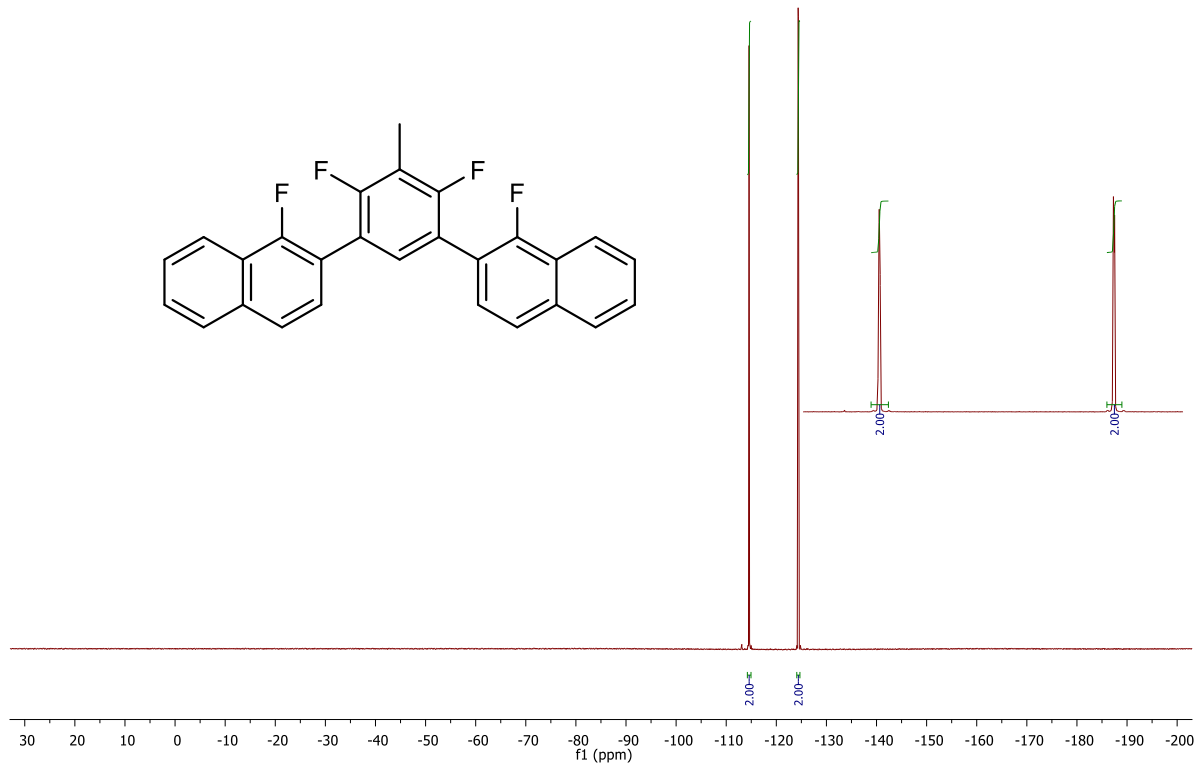

Figure A104. ^{19}F NMR (376 MHz, $CDCl_3$) of 25.

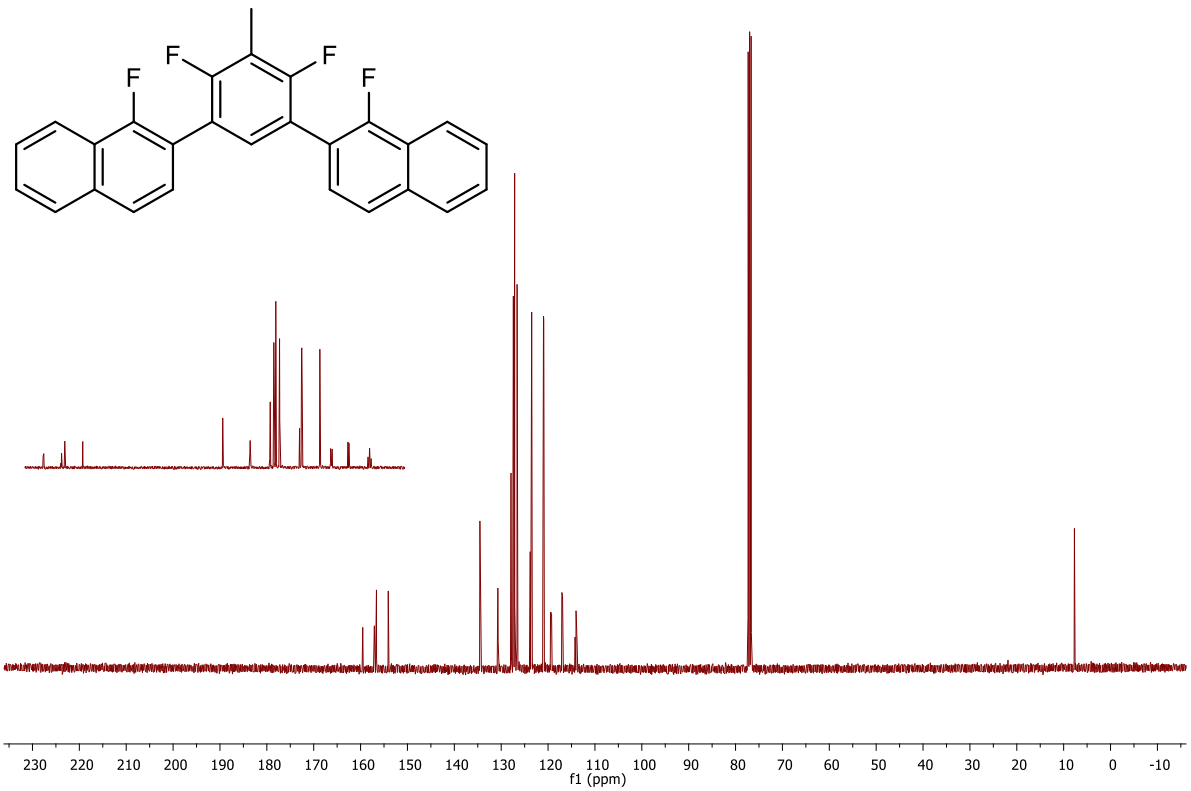

Figure A105. ^{13}C NMR (101 MHz, $CDCl_3$) of 25.

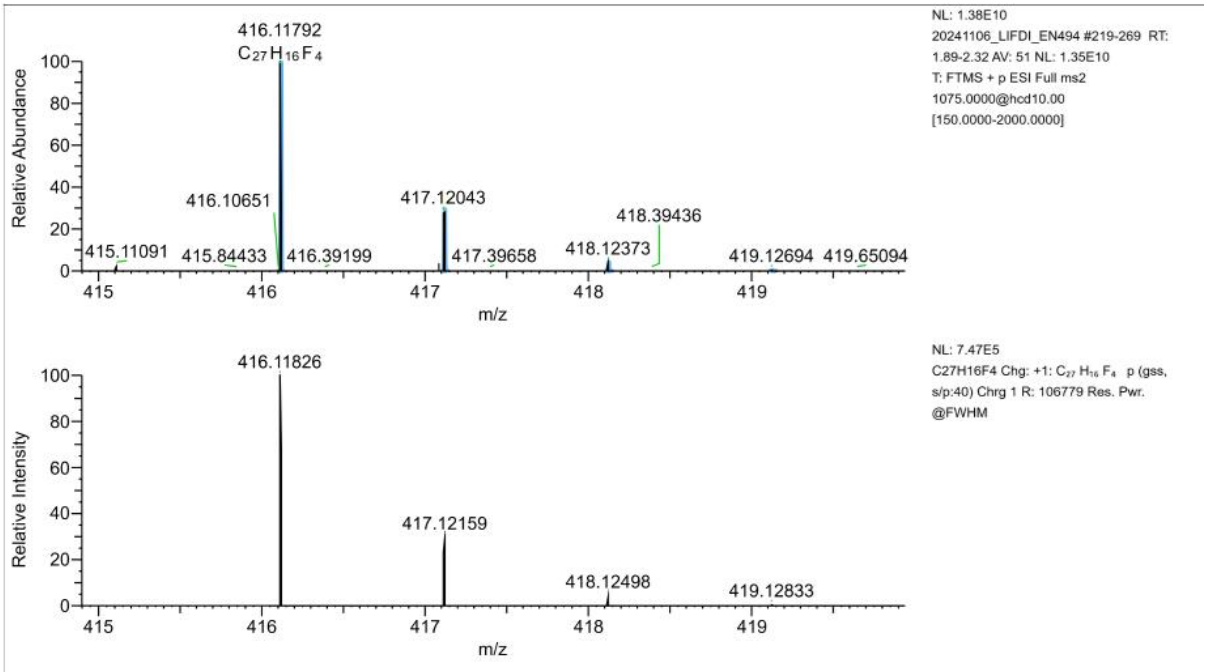

Peak Mass	Display F...	S Fit	RDB	Delta [pp...	Theo. ma...	Rank	Combine...	# Match...	# Missed...	MS Cov....	Pattern C...	MSMS M...
416.11792	$C_{27}H_{16}F_4$	59.752377299640 5	18.00	-0.84	416.11826	1	97.79	4	0	99.91	100	(Collection)

Figure A106. HRMS (LIFDI) of 25.

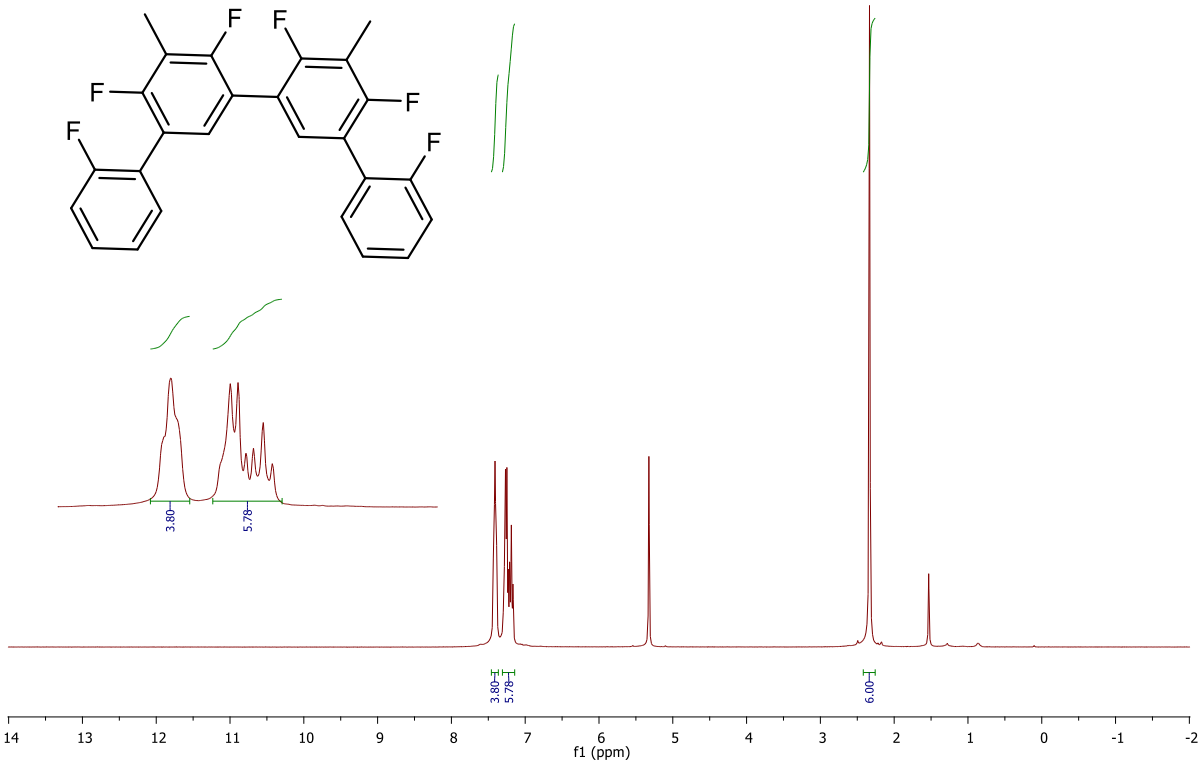

Figure A107. ^{1}H NMR (400 MHz, $CDCl_3$) of 26.

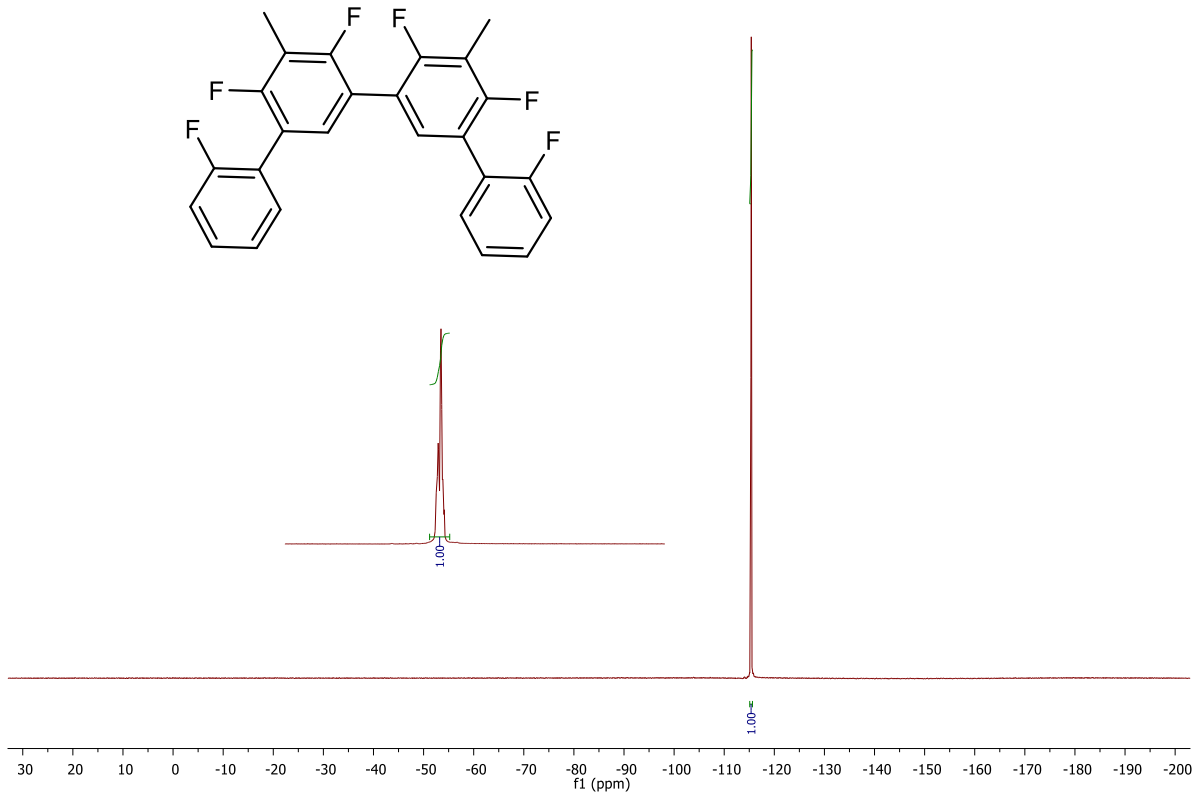

Figure A108. ^{19}F NMR (376 MHz, $CDCl_3$) of 26.

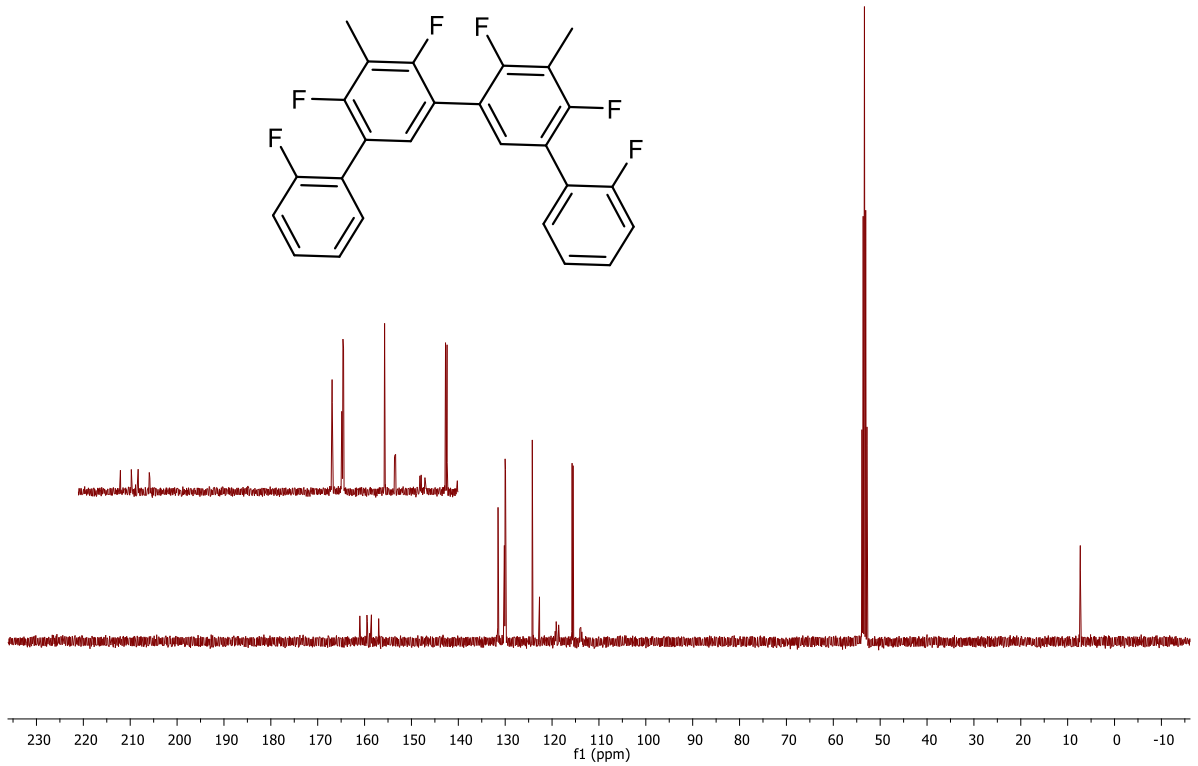

Figure A109. ^{13}C NMR (101 MHz, $CDCl_3$) of 26.

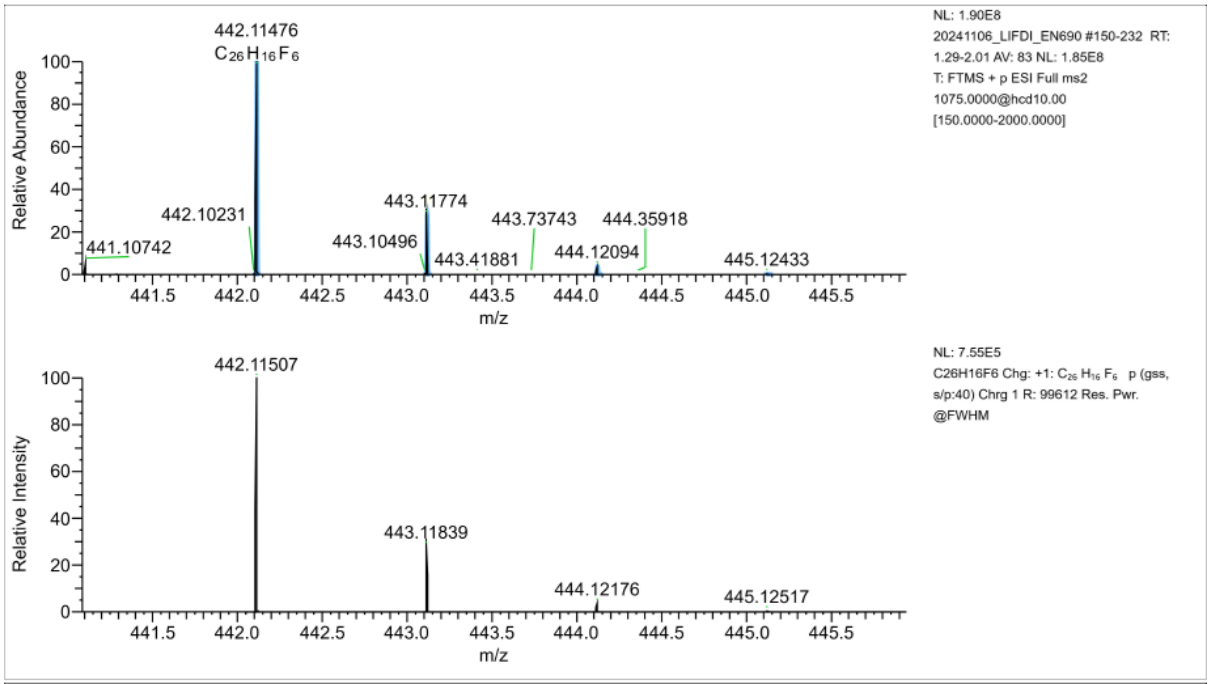

Peak Mass	Display F...	S Fit	RDB	Delta [pp...	Theo. ma...	Rank	Combine...	# Match...	# Missed...	MS Cov....	Pattern C...	MSMS M...
442.11476	$C_{26}H_{16}F_6$	75.980527133933 2	16.00	-0.70	442.11507	1	98.62	4	0	99.88	100	(Collection)

Figure A110. HRMS (LIFDI) of 26.

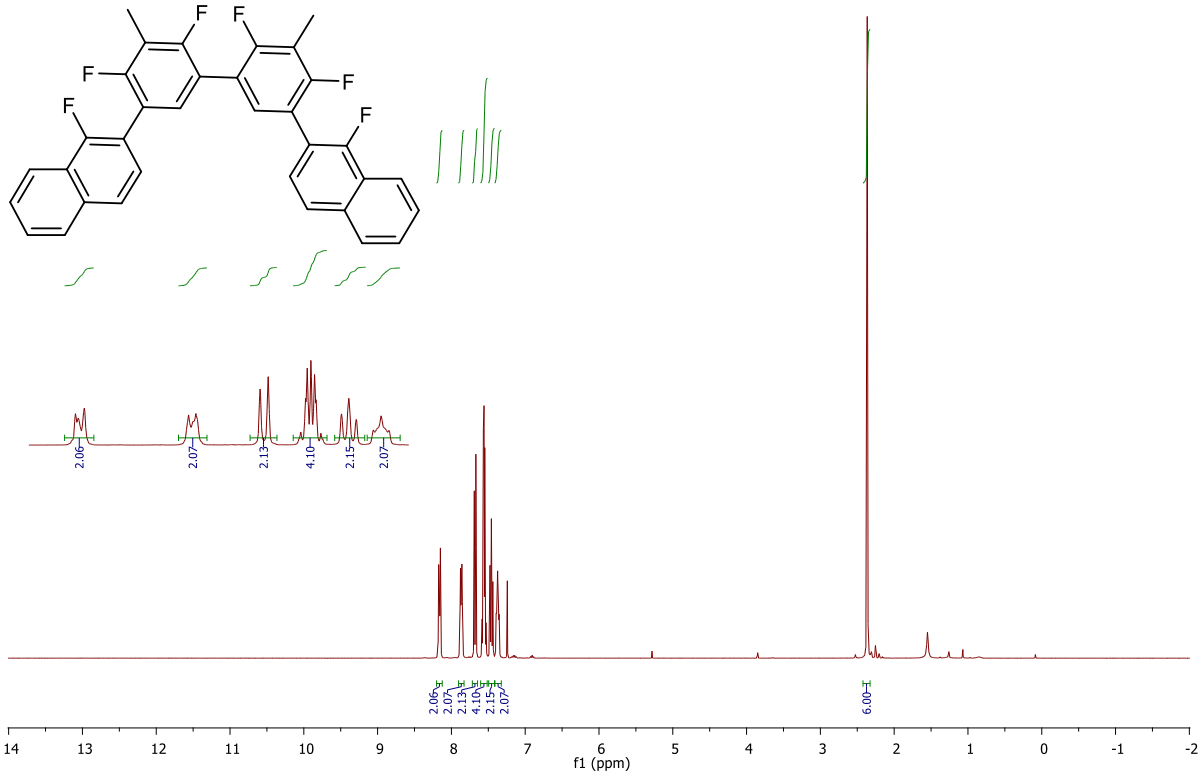

Figure A111. ^{1}H NMR (400 MHz, $CDCl_3$) of 27.

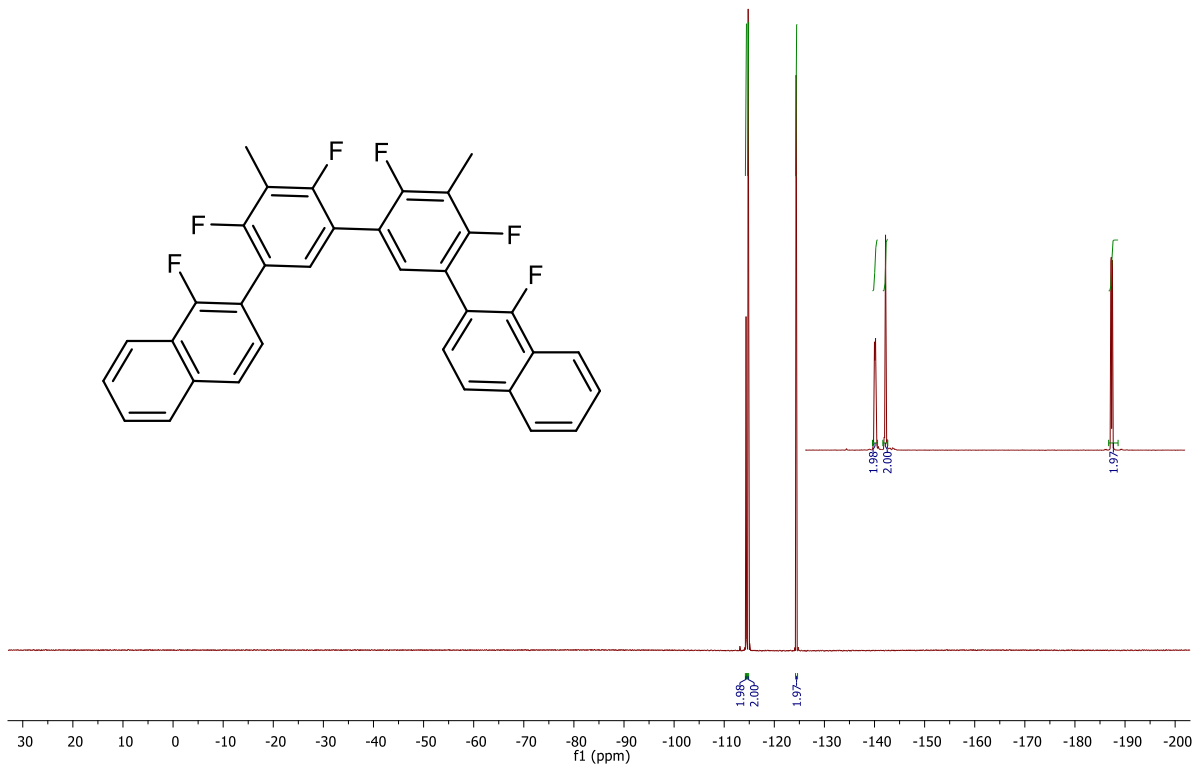

Figure A112. ^{19}F NMR (376 MHz, $CDCl_3$) of 27.

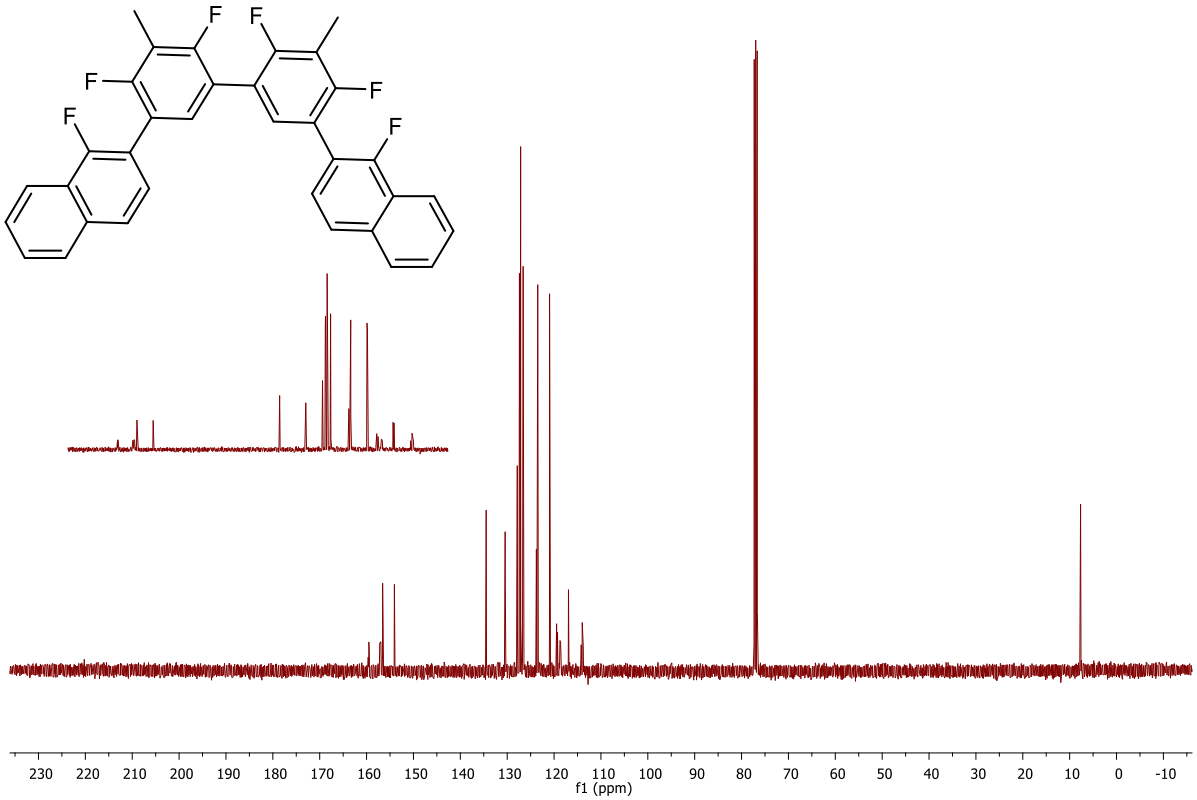

Figure A113. ^{13}C NMR (101 MHz, $CDCl_3$) of 27.

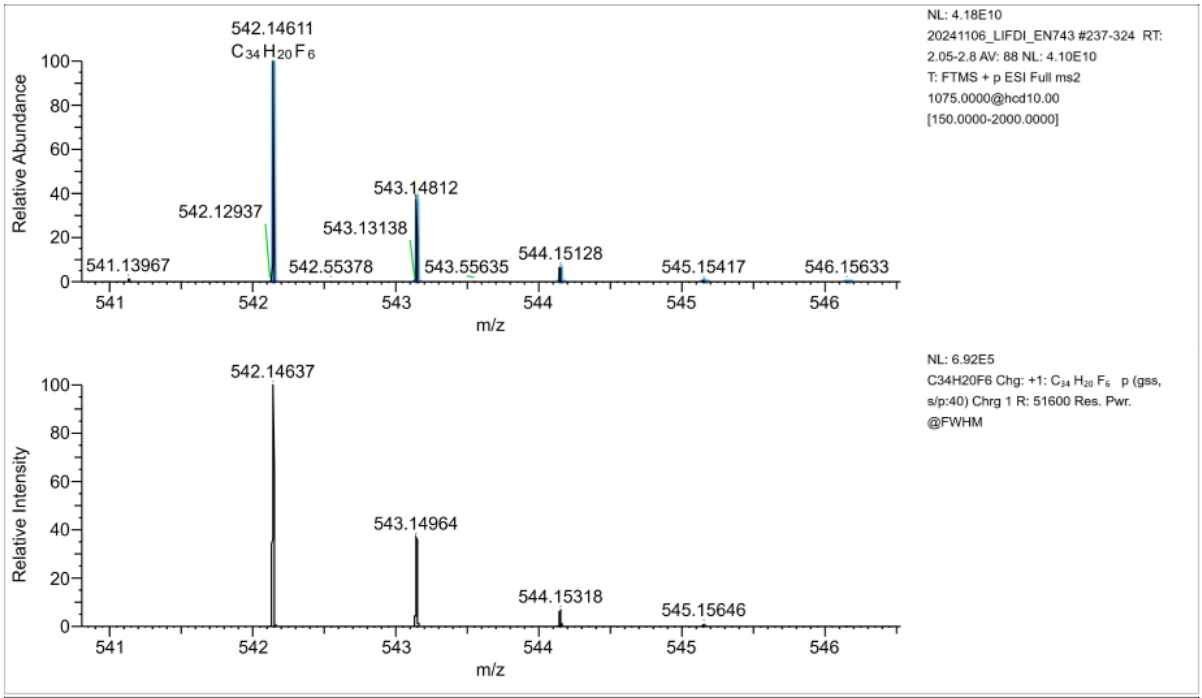

Peak Mass	Display F...	S Fit	RDB	Delta [pp...	Theo. ma...	Rank	Combine...	# Match...	# Missed...	MS Cov....	Pattern C...	MSMS M...
542.14611	$C_{34}H_{20}F_6$	40.570919089432	22.00	-0.48	542.14637	1	96.33	4	0	99.43	99.47	(Collection)

Figure A114. HRMS (LIFDI) of 27.

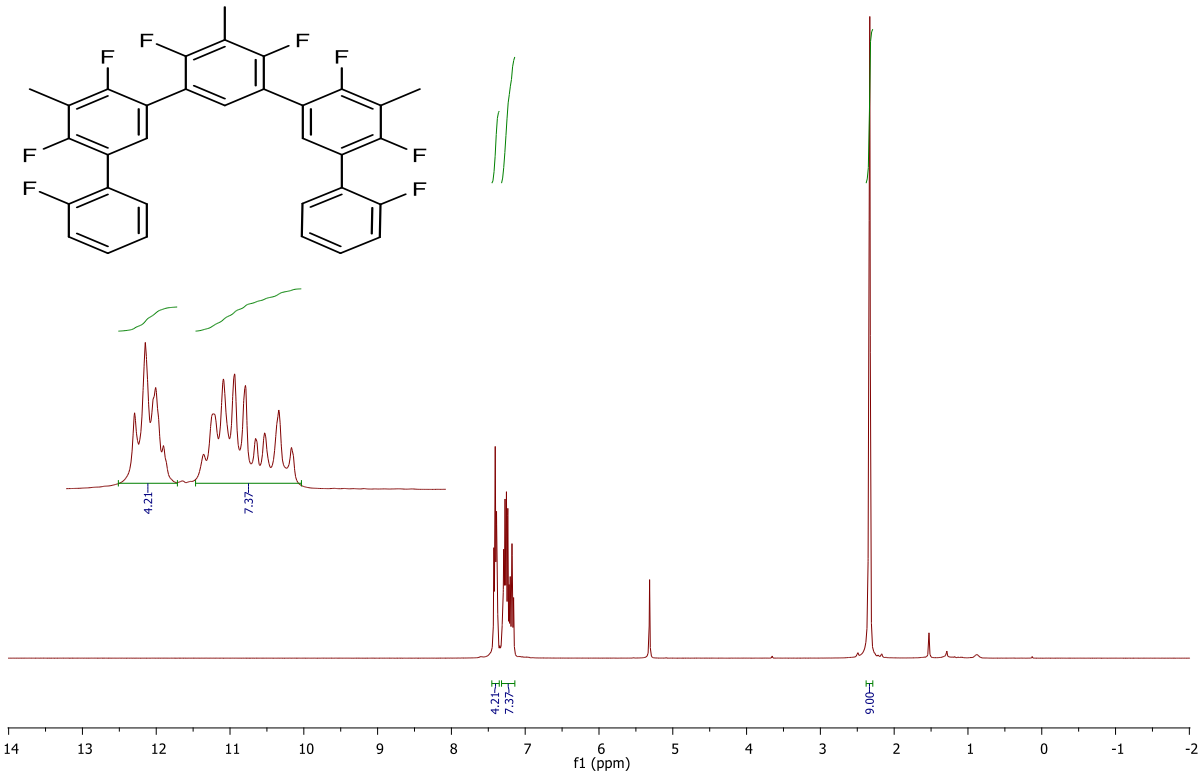

Figure A115. ^{1}H NMR (400 MHz, $CDCl_3$) of 28.

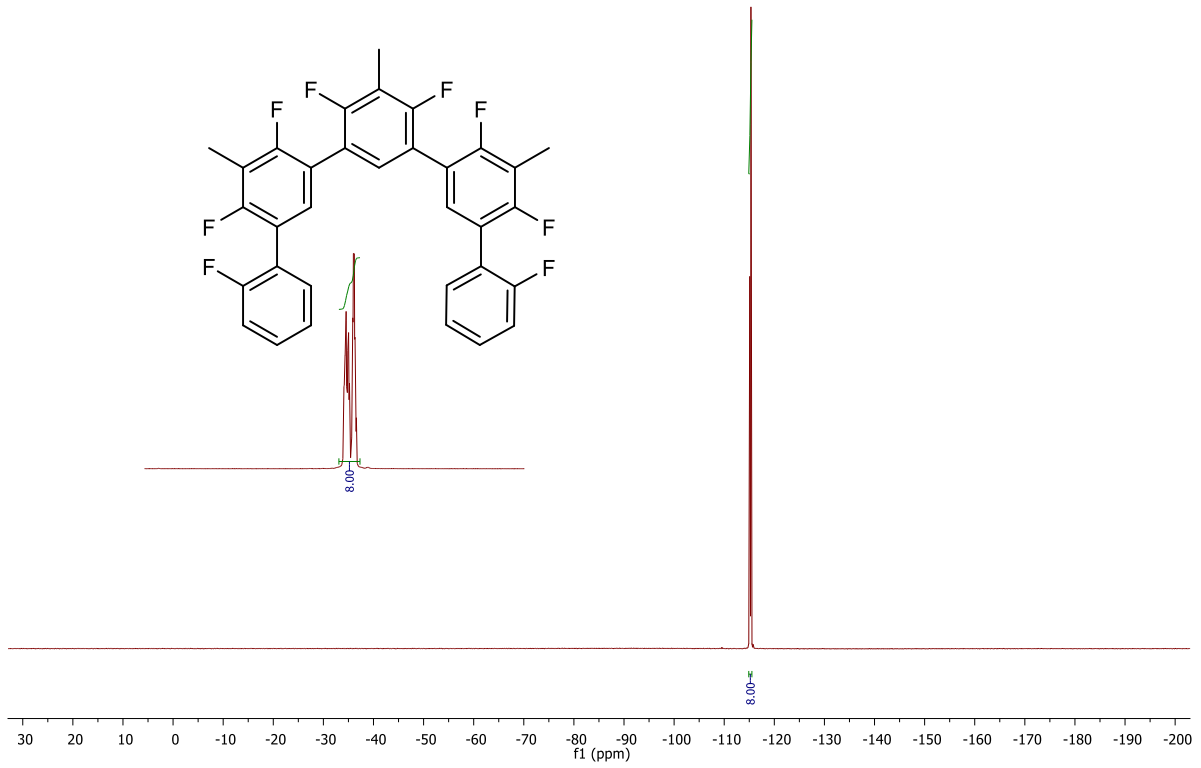

Figure A116. ^{19}F NMR (376 MHz, $CDCl_3$) of 28.

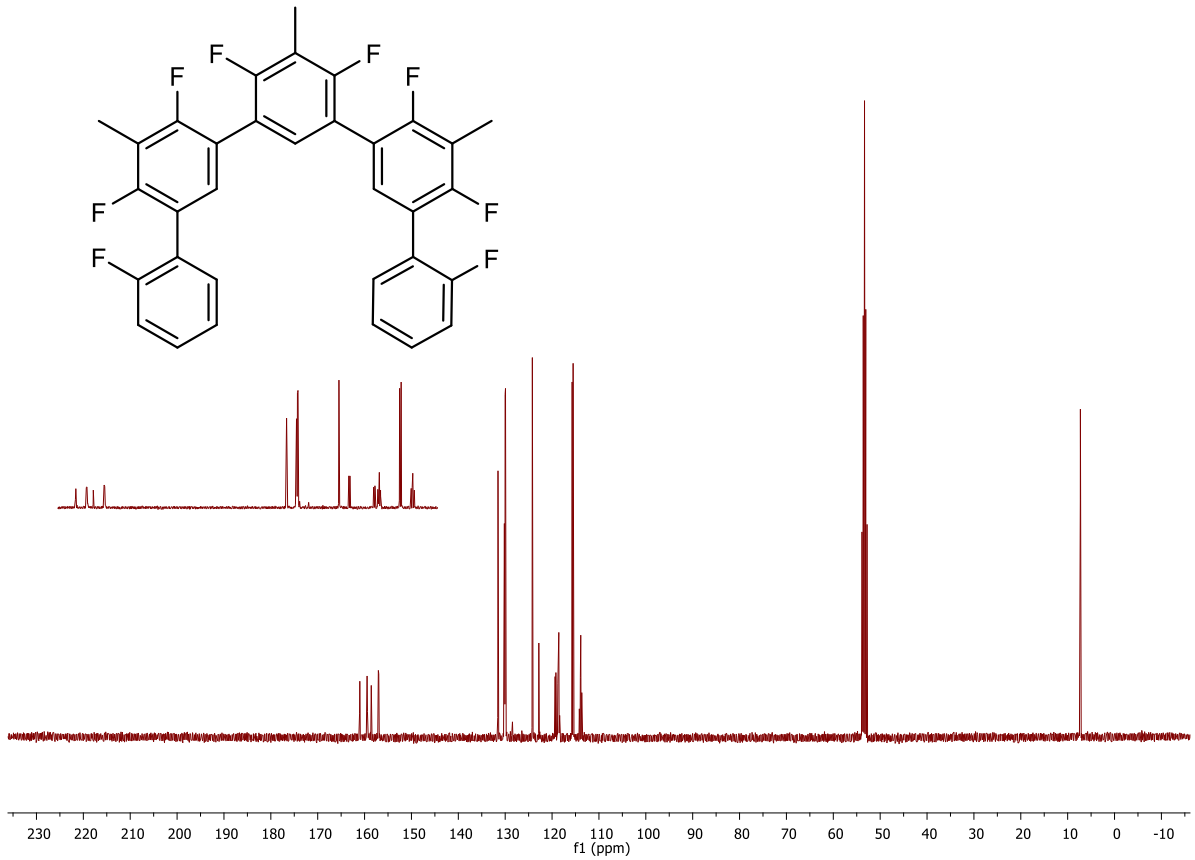

Figure A117. ^{13}C NMR (101 MHz, $CDCl_3$) of 28.

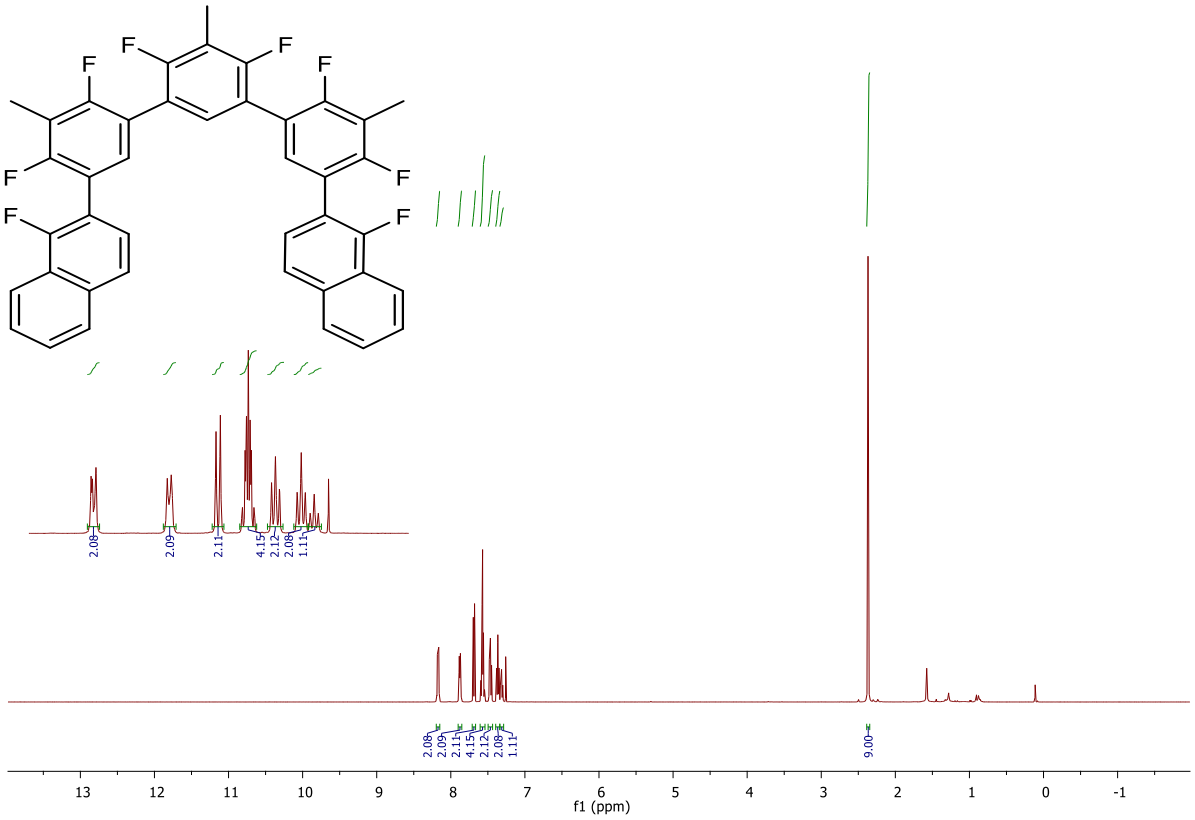

Figure A118. ^{1}H NMR (400 MHz, $CDCl_3$) of 29.

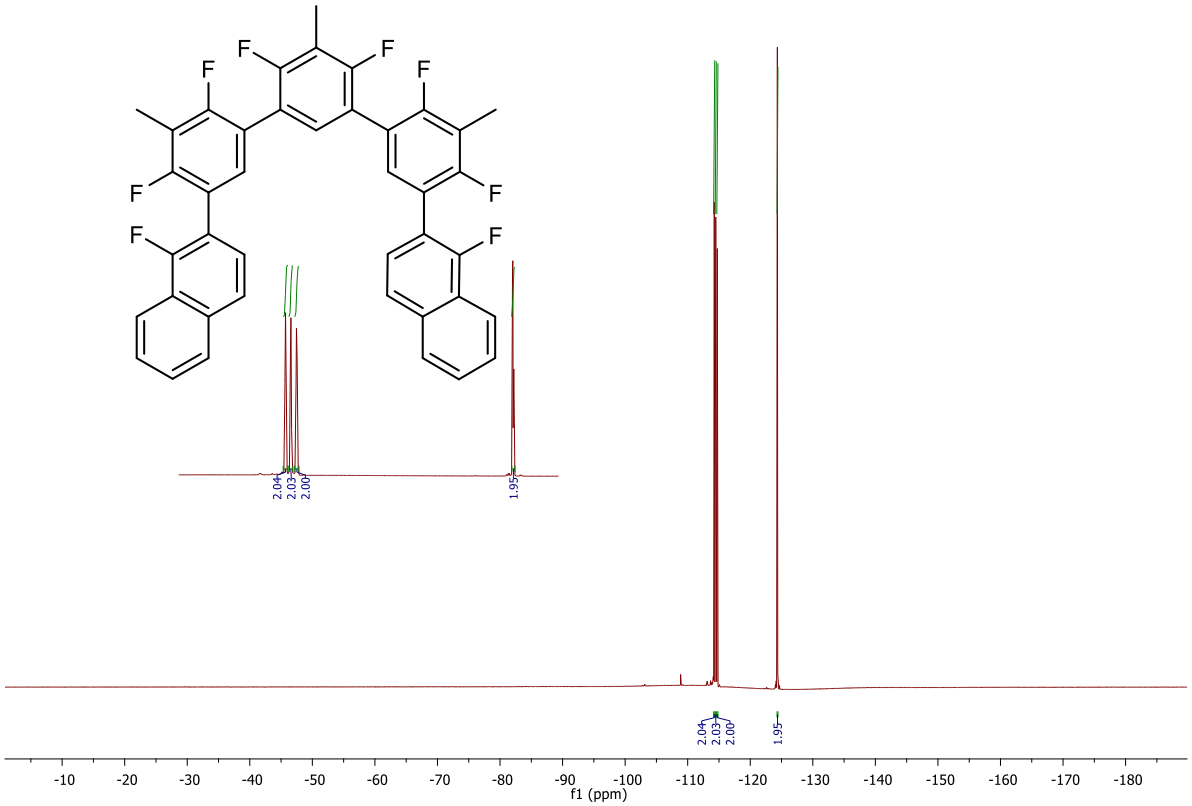

Figure A119. ^{19}F NMR (376 MHz, $CDCl_3$) of 29.

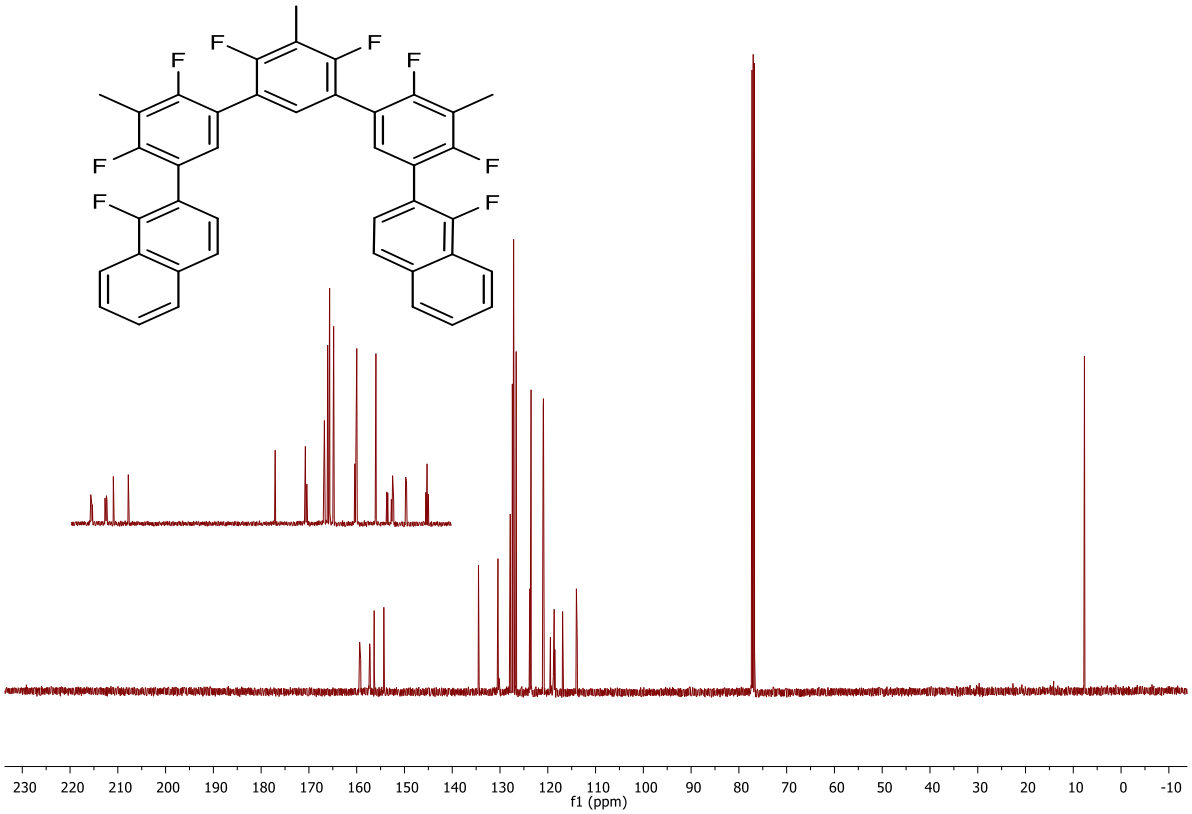

Figure A120. ^{13}C NMR (101 MHz, $CDCl_3$) of 29.

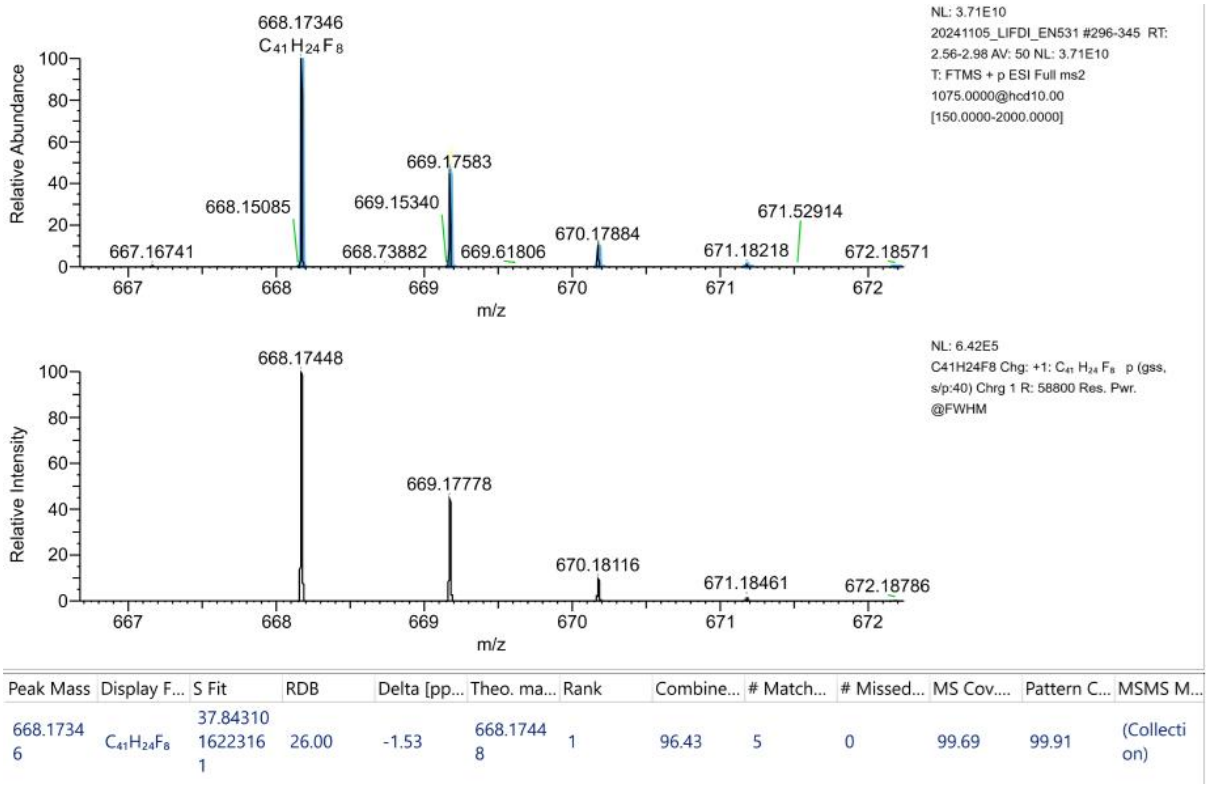

Peak Mass	Display F...	S Fit	RDB	Delta [pp...	Theo. ma...	Rank	Combine...	# Match...	# Missed...	MS Cov....	Pattern C...	MSMS M...
668.17346	$C_{41}H_{24}F_8$	37.843101622316 1	26.00	-1.53	668.17448	1	96.43	5	0	99.69	99.91	(Collection)

Figure A121. HRMS (LIFDI) of 29.

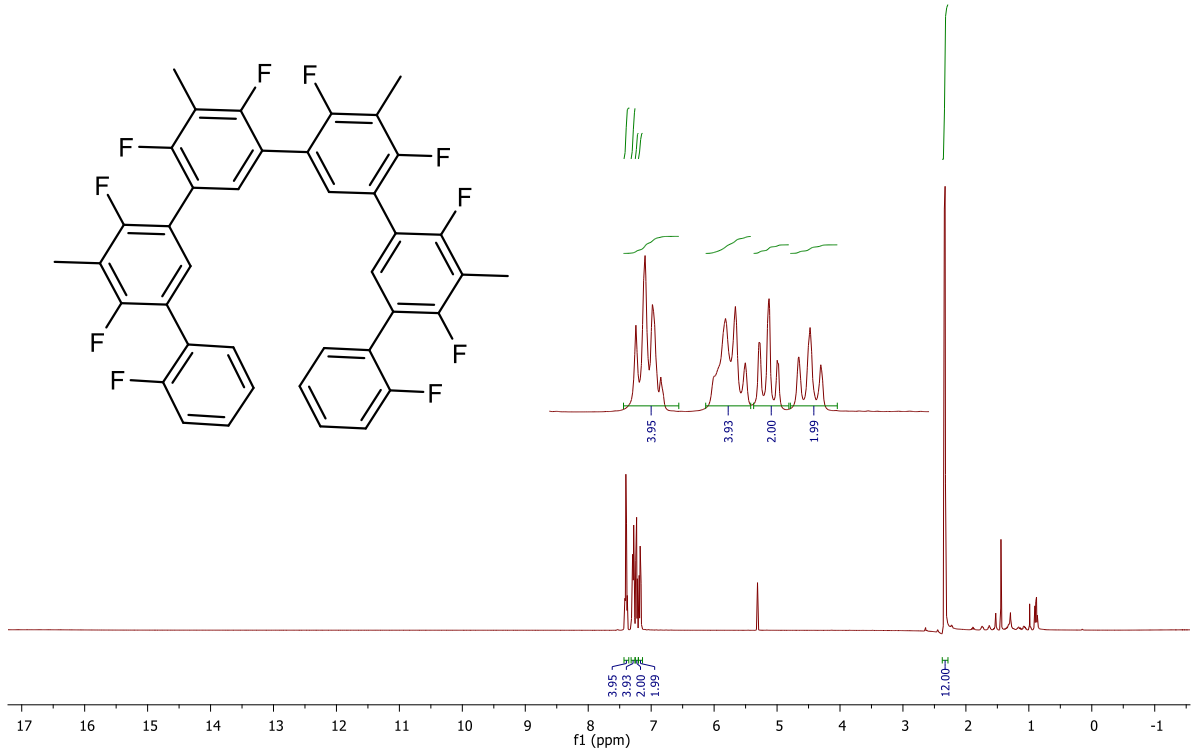

Figure A122. ^{1}H NMR (400 MHz, $CDCl_3$) of 30.

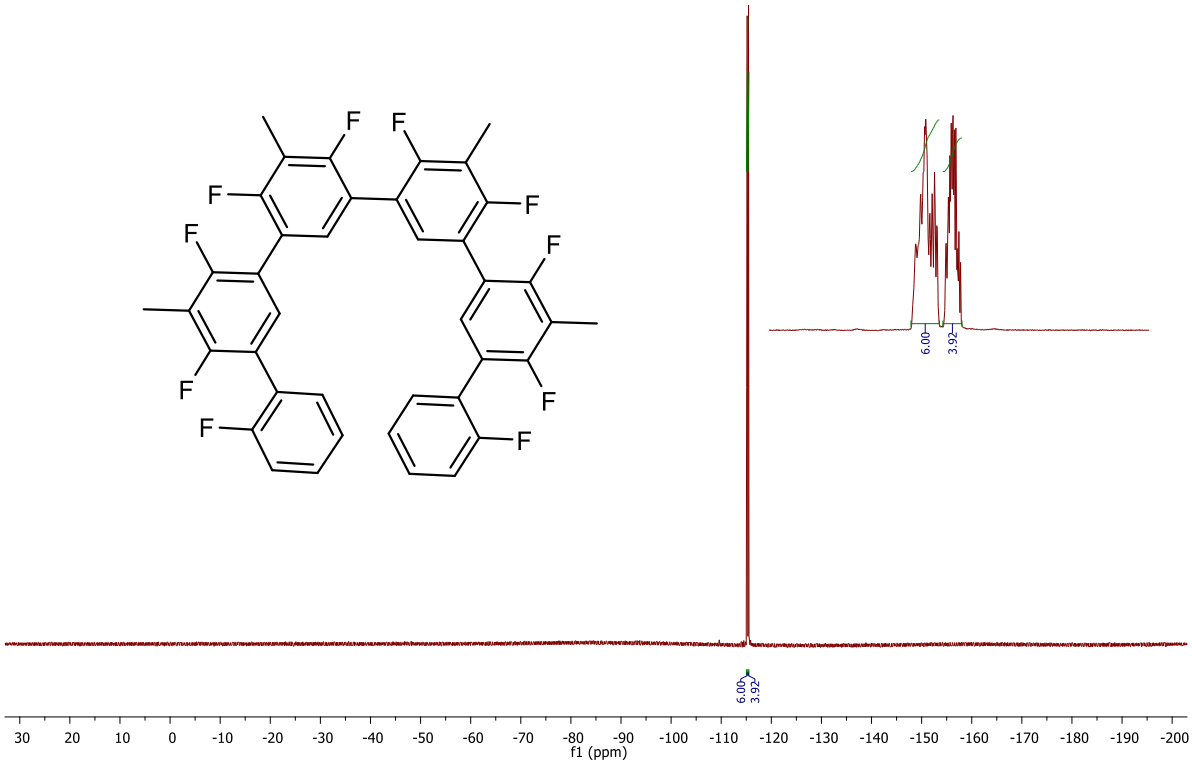

Figure A123. ^{19}F NMR (376 MHz, $CDCl_3$) of 30.

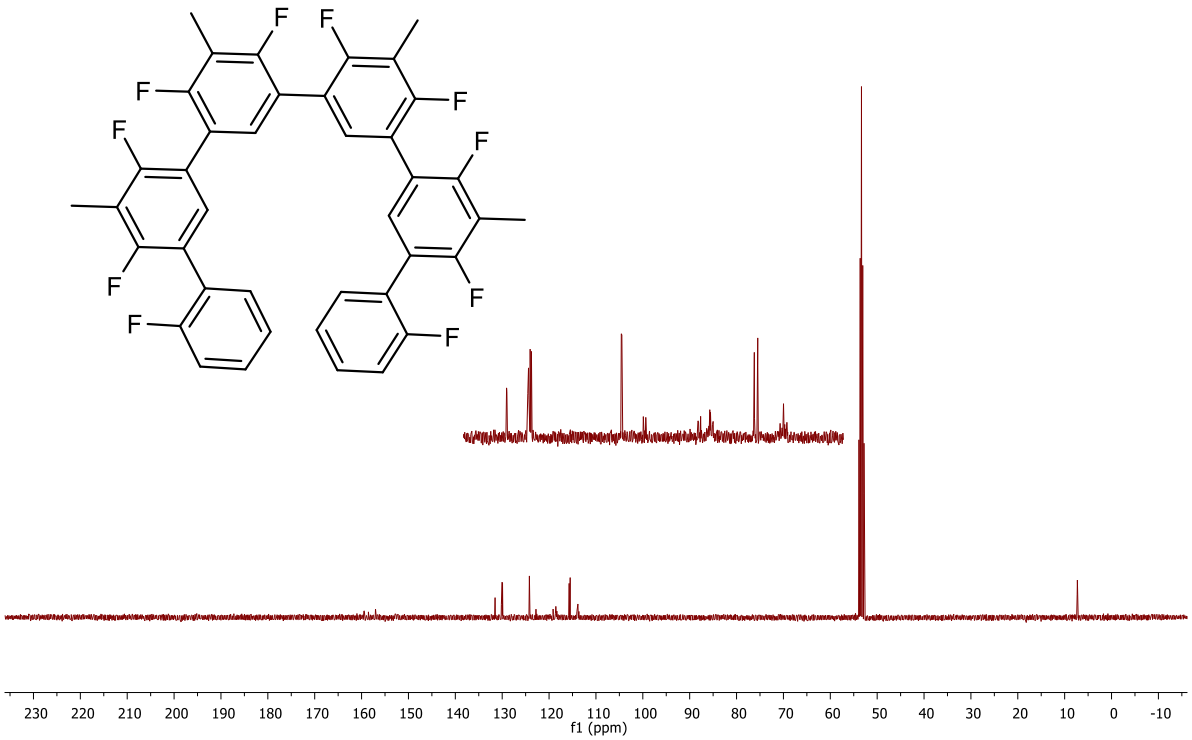

Figure A124. ^{13}C NMR (101 MHz, $CDCl_3$) of 30.

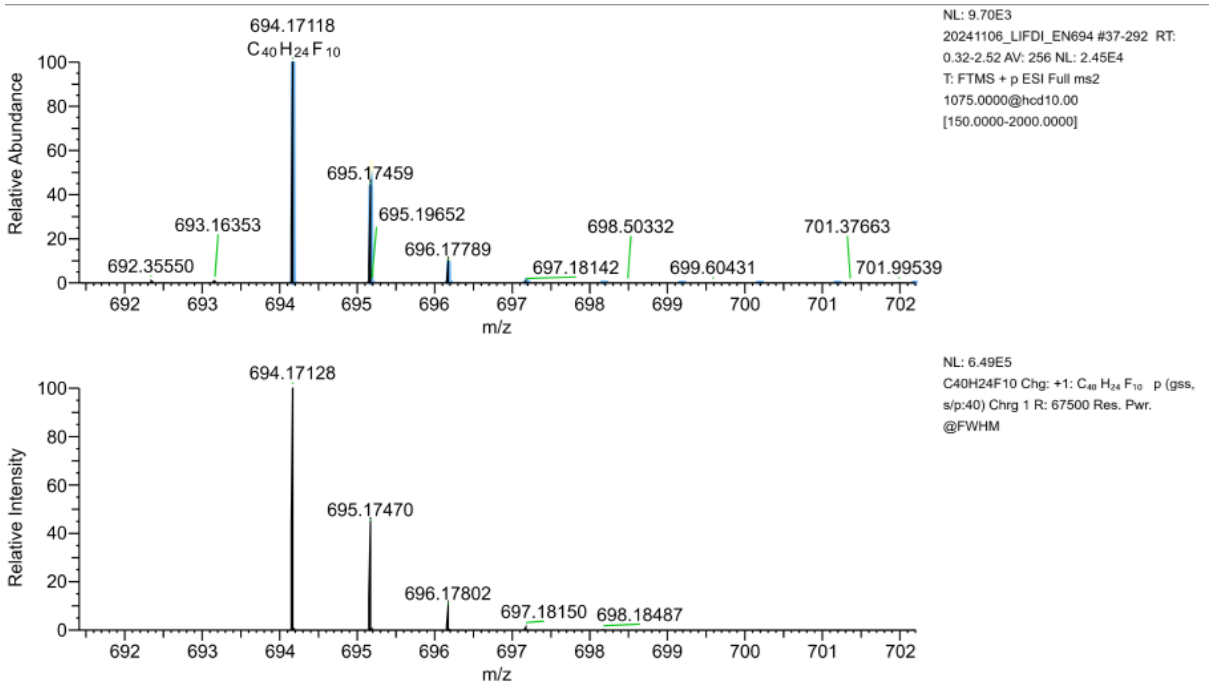

Figure A125. HRMS (LIFDI) of 30.

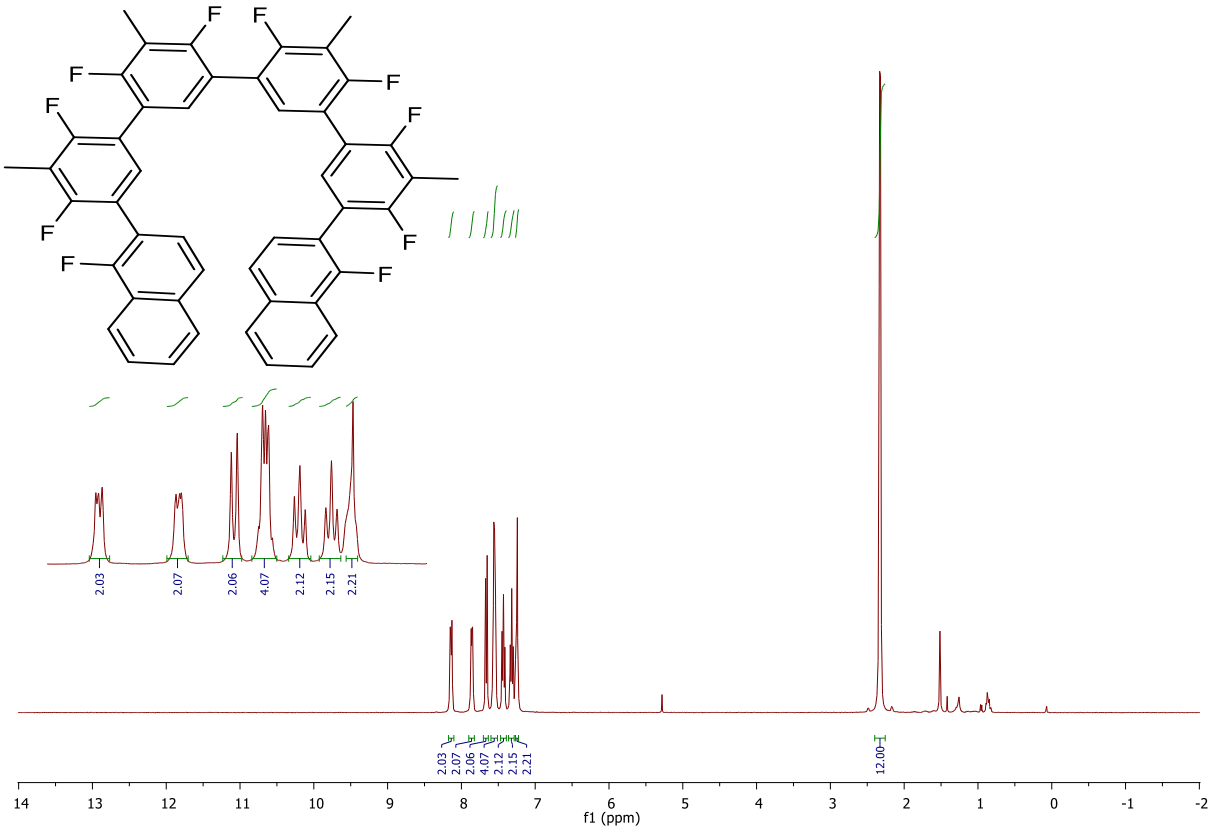

Figure A126. ^{1}H NMR (400 MHz, $CDCl_3$) of 31.

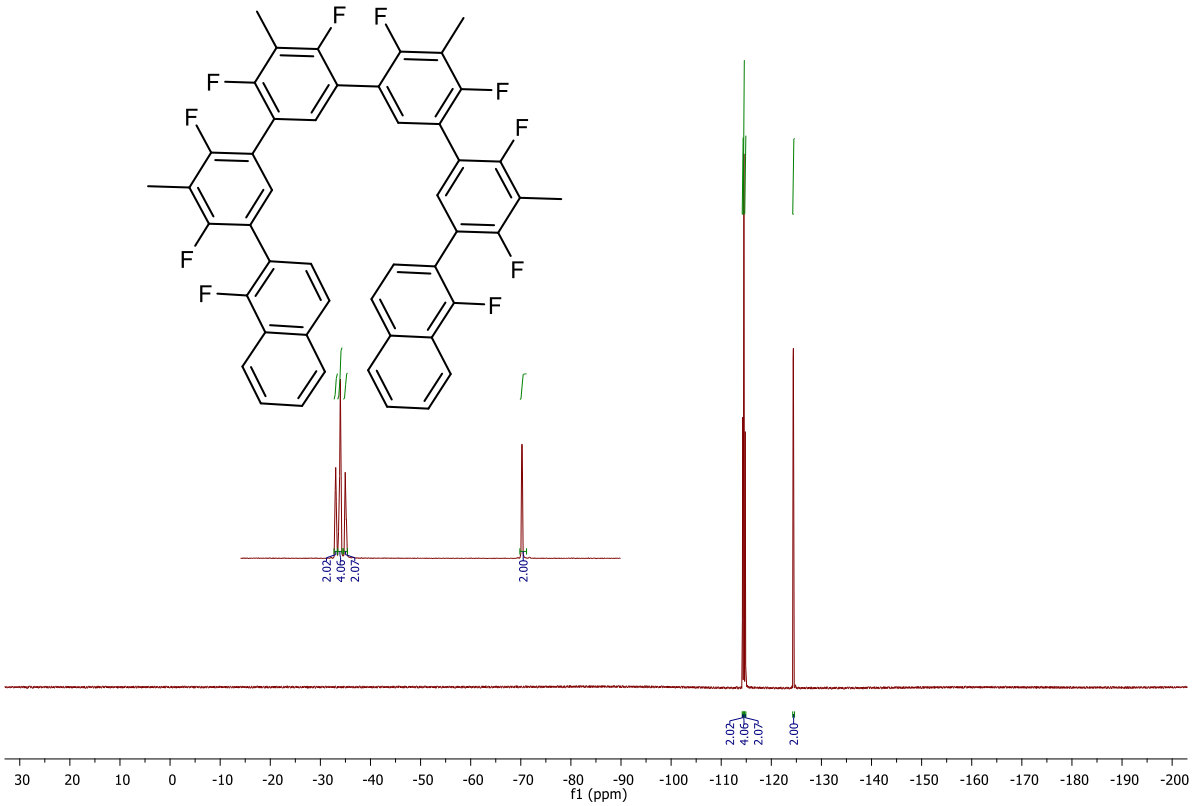

Figure A129. ^{19}F NMR (376 MHz, $CDCl_3$) of 31.

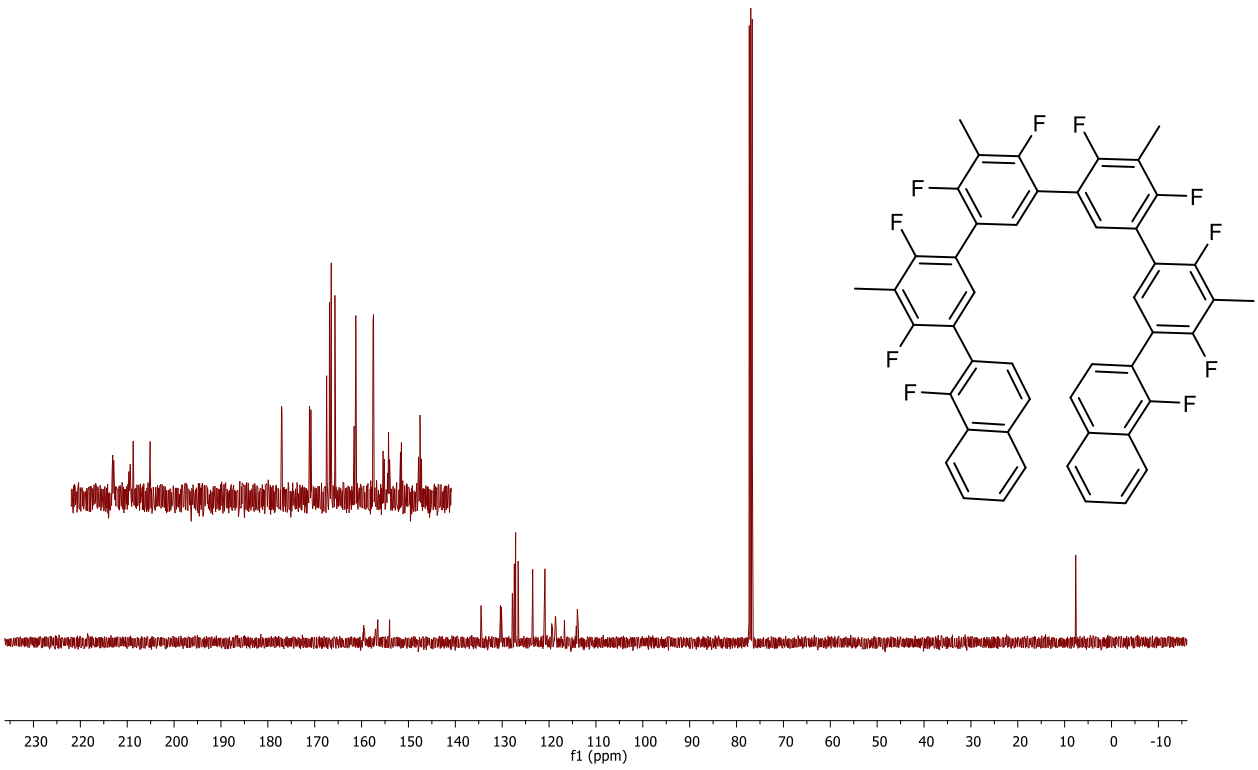

Figure A130. ^{13}C NMR (101 MHz, $CDCl_3$) of 31.

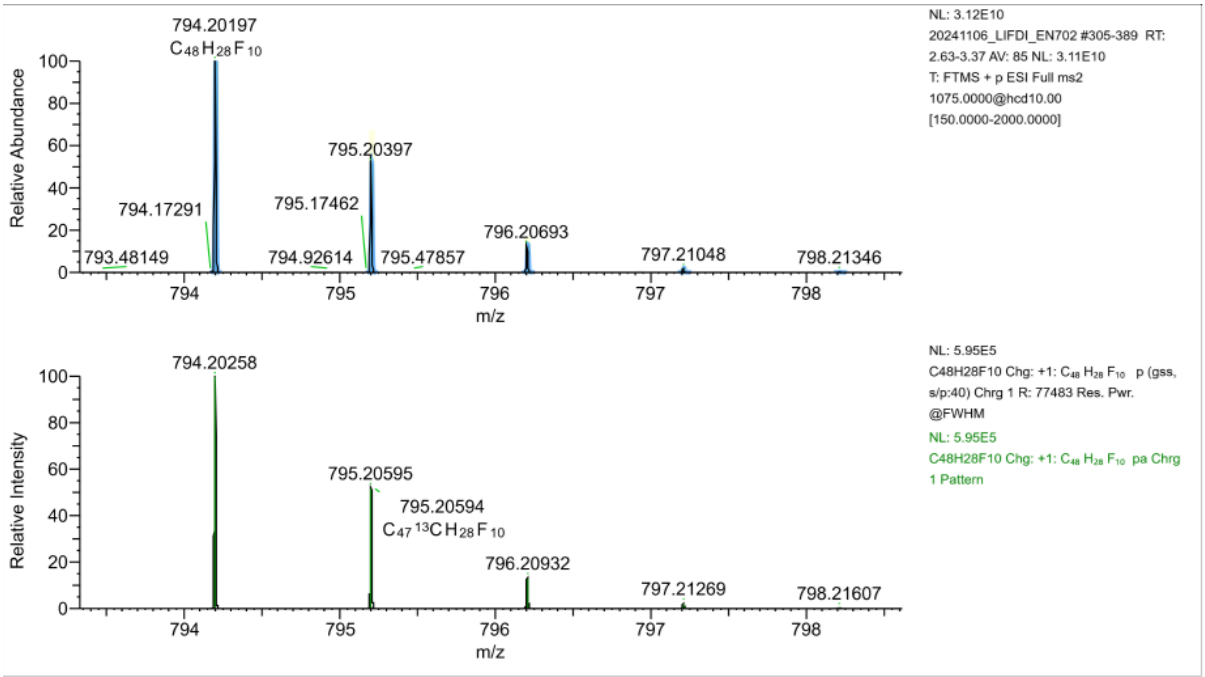

Peak Mass	Display F...	S Fit	RDB	Delta [pp...	Theo. ma...	Rank	Combine...	# Match...	# Missed...	MS Cov....	Pattern C...	MSMS M...
794.20197	$C_{48}H_{28}F_{10}$	53.639662646525 9	30.00	-0.78	794.20258	1	97.43	5	0	99.87	100	(Collection)

Figure A131. HRMS (LIFDI) of 31.

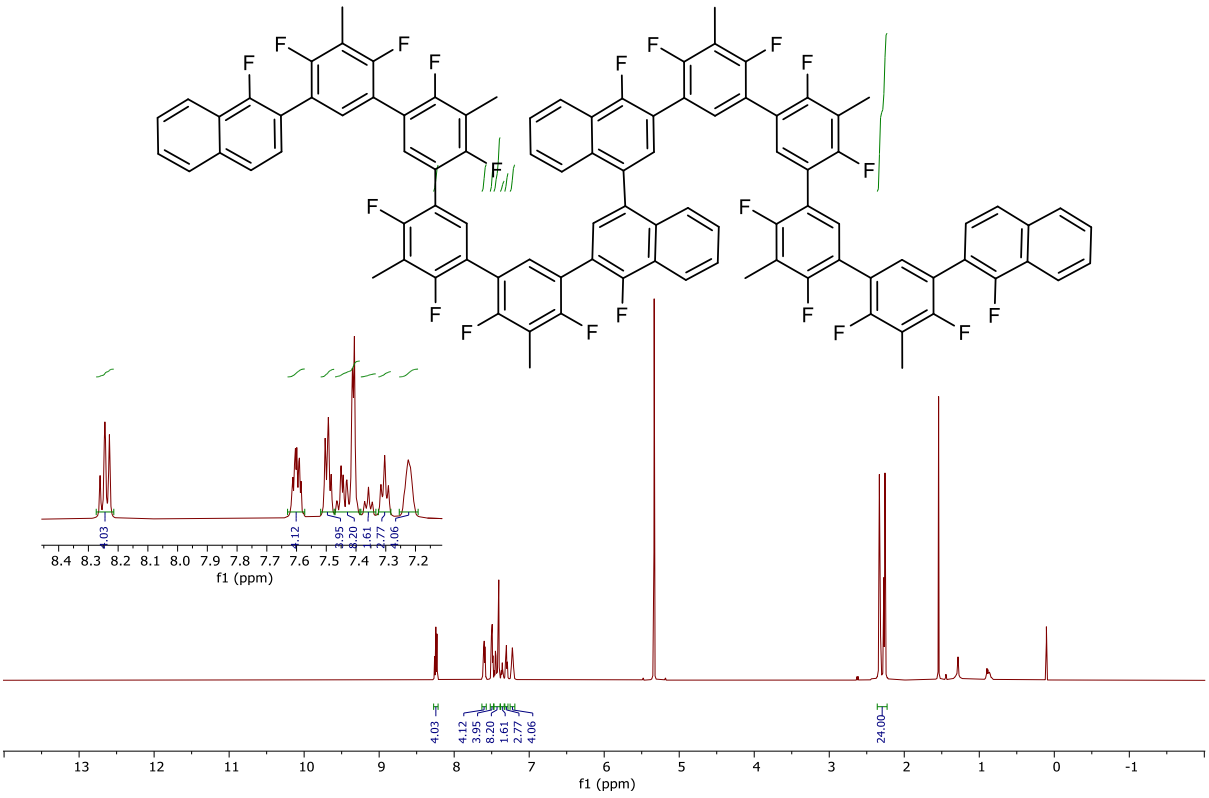

Figure A132. ^{1}H NMR (400 MHz, $CDCl_3$) of 32.

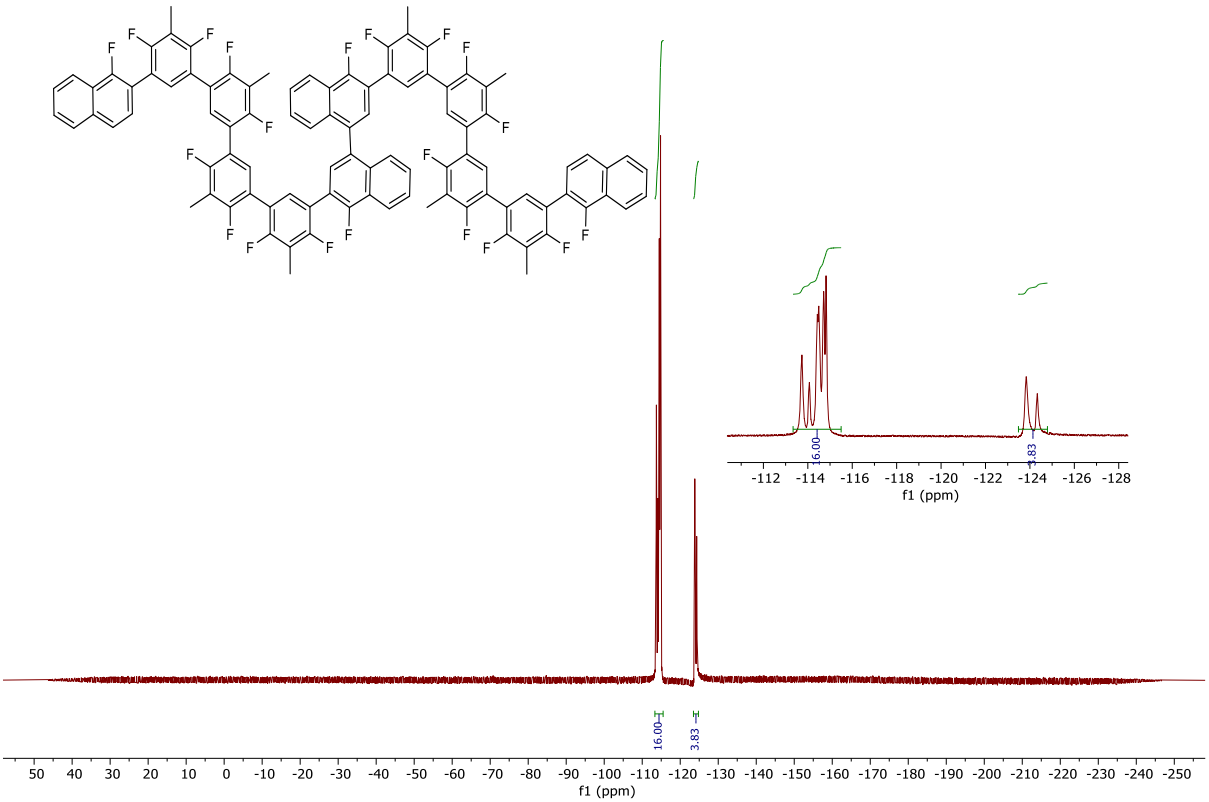

Figure A133. ^{19}F NMR (376 MHz, $CDCl_3$) of 32.

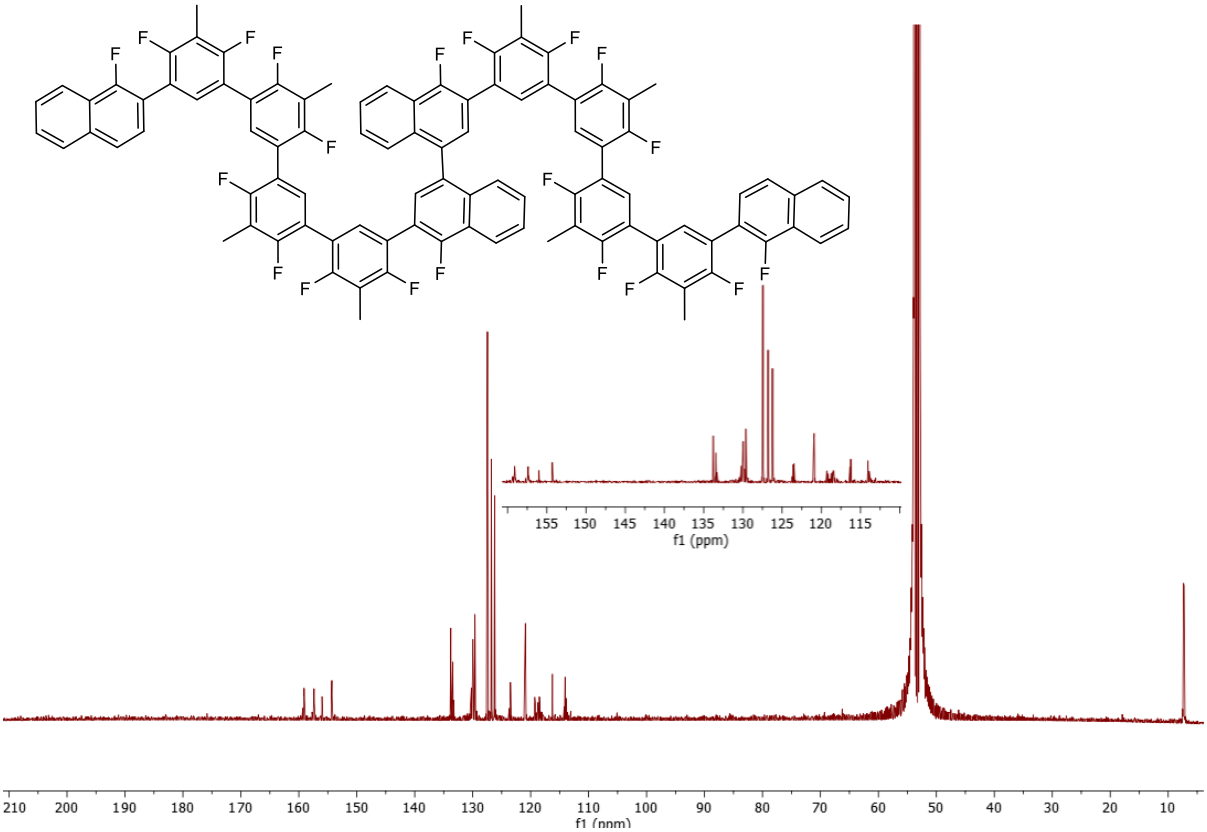

Figure A134. ^{13}C NMR (101 MHz, $CDCl_3$) of 32.

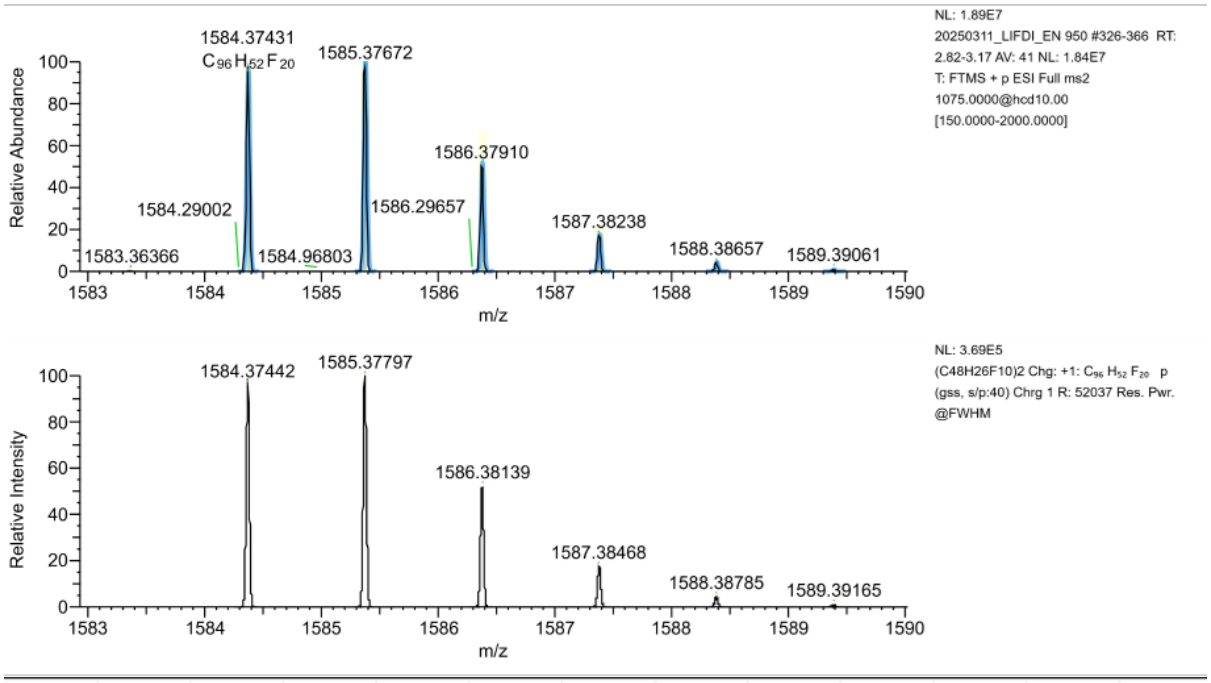

Peak Mass	Display F...	S Fit	RDB	Delta [pp...	Theo. ma...	Rank	Combine...	# Match...	# Missed...	MS Cov....	Pattern C...	MSMS M...
1584.37431	$C_{96}H_{52}F_{20}$	83.47955 9656347	61.00	-0.41	1584.37497	1	99.1	7	0	99.97	100	(Collection)

Figure A135. HRMS (LIFDI) of 32.

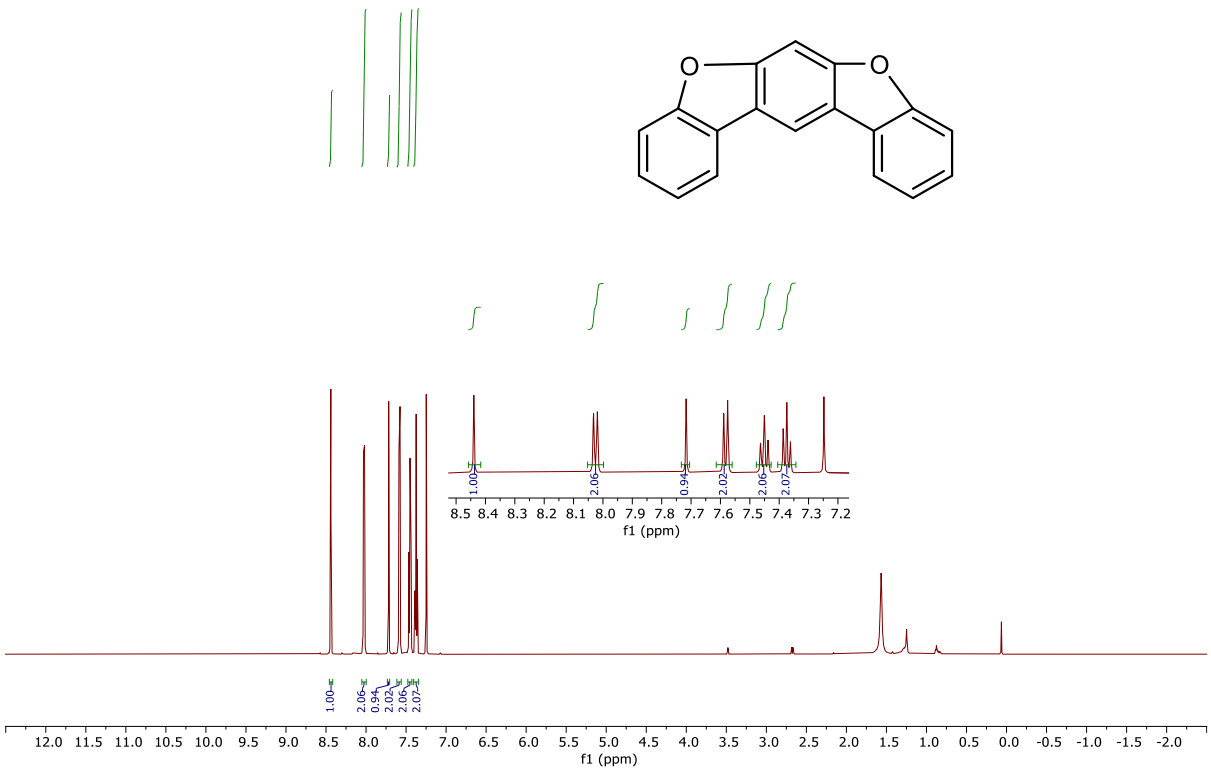

Figure A136. ^{1}H NMR (400 MHz, $CDCl_3$) of 33.

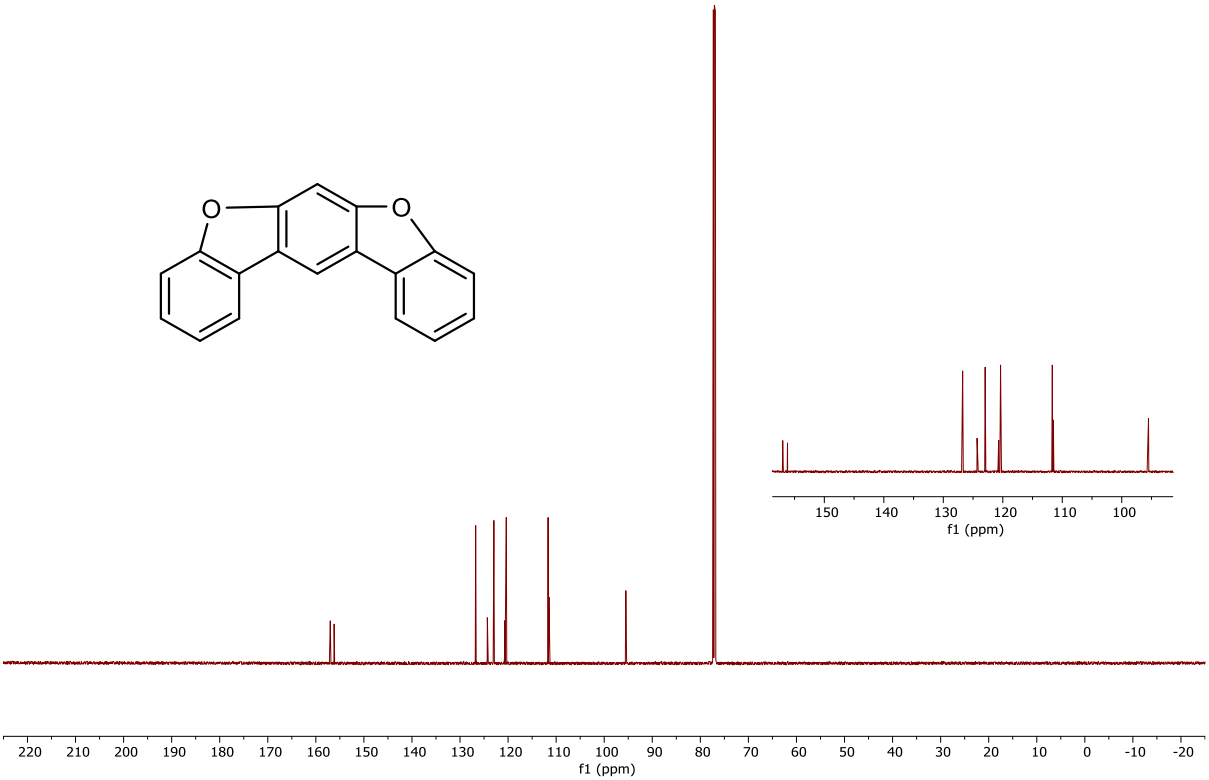

Figure A137. ^{13}C NMR (101 MHz, $CDCl_3$) of 33.

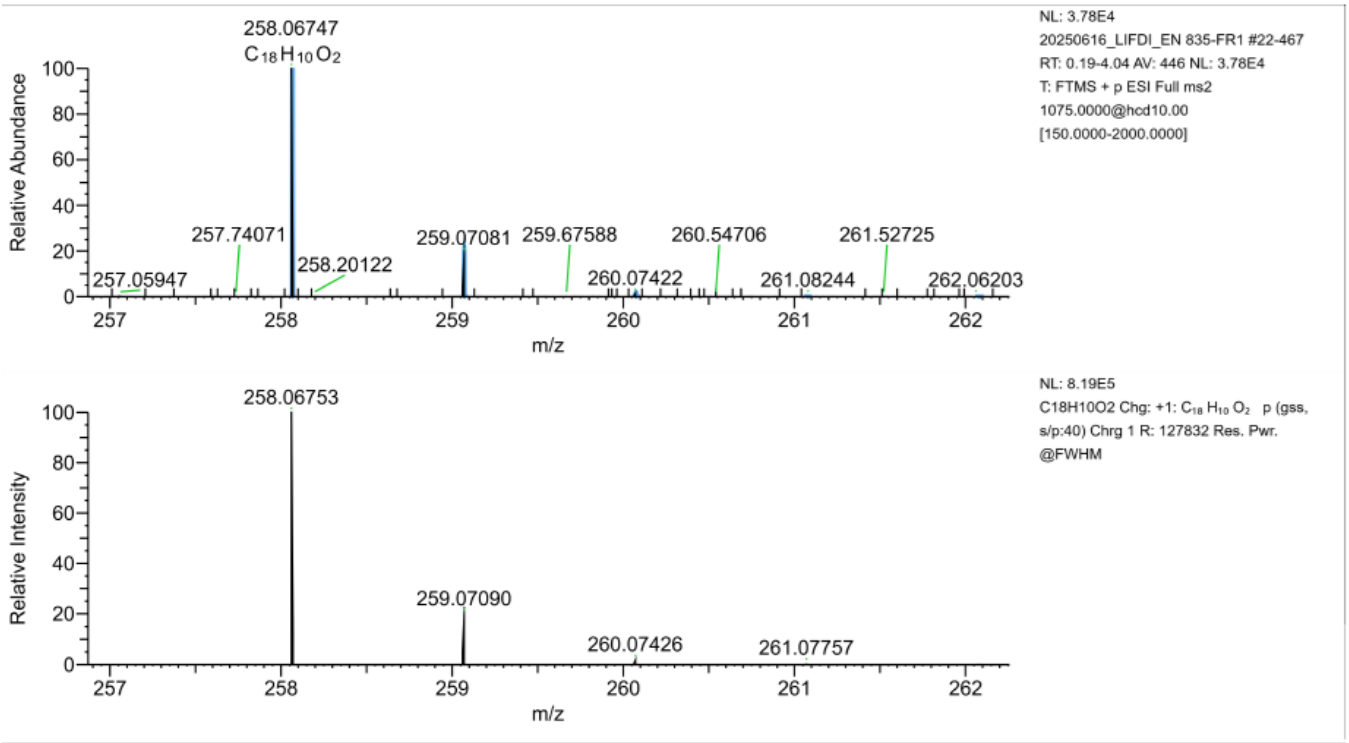

Peak Mass	Display F...	S Fit	RDB	Delta [pp...	Theo. ma...	Rank	Combine...	# Match...	# Missed...	MS Cov....	Pattern C...	MSMS M...
258.06747	$C_{18}H_{10}O_2$	45.351213415590	14.00	-0.24	258.06753	1	96.91	4	0	99.77	99.91	(Collection)

Figure A138. HRMS (LIFDI) of 33.

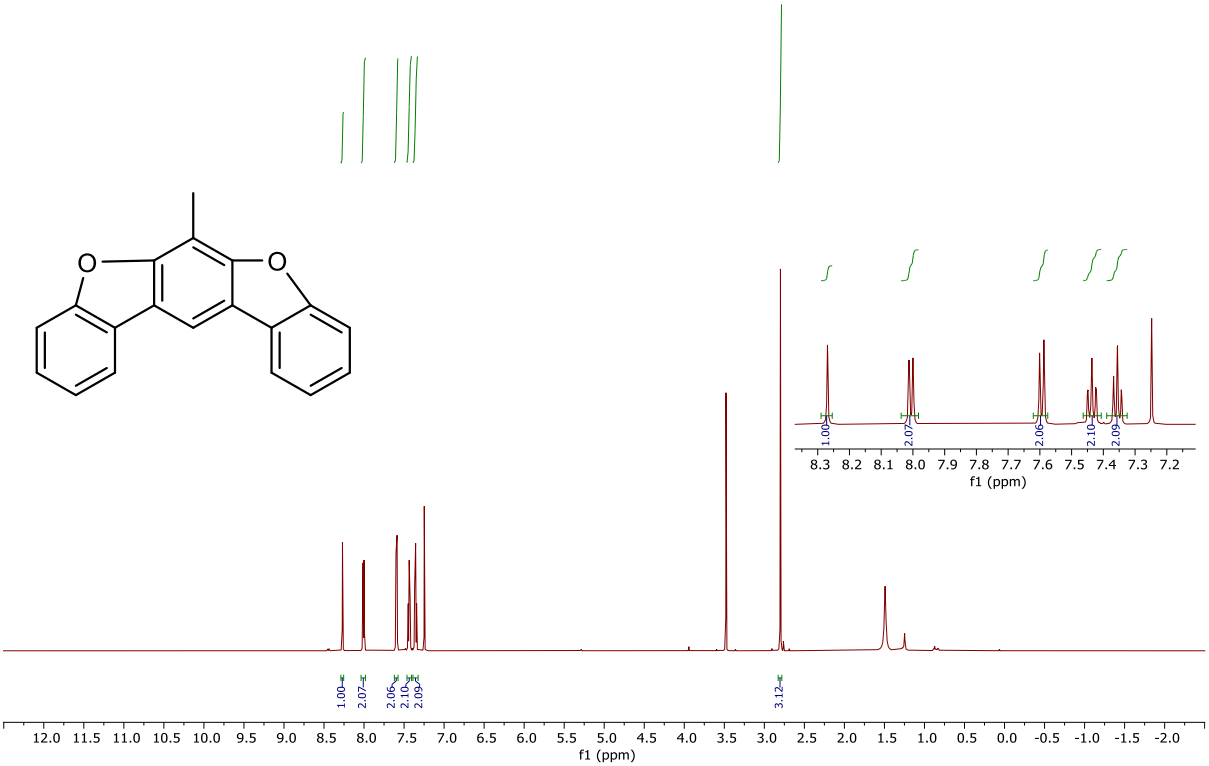

Figure A139. ^{1}H NMR (400 MHz, $CDCl_3$) of 34.

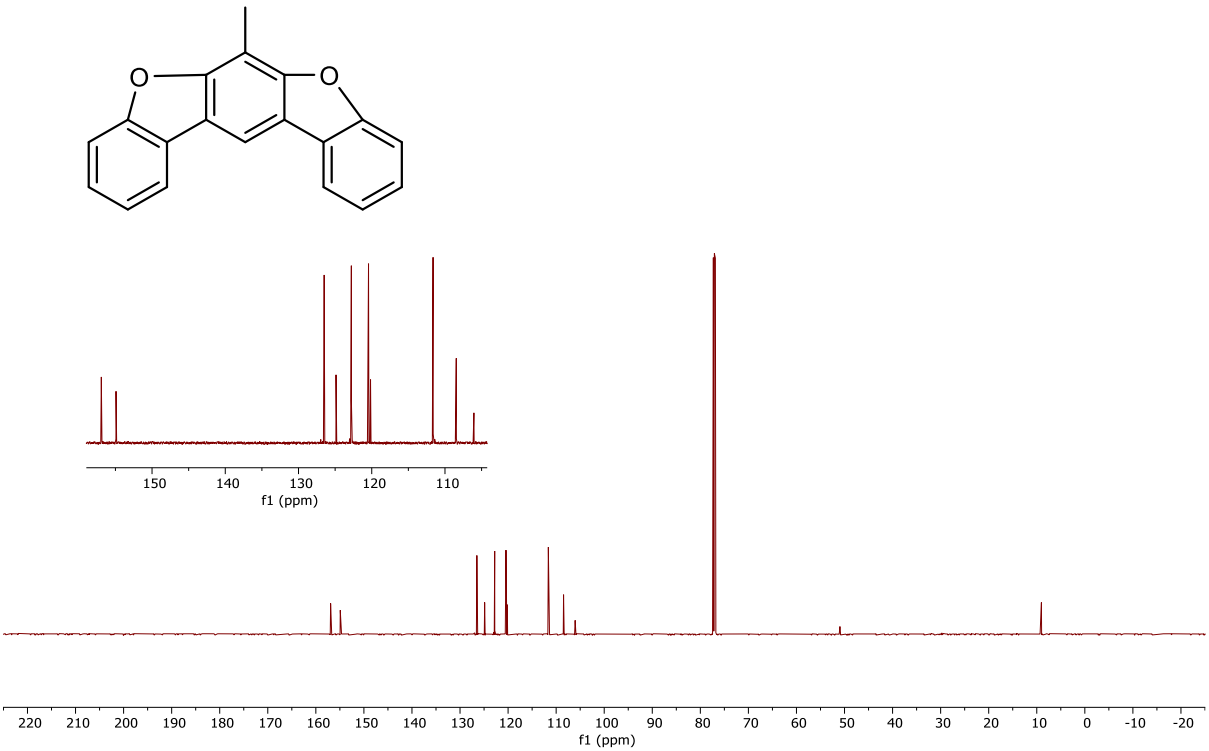

Figure A140. ^{13}C NMR (101 MHz, $CDCl_3$) of 34.

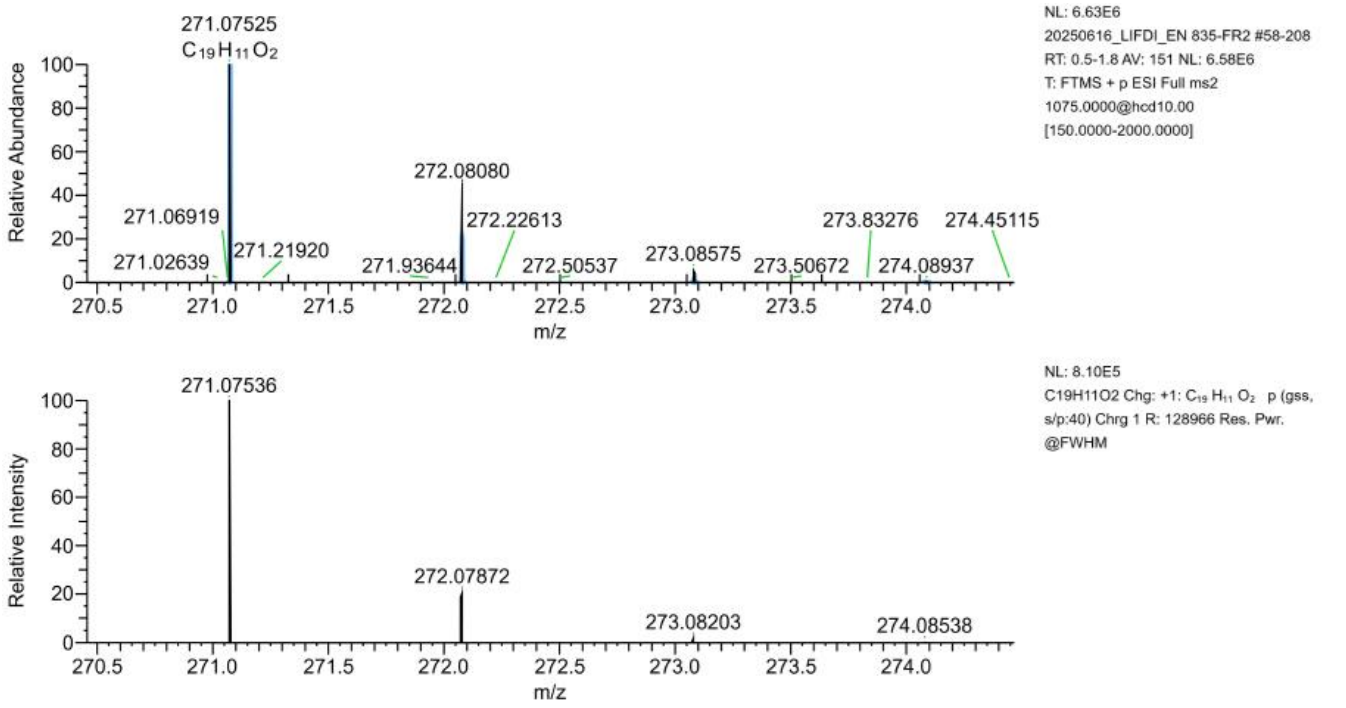

Peak Mass	Display F...	S Fit	RDB	Delta [pp...	Theo. ma...	Rank	Combine...	# Match...	# Missed...	MS Cov....	Pattern C...	MSMS M..
271.07525	$C_{19}H_{11}O_2$	26.143815860180 7	14.50	-0.39	271.07536	1	64.55	3	1	66.69	83.12	(Collection)

Figure A141. HRMS (LIFDI) of 34.

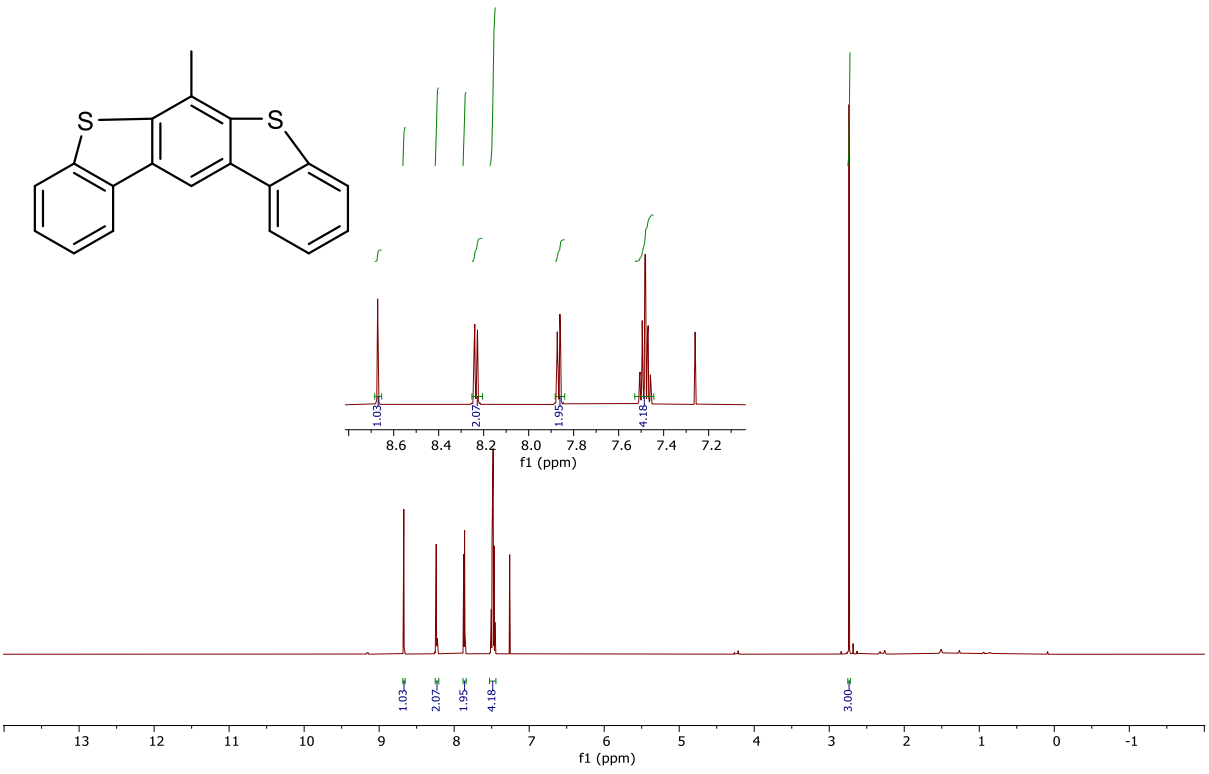

Figure A142. ^{1}H NMR (400 MHz, $CDCl_3$) of 35.

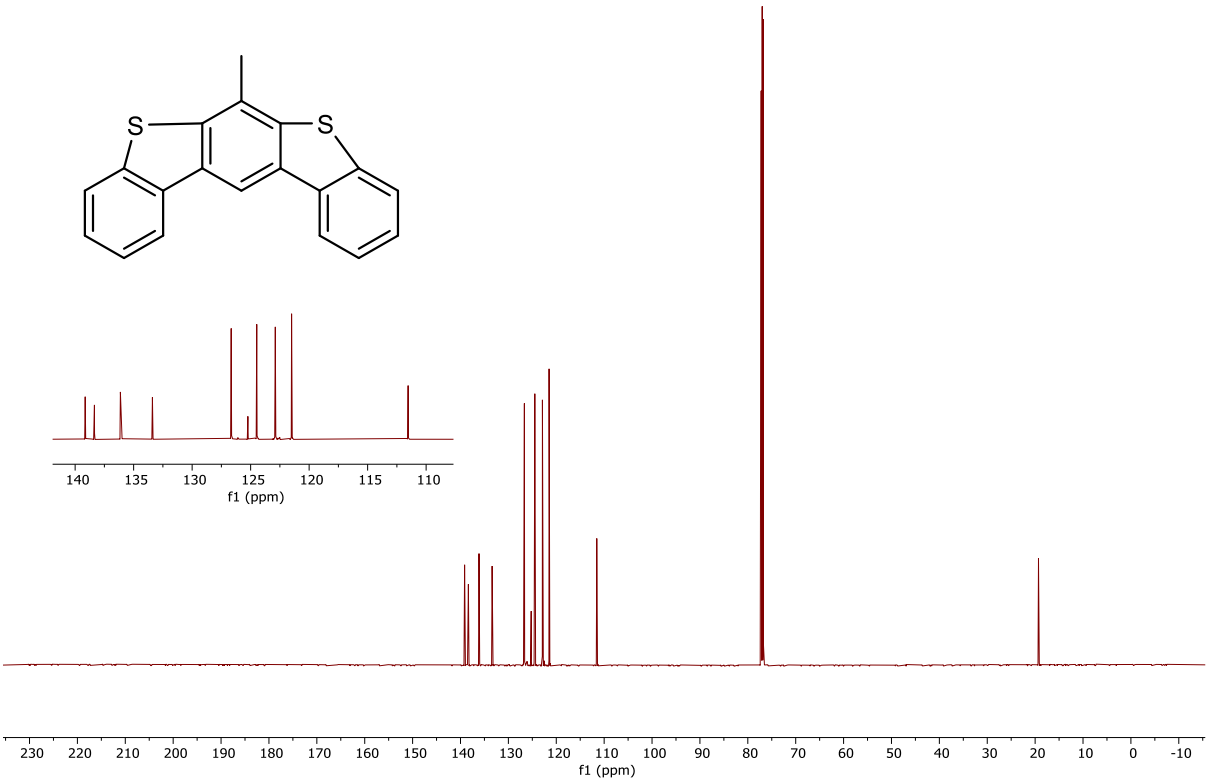

Figure A143. ^{13}C NMR (101 MHz, $CDCl_3$) of 35.

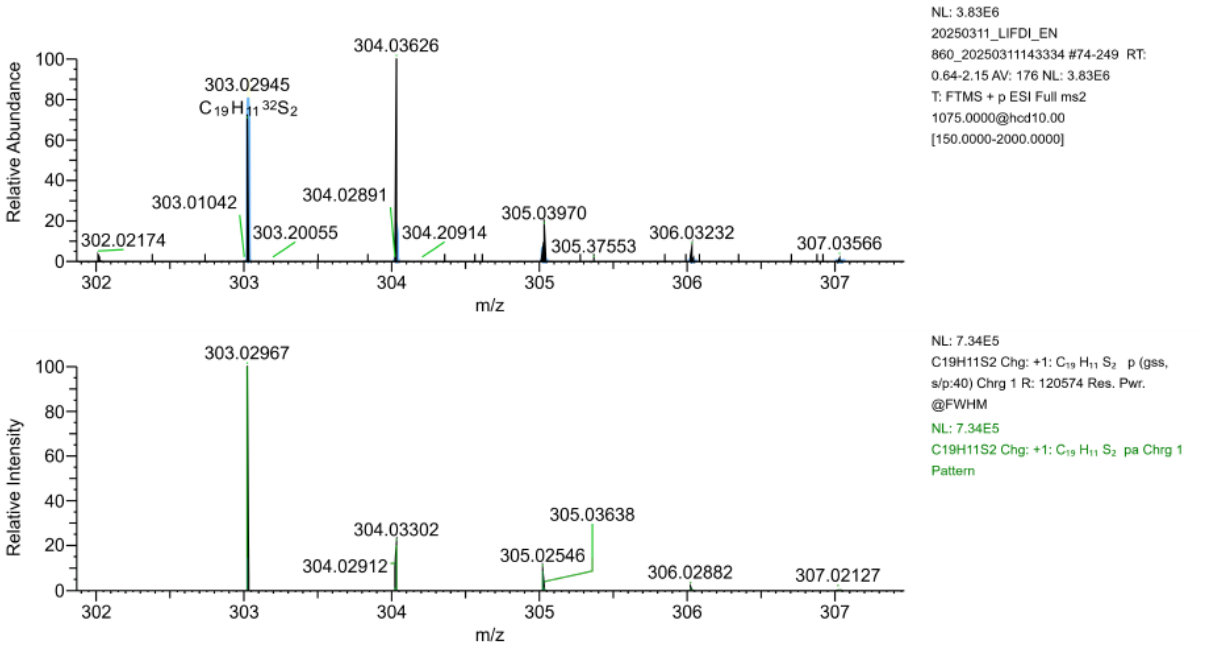

Peak Mass	Display F...	S Fit	RDB	Delta [pp...	Theo. ma...	Rank	Combine...	# Match...	# Missed...	MS Cov....	Pattern C...	MSMS M...
303.02945	$C_{19}H_{11}{}^{32}S_2$	23.74017 0884407	14.50	-0.71	303.02967	1	36.93	8	2	37.66	81.82	(Collection)

Figure A144. HRMS (LIFDI) of 35.

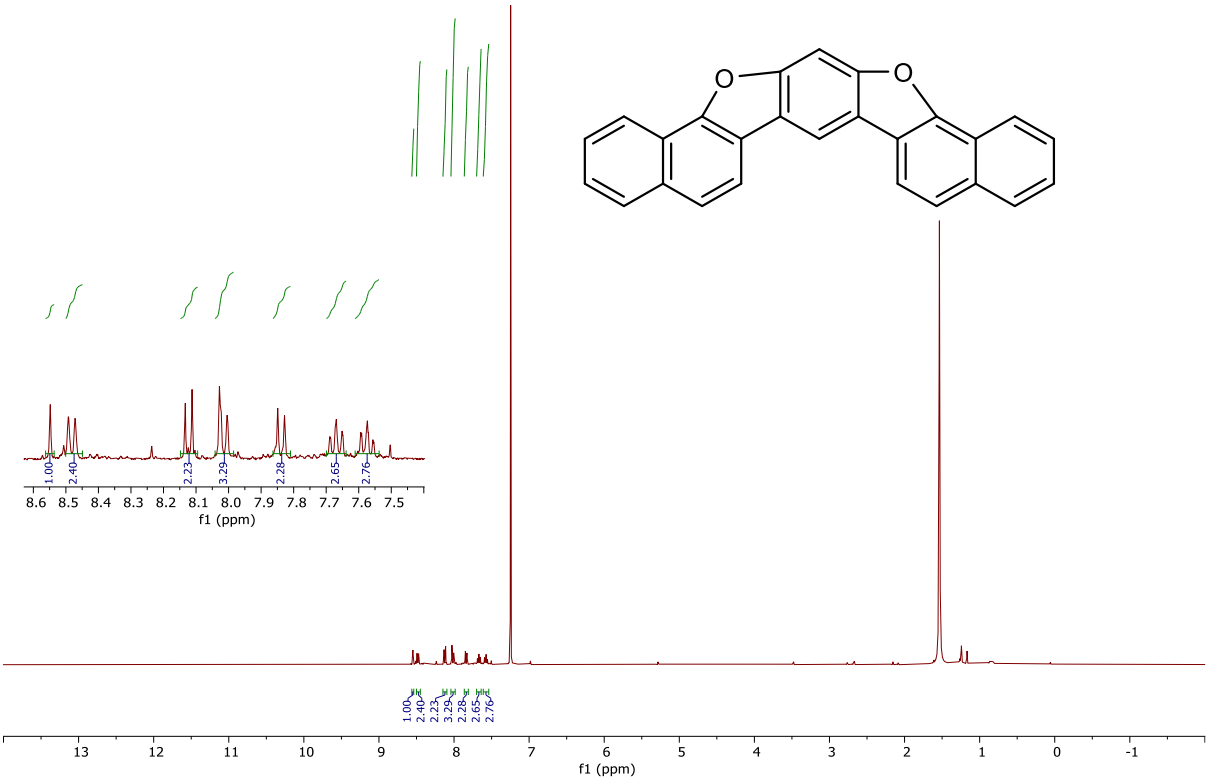

Figure A145. ^{1}H NMR (400 MHz, $CDCl_3$) of 36.

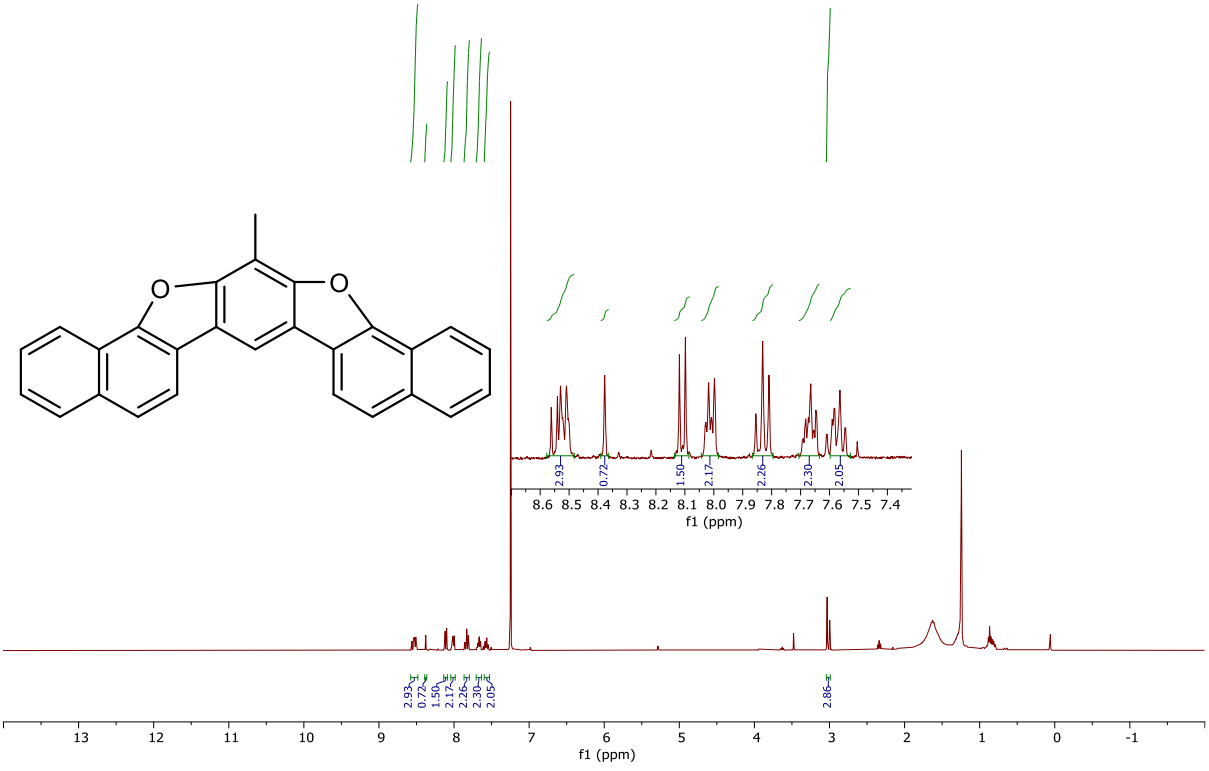

Figure A146. ^{1}H NMR (400 MHz, $CDCl_3$) of 37.

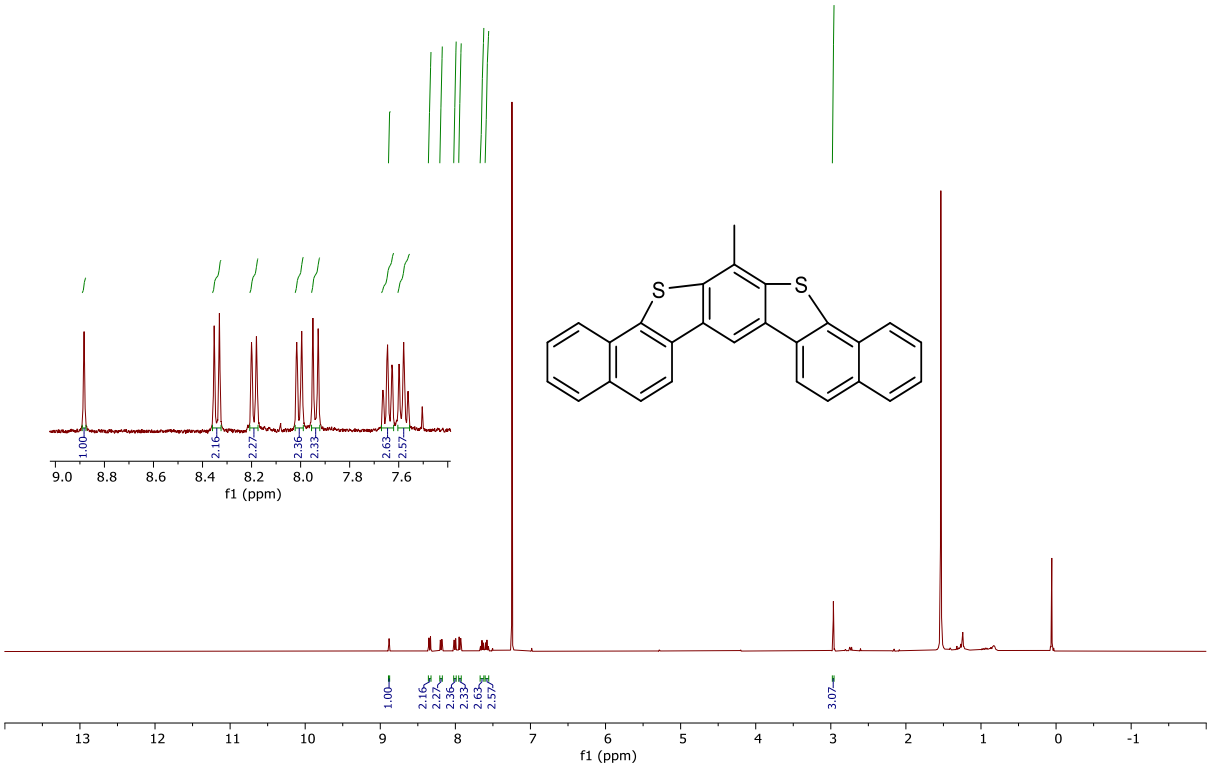

Figure A147. ^{1}H NMR (400 MHz, $CDCl_3$) of 38.

Eidesstattliche Erklärung

Hiermit erkläre ich, Nour-Eddine El Alaoui, die vorliegende Arbeit „ Specific bromination of fluorinated oligophenylenes, towards cyclo-para- and cyclo-meta-phenylenes “ selbständig und ohne fremde Hilfe verfasst zu haben. Es wurden keine anderen als die von mir angegebenen Quellen und Hilfsmittel benutzt. Die den benutzten Werken wörtlich oder inhaltlich entnommenen Stellen sind als solche kenntlich gemacht worden. Ich erkläre, die Angaben wahrheitsgemäß gemacht, keine vergeblichen Promotionsversuche unternommen und keine Dissertation an einer anderen wissenschaftlichen Einrichtung zur Erlangung eines akademischen Grades eingereicht zu haben. Ich bin weder vorbestraft noch sind gegen mich Ermittlungsverfahren anhängig.

Liste of Publications

1- **El Alaoui, N.E**. and Amsharov, K., 2025. Regioselective Terminal Bromination of Fluorinated Oligophenylenes. **Chemical Communications.**

2- Han, D., Schramm, J., Ruan, Z., Naumann, T., **El Alaoui, N.E**., Amsharov, K.Y., Tonner-Zech, R. and Gottfried, J.M., 2025. Quasi-Planar π-Extended Cycloparaphenylenes: On-Surface Synthesis, Characterization, and Electronic Properties. **Journal of the American Chemical Society**.5c07471.

3- **Alaoui, N.E.E**., Boulhaoua, M., Hutai, D., Oláh-Szabó, R., Bősze, S., Hudecz, F. and Csámpai, A., 2022. Synthetic and DFT Modeling Studies on Suzuki–Miyaura Reactions of 4, 5-Dibromo-2-methylpyridazin-3 (2 H)-one with Ferrocene Boronates, Accompanied by Hydrodebromination and a Novel Bridge-Forming Annulation In Vitro Cytotoxic Activity of the Ferrocenyl–Pyridazinone Products. ***Catalysts*****,** *12*(6), p.578.

4- Thari, F.Z., Tachallait, H., **El Alaoui, N.E**., Talha, A., Arshad, S., Álvarez, E., Karrouchi, K. and Bougrin, K., 2020. Ultrasound-assisted one-pot green synthesis of new N-substituted-5-arylidene-thiazolidine-2, 4-dione-isoxazoline derivatives using NaCl/Oxone/Na3PO4 in aqueous media. ***Ultrasonics sonochemistry***, *68*, p.105222.

Curriculum vitae

Personal Data.

Name	Nour-eddine EL Alaoui
Gender	Male

Education.

Since May. 2021	PhD studies at Martin Luther University Halle-Wittenberg, Halle (Saale), Germany, Supervisor: Prof. Dr. Konstantin Amsharov
Sep 2014-June 2016	Master (specialist) Organic chemistry at Mohammed V University, Morocco. Thesis: Synthesis and reactivity of new derivatives of Thiazolidine-2,4-dione. Supervisor: Prof. Dr. Khalid BOUGRIN Final grade: 2.9
Sep 2011-June 2014	Bachelor (specialist) Organic chemistry at Mohammed V University, Morocco. Thesis: synthesis of aroma molecules. Supervisor: Prof. Dr. Smoumia LAFQUIH TITOUANI Final grade: 3.5
Sep 200-June 2011	Secondary school, les orangers, Morocco. Final grade: 3.4

Academic work experience.

Since May. 2021	Research assistant at Martin Luther University Halle-Wittenberg, Halle (Saale), Germany. Supervisor: Prof. Dr. Konstantin Amsharov
Mar. 2020–Feb. 2021	Research assistant at the Friedrich-Alexander University Erlangen-Nürnberg, Germany Supervisor: PD. Dr. evgeny kataev